SWITCHING EFFECT

IN CHALCOGENIDE GLASSES

by

P. NESVADBA, M.Sc.

A dissertation submitted
to the University of Warwick for
admission to the degree of
Doctor of Philosophy.

1973

SWITCHING EFFECT

IN CHALCOGENIDE GLASSES

by

P. NESVADBA, M.Sc.

A dissertation submitted
to the University of Warwick for
admission to the degree of
Doctor of Philosophy.

1973

Dedicated to my loving mother, VLASTA

to my exemplary father, OTA

to my devoted wife, ZUZANA

and to my beloved brother, OŠEK

MEMORANDUM

This dissertation is submitted to the University of Warwick in support of my application for admission to the degree of Doctor of Philosophy. It contains an account of my own work performed at the School of Physics of the University of Warwick in the period October 1970 to November 1972 under the general supervision of Dr. P. W. McMillan. No part of it has been used previously in a degree thesis submitted to this or any other university. The work described in this thesis is the result of my own independent research except where specifically acknowledged in the text.

August 1973. P. Nesvadba.

ACKNOWLEDGEMENTS

I am extremely grateful to Dr. P.W. McMillan for his supervision, continued interest and encouragement throughout the course of this work and in preparation of the manuscript.

I should also like to thank Professor A.J. Forty for making the facilities for research within the School of Physics available to me.

Furthermore, I should like to thank many of the members of staff for their interest and valuable discussions, in particular Dr. T.A. Delchar who kindly let me use his vacuum system and Dr. H. Mykura who helped me to set up the experiment described in section 5.6.4. I am grateful to the members of the glass-ceramics group for their friendship, especially to Dr. D.N. Jarrett and to Mr. D.I. Atkinson, who was kind enough to run some of the computer programmes for me.

An invaluable technical assistance was given to me by Mr. I.D. Ward and Mr. G. Smith (electron microscopy), by Mr. J.S. Huckfield (glass apparatuses in Fig. 5.14 and 5.18) and by Mr. R.A. McLeod (photography), which I gratefully acknowledge.

I should also like to thank the librarians, Mr. L. Bulmer and Mr. M. Davies for their efficiency in dealing with my requests.

My thanks are due to Mrs. B.A. Kerton for attentive typing of this thesis and to Mrs. C.A. Allsopp for skilful tracing of the diagrams.

Finally I wish to thank the General Electric Co. Ltd. of Stafford for the provision of a grant for my maintenance.

ABSTRACT

The overall aim of the research programme was to investigate threshold switching, both experimentally and theoretically, in thick devices based on chalcogenide glasses.

The experimental study included characterization of the switching material Si_{12} Ge_{10} As_{30} Te_{48} by measurement of its electrical conductivity as a function of temperature and electric field.

The temperature dependence of threshold voltage was measured over a broad temperature range and could be explained in terms of two theoretical models. The models had a common feature in that they were based on the one-dimensional thermal model with an added independent condition for switching involving the presence of electric field. The importance of the restriction to one dimension was illustrated by solving the equations of the thermal model in two dimensions using a digital computer. The validity of the models was limited, however, because no modifications due to the presence of structural changes in the switching material were included in the models. It was concluded that the structural changes have to be studied and understood before a realistic quantitative model of switching can be developed.

The experimental study of structural changes in the threshold switching material comprised direct evidence of microcrystallites by the use of electron microscope and observations of changes in switching parameters during and after the forming stage.

The variation in threshold voltage and delay time has been analyzed by statistical methods which revealed that the variation has two components:

(i) slow semi-reversible ageing taking place throughout the life of the device,

(ii) fast fluctuations occurring from operation to operation.

It was further shown that the latter variation is not random but that correlation exists between sequential fluctuations. A semi-quantitative theoretical model was presented to explain the observed phenomena in terms of microstructural changes in the glass during switching. This model incorporates some simplifying assumptions but nevertheless it is capable of satisfactorily predicting the experimental observations and of suggesting areas for future research.

Some direct experiments aimed at the elucidation of the mechanism of switching were conducted, but no definite conclusion could be reached. However, the overall results indicate that a satisfactory description of the switching phenomena could be achieved in terms of a thermal model with the inclusion of electric field effects and aspects of structural changes.

CONTENTS

CHAPTER 1

GENERAL INTRODUCTION

Since the subject matter of this thesis is related to the switching effect in chalcogenide glasses it is appropriate in this introductory chapter to discuss the nature of the materials and the physical effects with which we shall be concerned.

1.1 Chalcogenide Glasses

Chalcogenide glasses are non-crystalline solid substances containing one or more of the chalcogens: Selenium (Se), Sulphur (S) and Tellurium (Te). Selenium forms glass readily by cooling of the melt; amorphous sulphur is obtained by fast cooling of the liquid form; amorphous tellurium cannot be prepared in bulk, only as a chemical precipitate or by a vapour deposition technique. The fact that many elements can be added to these three basic elements and form two or more component chalcogenide glasses means that this class of substances is extremely large; already the number of binary glasses runs into several tens. For a given system of chalcogen elements there will be a range of compositions that can be quenched to the glassy state. Outside this range, the final material will be partly or wholly crystalline.

The most important non-chalcogen constituents of chalcogenide compounds are Lead (Pb), in crystalline, and Arsenic (As) in glassy compounds. Lead chalcogenides are highly photoconductive and are used for manufacture of infra-red detectors. Chalcogenide glasses are transparent to infra-red radiation to considerably longer wavelengths than oxide glasses; $As_2 Se_3$ glass has been an important material for making infra-red prisms. Amorphous selenium is the only known material suitable for xerography.

Not all of the chalcogenide glasses show the switching effect. It appears at present that the most suitable materials for switching applications are three or four component chalcogenide glasses containing germanium (Ge), silicon (Si), Indium (In), Antimony (Sb) or other elements.

So far nothing has been said about the properties of chalcogenide glasses apart from that they are solid, non-crystalline and exhibit the switching effect. The other important property of the chalcogenide glasses is their semiconductivity. This means that their electrical conductivity at room temperature is in the range between a "bad" metal and a "bad" insulator. However, more important than the actual magnitude of the electrical conductivity is the way in which the conductivity changes with temperature. The conductivity of the chalcogenide glasses can in many cases be considered as being thermally activated over large ranges of temperature as found in the case of crystalline semiconductors. The activation energy roughly corresponds to one half of the energy of light quanta for which the chalcogenide glasses become transparent to light. As this energy is of the order of 1 eV, the chalcogenide glasses are opaque in the visible range and are transparent to infra-red radiation.

An important property of chalcogenide glasses is that they can be prepared relatively easily. Although Chapter 4 indicates that the process of preparation is not as simple as taking a few components and melting them in a test-tube it is nevertheless much easier than the method of preparing crystalline semiconductors. The main reason for this is the relative insensitivity of the properties of chalcogenide glasses to the addition of impurities[1].

Some of the properties of chalcogenide glasses which are relevant for the switching effect are discussed in a greater detail in the next Chapter 2. This section is concluded by several remarks concerning the history of the chalcogenide glasses.

Amorphous selenium was discovered by Berzelius in 1817 and is perhaps the oldest and the most famous of the chalcogenide glasses. Although several glassy chalcogenide compounds were known and used in some technical applications for a long time, it was not until late 1950's when serious interest and systematic research in chalcogenide glasses started[2-4]. As more chalcogenide glasses and amorphous semiconductors in general were prepared and their properties reported the need arose for theoretical explanations. The first attempts to explain theoretically the electrical and optical properties of amorphous semiconductors are of a relatively recent date (1960's) and it is possible to say that the subject is still in its very beginings[5]. The central problem is to calculate the electron energy spectrum in an amorphous semiconductor. The main difficulty here is the lack of a theoretical method which would give reliable wave-functions for the calculation of transport properties. The application of the methods used for the calculation of the electron energy spectrum of crystalline semiconductors during the past few decades to amorphous materials yields in all cases wave-functions which are incoherent (due to the disorder) to such a degree that the gap in the energy spectrum is not preserved and thus the classical method of calculation predicts always metallic properties contrary to the experimental observations[8]. The search for new theoretical concepts of amorphous semiconductors becomes more widespread every year judging by the number of published papers and contributions at the conferences held on the subject[6,7].

The discovery of the switching effect has undoubtedly played a major role in the stimulation of the theoretical interest in amorphous semiconductors.

1.2 Switching Effect

The switching effect can be somewhat loosely defined as a reversible change in the electrical conductivity of a solid under the influence of an

applied electric field. Some amendments to this definition are required to make it more precise and a few remarks are made relating to this.

Let us first describe how the reversible change in the electrical conductivity of the switching material is achieved technically. In the case of a two-terminal device a layer of the switching material (e.g. chalcogenide glass) is furnished with two electrodes (for the possible geometries see Fig. 4.1 and 4.2). This provides the means of changing the conducting state of the device by an applied electric potential difference. As the applied potential difference is increased to a certain critical value the change in the conductance of the switching device (usually an increase of conductance by several orders of magnitude) occurs. (This change in the conductance of the device is not necessarily due to the change in the conductivity of the switching material in the whole of the volume between the electrodes). The new state may last only for the time of application of the electric potential difference in which case the switching effect is specified as "the threshold switching effect", or the new conducting state may persist after the applied potential difference is removed and then we deal with "the memory switching effect". The memory switching effect is distinguished from dielectric breakdown by its reversibility; if a suitable electric pulse (re-setting pulse) is now applied to the memory device, its state will revert back to the initial one.

There are many materials exhibiting the switching effect and accordingly a great variation in the switching characteristics. Apart from the chalcogenide glasses which are, at present, most widely used for the investigation of the switching effect and also promise the most useful applications, there is a large group of transition metal oxide glasses exhibiting the switching effect; some elemental amorphous semiconductors can be switched in thin film form and also a small group of crystalline semiconductors shows the switching behaviour. At present there is no

criterion which could be used for predicting whether a given material will show switching or not. (This question is discussed in section 2.2.5).

The large number of the switching characteristics can be classified broadly according to whether the performance of the device is current controlled (Fig. 1.1.a) or voltage controlled (Fig. 1.1.b). In the first case the voltage-current characteristic (V-I characteristic) is multivalued in voltage ("S" shaped), in the second case of the voltage controlled device the V-I characteristic is multivalued in current ("N" shaped characteristic). Although strictly speaking both the "S" and "N" shaped characteristics conform to the above definition of switching, only the first behaviour is usually designated (and even then only in some cases) as the switching behaviour; the second type of behaviour is described as "voltage controlled negative resistance".

Fritzsche[9] subclassifies the performance of the devices having the "S" shaped V-I characteristics according to whether their working point can be stabilised in the negative differential resistance region $\frac{dV}{dI} < 0$ and whether the device exhibits the memory action into four groups:

(i) negative differential resistance without memory (e.g. thermistor)

(ii) switching without memory (threshold switching)

(iii) negative differential resistance with memory

(iv) switching with memory.

In the cases (i) and (iii) the working point can be stabilised in the region of the negative differential resistance whereas the opposite is true in the cases of switching ((ii) and (iv)). The switching characteristics corresponding to the four groups of the above classification are schematically given in Fig. 1.2. Only the switching action of type (ii) is the subject of the present thesis.

Several further categories can be added to supplement the above classification. For example Drake et al[10] have added a further class

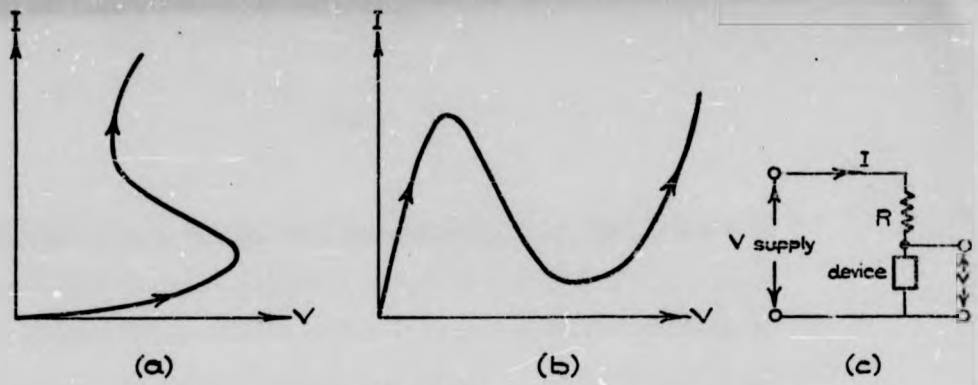

Fig. 1.1.

SCHEMATIC DIAGRAMS OF:

(a) current controlled negative differential resistance device
(b) voltage controlled negative differential resistance device.
(c) measuring circuit.

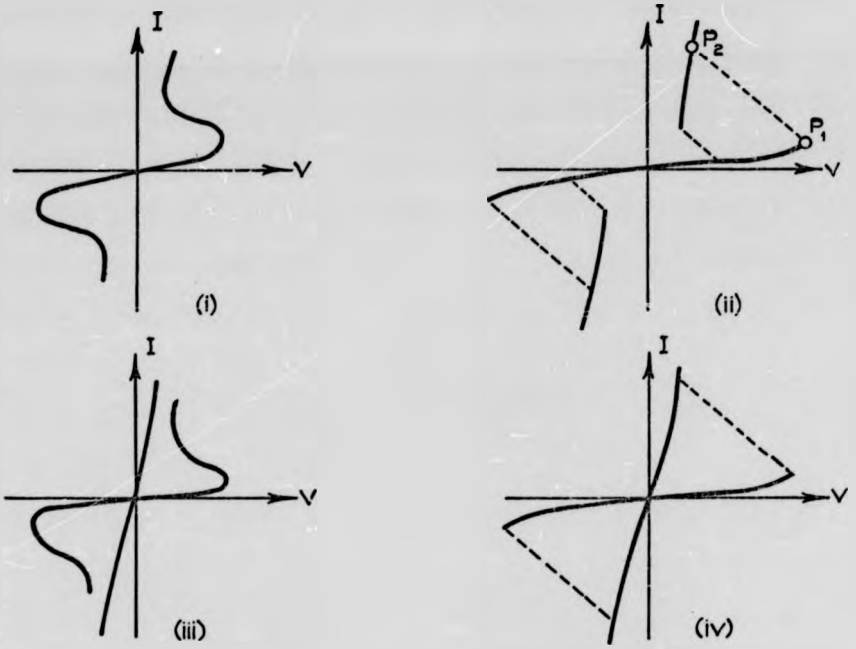

Fig. 1.2.

CLASSIFICATION OF DEVICES AFTER FRITZSCHE, REFER TO TEXT IN SECTION 1.2.

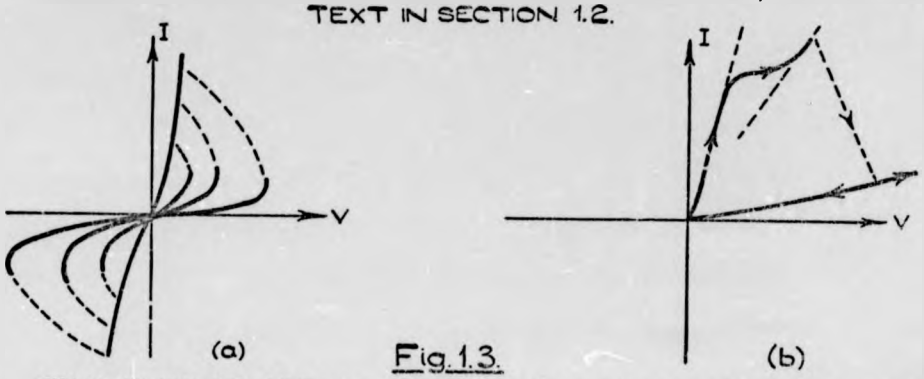

Fig. 1.3.

EXAMPLES OF SPECIAL TYPES OF SWITCHING CHARACTERISTICS.

of a switching device with multistable series of characteristics. The performance of the device can be "switched" between these characteristics by suitable electrical pulses. A schematic representation of the characteristics of such a device is given in Fig. 1.3.a. In many cases the first switching performance of a device is different from the rest of the subsequent operations. An example of this behaviour[11] is given in Fig. 1.3.b. The device is initially in a high conductance state. At a certain value of the applied voltage a transition to the second high conductance state occurs. If the voltage is increased still further then switching into a highly resistive state occurs. Thereafter the device shows a normal switching behaviour. There are many special types of switching which, perhaps, would deserve to have their own category. At present new types of switching are still being reported in the literature[29] and any attempt to classify them, other than the basic classification of Fritzsche, would be premature.

The switching behaviour is sometimes reported to be polarity dependent, i.e. the switching characteristics are asymmetric unlike those shown in Figs. 1.1 - 3. The polarity effects occur when two different electrode materials are used for the construction of a two-terminal device and they seem to be pronounced only at low temperatures[12].

In this section an attempt has been made to introduce some basic features of the switching effect and its complexity in terms of the switching V-I characteristics. It has to be said, however, that the description of the switching effect in terms of the switching V-I characteristics is not sufficient and additional, secondary characteristics are needed to account for other essential features of the switching process. These are, for example, the dynamic response of a switching device to rectangular electrical waveforms, variation of the switching parameters with device geometry, ambient temperature or pressure, illumination, long term variation

of the parameters of the switching device, structural changes in the device, its life-time and other secondary characteristics.

The switching effect was defined as a reversible change in the electrical conductivity of a solid under the influence of an electric field. This definition thus excludes gases and liquids from consideration. The reversible changes in the conductivity of gas media have been known for a long time (lightning, gas discharge). Reversible changes in the conductivity of liquids have been reported more recently[13]. The reversibility of the changes in electrical conductivity of gases and liquids may seem to be in many cases a trivial effect owing to their fluidity. In some cases, however, the essential mechanism of the reversible change may be closely related to that in switching solid materials (e.g. switching in liquid chalcogenides is probably closely related to the switching in chalcogenide glasses) and the fluidity is not an essential requirement for reversibility of the change in electrical conductivity.

The definition of the switching effect also eliminates from consideration the changes in the electrical conductivity of a solid by means other than electrical. It is known that certain solids change their electrical conductivity abruptly on heating as a result of a thermodynamic phase transition (e.g. VO_2 at $68^{\circ}C$)†. It can be seen that such materials will also change their electrical conductivity under the influence of the electric field if the conditions are so arranged that the development of joule heating will effect the temperature rise necessary for the phase transition to occur. Such effects (when known to be operative) are excluded from the switching class as trivial. Another important non-electrical means of changing the properties of a switching material is high intensity illumination of certain switching materials by enegetic photons (by laser beam) or by electrons of suitable energy (by electron beam). There are

† E. N. Fuls et al., Appl. Phys. Lett. 10 (1967) 199.

indications that the resulting phase transformation of the material is not achieved by straight forward heating as in the case discussed above but that the effect of the photon-electron interactions or electron-electron interactions is decisive in these experiments, although the inevitable heating plays a certain role[14,15]. The important feature is that not only can the electrical conductivity of the material be reversibly changed by these means but also that other properties such as reflectivity, secondary emission yield, wettability, can be reversibly changed. This creates immense opportunities for technological applications of these effects. Some of these applications (e.g. information storage) are mentioned in the next section (1.3).

It was S. R. Ovshinsky who first realized the possibility of the application of the switching effect and also developed the first commercial devices*[16] in 1968. This year is usually considered as the date of the discovery of the switching effect although several reports of this effect appeared earlier[17,18]. The possibility of technological applications of the switching effect and related phenomena has stimulated much of the experimental and theoretical research into amorphous semiconductors. At the present date by no means all of the effects of reversible changes in the non-crystalline materials are sufficiently well understood. Thus the understanding of the electrical switching effect, which is just one aspect of the more general reversible changes observed in non-crystalline semiconductors, will contribute to the elucidation of the related mechanisms.

1.3 Application of the Switching and Related Phenomena

The structure of all non-crystalline solids is, strictly speaking, a non-equilibrium one and as such is liable to change in time. In some technological applications it is desirable that

(i) this change occurs as slowly as possible; in other applications,

* Ovonic devices by Energy Conversion Devices Inc., Troy, Michigan, U.S.A.

however, one is interested in

(ii) a fast change of the state of the solid under certain controlled conditions and when these conditions are removed the resultant state should again be, practically, a stable one.

It is not possible to review all applications which non-crystalline solids have found in their apparently "stable" state, nor to stress sufficiently the importance of such applications within the scope of this thesis. (For a short review see (19)). The switching phenomena are of the kind belonging to the group (ii), in which the state of the non-crystalline system is changed rapidly and reversibly under the influence of electric field. There are other means by which this change can be brought about (e.g. light and electron beams), as mentioned in Chapter 2. The reversible changes can occur extremely fast (in $< 10^{-9}$s) and also in a very small volume; both these circumstances are of great importance for the application of the memory switching phenomenon to information storage. It is estimated that the densities of the information in light operated stores (ECD) could succesfully compete with the presently used magnetic memories[20]. The feasibility of the application of the RM-256 memories (see section 4.1.2) in computer memories (micro-programmes and code inversion) is, perhaps, sufficiently demonstrated by the interest of the big computer-producing firms[21]. Another possible applications of the switching devices are in telephone networks as switches, in alphanumerical displays as controlling elements or in logic circuits in general[22]. Reviews of the applications of Ovonic devices can be found in[23]. The possibilities of the threshold switching device alone remain largely unexplored but in the least it can be used as a voltage regulator[24], artificial inductance[22] or an oscillator in a MHz range[25].

The possibility of three terminal (or more) controllable switching devices is indicated by recent reports by Schuöcker and others[26].

The power capability of the switching devices can be quite high, especially those employing liquid chalcogenides[27].

Devices employing amorphous materials are less susceptible to radiation damage than similar devices using crystalline materials[28]; this would be a definite advantage in conditions in which large radiation fields are present. The apparent insensitivity of the amorphous semiconductors to the addition of impurities[1] is another advantage, which makes the preparation of the materials a relatively trivial process.

The potential usefulness of amorphous semiconductors (not necessarily switching ones) is indicated by the recent developments of new vidicon targets and new xerographic materials.

1.4 Choice of Experiments

One of the basic restrictions placed on the choice of experiments dealt with in this thesis was to work with devices prepared from chalcogenide glass in bulk form. As explained in Chapter 4 dealing with preparation, this decision was made in order to ensure that

(i) the composition of the chalcogenide glass could be controlled easily

(ii) the properties of the glasses of a particular composition were reproducible.

Some restrictions also had to be placed on the range of compositions of the chalcogenide glasses which were investigated. Although several types of glasses were prepared (see Table 4.2.1) most of the switching experiments were carried out using the most stable 4-component glass $Si_{12}Ge_{10}As_{30}Te_{48}$ (Ovshinsky composition) and all the results contained in this thesis refer to this composition unless stated otherwise.

The primary objective which was kept in mind during the choice of the switching experiments themselves was to devise experiments which would elucidate the nature of the switching mechanism; more specifically

this meant an attempt to decide the extents to which the thermal and the electronic mechanisms are responsible for the overall switching behaviour. During the course of experimentation it became obvious that structural changes in the threshold glass are a relevant factor and the need for structural investigations therefore arose.

The switching experiments were supplemented by measurements of d.c. conductivity over a wide temperature range and at various strengths of the electric field.

From the theoretical side, the problem of the initiation of the switching transition was considered in order to explain the change in the threshold field with ambient temperature observed and reported earlier[30]. The study of the initiation of switching was done using the assumption that the conductivity of the switching material is electric field dependent and solving the appropriate 1-D model using a digital computer. An attempt to consider the 2-D problem was made but only partial success was achieved.

A theoretical model for the statistical aspects of the variability of switching parameters was set up; the basic assumption in the model was the presence of structural changes in the switching chalcogenide glass.

1.5 Plan of Thesis

The contents of the thesis, which is divided into eight chapters, are listed on pages preceding this introductory Chapter 1.

Chapter 2 consists of two parts:

(i) a condensed introduction to amorphous semiconductors and their properties relevant to the switching effect with some indication of the outstanding problems in the theory of the amorphous state.

(ii) a review of the theories of the switching effect.

The third Chapter presents the theoretical models employed in this work to explain the results of the experiments presented in Chapter 5.

Chapter 4 deals with the methods of preparation of chalcogenide

glasses and fabrication of switching devices employed in this work and also gives a brief review of the methods of preparation.

Chapter 6 compares the experimental results with the predictions of the theoretical models. The main implications of the comparison and conclusions are summarized in Chapter 7.

Suggestions for future work are made in Chapter 8.

References Quoted in Chapter 1

(1) Duwez P. and Tsuei C.C., J. Non-Cryst. Solids 4 (1970) 345.
Kolomiets B.T. and Nazarova T.S., Sov. Phys. Solid State 2 (1960) 159.

(2) Gorynuova N.A., et al., Sov. Phys.-Tech. Phys. 3 (1958) 912.

(3) Kolomiets B.T. and Gorynuova N.A., Zhur. Tek. Fiz. U.S.S.R. 25 (1955) 984.

(4) Pearson A.D., et al, Advance in Glass Technology, (1967) 357 (Plenum Press).

(5) Mott N.F. and Davis E.A., "Electronic Processes in Non-Crystalline Solids", Oxford Press, 1971.

(6) Proceedings of the 3rd Int. Conference on Amorphous and Liquid Semiconductors, Cambridge, England, 24th - 27th September, 1969, published in J. Non-Cryst. Solids 4 (1970).

(7) Proceedings of the 4th Int. Conference on Amorphous and Liquid Semiconductors, Ann Arbor, Michigan, U.S.A., August 1971, in J. Non-Cryst. Solids 8-10, (1972).

(8) Ziman J.M., J. Non-Cryst. Solids, 4 (1970) 426.

(9) Fritzsche H., I.B.M. J. Res. Dev. 13 (1969) 515.

(10) Drake C.F., et al, Phys. Status Solidi 32 (1969) 193.

(11) Ashara Y. and Izumitani T., J. Non-Cryst. Solids 11 (1972) 97.

(12) Henisch H.K., Paper 8 of the European Semiconductor Device Research Conference, Munich, March 1971.

(13) Andreev A.A., et al, Sov. Phys.-Semicond. 5 (1972) 1900.
Busch G., et al, Phys. Lett. 33A (1970) 64.
Regel A.R., et al, J. Non-Cryst. Solids 8-10 (1972) 455.

(14) Feinleib J., et al, Appl. Phys. Lett. 18 (1971) 254.

(15) Chen A.C., et al, J. Non-Cryst. Solids 8-10 (1972) 917.

(16) Ovshinsky S.R., Phys. Rev. Lett. 22 (1968) 1024.

(17) Pearson A.D., et al, Advances in Glass Technology, 6th Int. Congress on Glass, 1962, p. 357.

(18) Ovshinsky S.R., Electronics 32 (1959) 76.
Lebedev A.A., et al, Sov. Phys.-Techn. Phys. 1 (1956) 2071.

(19) Goodman C.H.L. (STL, Harlow), "The Technological Importance of Amorphous Materials", contribution at the summer school on Electrical Properties of Non-Crystalline Solids, Cambridge, 29.6 - 3.7 1970.

(20) Aseltine J., (Ovonic Memories Inc., Los Angeles, Calif.) Electronic Design 20 (No.6) 1972, March 16.

(21) Lee, G.C., (ICL), contribution at the IEE Discussions Meeting on "Experiences with amorphous semiconductors", London, Savoy Place, 8.5.1972.

(22) Bosnell J.R. (RRE), contribution of the meeting as in (21).
Neale R.G. and Ovshinsky S.R., 4th Int. Congress in Munich, West Germany, November 1970.

(23) Nelson D.C., J. Non-Cryst. Solids 2 (1970) 528
Kobylarz T.J., ibid, 515
Fritzsche H., Proc. Ind. Conf. on low mobility materials, Eilat, Israel, April 1971, p. 279.

(24) Morgan D.V. and Howes M.J., "Solid State Electronic Devices," Wykeham Publications, London, 1972, p. 150.

(25) Zaliva V.I. and Zakharov V.P., Sov. Phys. JETP Letters 13 (1971) 93.
Shadrin V.D., Kogan Sh. M., Sov. Sol. State Phys. 13 (1971) No. 4.
Haden C.R. et al, J. Non-Cryst. Solids 8-10 (1972) 432.

(26) Schuöcker D., J. Non-Cryst. Solids 8-10 (1972) 427.
Appl. Phys. Lett. 19 (1971) 7.
et al, J. Appl. Phys. 43 (1972) 2647.
Kikuchi M. and Iizima S., Appl. Phys. Lett. 15 (1969) 323.

(27) Regel A.R., et al, J. Non-Cryst. Solids 8-10 (1972) 455.

(28) Electronics 28.9.1970.
Suntola T. et al, (and references therein)
Acta Polytechnica Scandinavica, Series 85, Helsinki, 1971.
Smith R.A. et al, J. Non-Cyst. Solids 8-10 (1972) 862-867.
Nicolaides R.V. and Doremus L.W. ibid, 857.

(29) e.g. Hamakaura Y., et al, p. 868, Mahdjuri F., p. 992 in J. Non-Cryst. Solids 8-10 (1972).

(30) McMillan P.W. and Nesvadba P., J. Phys. D. (Applied Physics) 4 (1971) 1401.

CHAPTER 2

REVIEW OF THE PROPERTIES OF CHALCOGENIDE GLASSES AND THE THEORIES OF SWITCHING

The second part of this chapter reviews the theories of the switching effect. Any theoretical model of the switching effect has to take into account at least some properties of the switching material; therefore the basic properties of chalcogenide glasses relevant to the switching effect are also reviewed in the first part of this chapter. Although the chalcogenide glasses are the primary subject of the review certain parts of the review are applicable to amorphous materials in a more general sense. The term chalcogenide glass is synonymous with the term amorphous semiconductor in sections 2.1.1 and 2.1.3.

2.1 Properties of Chalcogenide Glasses

Some properties of chalcogenide glasses were mentioned in section 1.1. The following three sections give more detailed account of the properties with particular reference to the points pertaining to the switching effect.

2.1.1 Disorder

The chalcogenide glasses belong to the group of non-crystalline substances. There is no precise definition of non-crystallinity, but usually the absence of long range order in the atomic arrangement of a solid over distances $\gtrsim 100$ Å is taken as a condition for non-crystallinity. According to this definition a crystalline solid containing more than 10^{19} randomly distributed point defects in one cm^3 or a polycrystalline solid composed of small ~100 Å crystallites are classed as non-crystalline.

The term "amorphous" is usually used to characterize thin films of deposited non-crystalline material; the term "glass" is used to describe non-crystalline substances prepared by quenching from the melt in bulk quantities.

Recently a work appeared (1) which suggests that in many cases the disorder of amorphous films differs in a fundamental way from the disorder of bulk glass.

Detailed knowledge of the atomic arrangement of a non-crystalline solid is extremely important for a number of considerations, e.g. glass formation, calculation of electron band structure etc.. Apart from the atomic arrangement other properties of the solid are important characteristics, for example the thermodynamic properties or mechanical properties (e.g. fracture). These can also serve as a measure of non-crystallinity and are discussed at some length later.

There are two basic approaches to making a model of a non-crystalline solid. In the case where the long range order distance r is comparable with the interatomic distances it is possible to imagine the atomic network of the non-crystalline solid as a modification of the corresponding crystalline structure in which the atomic bonds are randomly stretched or shortened or in some way mutually rotated. This approach assumes that no bonds are broken during this modification which means that the number of the nearest neighbours z_1 is the same in both substances. The practical consequence is that liquids having the same number of nearest neighbours z_1 as in the solidified phase can in principle form glasses having the random network (subject to certain restrictions given by the kinetic theory of glass formation). An example of a substance which cannot form glass by melt quenching is germanium; in liquid germanium $z_1 = 6$ whereas in solid form $z_1 = 4$. The hypothesis of random network was first used by Zacharaisen to describe the structure of oxide glasses[2] and is still a source of inspiration at present[3].

The second approach is to imagine the structure of the disordered material to be composed of small domains of high order surrounded by a matrix of low degree of long range order. This "small crystallite" theory

is due to Lebedev, Valenkov and Porai-Koshits[4,5].

In certain substances atoms are grouped in molecular units (e.g. eight-membered rings in sulphur, selenium, chains in tellurium) which are connected together by other atoms (the bonds between units can be of a different chemical nature from the bonds inside the molecular units). The molecular group theory[6] is intermediate between the random network and small crystallite theories and has been applied to silica glasses[6] but can also be applied to chalcogenide glasses.

If the disordered solid is composed of only one kind of atom, the two dimensional representation of the solid according to the random network hypothesis is given in Fig. 2.1.a. The corresponding crystalline arrangement is drawn in Fig. 2.1.b. It is seen that the atoms in the first case are spaced by nearly the same distances as in Fig. 2.1.b. This is due to the similarity between the nature of the atomic forces acting in amorphous and crystalline substances; the nature of the repulsive and attractive forces is apparently very little changed with disorder. Repulsive forces increase very rapidly with decreasing interatomic distance; this is one reason why the network in Fig. 2.1 cannot be completely random - the interatomic distance cannot be arbitrarily small. If this were the case, then following the analysis made by Hertz[7] it is possible to show that the most probable nearest neighbour distance in a random mixture of silicon atoms would be 1.49 Å; in fact it is 2.35 Å in amorphous and crystalline silicon[8].

If we deal with a solid containing two (or more) kinds of atoms, say A,B,(C,...) and if the atomic bonding allows interchange of atoms between their sites without changing the distances between the lattice sites, there is the possibility (subject to further restrictions) of disordering the crystalline alloy AB by permuting the atoms randomly between the sites. This type of disorder is termed compositional disorder

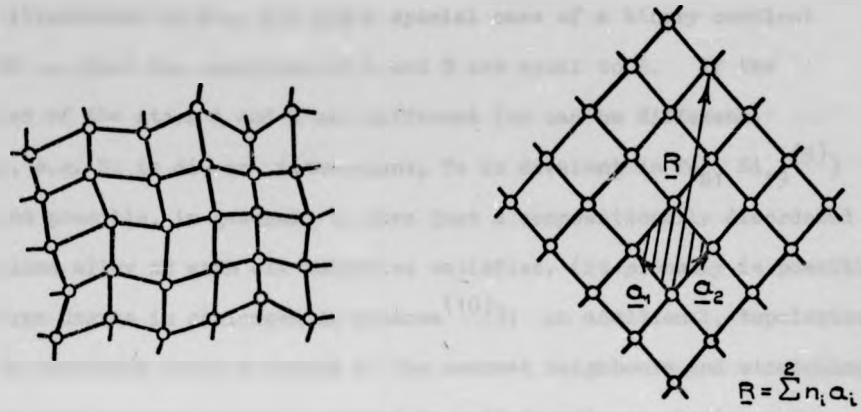

Fig. 2.1.

EXAMPLES OF AMORPHOUS AND CRYSTALLINE SUBSTANCES WITH ONE KIND OF ATOM.

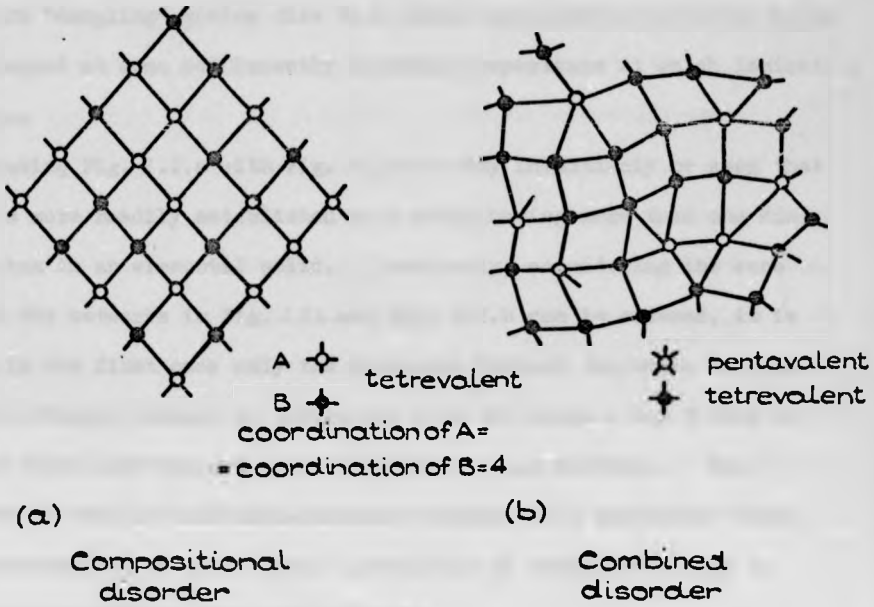

Fig. 2.2

and is illustrated in Fig. 2.2 for a special case of a binary covalent alloy AB in which the valencies of A and B are equal to 4. If the valencies of the atoms A and B are different (or can be different, varying, e.g. Si is di - or tetravalent, Te is divalent in Te_{81} Si_{19} [9]) it is not possible, in general, to have just a compositionally disordered crystalline alloy AB with all valencies satisfied, (it probably is possible to a large degree in chalcogenide glasses[10]); an additional, topological, disorder involving varying number of the nearest neighbours and stretching bonds or varying bond angles is needed to satisfy valence requirements. In certain materials in which the atomic rearrangement is a relatively difficult process it may be favourable to leave some valencies unsatisfied. The situation then arises as shematically shown in Fig. 2.2.b. A number of bonds are "dangling" giving rise to a large concentration of sites which will be charged at some sufficiently elevated temperature at which ionization takes place.

Comparing Fig. 2.2.a with Fig. 2.2.b it may intuitively be seen that disorder is more readily established in a solid having more than one kind of atoms than in an elemental solid. Conversely, considering the ease with which the networks in Fig. 2.2.a and Fig. 2.2.b can be ordered, it is seen that in the first case only the distances between the atoms need to be slightly changed whereas in the second case the atoms A and B have to be in some cases interchanged over a relatively long distance. The consequence of this is that multicomponent glasses in a particular class (e.g. chalcogenides) do not usually crystallize as easily as binary or single component glasses when heat treated.

So far only atomic disorder has been discussed. The perfect order of a crystal will be destroyed also if various atoms are in varying energetical states because of some "exciton" being present at the atomic site. Excitons, magnetic disorder etc. represent an additional disorder which we do not consider here. The concept of the radial distribution

function outlined below is not applicable to this type of disorder.

The atomic structure of a perfect crystal is easily described by defining a unit cell containing a small number of atoms (2 atoms in case of Fig. 2.2.b) and giving the elementary lattice vectors R_1 and R_2 through which the unit cell has to be translated to obtain the whole crystal. This approach is not possible in the case of a non-crystalline solid as there is no simple pattern which could be repeated exactly to obtain the whole non-crystalline solid of macroscopic dimensions. The disorder has to be described by some statistical entity which gives an "average" of the atomic arrangement. An example of a statistical function giving the probability of finding an atom A in a sperical shell of a radius r and thickness dr around an atom B placed in the centre of the shell is the radial distribution function[11]. For a solid containing one kind of atom, only one radial distribution function ϱ_{AA} exists, but for a solid containing n components one can define n^2 functions describing the distribution of atoms of kind k around an atom of kind l, where $1 \leq k \leq n$, $1 \leq l \leq n$ (e.g. in the case of a binary alloy AB four radial distribution functions are in general required: ϱ_{AA}, ϱ_{AB}, ϱ_{BA}, ϱ_{BB}). A set of radial distribution functions does not give a complete statistical description of the disorder. Additional information can be given in terms of the distribution functions for bond angles between various atoms. Correlation functions of order $n > 2$ can be introduced, giving the probability of n atoms being in a particular position (for $n = 2$ this reduces to the pair correlation functions discussed above).

The problem of the description of the disorder has not yet been satisfactorily solved[12]. Solid state physics should ideally be able to predict the properties of a solid, given the kinds and numbers of atoms constituting the solid. In the case of crystalline solids this can be done in many cases quite satisfactorily; in the case of an

function outlined below is not applicable to this type of disorder.

The atomic structure of a perfect crystal is easily described by defining a unit cell containing a small number of atoms (2 atoms in case of Fig. 2.2.b) and giving the elementary lattice vectors R_1 and R_2 through which the unit cell has to be translated to obtain the whole crystal. This approach is not possible in the case of a non-crystalline solid as there is no simple pattern which could be repeated exactly to obtain the whole non-crystalline solid of macroscopic dimensions. The disorder has to be described by some statistical entity which gives an "average" of the atomic arrangement. An example of a statistical function giving the probability of finding an atom A in a sperical shell of a radius r and thickness dr around an atom B placed in the centre of the shell is the radial distribution function[11]. For a solid containing one kind of atom, only one radial distribution function ϱ_{AA} exists, but for a solid containing n components one can define n^2 functions describing the distribution of atoms of kind k around an atom of kind l, where $1 \leq k \leq n$, $1 \leq l \leq n$ (e.g. in the case of a binary alloy AB four radial distribution functions are in general required: ϱ_{AA}, ϱ_{AB}, ϱ_{BA}, ϱ_{BB}). A set of radial distribution functions does not give a complete statistical description of the disorder. Additional information can be given in terms of the distribution functions for bond angles between various atoms. Correlation functions of order $n > 2$ can be introduced, giving the probability of n atoms being in a particular position (for $n = 2$ this reduces to the pair correlation functions discussed above).

The problem of the description of the disorder has not yet been satisfactorily solved[12]. Solid state physics should ideally be able to predict the properties of a solid, given the kinds and numbers of atoms constituting the solid. In the case of crystalline solids this can be done in many cases quite satisfactorily; in the case of an

amorphous solids we do not know even how to predict and describe the structure of the substance satisfactorily. This is an indication of the size of the problems awaiting solution in amorphous solid state physics.

Let us consider a specific example of a radial distribution function for silicon (Fig. 2.3) and discuss in some detail the interpretation of the differences between the radial distribution function of amorphous silicon (full line) and crystalline silicon (dashed line). Theoreticaly (at absolute zero) the radial distribution function in a crystal should be a series of sharp lines at the values of r corresponding to the distances between atoms, r_1, r_2, r_3 ... However, due to the thermal vibrations of the atoms at finite temperatures (Debye-Waller factor) the lines are broadened to a great extent. In fact, the curves for the crystalline and amorphous modifications of silicon do not differ markedly for the values of r smaller than the third nearest neighbour distance and this means that the structural disorder becomes greater than the "thermal" disorder only at distances greater than the third nearest neighbour distance. The peaks in the radial distribution function give the most probable spacing between atoms and the areas underneath the peaks give the numbers of neighbours at the particular distances. Fig. 2.3 indicates that the short range order in amorphous silicon does not markedly differ from the short range order in crystalline silicon. This, together with the observation that the electronic and optical properties of the two modifications of silicon do not differ drastically leads to the conjecture that it is the short range order which is important for the electronic and optical properties of semiconductors. Hill[13] points out that in most cases the category (metal, semiconductor, insulator) is preserved on transformation from the crystalline form to the amorphous form. This is of importance for the calculation of the electron energy spectrum in amorphous solid (section 2.1.3.1). The lack of long range order in the case of amorphous silicon can then be considered as a perturbation in a

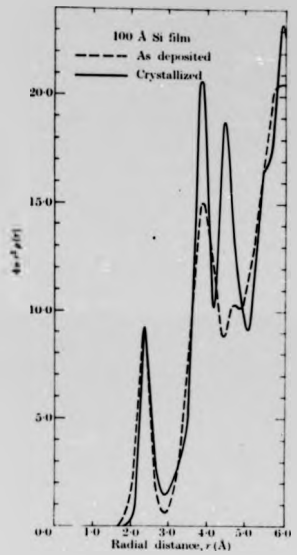

FIG. 2.3.

RADIAL DISTRIBUTION OF ATOMS IN SILICON

After Moss and Graczyk, ref. 8.

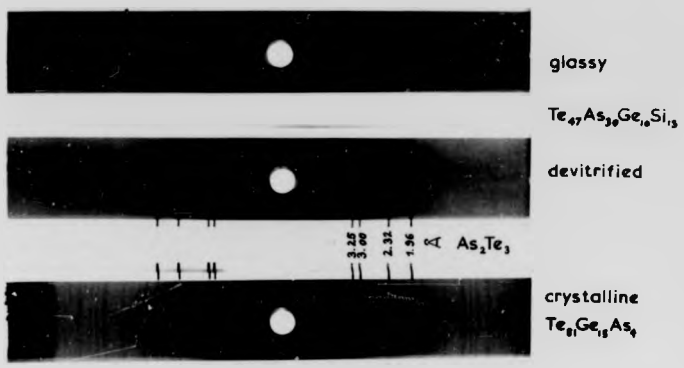

FIG. 2.4.

X-RAY POWDER PATTERNS OF CHALCOGENIDE ALLOYS.

method of calculating the properties from the local atomic arrangement. It should be noted, however, that certain substances (e.g. Ge Te) exist in amorphous and crystalline modifications the short range order of which is completely different[14]. (Such substances are therefore of interest because their study can also contribute to the realization of the role which short range order plays in the properties of an amorphous solid.)

As there is a close correspondence between the radial distribution function of a solid and its diffraction pattern (x-ray, electron, or neutron diffraction patterns) it is relatively easy to determine the radial distribution function from the diffraction data (by taking the Fourier transform of the intensity of the diffracted beam as a function of the diffraction angle[11]) or to judge the degree of order in the solid just from the appearance of the diffraction pattern. In Fig. 2.4 there are three examples of an x-ray powder (or Debye-Scherer method) of chalcogenide alloys with various degree of disorder.

Note: The powder x-ray test is a fast procedure which can be used as a routine check for amorphousness. Unfortunately there is a fundamental limit of resolution in this method, very small crystallites present in the non-crystalline material will not be detected by this method[15] and radiation with a shorter wavelength has to be used (e.g. high energy electrons). (We may mention in this context that a fast test for amorphousness which can give a rough guide about the state of the solid is the mechanical fracture test. The appearance of the fracture surface gives an indication of the degree of crystallinity (glass : conchoidal fracture surface, crystal : usually much more ductile, fracture surface reveals grains of crystals)).

In recent years another "experimental" approach for determining the structure of an amorphous solid was employed[3,16]. This involves postulating a structural unit of the amorphous solid (e.g. tetrahedron of Ge atoms in case of Ge) and postulating the way in which to construct the

method of calculating the properties from the local atomic arrangement. It should be noted, however, that certain substances (e.g. Ge Te) exist in amorphous and crystalline modifications the short range order of which is completely different[14]. (Such substances are therefore of interest because their study can also contribute to the realization of the role which short range order plays in the properties of an amorphous solid.)

As there is a close correspondence between the radial distribution function of a solid and its diffraction pattern (x-ray, electron, or neutron diffraction patterns) it is relatively easy to determine the radial distribution function from the diffraction data (by taking the Fourier transform of the intensity of the diffracted beam as a function of the diffraction angle[11]) or to judge the degree of order in the solid just from the appearance of the diffraction pattern. In Fig. 2.4 there are three examples of an x-ray powder (or Debye-Scherer method) of chalcogenide alloys with various degree of disorder.

Note: The powder x-ray test is a fast procedure which can be used as a routine check for amorphousness. Unfortunately there is a fundamental limit of resolution in this method, very small crystallites present in the non-crystalline material will not be detected by this method[15] and radiation with a shorter wavelength has to be used (e.g. high energy electrons). (We may mention in this context that a fast test for amorphousness which can give a rough guide about the state of the solid is the mechanical fracture test. The appearance of the fracture surface gives an indication of the degree of crystallinity (glass : conchoidal fracture surface, crystal : usually much more ductile, fracture surface reveals grains of crystals)).

In recent years another "experimental" approach for determining the structure of an amorphous solid was employed[3,16]. This involves postulating a structural unit of the amorphous solid (e.g. tetrahedron of Ge atoms in case of Ge) and postulating the way in which to construct the

solid using the structural units; then the "experiment" is undertaken in which it is investigated whether the solid can really be built in the postulated way without breaking the original assumptions. If it can be done then it is plausible to assume that the postulated structure corresponds to the real structure. This assumption can be further tested by measuring the radial distribution function for the model and comparing it with one for the real substance. Polk[3] built a model of amorphous germanium using plastic rods and joints* containing 440 tetrahedral units ($z_1 = 4$) and allowed a small variation in the bond length ($r_1 = 3$ cm) and variation in the tetragonal bond angle and rotation about bonds. He was able to complete the model (~1 m in diameter) without breaking the original assumptions. He also measured the radial distribution function for the model (by cathetometer) which agreed reasonably with the one for amorphous germanium. This supports the applicability of random network hypothesis to amorphous germanium in contradiction with the observations made by Rudee[1]. However, Polk's approach, when perfected may give a new method of the investigation of structure of amorphous solids. Similar approach was used by Grigorovici and Manaila[16] who used a new concept of the amorphon - a cluster of several tens of atoms regularly arranged but having 5-fold non-crystallographic symmetry. Computer simulation of the atomic arrangements in amorphous silicon and germanium was done by Henderson and Herman and others[17].

2.1.2 Glass Formation and Thermodynamic Properties

There are several ways in which the answer to the question whether a given substance will form an amorphous modification (under given experimental conditions) can be attempted.

In the preceding section some points concerning the concept of disorder were reviewed; the considerations of the structure are obviously one way in which to predict whether a given substance will form an amorphous

* manufactured by Rinco Instruments, Greenville, Illinois.

modification. If an amorphous network can be "built" by using a postulated structural unit in a certain way (both the unit and the way plausible from the chemical point of view) then there is a reason to believe that the substance will, in fact, form an amorphous modification. This approach has been succesfully applied to oxide glasses by Zacharaisen[2] and more recently invoked again, as mentioned in the last section, and applied to semiconducting materials. There are special cases of this approach; in some glasses (e.g. chalcogenide glasses) the atoms tend to form well defined molecular groups ((6) for silicate glasses) and the structural approach proceeds with consideration of the possible interaction between the molecular units. This interaction will to a certain extent depend on the kinetic processes during melt quenching which are investigated by the kinetic theory of glass formation discussed in a greater detail below.

The structural approach thus looks at the geometrical arrangement of atoms and assumes that the question of glass formation can be answered considering solely this arrangement, bond type and bond strength in the elementary unit. An approach which does not look at a static situation but considers the time development of the structure of the substance being formed by melt quenching is qualitatively opposed to the structural approach and is called the kinetic approach. The kinetic theory of the formation of amorphous substances has been so far developed only for the case in which a liquid is cooled at a certain rate to produce a glass and has not been applied to the case of preparation by evaporation or by other means (see also Chapter 4). The theory enables one to find the condition for crystallization of a supercooled liquid. Turnbull and Cohen[18] found under certain assumption the criterion

$$G < 30\ RT_m \qquad (2.1)$$

where G is the activation energy for nucleation of crystallites or their growth, T_m is the melting temperature and R is the universal gas constant.

In order to obtain the criterion for glass formation the inequality sign in (2.1) is reversed. The activation energy G has to be related to the activation energies involved in the construction of a crystalline particle inside a solidifying liquid by the process of mass transfer. If the inequality (2.1) does not hold then glass formation is to be expected.

In practice the glass formation region of a particular system is predicted by using an empirical diagram giving the glass forming regions as a function of composition. Fig. 2.5 shows such a diagram for the ternary glass Ge-Te-As[19,20]. Such diagrams are sometimes incorrectly called phase diagrams in analogy with the phase diagrams for crystalline alloys. The latter are well defined in the thermodynamic sense as the crystalline phases are in thermodynamic equilibrium at all temperatures whereas the glassy phase is a non-equilibrium phase. One consequence of this fact is the dependence of the size of the glass forming regions on the rate of cooling, the greater is the rate of cooling the greater the region of glass formation will be.

One of the most important features of amorphous solids is the dependence of their properties and behaviour on the previous treatment of the solid. The reason for this can be intuitively seen by making reference to Fig. 2.6 which schematically shows the changes in volume of a substance when cooled from the liquid state. The structure of a liquid is an equilibrium one and follows quickly changes in temperature (small relaxation time), region AA' in Fig. 2.6. On cooling the substance at some finite rate, at some temperature T_2 the changes in structure start to lag behind the changes in temperature and the structure ceases to be an equilibrium one. This temperature T_2 is the upper limit of the glass transition region. In the region of glass transition a non-equilibrium change in structure takes place. Below some temperature T_1 the relaxation times become so large that the structure practically stops changing. Below T_1 (lower limit of

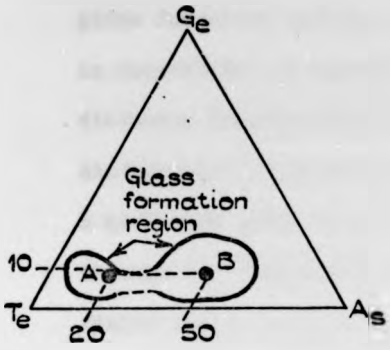

A : memory glass $Ge_{10}Te_{70}As_{20}$
B : threshold glass $Ge_{10}Te_{40}As_{50}$

Fig. 2.5.

GLASS FORMATION REGIONS OF THE TERNARY CHALCOGENIDE SYSTEM Ge-Te-As.
(after Matsushita et.al, ref. 19).

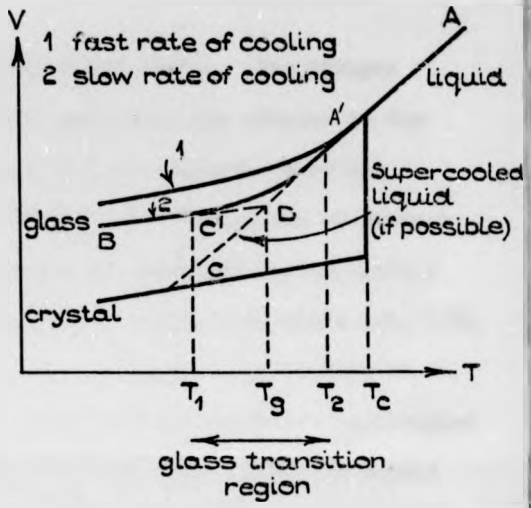

Fig. 2.6.

CHANGES IN SPECIFIC VOLUME DURING GLASS FORMATION.

Fig. 2.7.

DTA CURVE OF $Ge_{18}Te_{82}Sb_2$
(after Fritzsche and Ovshinsky ref. 32).

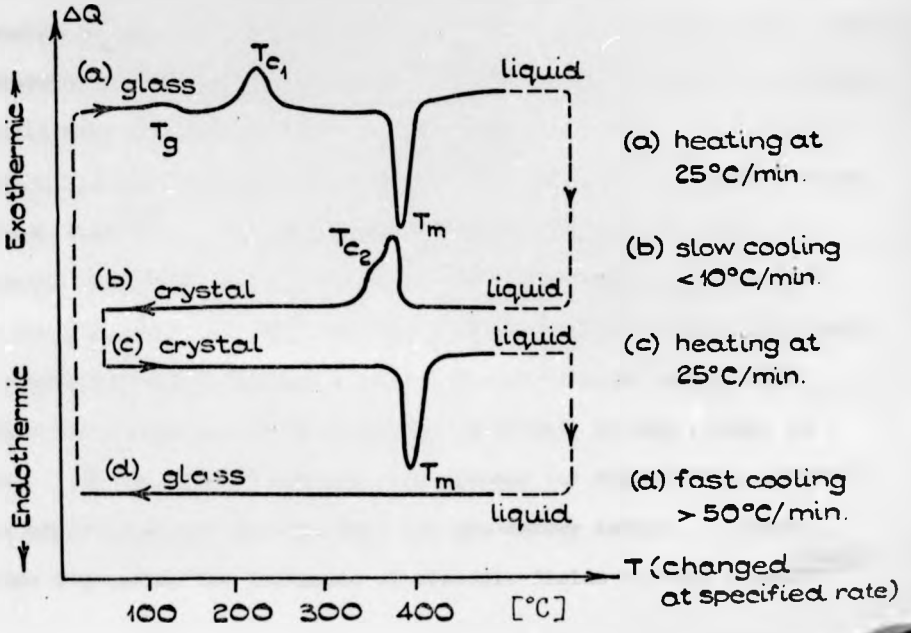

glass formation region) the substance is in solid state. The changes in properties are associated in this region only with the changes in the distances between atoms (section C'B), not with the changes in mutual distribution of atoms as in the liquid state (therefore C'B has in general a different slope than AA'). As the changes in structure during cooling through the temperatures in the glass transition region take place only with finite speed, at higher rates of cooling the structure of glass will be further from equilibrium represented by the metastable state of supercooled liquid (section DC). The properties of the glass will therefore depend on the rate of cooling w, in particular the glass transition temperature Tg (for definition see Fig. 2.6) will change (increase) with (increasing) rate of cooling. An empirical formula for glasses

$$\frac{1}{Tg} = \text{const}_1 - \text{const}_2 \ln w \qquad (2.2)$$

relates the glass transition temperature Tg to the rate of melt quenching w.

If the glass is heated at sufficiently high temperature T such that $RT \geq G$ a change in the structure of the glass will start to occur and at sufficiently high temperature the glass may crystallize. This is important industrially in producing glass-ceramics by controlled nucleation and growth.

Recently a considerable interest has been aroused in the possibility of crystallizing certain amorphous phases under the influence of electric field and/or strong illumination by light[21,24] and in some cases also by an electron beam[25]. In conventional glasses this effect would have considerable importance in the production of strong composite materials because the direction of growth of the crystalline phase can be influenced by the electric field to produce needle-like crystallites which would strengthen the glassy matrix considerably (similarly as steel wires in concrete). In the case of chalcogenide glasses the effect of an electric field on crystallization is important for the memory action. General references concerning the influence of electric fields on mass transfer

are given in (26 - 30).

Experiments by Feinleib et al[21] suggest that the crystallization of chalcogenide glasses is accelerated enormously by the production of non-equilibrium carriers photo-excited by the action of laser beam. As non-equilibrium carriers are expected to be present in the switching devices during the on-state (according to the theories reviewed in section 2.2.2), the explanation by Feinleib would also account for the fast switching memory action. The transformation of the amorphous phase by the action of light or electron beam has an important potential application in information storage[31].

The most widely used technique for the investigation of the structural changes in glass during heating is differential thermal analysis (DTA). By this technique small changes ΔQ in the heat content of a small quantity of the tested material due to the latent heats associated with various structural changes occurring during the temperature change can be detected. Fig. 2.5 shows DTA curves for $Te_{82}\ Ge_{16}\ Sb_2$ memory chalcogenide glass[32]. Curve (a) corresponds to heating of a glassy form of the chalcogenide alloy, showing first structural relaxations at T_g followed by crystallization at T_c and melting at T_m. If the liquid alloy is cooled very slowly (curve (b)), crystallization will occur at Tc; on the other hand fast cooling (curve (d)) prevents crystallization and the subsequent test (a) reveals that the solid was in glassy state.

For materials which cannot be prepared by melt quenching (e.g. amorphous Ge, Si) because the structure of the liquid ($z_1 = 6$) is vastly different from that of solid ($z_1 = 4$), and are therefore prepared by atom deposition the rate of quenching w is difficult to define and, what is more important, we cannot speak of a "frozen-in" structure of a liquid as there is no collective interaction between atoms in the volume as is the case during preparation of glass by melt cooling. Therefore the meaning of the glass

transition temperature (if there is any) is not the same in these thin film materials as in glasses.

If a glass is heated to some temperature $T<Tc$ and then kept at this temperature, the properties of the glass will change with time as the structure of the glass will tend to some equilibrium configuration (The speed with which this occurs depends on the temperature and in some cases can be represented by relaxation times). It has been shown (33) that an isolated system whose properties change with time at a constant temperature T and a constant pressure p has to be described by the thermodynamics of non-equilibrium processes. It can be shown that in certain cases the non-equilibrium properties of a glassy system can be described by an equation of state which includes additional "inner parameters". The equation of state given by the "equilibrium" thermodynamics

$$f(p,V,T) = 0 \qquad (2.3)$$

is thus modified by the inclusion of additional parameters $Q_i(t)$

$$f(p,V,T_{ph};\ Q_1,Q_2 \ldots) = 0 \qquad (2.4)$$

where T_{ph} is the phenomenological temperature. The number of the inner parameters may, theoretically, be infinite and they also can be interlinked by additional relationships. In most practical cases, however, one or two inner parameters usually suffice to account for the behaviour of the glassy system. They may be identified with the glass transition temperature or other quantities (concentrations of frozen-in point defects, ordering parameter, fictive temperature). The description of amorphous solids by non-equilibrium thermodynamics still remains to be developed. For this a general improvement in understanding of the structural relaxation processes is required (relaxation analysis[33]). Duwez and Tsuei[34] quote certain relaxation times for the structural changes in chalcogenide glass $Te_{70}\ Cu_{25}\ Au_5$. To warrant resistance against pronounced ageing the

relaxation times at room temperature have to be practically infinite, but if fast changes are required at moderately high temperatures to allow for memory effects the relaxation times must be sufficiently short at these temperatures. Duwez and Tsuei estimate for the above glass $\tau(20^{\circ}C) = 4$ years; $\tau(89^{\circ}C) = 20$ minutes.

2.1.3 Semiconductivity

2.1.3.1 Electron Energy Spectrum

The classification of solids into metals, semiconductors and insulators has been possible on the basis of the electron energy band theory. This theory depends heavily on the presence of the periodicity in the atomic arrangement of solids and is therefore, strictly speaking, applicable only to crystalline solids. Nevertheless, the absence of a satisfactory theory for the electron energy spectrum in a general amorphous solid makes the band theory useful as a starting point for various conjectures which are necessary at present for the development of the theory for non-crystalline solids.

Following Slater[35] it can be illustrated how intimately are connected the most important features of the solution of the one-electron Schrödinger equation for a crystalline solid with the periodicity in the structure of the solid. Introducing the translation operators $T(\underline{R})$ defined for each lattice vector $\underline{R}$ (see Fig. 2.1.b) by the relation

$$T(\underline{R})\, f(\underline{r}) = f(\underline{r} + \underline{R}) \qquad (2.5)$$

where f is any function of position, we investigate their basic properties. Firstly, these operators commute with each other because translation through a number of lattice vectors does not depend on the order in which the individual translations are carried out. Secondly, the translation operators commute with the one electron Hamiltonian

$$H = -\frac{\hbar^2}{2m}\nabla^2 + V(\underline{r}) \qquad (2.6)$$

because H is the same for any cell so that operating by H and translating by $T(\underline{R})$ is the same thing as translating by $T(\underline{R})$ and then operating by H.

The eigenfunction ψ of the operator $T(\underline{R})$ satisfies the relation

$$T(\underline{R})\psi(\underline{r}) = \psi(\underline{r} + \underline{R}) = \lambda(\underline{R})\psi(\underline{r}) \tag{2.7}$$

If (2.7) is multiplied by its complex conjugate the resultant condition

$$|\psi(\underline{r} + \underline{R})|^2 = |\lambda(R)|^2 \, |\psi(r)|^2 \tag{2.8}$$

demands that $\lambda(R)$ is a complex number of modulus unity: $\lambda(R) = e^{i\theta(R)}$ (2.8a)

since the electron distribution determines in part the potential $V(r)$ in which the electrons move and for consistency it is necessary that the electron distributions have the same periodicity as the potential.

Now let two translation operators, say $T(\underline{R}_i)$ and $T(\underline{R}_j)$ act in succession. This translation is equivalent to that produced by the single operator $T(\underline{R}_i + \underline{R}_j)$:

$$\begin{aligned} T(\underline{R}_i)T(\underline{R}_j)\psi(\underline{r}) = \psi(r + R_j + R_i) &= \lambda(\underline{R}_j)\lambda(\underline{R}_i)\psi(\underline{r}) \\ &= \lambda(\underline{R}_j + \underline{R}_i)\psi(\underline{r}) \end{aligned} \tag{2.9}$$

which means that the product of the eigenvalues corresponding to different displacements must be equal to the eigenvalue of the combined translation. This condition will be satisfied if

$$\theta(\underline{R}) = \underline{k} \cdot \underline{R} \tag{2.10}$$

where $\underline{k}$ is an arbitrary vector that is the same for each of the operations. The wave function of an electron in a periodic field is characterized by the particular vector $\underline{k}$ which appears in the eigenvalue of each translation and the vector $\underline{k}$ is generally written as a subscript on ψ. It can be shown that in order to get all different solutions of the eigenvalue problem it suffices to consider vectors $\underline{k}$ restricted to a finite volume in the reciprocal space which is called the Brillouin zone. Furthermore, by applying Born-von-Karman boundary conditions it is possible to show that for finite crystals of volume V the vector $\underline{k}$ changes in the Brillouin zone quasi-continuously by small steps of the order $2\pi/V^{1/3}$.

Combining (2.10) and (2.8a) and (2.7) we have the Bloch theorem[36]

$$\psi_{\underline{k}}(\underline{r} + \underline{R}) = e^{i\underline{k}\underline{R}}\psi_{\underline{k}}(\underline{r}) \tag{2.11}$$

which may be rewritten in the form

$$\psi_k(\underline{r}) = e^{i\underline{k}\underline{r}}\, u_{\underline{k}}(\underline{r}) \tag{2.12}$$

where $u_{\underline{k}}(\underline{r})$ is periodic in the lattice because

$$\psi_{\underline{k}}(\underline{r} + \underline{R}) = e^{ik(\underline{R} + \underline{r})}\; u_{\underline{k}}(\underline{r} + \underline{R}) = e^{i\underline{k}\underline{R}}\left[e^{i\underline{k}\,\underline{r}}\, u_{\underline{k}}(\underline{r})\right].$$

(2.12) gives the general form of the eigenfunctions of the translation operators. Now as the translation operators commute with the Hamiltonian, functions given by (2.12) are also the eigenfunctions of the Hamiltonian. The functions $u_{\underline{k}}(\underline{r})$ are determined by one of many methods of the band structure calculation.

The general form of the wavefunctions (2.12) of the one electron Hamiltonian was determined solely on the assumption of the periodicity of the crystal. Thus the assumption of periodicity is seen to be very powerful. In the case of an amorphous solid the one electron potential $V(\underline{r})$ will generally change on the translation through a "lattice" vector $\underline{R}$.

$$V(\underline{r}) \neq V(\underline{r} + \underline{R}) \tag{2.13}$$

If we denote by $f_{\underline{r}}$ the result of ~~acting of~~ the one electron Hamiltonian $H(\underline{r})$ acting on a function f and investigate the commutation of the translation operator $T(\underline{R})$ with the Hamiltonian we have

$$T(\underline{R})H(\underline{r})f(\underline{r}) = T(\underline{R})f_{\underline{r}}(\underline{r}) = f_{\underline{r}+\underline{R}}(\underline{r} + \underline{R}) \tag{2.14a}$$

and

$$H(\underline{r})T(\underline{R})f(\underline{r}) = H(\underline{r})f(\underline{r} + \underline{R}) = f_{\underline{r}}(\underline{r} + \underline{R}) \tag{2.14b}$$

which means that the operators do not commute since $f_{\underline{r}+\underline{R}} \neq f_{\underline{r}}$ in view of (2.13). Therefore $T(\underline{R})$ and H do not have simultaneous eigenfunctions and nothing can be said about the nature of the one-electron wavefunctions using the approach for the case of a crystalline solid outlined above.

The main consequence of the lack of spatial periodicity in general amorphous solid is that the wave vector $\underline{k}$ is no longer a good quantum number for the electron state in general amorphous solid. In the situation where the potential (2.13) is weak (or can be transformed into a weak

pseudopotential) the scattering of the electrons states will also be weak and moving electrons will have a large mean free path L so that $kL \gg 1$ and $\underline{k}$ is still a good quantum number. This is the case in most liquid metals, and in the conduction band of liquid rare gases where the valence electrons are nearly free and no strong band gap is produced. The theory for this case was developed by Ziman[32] and was relatively very successful.

However, if in a liquid or amorphous material the atomic potential is strong to produce a band gap, or any large deviation from the free electron form, then it must give strong scattering and a short mean free path ($kL \sim 1$) (Mott[38]). This is so for the carriers in most amorphous and liquid semiconductors and the development of concepts of the theory for these substances started only in recent years. The reason for this is that one is called upon to predict the wavefunctions of electrons moving in a spatially non-periodic potential with wells of random depth and even this is an idealized situation. In practice there may be further complications in that materials designated as amorphous by various physical tests may contain small regions which are ordered and/or different composition. Such structures would be difficult to detect but would strongly influence the conduction[39].

Most approaches to date have started with the standard band theory of crystalline solids as the zero approximation and have applied perturbation theory to this model, the perturbation taking the form of annihilating the long-range order, say over a few atomic spacings, whilst maintaining the short range order. Klima and co-workers[40] from the Bristol school used an alternative approach in which a certain disordered structure is approximated by a cluster of atoms and scattering theory is used to study the electron states. One of the difficulties in this approach is that the number of atoms in the cluster has to be very large to obtain results comparable with experiment. It may be possible, as the theoretical

research in this field goes on, that a satisfactory method will be found in which the two approaches are brought together and in which the short range order is given by a cluster of a small number of atoms and the surroundings of the cluster is approximated by some "averaged" background determined by the first approach (connected band theory and chemical band theory[41]).

A review of the present theoretical ideas concerning amorphous semiconductors is given in (39), including approaches due to Cohen[42] Mott-Anderson[43] and Gubanov[44]. Although the three approaches are in some ways quite different they have a unifying feature in the results they predict. The novel universal feature of the electron energy spectrum of non-crystalline solids is the existance of a quasi-continuous range of energies for which the electron states are all localized. The theories differ in the origin of the localized states and the features of the band structure vary accordingly. Cohen et al consider the fluctuations of the density of atoms as the main origin of the localized states and predict that "tails" of localized states will extend well into the original band gap of the crystal (see Fig. 2.8) so that they overlap at the centre of the gap. The density of states at the Fermi level is estimated to be $10^{19} - 10^{20}$ cm^{-3} eV^{-1}. At a finite temperature localized states within kT of the Fermi level will be ionized and will give rise to charged traps. At room temperature their concentration is estimated at $10^{18} - 10^{19}$ cm^{-3}. Anderson-Mott model associates the origin in the localized states with the random variation in the strength of the one-electron potential wells which are assumed in the first approximation to be regularly spaced whereas Gubanov considers the spatial variation of the position of atomic wells more important than the variation in strength of the potential.

The model of Mott favours a band of localized states at the Fermi level rather than the featureless tails of the Cohen's model[42]. The concepts of the electron energy spectrum in amorphous solids are so far

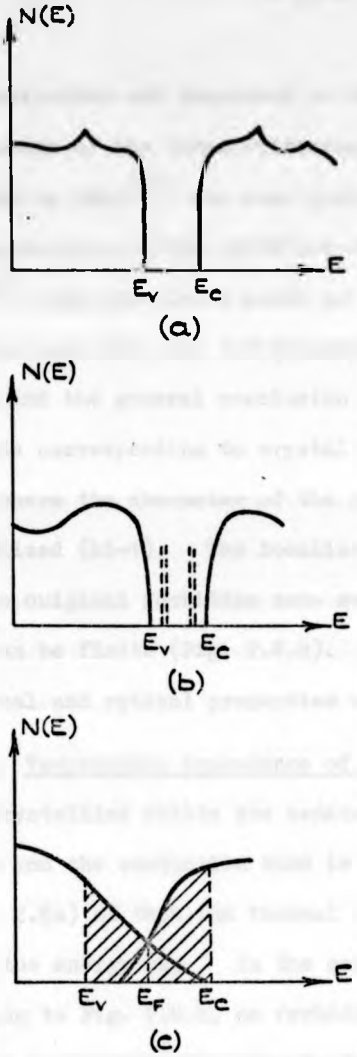

Fig.2.8.

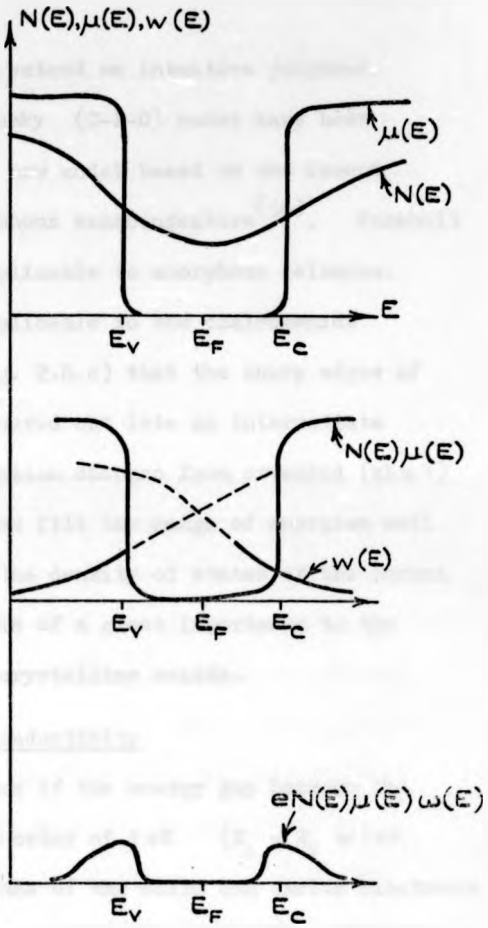

Fig.2.9.

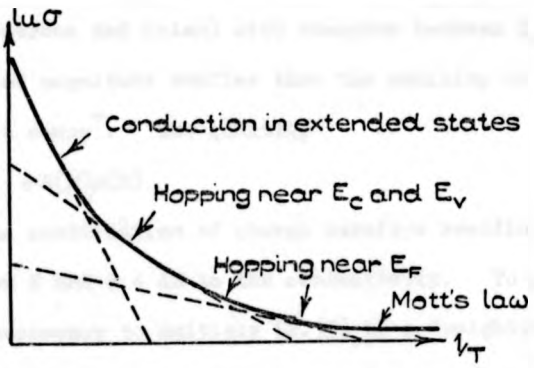

Fig.2.10.

SCHEMATIC PLOT OF $\ln\sigma$ VS $1/T$.

only qualitative and dependent to a large extend on intuitive judgment. Improvements of the Cohen-Fritzsche-Ovshinsky (C-F-O) model have been suggested by Böer[45] who also proposed a new model based on the recent findings concerning the structure of amorphous semiconductors[46]. Marshall et al[47] show that C-F-O model is not applicable to amorphous Selenium. We assume here that the C-F-O model is applicable to the chalcogenide glasses and the general conclusion is (Fig. 2.8.c) that the sharp edges of the bands corresponding to crystal are smeared out into an intermediate region where the character of the wavefunction changes from extended ($kL \gg 1$) to localized ($kL \sim 1$). The localized states fill the range of energies well into the original forbidden zone so that the density of states at the Ferrmi level can be finite (Fig. 2.8.c). This is of a great importance to the electrical and optical properties of non-crystalline solids.

2.1.3.2 Temperature Dependence of d.c. Conductivity

Crystalline solids are semiconductors if the energy gap between the valence and the conduction band is of the order of 1 eV. ($E_c - E_v \approx 1$ eV in Fig. 2.8a) so that the thermal vibrations of the solid can excite electrons across the energy gap. In the case of an amorphous semiconductor there is, according to Fig. 2.8.c, no forbidden range of energies; the experimentally observed semiconductivity has to be interpreted quite differently from the crystalline semiconductivity. It is expected that the mobility of the charge carriers (electrons and holes) with energies between E_v and E_c is two or three orders of magnitude smaller than the mobility of carriers with energies outside this range*. The quantity

$$e N(E) \mu(E) \qquad (2.15)$$

is the measure of the contribution of charge carriers residing in states with energies between E and E + dE to the conductivity. To get the total conductivity it is necessary to multiply (2.15) by a "weighting" function[48], which in the case of carriers whose wave vector is $k \gtrsim 1/L$ is $-kT\partial f(E,T)/\partial E$,

* P.N. Butcher[48] suggests discarding the term "energy dependent mobility" in favour of "energy dependent diffusivity".

where f(E,T) is the Fermi-Dirac function, and to integrate the product over all energies. The quantity (2.15) and the "weighting" function at some temperature T > 0 are drawn schematically in Fig. 2.7.b as a function of energy. The result of integration, (if it is assumed that $\mu(E)$ does not depend on temperature and that f(E,T) can be replaced by the Boltzman function),

$$\sigma(T) = \sigma_o \exp(-{}^{(E_c-E_v)}/_{2kT}) \qquad (2.16)$$

is analogous to crystalline semiconductors as the quantities in Fig. 2.7.b have similar dependence on energy as in the case of the crystalline semiconductor, albeit for different reasons. In the case of a crystalline semiconductor the function N(E) has a sharp fall-off at the energies E_v and E_c; in the case of an amorphous solid the density of states does not change markedly and it is the mobility dependence on energy which produces the sharp drop in the quantity (2.15) in the region of energies between E_v and E_c. The region is therefore referred to as the mobility gap.

A more rigorous analysis than the one presented here reveals that the activation energy $(E_c - E_v)/2$ in (2.16) changes slightly with temperature. At low temperatures the conduction by the carriers in the extended states ($E > E_c$, $E < E_v$) may be less significant than the conduction by the carriers in the localized states near E_F. This latter will have a different activation energy and a different pre-exponential factor than those in (2.16) and also at very low temperatures the argument of the exponential function will be replaced by - const $(T)^{1/4}$ [38]. Thus over a large temperature range the plot of $\ln\sigma$ against 1/T is expected to have variable slope with more or less pronounced breaks in the slope (Fig. 2.10) at the temperatures at which the dominant conduction mechanism changes. The behaviour shown schematically in Fig. 2.10 was observed in many amorphous semiconductors. In the case of chalcogenide glasses measurements by Hulls[49] and Croitoru et al[50] may serve as examples.

2.1.3.3 Non-Ohmic Conduction in Strong Fields

At sufficiently high fields ($\geq 10^4$ V/cm) it can be observed in many cases that the current flowing through an amorphous semiconductor at a constant ambient temperature increases more rapidly than the applied field (as indeed it does in many crystalline materials). The interpretation of the results obtained by the measurements is difficult because there is a great uncertainty about the distribution of trapping centres which will influence the conduction in thin layers and in thick layers the effects of Joule heating are difficult to exclude[51]. Furthermore, there is evidence (49,52) that structural inhomogenieties present in amorphous semiconductors influence the field dependence of conductivity. As the structure of (especially thin film) amorphous semiconductors is dependent on the preparation conditions[128], the correlation between measurements made in different laboratories is not an easy task. In (53) it is argued that our present knowledge of detailed microscopic processes in amorphous semiconductors is insufficient to permit their unambiguous identification from I - V characteristics.

There are many examples in the literature of a linear relationship between the logarithm of the current and $(\text{field})^{1/2}$, some of which are mentioned in (10) together with a summary of the possible mechanisms which may be responsible for the observed behaviour. Other observations suggest an exponential dependence of conductivity on the applied field[52,54,55].

The non-ohmic effects can be divided into two groups according to whether they

(i) are bulk controlled

(ii) originate from the processes near electrodes

The significance of this division is that in the first case one can phenomenologically describe the non-ohmic behaviour in terms of field dependent conductivity whereas in the second case this is not possible.

A third effect, not considered in the above division, could be Joule heating inside the semiconductor as suggested by Thomas and Warren[56].

The classical Poole-Frenkel effect[57] belongs to the group (i) and has been used for interpretation of the non-ohmic conduction in a number of materials. Conduction in As-Te-Ge-Si glass has been interpreted in this way by several researchers[58,59]. The effect of field ionization of the weakly localized states near the extremities of the conduction and valence band was invoked by Dussel and Böer[60] and may be responsible for the rapid increase in current observed in chalcogenide glasses prior to switching[61]. The high fields close to the threshold of switching may lead to the acceleration of electrons owing to the increase in the mobility (or diffusivity) of the carriers with their energy. If the rate of increase of the kinetic energy of the carriers is faster than the rate of loss of the energy to phonons, secondary electrons may be formed and eventually an avalanche. This process has been analysed by Mott[62] and Hindley[63].

The variety of the effects which originate from the processes near the electrodes and which can cause the departure from the Ohm's law is much greater than for the processes in group (i). The quality of the electrode metal will influence the injection processes at high fields according to the value of its work function (Schottky effect). The formation of space charges, which is a likely effect in amorphous semiconductors in view of the concentration of trapping centres present, can greatly influence the non-ohmic behaviour; some references relevant to this problem are given in (63 - 67).

The non-ohmic processes near electrodes can be responsible for the initiation of the switching effect. Adam and Duchene[68], used the condition of the critical tunnelling through a potential barrier near the electrodes analysed by Tantraporn[69] as a criterion for the onset of switching in thin film devices. On the other hand single-space-charge-limited injection process is considered by Allison and Dave[70] to explain

the pre-switching characteristics of chalcogenide threshold devices while Henisch et al[96] favour double-injection process to explain the initiation of switching at low temperatures. These models are reviewed in a greater detail in section 2.2.2.

2.1.3.4 Surface Conduction

The section on semiconductivity is concluded by a few remarks on the surface conduction in chalcogenide glasses. They are meant to constitute a kind of caution against possible misinterpretation of experimental results rather than to suggest that the topic of surface conduction has an importance comparable with the importance of the effects discussed in the preceding two sections. Measurements of the conductivity, Seebeck coefficient etc. of chalcogenide glasses can be seriously distorted by the presence of a conductive "skin" on the surface of the glass[71]. Equally, certain switching experiments performed on the surface of the glass (72-76) can be effected by the surface condition.

The changes in the surface conductivity have been reported by several authors[71,77-79] and they are interpreted as the result of chemical interaction of the glass with atmospheric oxygen and water which is accelerated by elevated temperature. Heating in high vacuum does not produce the "skin"[77]. Phillips et al[79] have shown that if the surfaces of the glass are lightly abraded, with a layer of ~10μm removed, the true bulk properties of the material are retrieved.

The geometry of the switching devices used in the present work was such that the surface conduction could be of importance (see Chapter 4). However, experiments carried out in normal atmosphere at room temperature and experiments carried out in high vacuum (10^{-7} torr) at room temperature did not yield noticeably different results. It is therefore concluded that the results of the switching experiments performed were not influenced by possible surface layer of extreme properties.

2.2 Review of the Theories of Switching Effect

In section 2.1 the basic properties of amorphous materials were outlined and it could be seen that the present state of knowledge concerning these materials is by no means satisfactory. There is a great deal of uncertainty about the exact structure of amorphous semiconductors and even if the exact amorphous structure were known there is a lack of a theoretical method by which the electronic structure (required for the calculation of transport properties) could be properly calculated. Furthermore, the thermodynamic description of a non-equilibrium state has not yet been fully developed.

These shortcomings of the theory of the amorphous state are reflected in the ambiguity in the interpretation of the experimental data concerning amorphous semiconductors accumulated during the past years. The switching effect is no exception in this respect; also it is a phenomenon in which it is difficult to distinguish between thermal and electronic effects, between macroscopic and microscopic feedbacks and between cause and consequence. It is, perhaps, therefore not surprising that at present there is more than one theory claimed to be capable of explaining the switching phenomena in a single material. Additional "variety" in the theories is, of course, due to the fact that switching occurs in a large number of materials and it is unlikely that the same mechanism is responsible in all cases. The main theories of switching are outlined in the next sections. It is helpful to distinguish between models of the initiation of switching which describe mechanism by which the switching threshold is reached and between models which describe the situation in the "on"-state and possibly also the reverse "on"-"off" transition. It is not always the case that the two models are of the same nature, e.g. one can conceive of a model in which the switching transition is initiated by thermal runaway and the "on"-state is essentially non-thermal.

The experimental evidence available (80 - 82) shows always that the "on"-state is associated with the formation of a narrow conducting channel (or "filament") whatever the mechanism of switching may be; thus the theoretically predicted "on"-state must be filamentary - one of the very few common features of the various theories. The formation of the filament is apparently associated with the transition between points P_1 and P_2 on the I - V characteristic in Fig. 1.2 (ii), i.e. the negative differential resistance region of the I - V characterstic. Ridley[83] gave a general proof that all current controlled negative resistance devices have to have the filamentary character of current flow in the "on"-state.

A direct experimental observation of the filament is not possible (unless the switching experiment is performed on the surface of the material using coplanar electrodes (72-74,76), but then its character may be different from bulk filament) and indirect observations are made difficult by the small dimensions of the filament. The radius of the filament is of the order of the device thickness and for thin film devices it probably never exceeds 25 μm. This follows from the observations made by Sie et al[80] on the memory devices; they used preferential etching to reveal the morphology of the filament. Uttecht et al[81] used an infrared microscope to look at the localization of temperature rise in the "on"-state which gives a rough measure of the filament dimensions. Cholesterol ester coating which changes its colour with temperature was used by Moorjani and Feldman[82] for the same purpose. The intensity and localization of recombination radiation could be also used for the estimation of the filament volume[75,84].

A very wide range of papers has appeared on the subject of switching during the past four years; moreover, the emphasis placed on the various theories changes very rapidly as new experiments are being devised to

prove or disprove various theories. It is therefore not possible to elaborate a complete review nor it is really sensible in view of the fast changes in this field. The review of the theories of switching is divided into four sections according to the essential assumptions of the theories (another possibility would be to classify the theories according to the devices (thin-thick, chalcogenide - other materials) or experimental data (e.g. polar switching - bipolar switching, etc.)). The review is concluded by a section containing some thoughts about the special position which non-crystalline materials take in the switching effect.

2.2.1 Thermal Theory of Switching

The switching materials behave mostly as intrinsic semiconductors and their conductivity is therefore strongly increasing function of temperature (2.16). As the heat dissipated in a unit volume

$$\sigma(T)F^2 \qquad F = \text{intensity of el field} \qquad (2.18)$$

is proportional to the conductivity, a rise in the temperature results in a greater quantity of the heat generated in the volume per unit time which must be conducted away from the volume if an equilibrium is to be maintained. The rate at which the heat is conducted away from the switching material depends on the geometry and on the boundary conditions imposed. In the most simple case of a semi-infinite slab of the switching material of thickness d which faces are held at a constant ambient temperature T_d the rate of cooling per unit area of the surface will be approximately

$$\frac{K}{d}(T - T_d) \qquad T = \text{temperature inside the switching material} \qquad (2.19)$$

where K is a constant proportional to the thermal conductivity of the switching material. As the applied field is increased to a value F_1 the temperature inside the material will increase to a new value T_1 as both terms (2.18) and (2.19) have to increase. Geometrically the steady state equilibrium solution can be represented for each field F by a point

of intersection of the graphs of the quantities (2.18) and (2.19) as a function of temperature. An unstable situation will arise when the point of intersection becomes a tangent point as the graph of (2.18) changes with the parameter F, i.e. when the graphs touch each other in that point. Then for an infinitesimal change in F a finite change in T can occur as the point of contact (and hence the solution represented by that point) vanishes. The condition for such unstable situation is obtained by equating the slopes of the graphs of functions (2.18) and (2.19) (condition for the tangent point, equivalent with the requirement of a vanishing Jacobian in more general cases):

$$F^2 \frac{d\sigma}{dT} = \frac{K}{d} \tag{2.20}$$

from where the critical field is obtained

$$F_c = \left(\frac{K}{d}\Big/\frac{d\sigma}{dT}\right)^{\frac{1}{2}} \tag{2.21}$$

The relation (2.21) is the condition for the critical field F_c at which the thermal instability occurs and switching is thus initiated. In mathematical terms the field F represent the bifurcation parameter; $F = F_c$ is the bifurcation value of F at which the character of the solution changes qualitatively. The qualitative change in the solution means in physical terms a change to the filamentary type of conduction from a relatively uniform distribution of current in the "off"-state. The equations (2.18) and (2.19) cease to describe the situation accurately in the "on"-state. Moreover, in practice (2.19) does not accurately describe the heat dissipation from devices with usual geometries. If an accurate value of the critical field is required, (2.19) has to be replaced by the rigorous term

$$\nabla(K\nabla T) \tag{2.22}$$

where ∇ denotes the gradient operator and K is the thermal conductivity of the switching material. The term (2.18) also has to be modified in

cases where the assumption of a constant electric field $F = -\nabla\varphi$ is not justified; then the term (2.18) becomes

$$\sigma(T)\ (\nabla\varphi)^2 \qquad \varphi = \text{electric potential} \tag{2.23}$$

When one wishes to consider time development of the temperature profile, another term associated with the time changes in the heat stored in a unit volume of specific heat c has to be taken into account

$$-\ c\ \frac{\partial T}{\partial t} \tag{2.24}$$

Conservation of energy requires that the sum of the terms (2.22 - 2.24) be zero

$$c\ \frac{\partial T}{\partial t} = \nabla(\kappa\nabla T) + \sigma(T)(\nabla\varphi)^2 \tag{2.25}$$

This non-linear elliptic equation can give the time development of the temperature distribution in the domain of integration if the electric potential distribution and appropriate boundary conditions are specified. The potential has to satisfy the condition

$$\nabla(\sigma(T)\nabla\varphi) = 0 \tag{2.26}$$

which originates from the requirement of conservation of the electric charge[85]. As (2.26) depends on temperature T, the two equations (2.25) and (2.26) have to be considered as a system of two equations. The bifurcation parameter in this case is the potential difference $V = \varphi(\text{anode}) - \varphi(\text{cathode})$ and the potentials of the electrodes appear in the boundary conditions. The geometrical interpretation of the bifurcation becomes more complicated for the system (2.25 - 2.26); it was shown by Thom[86] that every bifurcation process can be topologically classed into one of seven categories. Bifurcation and other topological properties of a simplified system similar to (2.25) have recently been studied by Kroll and Cohen[87].

To the author's knowledge the system (2.25 - 2.26) with a set of boundary conditions which would be realistic for the case of switching has not yet been solved. The one-dimensional form of the system can only account satisfactorily for the situation before the critical point

$V = V_c$ is reached; the form of the solution for $V > V_c$ is expected to be of the filamentary type and more than one-dimensional (1-D) solutions are needed. The first considerations of the 1-D solution of the set (2.25 - 2.26) were associated with the theory of the thermal breakdown in dielectrics nearly fifty years ago (88). Although the physical principles behind the solution of (2.25-2.26) are clear, to solve the problem mathematically in a practicable way one is forced to introduce various simplifications; this explains the large number of publications on the theory of thermal breakdown which appeared during the past decades (89). In the last years of the decade 1960 - 1970 a new interest in the old theory was stimulated by the need to explain the switching effect (90). For the reasons given above in order to model satisfactorily the "on"-state using the thermal theory one needs to solve (2.25-2.26) at least in two dimensions. Results of 2-D and 3-D numerical calculations using a simplified system derived from (2.25-2.26) were published by Thomas and Male[91], Kroll and Cohen[87] and by Kaplan and Adler[92]. The general feature of these solutions seems to be, as Mott[93] points out, initial localized rise in temperature in the central region of the switching device before switching followed by a decrease and more uniform distribution of temperature; the reverse is expected if the switching is due to an electronic process; the heating effects take place after the voltage across the device has collapsed ("off"-"on" transition).

The predictions yielded by the thermal model which uses only one critical assumption - sufficiently large rise of conductivity with temperature - show a certain degree of discrepancy with the experimental observations; it is likely that some discrepancies will still exist even when the system (2.25-2.26) is resolved mathematically in complete generality. Henisch[94] points out that the thermal model gives unsatisfactory prediction of the following observations:

(i) Scaling of the critical voltage V_c with the thickness d of the device. (At low enough d predicted V_c is greater than the observed V_c).

(ii) Dependence of the critical voltage V_c on ambient temperature. (At low enough temperatures the observed V_c is lower than that predicted by the termal model.)

(iii) Delay times between the application of a voltage $V > V_c$ and the switching transition (observed shorter than those predicted).

(iv) Polarity effects at low temperatures. (The thermal model is insensitive to polarity reversal in view of the quadratic dependence in (2.23)).

(v) Systems which are known to be thermal show I - V characteristics strongly dependent on frequency, do not have a sharply defined filament and their working point can be stabilized in the negative differential resistance region. On the other hand switching I - V characteristics do not greatly depend on frequency of the applied voltage, have extremely narrow filaments and their working point cannot be stabilized in the negative diff. resistance region.

(vi) Statistical variation of switching parameters (cannot be convincingly accounted for in terms of the thermal model).

(vii) Special position of chalcogenide glasses in switching phenomenon is difficult to understand on the basis of one key requirement only - sufficiently high activation energy for d.c. conduction.

Some of the listed discrepancies, which are particularly noticeable in thin film devices, can be reconciled by allowing the conductivity of the material to depend on both the temperature and the electric field. This means admitting some electronic processes to be operative besides the thermal effects and models of this kind are reviewed in the section 2.2.3. In the next section the diametrically extreme mechanism to the thermal one is considered.

2.2.2 Electronic Theories of Switching

In the preceding section a mechanism was described in which the increase in the electrical conductivity of a semiconducting solid was caused by heating effects. In that model the phonon and electron (and hole) temperatures are equal and therefore the corresponding quasi-particles are in a thermodynamic equilibrium. The increase in conductivity is achieved by redistribution of carriers into states with greater mobility. The distribution function is assumed to depend explicitly only on temperature. This is an idealized case because as the electric field is applied to the solid by means of electrodes the injected carriers will not be in thermal equilibrium within a diffusion length off the electrodes. For small applied fields, the distribution function will not require any significant corrections due to the electric field and the thermal approximation will be satisfactory. In thick layer switching devices the magnitudes of fields attainable without inducing the thermal instability of section 2.2.1 are usually sufficiently small to warrant the self-consistancy of the assumption that the distribution function depends explicitly only on temperature. Also at large thicknesses the ratio between volumes of true bulk and the "non-bulk" regions near the electrodes is large so that the processes in the device can with a greater confidence be regarded as bulk processes at low fields and parameters of the theoretical model can be determined by measuring the bulk properties of bulk material from which the device is manufactured.

The situation is likely to change as the thickness of the switching layer is decreased to the region of tens of micrometers. The magnitude of electric fields which can be applied to the device without causing thermal instability at room temperature is reaching 10^5 V/cm. At these fields and thicknesses the manifestation of non-thermal effects becomes apparent. (The value of the electric field which can be applied to a

thick device without causing thermal instability can be increased by providing more efficient cooling to the device - hence at low temperatures the possibility of electronic effects in thick devices (few hundred micrometers) is plausible).

In these regimes the distribution of carriers in the energy states is likely to be governed by both the temperature and the electric field. It seems plausible that any non-ohmic effects (section 2.1.3.3) taking place at fields below the threshold field of (electronic) switching can constitute a precursor to the switching transition. Thus to construct an electronic model of switching it needs to be shown that

(i) the suggested electronic process is responsible for the non-ohmic effects

(ii) a current controlled positive feedback exists in the electronic mechanism and is responsible for the switching transition[95].

It was only recently that some progress was made in identifying various electronic processes responsible for the non-ohmic conduction in amorphous semiconductors and with regard to point (ii) a considerably improved understanding is necessary. Correspondingly, the degree of elaboration of the various electronic theories of switching is in many cases only qualitative at present. The uncertainty in the mechanism of charge transport processes in amorphous semiconductors is also reflected in the presence of several alternative "electronic" models put forward to explain switching in chalcogenide glasses and surviving experimental elimination. At any rate, the possibility of various mechanisms for different substances has to be, at present, admitted and also in a single device the mechanism can change with temperature[94].

Mott[96] first suggested that the potential energy of an electron in the "on"-state plotted against position across the switching layer should appear as in Fig. 2.11.d. (similarly to the case of gas discharge).

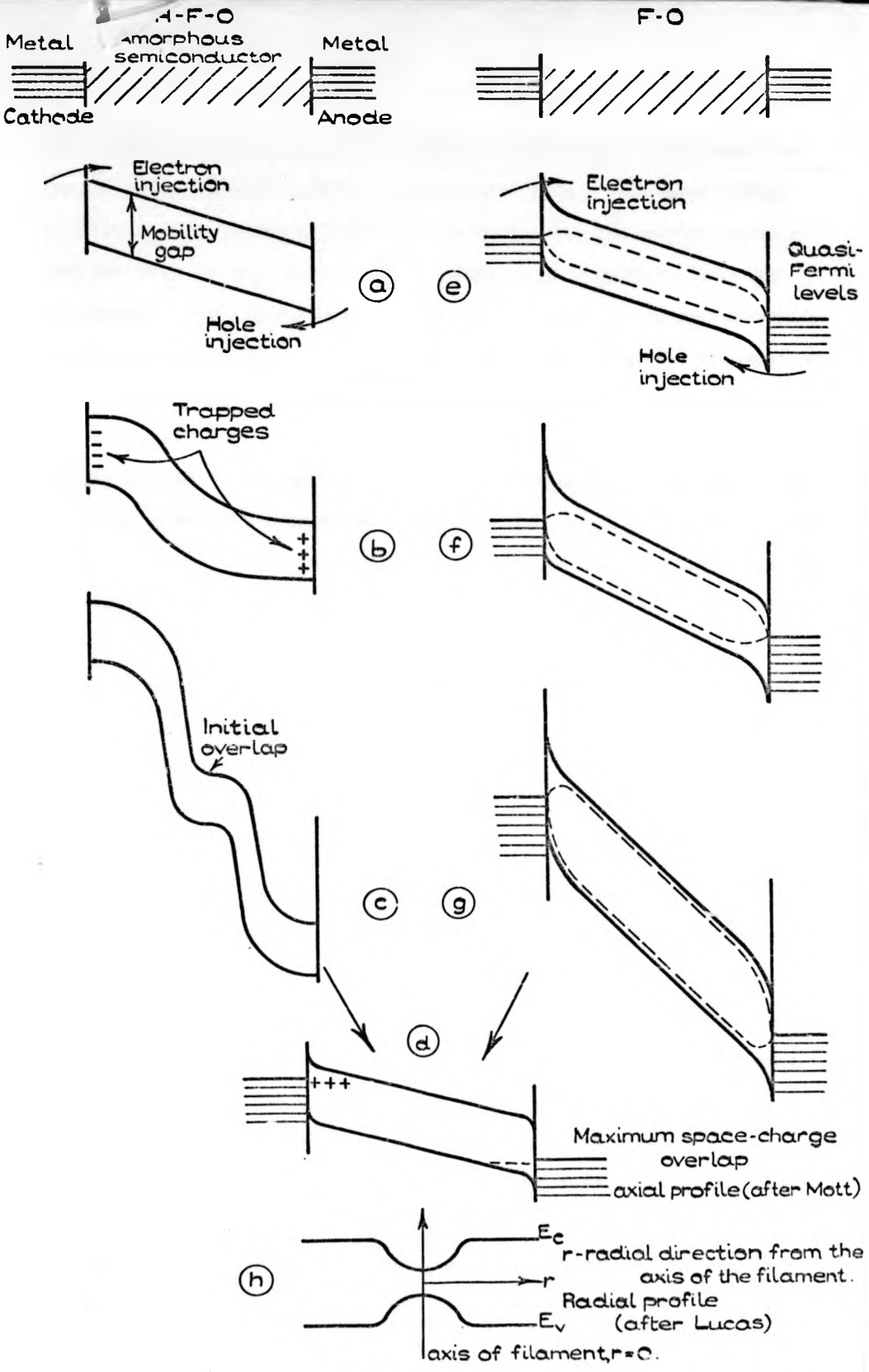
M-F-O
Metal
amorphous semiconductor
Metal
Cathode
Anode
F-O
Electron injection
Mobility gap
Hole injection
a
e
Electron injection
Quasi-Fermi levels
Hole injection
Trapped charges
b
f
Initial overlap
c
g
d
+++
Maximum space-charge overlap
axial profile (after Mott)
h
E_c
r-radial direction from the axis of the filament.
r
Radial profile (after Lucas)
E_v
axis of filament, r=0.

Fig. 2.11 a-h.

He postulates the existence of a positive trapped space charge near the cathode and a negative space charge near the anode. The space charge regions must not be too close to the electrodes so they cannot tunnel to them and also not too wide to prevent tunnelling of carriers from the electrodes. Mott shows that the conditions prevailing in most switching materials (transit time $\ll$ recombination time, small mobility for carriers in deep traps) are consistent with the proposed model in Fig. 2.11.d and also he is able to show (97) that the profile leads to a self-stabilizing holding voltage. In the central region all traps are filled and it has therefore a very low resistance. The holding voltage is practically the sum of the voltage drops across the space-charge regions; their existence can therefore explain why the holding voltage is bigger than the band gap.

The exact mechanism by which the "on"-state in Fig. 2.11.d is attained is controversial. Mott[93,98] suggests strong field emission from the electrodes into the conduction or valence bands of the glass, Zener tunnelling from the valence band into the conduction band or an electron avalanche caused by a mechanism proposed by Hindley[99] or an initiation by a thermal instability in the central region of the semiconducting film (this was first proposed by Böer et al[100] and by Owen[101]).

Certain doubts about these mechanisms as being operative were raised by the supporters of the Cohen-Fritzsche-Ovshinsky (C-F-O) model, which was discussed earlier. Adler[108] expresses the opinion that the short mean free path ≤ 10 Å of free carriers makes the impact ionization avalanche process unlikely. The rates of Zener tunnelling at fields of 10^5 V/cm would probably be smaller than that of recombinations besides the fact that such a process would not be compatible with the requirement (ii). There are also objections against the thermal instability, primarily because of the short delay times and small energies available to heat the required volume of material to a high enough temperature fast enough[102].

Henisch, Fagen and Ovshinsky (H-F-O)[94] have proposed a model for switching which makes use of the C-F-O model of the density of states (section 2.1.3.1) originally put forward to explain experimental data on the electronic and optical properties of amorphous semiconductors in bulk. The sequence of events during the formation of the "on"-state according to this model is shown in Figs. 2.11.a-c. Two space-charge systems are developed due to the trapping of injected carriers near the electrodes. Schottky barriers are assumed to be very thin, <30 Å, to prevent tunnelling from the electrodes and are omitted in Figs. 2.11.a-c). In the negative (positive) space-charge region near the cathode (anode) all electron (hole) traps are filled; with increasing applied voltage the space charge regions are assumed to grow and finally to start overlap at the centre (or close to it, depending on the similarity in electron and hole mobilities) of the layer. In the overlap region all traps effective at given temperature are filled and thus free conduction occurs in that region which has thus much lower resistivity than the rest of the specimen. This means that the electric field in the overlap region is decreased (Fig. 2.11.b) and increased fields appear across the space-charge regions. Thus the injection of carriers is increased which leads to a greater overlap of space-charges; this represents a positive feedback according to (ii) and a collapse of specimen resistance followed by space-charge reversal (Fig. 2.11.d). A semi-quantitative study of this process has been made by Lucas[103]. A trap controlled double injection process was also considered quantitatively by Bowers and Barnett[110].

Fritzsche and Ovshinsky (F-O)[104] suggested an alternative mechanism which is more likely to occur at intermediate temperatures where screening is more efficient than at low temperatures (screening length = $(kT\varepsilon/4\pi e^2 n)^{\frac{1}{2}}$ (where n is concentration of mobile charges and ε is dielectric constant) is short at high temperatures) and space charges are therefore not likely to be developed. They assume that the traps can become filled

by a process without space-charge formation by injection of carriers or by internal field ionization. The excess non-equilibrium charges which cannot condense to traps at given temperature and field are swept towards the electrodes where they form depletion layers since the anode and cathode are unable to supply the holes and electrons to maintain the non-equilibrium current. The resulting Schottky barriers grow with increasing voltage but their thickness remains in the limits permitting tunnelling ($<50\,\text{Å}$) so that ohmic contacts are maintained and injection of carriers not impeded (Fig. 2.11.e). As the injected electron and hole currents are increased a level is reached at which it is sufficient to support the non-equilibrium distribution of carriers (i.e. to keep the traps filled). This represents the conducting state; the Schottky barriers are decreased by the incoming non-equilibrium charges (Fig. 2.11.d).

The transition from the mechanism just described (F-O) to H-F-O mechanism is expected just below room temperature. Experiments in which the polarity of the applied voltage is reversed during the delay period show that the delay time is lengthened if the experiment is performed at low temperatures[51,105] and that this dependence ceases at certain temperature. This is interpreted as the transition between the H-F-O and F-O models. A change in the character of the pre-switching characteristics at this temperature also favours the idea of the transition [59,106]. At a given over-voltage $V > V_c$ the delay time to switching in both models is associated with the time necessary for the trap filling (time $\geq$ charge of traps/current)[107]. The holding current corresponds to a minimum current density necessary to keep the traps filled against the recombination process. As the number of effective traps (those which are not thermally ionized and within the filament) diminishes with increasing temperature, the minimum current density necessary to keep them filled should likewise diminish (as observed).

In both models (H-F-O and F-O) filaments are formed in the "on"-state and Fig. 2.11.d refers only to the axial direction of the filament. The conducting channel is expected to expand with increasing "on"-state current, similarly as in gas discharge. It is not known whether the constriction of the current flow into the filament is due to thermal initiation or can arise from essential plasma relationships[94]. Lucas[103] points out that the electric potential irregularities of the localized states in the mobility gap can be partially offset by the shielding action of the injected carriers. Thus the mobility edges would be altered radially as shown in Fig. 2.11.h and in the region of depression of the edges the plasma is protected against lateral diffusion. Below a certain value of the (holding) current density the bending of the edges is insufficient to protect the plasma against lateral diffusion and "on"-"off" transition occurs. To calculate this holding current density it would be necessary to consider collective electron interactions (the Anderson and Mott theory is an one-electron theory).

Electron correlation effects have been considered in a model of switching developed by Mattis[109] in which the basic assumption is that the activation energy which determines the concentration of mobile carriers decreases with increasing concentration of the carriers. Assuming further that the carrier injection takes place by Zener tunnelling, Mattis is able to show that at certain critical field the concentration of carriers sharply increases and the I - V characteristic displays a region of negative differential resistance. Similar theories of switching have been outlined by Sandomirski[111] and Iida and Hamada[112].

A completely different model of switching involving cooperative phenomena has been proposed by Drake et al[113]. By considering structural arrangements of metal ions in vitreous switching materials they show that the local environment of ions with different valencies (Cu^{+}, Cu^{2+} in the case of copper oxide glasses) are nearly identical except for polarization

of the surrounding matrix and slightly different positions of the neighbours. Assuming certain spread of energies of electrons in these states in weak electric fields ($<10^4$ V/cm) the transport is shown to take place by polaron hopping between the ion sites of different valencies. At high field strengths transport (or hopping) of electrons will be favoured into sites in which the resulting dipole moment of the metal ion centre and its environment (highly polarizable matrix) is a maximum. In the case of the copper oxide glasses the application of high fields will favour delocalization of one electron on the cuprous ion site (Cu^{2+}) thereby tending to make the Cu^+ and Cu^{2+} sites nearly identical. This is expected to occur at some sufficiently high field strength at which a cooperative rearrangement of the structure involving the shift of appropriate coordinating ions by several tenths of an Angström will effect a ferro-electric-like transition. In this new ordered state the metal ions initially present in two different valence states and in different environments have now same valence states and more nearly identical environments. This is shown to result in semimetallic highly conductive "on"-state. Drake et al do not discuss filament formation but this is probably due to some macroscopic feedback ("weak spot" or thermal effect). It is difficult to see how Drake's model could be applied to chalcogenide glasses in which chemical bonding is believed to be predominantly covalent.

2.2.3 Electrothermal Theories of Switching

Any heating present in the switching device will increase the electric fields near the electrodes because these regions will be cooler than the central region of the device. (This was first pointed out by Böer et al[100] and by Owen[101]). Thus an initial small rise in the temperature of the central region of the device may enhance the electric field at the electrodes to a degree which is sufficient to cause electronic switching originating at the electrodes by one of the mechanisms suggested by Mott[93] and

mentioned in the last section. This combined action of heating and electronic effects is an example of so-called electrothermal mechanism of switching.

A somewhat different situation arises when the conductivity of the bulk is a function of both the temperature and the intensity of the electric field. As mentioned in section 2.1.3.3 the conductivity of the bulk of the switching materials is often found to be field dependent. The Joule heating term (2.18) in the thermal model (section 2.2.1) is then replaced by

$$\sigma(T,F)F^2 \qquad (2.27)$$

and the model of switching then is electrothermal.

Some authors[114] have assumed the field dependence of conductivity in order to explain the fast switching speeds. Other authors maintain that the introduction of field dependence of conductivity is a necessary modification of the equations of the thermal model (2.25 - 2.26) if their solution is to exhibit the region of negative differential resistance[87,92]. At present there is a marked tendency in the literature (e.g. Proceedings of the 4th int. conference on amorphous and liquid semiconductors, Ann Arbor, August 1971) to favour the electrothermal model, although the field dependence is not clearly understood. Great care has to be taken to ensure that (2.27) represents true bulk heating effects if the conductivity law is derived from an experiment in which overall conductance has been measured. Further, mathematical complication arise in solving the modified system (2.25 - 2.26). The first case in which it is the field enhancement in the regions near electrodes, and only there the conductivity is assumed to be field dependent, is in many cases easier and also less ambiguous to deal with. Adam and Duchene[68] have used the assumption that strong field emission from the electrodes begins at the field

$$F_{crit} = (\text{const. } T_e)^{4/3} \qquad (2.28)$$

T_e = temperature at the electrodes

following analysis by Tantraporn[69], and by solving the one-dimensional heat equation with (2.28) as the criterion for the switching initiation were able to obtain the dependence of the threshold voltage on temperature in good agreement with experiment.

By substituting the conductivity law (2.16) into (2.21) it can easily be shown that the critical field predicted will increase with decreasing temperature without limit. McMillan and Nesvadba[115] have shown that the switching field in chalcogenide devices with layer thickness of about 200 μm in fact departs from the value predicted by the thermal model at temperatures only several tens of degrees below room temperature and tends to a certain asymptotic value. If F_{crit} in (2.28) is constant and equal to this asymptotic value then the approach of Adam and Duchene will explain the observed behaviour as shown in Chapter 3.

2.2.4 Structural Change Model of Switching

In many cases it is found that the conductivities of amorphous semiconductors increase by several orders of magnitude on crystallization. If the switching device is made using chalcogenide glass with the composition which corresponds to a point near the boundary of the glass forming region (e.g. point A in Fig. 2.5) the glass will be likely to crystallize during the operation of the switching device and a highly conductive state will persist even if the external applied field is removed. If the device can be brought back to the original highly resistive "off"-state by heating the crystallized region and quenching it quickly (applying a suitable re-set current pulse e.g. 150 mA for 6 μs) then the useful property of memory action is exhibited by the device (for characteristics see Fig. 1.2 (iv)).

The action of the set and reset pulse are interpreted in terms of slow and fast quenching of the glass (curves (b) and (d) in Fig. 2.7) and corresponding changes in the structural ordering. The structural change in a conducting channel (initially hot and then cooled relatively slowly)

on the surface has been demonstrated in several experiments[116] in which the growth of the channel originated at the anode and took place over relatively long periods of time (in some cases the growth speed was only a fraction of mm/s). Polarity effects were observed in such grown filaments - reversal of polarity caused the channel to retreat and a new filament started at the (new) anode. Thus a field dependent mass transport is evidenced in these experiments, probably due to solid state electrolysis. However, even when considering field dependence of the mass transfer, the observed speeds with which the transformations take place in thin sandwich devices are surprisingly high. It is thought that the presence of non-equilibrium carriers in the "on"-state following threshold switching action is decisive for the acceleration of the crystallization process[21]. The experiments concerning the transformation of amorphous semiconductors by laser beam lend support to this hypothesis.

It is worth mentioning that the theory of switching developed by Drake et al[113] is able to account for the memory switching just by making the additional assumption that the ferroelectric-like ordering persists when the external electric field is removed. Then the difference between memory and threshold switching is only quantitative (depending on the amount of perturbation necessary to destroy the ferroelectric ordering).

Recently a view was expressed[117] that the switching chalcogenide devices undergo certain changes during the first few operations, called forming; during the forming process regions of ordered or phase separated (and hence highly conductive) material are developed[127]. (A certain amount of this material can be present already in the starting glass). Thus only a small amount of growth needs to occur in order to produce in a very short time a highly conducting path, connecting the regions already present, when the set-pulse is applied to the device. On the application of the re-set-pulse the connectivity of the path is destroyed at one or more places.

It is feasible that structural changes play an essential role also in threshold switching. If the thermal model is modified by introducing a step function dependence of the conductivity on temperature instead of (2.16), the step occuring at the temperature of melting[87], or a saturation requirement[118], then a substantially improved agreement with the prediction of the thermal theory results. In Chapter 3 it is shown that statistical aspects of switching can be accounted for in terms of small variations in the volume fraction of a highly conductive material in the switching layer.

2.2.5 What is the Key Requirement for Switching?

In the preceding sections the current theories of the switching effect were reviewed, based on various assumptions which are in many cases completely different (e.g. thermal vs. electronic model). The switching effect is observed in large classes of materials

(i) chalcogenide glasses

(ii) oxide glasses[113]

(iii) amorphous materials like

$CdXAs_2$ X = Ge,Si,Mg,Al,Ga,In,Te,Sb[120]

SbISX, X = Cu,Ag,Au,Te[130]

SiN_4[122]

(iv) elemental amorphous semiconductors = Ge,Si,B[82]

(v) some liquid semiconductors (e.g. Se)

(vi) polymer thin films[131]

(vii) small group of crystalline semiconductors:
e.g. Sb_2S_3[119], ZrS_2[121]

The questions which arise are why switching occurs

(a) in semiconductors

(b) mainly in amorphous semiconductors

The answer to the first question is easier than to the second question. In semiconductors changes in electric field and temperature usually result

in large effects on the properties. Electric fields in metals are only vanishingly small and do not have much effect on the properties of metal; the resistivity of metals increases with temperature (the opposite is required by the thermal model of switching). On the other hand in insulators (i.e. large band gap semiconductors) very high fields are required to produce noticeable changes in conductivity; when these occur, they usually result in a permanent structural change in the insulator.

According to the thermal theory any substance having sufficiently large activation energy for conductivity ($>4\,kT$) can show switching providing that the "on"-state is not destructive and irreversible. In view of the list of substances above, however, it seems that something more is required and that "something" is usually found in amorphous semiconductors. The crystalline semiconductors (in p-n junctions) electrical breakdowns can occur (avalanche or Zener) neither of which is inherently destructive although the resultant generation of heat can in certain circumstances lead to a permanent damage. To obtain an effect similar to switching in crystalline p-n junctions a large amount of sophisticated engineering design and technological skill is required; on the other hand the amorphous semiconductor switching devices do not require any critical design and the ability to show switching seems to be inherent to the amorphous state.

In the case of memory switching the answer to the question (b) is relatively straightforward: memory switching is associated with a structural change from the glassy to the crystalline state and hence the semiconductor has to be obtainable in a glassy form. Amorphous germanium does not show bistable switching because it cannot be obtained in glassy form. Drake suggests that the tendency of a system to show memory switching and to form glass are intimately related. Some requirements which has to be satisfied by the glass in order to exhibit memory switching are suggested by Gildart[119].

It is much more difficult to ascertain the requirements for the occurence of the threshold switching. Threshold switching always precedes the memory action and therefore to find the requirements for the occurence of the threshold switching is essential in order to decide on the key requirement for the whole switching process (threshold and memory).

Let us consider the ways in which conductivity of a solid can be increased: either by increasing the concentration of mobile carriers or by increasing mobility of carriers present or by both processes. In the case of crystalline semiconductors the carrier mobility is very high and cannot be further increased by direct or indirect action of the electric field. Only the concentration of mobile carriers can be increased. On the other hand both mobility and number of mobile carriers can be increased in amorphous semiconductors by direct or indirect influence of the applied field. Thus for the same concentration of mobile carriers the increase in the conductivity of amorphous semiconductor will be higher by the factor $\mu_{crystal}/\mu_{glass}$ if the effective mobility of carriers in the "on"-state approaches the mobility of carriers in crystalline semiconductor of the same class.

This naive argument therefore suggests that the mobility of the carriers in switching material in the "off"-state has to be sufficiently small. This view seems to be directly or indirectly supported by several investigators. Krempaský and Červenák[122] relate the difference between the "off"-state and the "on"-state resistances of the switching device to the mobility of the carriers using an electronic model of switching in which non-ohmic contacts are made to the semiconductor. They found that the "off"-state resistance of the device is a function of the mobility and the contact potential and that the mobility has to be very small $\mu<0.1$ cm^2/Vs (for a reasonable value of the contact potential) to account for the large observed difference $R_{off} - R_{on} \approx 10^5 \Omega$. This value of mobility seems to be too small compared with one found by Böer[123] who finds the condition

μ = 100 cm^2/Vs for the observed short switching times ($<10^{-9}$s). Mattis[119] also mentions that μ should be small otherwise the Ohmic current will shunt out the applied voltage and eliminate the effects of cooperative phenomena which he considers in his model.

In switching crystalline materials a small value of mobility is probably also decisive in certain cases as can be inferred from the measurements performed on ZrS_2[121], which show that the mobility is greatly anisotropic due to the layer-like structure of this compound (ratio of the resistivity perpendicular to the layers to that measured parallel to the layers is about 10^{-3}). Switching liquid semiconductors also seem to conform with the requirement of small mobility[129].

It seems that not a too high mobility is also essential for the "on"-state. Mott[93] arrives at the condition that the width of the barriers near the electrodes (Fig. 2.11.d) is proportional to $\mu^{1/3}$ and hence mobility μ must not be too large to make the barriers incapable of being tunnelled by the carriers. Lucas in his model of recombination instability[103] visualizes the "off"-"on" transition as the extension of the diffusion length of the carriers L throughout the whole device of thickness d. As L_{off} = (0.05 to 0.15) 10^{-4}cm and d = 10^{-4}cm, he requires (very roughly)

$$\left(\frac{\mu_{off}}{\mu_{on}}\right)^{1/2} = \frac{L_{off}}{L_{on}} \leq \frac{L_{off}}{d} = 0.05 \text{ to } 0.15 \qquad (2.29)$$

and hence

$$\frac{\mu_{on}}{\mu_{off}} \geq (44 \text{ to } 400) \qquad (2.30)$$

Moreover, in his model he requires the existence of electron and hole traps in nearly equal concentrations. This is also the basic requirement for the H-F-O model of switching which, as pointed out by Henish et al[124], is very difficult to produce in crystalline semiconductors as producing nearly equal concentrations of donors and acceptors requires high degree

of artificiality and is practically never expected to happen naturally (when this happens something like switching is actually observed[125,126]). On the other hand, in the case of amorphous semiconductos, equal concentrations of electron and hole traps are automatically provided according to C-F-O model (Fig. 2.8.c), which also cause the low mobility of carriers which seems to be important for the occurence of the switching effect. This seems to explain the special position which amorphous semiconductors, especially chalcogenide glasses, take in the switching effect (question (b) above).

So far only the requirements concerning transport of charge carriers have been discussed. It is obvious, however, that apart from these requirements other conditions have to be satisfied if switching, rather than destructive breakdown, is to occur. It is suggested further (in section 6.3.2) that structural stability of switching devices is generally associated with the ability of the switching material to form a highly conducting phase during switching.

References Quoted in Chapter 2

(1) Rudee M.L. and Howie A., Phil. Mag. 25 (1972) 1001.

(2) Zacharaisen W.H., J. Amer. Chem. Soc. 54 (1932) 3841.

(3) Polk D.E., J. Non-Cryst. Solids 5 (1971) 365.

(4) Lebedev A.A., quoted by Evstropyev K.S. and Porai-Koshits E.A. J. Non-Cryst. Solids 11 (1972) 170.

(5) Valenkov N. and Porai-Koshits E.A., Z. Krist. 95 (1937) 195.

(6) Hägg G., J. Chem. Phys. 3 (1935) 42.

(7) Hertz P., Math. Ann. 67 (1909) 387.

(8) Moss S.C. and Graczyk J.F. (1970) Proceedings of the 10th International Conference on Physics of Semiconductors, Cambridge, Massachusetts, p. 658 (U.S. Atomic Energy Comission).

(9) Bartash G. and Just T., Z. Metallk. 63 (1972) 360.

(10) Mott N.F. and Davis E.A., "Electronic Processes in Non-Crystalline Materials" (Oxford Press 1971) p. 324.
Mott N.F., Advan. Phys. 16 (1967) 49.

(11) Gingrich N.S., Revs. Mod. Phys. 15 (1943) 90.

(12) Kopský V., Czech. J. Phys. B21 (1971) 1071.

(13) Hill, R.M., Contribution at the Discussions on Amorphous Semiconductors, Chelsea College, London, 17-18.12.1971.

(14) Betts F., et al, J. Non-Cryst. Solids 8-10 (1972) 364.

(15) Richter H. and Breitling G., Z. Naturforch. 13a (1958) 988.

(16) Grigorovici R. and Manaila R., Thin Solid Films 1 (1968) 343.

(17) Henderson D. and Herman F., J. Non-Cryst. Solids 8-10 (1972) 359.
Bennett C.H., J. Appl. Phys. 43 (1972) 2727.

(18) Turnbull D. and Cohen M., J. Chem. Phys. 29 (1958) 1049.

(19) Matsushita T. et al, Jap. J. Appl. Phys. 11 (1972) 923.

(20) Savage J.A., J. Mater. Sci. 6 (1971) 964.

(21) Feinleib J. et al, reference (14) quoted in Chapter 1.

(22) Evans E.J. et al, J. Non-Cryst. Solids 2 (1970) 334
Bienenstock A. et al, ibid 2 (1970) 347.

(23) Ovshinsky S.R. and Klose P.H., J. Non-Cryst. Solids 8-10 (1972) 892.

(24) Dresner J. and Stringfellow G.B., J. Phys. Chem. Solids 29 (1968) 303.
Belan S.A. et al, Izv. VUZ (USSR), Physics Section, No. 6 (1971) 106.

(25) Chen A.C. et al, reference (15) quoted in Chapter 1.

(26) Sinha O.P., J. Non-Cryst. Solids 8-10 (1972) 708 and references cited therein.

(27) Epstein S.G. and Puskin A., Phys. Lett. 24A (1967) 309.

(28) Verhoven J.D. and Hucke E.E., Am. Soc. Metals Trans. Quart. 55 (1962) 866.

(29) Scholten P.C., "The theory of Electrodiffusion" (Utrecht, 1962).

(30) Adler D. (M.I.T.), quoted by Henisch, reference (12) of Chapter 1.

(31) e.g. a number of papers in J. Non-Cryst. Solids, 8-10 (1972).

(32) Fritzsche H. and Ovshinsky S.R., J. Non-Cryst. Solids 2 (1970) 148.

(33) Eckstein B., ibid, 4 (1970) 366.

(34) Duwez P. and Tsuei C.C., reference 1 of Chapter 1.

(35) Slater J.C., quoted by Brown F.C. in "The Physics of Solids", p.405 (W. A. Benjamin, 1967).

(36) Bloch, F., Z. Physik 52 (1928) 555.

(37) Ziman J.M., Phil. Mag. 6 (1961) 1013.

(38) Mott N.F. and Davis E.A., reference (10), p. 2.

(39) Hulls K. and McMillan P.W., J. Phys. D. (Appl. Phys.) 5 (1972) 865.

(40) Klima J. et al, Discuss. Faraday Soc. 50 (1971) 20.

(41) Myuller R.L., "Solid State Chemistry" p.1. (edited by Borisova Z.U. Consultants Bureau, N.Y. 1966).

(42) Cohen M.H., Fritzsche H. and Ovshinsky S.R., Phys. Rev. Lett. 22 (1969) 1065.

(43) Anderson P.W., Phys. Rev. 109 (1958) 1492.
Mott N.F., Adv. Phys. 16 (1969) 49.

(44) Gubanov A.I., "Quantum Theory of Amorphous Conductors", 1st edition 1963. (Consultants Bureau, N.Y., 1965).

(45) Böer K.W., Phys. Stat. Solidi B47 (1971) K37.

(46) Böer K.W., J. Non-Cryst. Solids 8-10 (1972) 586.

(47) Marshall J.M. et al, J. Non-Cryst. Solids 8-10 (1972) 760.

(48) Cutler M., Phil. Mag. 25 (1972) 173.
Butcher P.N., to be published.

(49) Hulls K., reference (24) quoted in Chapter 4.

(50) Croitoru N. et al, J. Non-Cryst. Solids 4 (1970) 493.

(51) Henisch H.K. et al, ibid, 8-10 (1972) 415.

(52) de Wit H.J. and Crevecoauer C., Solid State Electron 15 (1972) 729.

(53) Murgatroyd P.N., Thin Solid Films 11 (1972) 125.

(54) Walsh P.J. et al, Phys. Rev. 178 (1969) 1274.
Robertson J.M. and Owen A.E., J. Non-Cryst. Solids 8-10 (1972) 439.

(55) Böer K.W. and Haislip R., Phys. Rev. Lett. 24 (1970) 230.
Door R.C. and Kaunewurf C.R., J. Non-Cryst. Solids 6 (1971) 113.

(56) Thomas D.L. and Warren A.C., Electron Lett. 6 (1970) 62.

(57) Poole H.H., Phil. Mag. 32 (1916) 112, 34 (1917) 195.
Frenkel J., Phys. Rev., 54 (1938) 647.

(58) Croitoru N. et al., reference (50).
Fagen E.A. and Fritzsche H., J. Non-Cryst. Solids 2 (1970) 170.

(59) Stubb T. et al., Solid State Electron, 15 (1972) 611.

(60) Dussel G.A. and Böer K.W., Phys. Stat. Solidi., 39 (1970) 375.

(61) Fritzsche H. and Ovshinsky S.R., J. Non-Cryst. Solids, 2 (1970) 148.

(62) Mott N.F., Phil. Mag. 24 (1971) 911.

(63) Hindley N.K., J. Non-Cryst. Solids, 5 (1970) 17, 31.

(64) Lampert M.A. and Mark P., "Current Injection in Solids" (Acad. Press 1970)

(65) Rose A., Phys. Rev., 97 (1955) 1538.

(66) Lanyon, H.P.D., Phys. Rev. 130 (1964) 134.

(67) Kröger F.A. et al., ibid., 103 (1956) 279.

(68) Adam G. and Duchene J., Solid State Commun., 9 (1971) 785.

(69) Tantraporn W., Solid State Electron, 7 (1964) 81.

(70) Allison J. and Dawe V.R., Electron Lett., 8 (1972) 437.

(71) Iizima S. et al., Solid State Commun., 9 (1971) 795.
c.f. ibid., 8 (1970) 1621.

(72) Pearson A.D., J. Non-Cryst. Solids 2 (1970) 1.

(73) Matsushita T. et al., reference (19), and references therein.

(74) Haberland D.R. and Kehrer H.P., Solid State Electron 13 (1970) 451.

(75) Kolomiets B.T. et al., Sov. Phys.-Semicond., 6 (1972) 167.

(76) Shimakawa K. et al., Jap. J. Appl. Phys., 10 (1971) 956.

(77) Johnson R.T. and Quinn R.K., Solid State Commun., 9 (1971) 393.

(78) Green M. et al., J. Phys. D. (Appl. Phys.) No. 7. (1972) L55.

(79) Phillips S. et al., J. Non-Cryst. Solids, 4 (1970) 510.

(80) Sie C.H. et al., ibid., 8-10 (1972) 877.

(81) Uttecht R. et al., ibid., 2 (1970) 358.
Stocker H.J. et al., ibid., 4 (1970) 523.
Sie C.H., ibid., 4 (1970) 548.

(82) Moorjani K. and Feldman C., ibid., 2 (1970) 82.
ibid., 4 (1970) 248.

(83) Ridley B.K., Proc. Phys. Soc., 82 (1963) 954.
also
Böer K.W. et al., Phys. Stat. Solidi., 1 (1961) 231.
Jahne E. and Nebauer E., ibid., 8 (1965) 881.

(84) Benc I. and Husa V., Czech. J. Phys., A21 (1971) 396.

(85) Koshlyakov N.S. et al., "Differential Equations of Mathematical Physics" (North-Holland Publ., 1964).

(86) Thom R., "Stabilitè Structurelle et Morphogénèse" (Benjamin, 1972, to appear).

(87) Kroll D.M. and Cohen M.H., J. Non-Cryst. Solids, 8-10 (1972) 544.

(88) Wagner K.W., Trans. A.I.E.E., 41 (1922) 288.
Fock V., Arch. f. Elektrot. 19 (1927) 71.

(89) a large number of references quoted in:
O'Dwyer J.J., "The Theory of Dielectric Breakdown of Solids" (Oxford Press, 1964).
Whitehead S., "Dielectric Breakdown of Solids" (Oxford Press, 1953).

(90) e.g.

Stocker H.J. et al., J. Non-Cryst. Solids, 4 (1970) 523.
Böer K.W., Phys. Stat. Solidi., A4 (1971) 571.

(72) Pearson A.D., J. Non-Cryst. Solids 2 (1970) 1.

(73) Matsushita T. et al., reference (19), and references therein.

(74) Haberland D.R. and Kehrer H.P., Solid State Electron 13 (1970) 451.

(75) Kolomiets B.T. et al., Sov. Phys.-Semicond., 6 (1972) 167.

(76) Shimakawa K. et al., Jap. J. Appl. Phys., 10 (1971) 956.

(77) Johnson R.T. and Quinn R.K., Solid State Commun., 9 (1971) 393.

(78) Green M. et al., J. Phys. D. (Appl. Phys.) No. 7. (1972) L55.

(79) Phillips S. et al., J. Non-Cryst. Solids, 4 (1970) 510.

(80) Sie C.H. et al., ibid., 8-10 (1972) 877.

(81) Uttecht R. et al., ibid., 2 (1970) 358.
Stocker H.J. et al., ibid., 4 (1970) 523.
Sie C.H., ibid., 4 (1970) 548.

(82) Moorjani K. and Feldman C., ibid., 2 (1970) 82.
ibid., 4 (1970) 248.

(83) Ridley B.K., Proc. Phys. Soc., 82 (1963) 954.
also
Böer K.W. et al., Phys. Stat. Solidi., 1 (1961) 231.
Jahne E. and Nebauer E., ibid., 8 (1965) 881.

(84) Benc I. and Husa V., Czech. J. Phys., A21 (1971) 396.

(85) Koshlyakov N.S. et al., "Differential Equations of Mathematical Physics" (North-Holland Publ., 1964).

(86) Thom R., "Stabilitè Structurelle et Morphogénèse" (Benjamin, 1972, to appear).

(87) Kroll D.M. and Cohen M.H., J. Non-Cryst. Solids, 8-10 (1972) 544.

(88) Wagner K.W., Trans. A.I.E.E., 41 (1922) 288.
Fock V., Arch. f. Elektrot. 19 (1927) 71.

(89) a large number of references quoted in:
O'Dwyer J.J., "The Theory of Dielectric Breakdown of Solids" (Oxford Press, 1964).
Whitehead S., "Dielectric Breakdown of Solids" (Oxford Press, 1953).

(90) e.g.

Stocker H.J. et al., J. Non-Cryst. Solids, 4 (1970) 523.
Böer K.W., Phys. Stat. Solidi., A4 (1971) 571.

(91) Thomas D.L. and Male J.C., J. Non-Cryst. Solids, 8-10 (1972) 522.

(92) Kaplan T. and Adler D., ibid., 8-10 (1972) 538.
Kaplan T. and Adler D., Appl. Phys. Lett., 19 (1971) 418.

(93) Mott N.F., Reference 62, p. 922.

(94) Henisch H.K., reference (12) of Chapter 1.
Henisch H.K. et al., J. Non-Cryst., Solids, 4 (1970) 538.

(95) Popescu C. and Croitoru N., ibid., 8-10 (1972) 531.

(96) Mott N.F., Contemp. Phys., 10 (1969) 125.

(97) Mott N.F., Festkörperproblemme 9 (1969) 22.

(98) Mott N.F., Phil. Mag., 19 (1969) 835.

(99) Hindley N.K., reference (63).
Hindley N.K., J. Non-Cryst. Solids, 8-10 (1972) 557.

(100) Böer K.W., Solid State Commun. 8 (1970) 1329.

(101) Owen A.E., Summer School on Electrical Properties on Non-Crystalline Materials, Cambridge, England, 29.6. - 3.7.1970.

(102) Fritzsche H. and Ovshinsky S.R., J. Non-Cryst. Solids 4 (1970) 464.

(103) Lucas I., ibid., 6 (1971) 136.

(104) Fritzsche H. and Ovshinsky S.R., ibid., 2 (1970) 393.

(105) Pryor R.W. and Henisch H.K., Appl. Phys. Lett., 18 (1971) 324.

(106) Fritzsche H., I.B.M. J. Res. Dev., 13 (1969) 515.

(107) Heywang W. and Haberland D.R., Solid State Electron, 13 (1970) 1077.
Haberland D.R., ibid., 13 (1970) 207.

(108) Adler D., Electronics, 28.9.1970, p. 61.

(109) Mattis D.C., Phys. Rev. Lett., 22 (1969) 936.

(110) Bowers H.C. and Barnett A.M., I.E.E.E. Trans., ED17, (1970) 971.

(111) Sandomirski V.B. et al., Sov. Phys. - JETP 21 (1970) 902.
also similar theoretical models by:
Bonch-Bruevich V.L., Sov. Phys., Solid State, 6 (1965) 1615.
Avak'yants G.M. et al., Izv. Akad. Nauk Arm. SSR (USSR), Fiz., 7 (No. 1), (1972) 55.

(112) Iida M. and Hamada A., Jap. J. Appl. Phys., 10 (1971) 224.

(113) Drake C.F. et al., J. Non-Cryst. Solids, 4 (1970) 234.
Drake C.F. et al., reference (10) of Chapter 1.

(114) Warren A.C. and Male J.C., Electron. Lett., 6 (1970) 567.

(115) McMillan P.W. and Nesvadba P., reference (30) of Chapter 1.

(116) Kikuchi M., Physics Meeting, Hannover, Germany, December 1970, p. 167, (German Phys. Soc., Stuttgart).
Tanaka K. et al., Solid State Commun., 8 (1970) 75.

(117) Barry (1971) quoted by
Thomas C.B. et al., Phil. Mag. 26 (1972) 617.
Contributions by
Bosnell J.R.
Brander R.W.
at the Discussion Meeting of I.E.E. on "Experiences with Amorphous Semiconductor Devices", Savoy Place, London, 8.5.1972.
Contribution by
Maghrabi Claude
at the "Switching Meeting", Cavendish Lab., Cambridge, 27.5.1971.
Inglis G.B. and Williams F., J. Non-Cryst. Solids, 5 (1971) 313.
Williams F., ibid., 8-10 (1972) 516.
Roy R. and Čáslavská Věra, Solid State Commun., 7 (1969) 1467.

(118) Suntola T., Acta Polytechnica Scandinavica Ph82 (1971).

(119) Gildart L., J. Non-Cryst. Solids 2 (1970) 240.

(120) Červinka L. et al., ibid., 4 (1970) 258.

(121) Yoffe A.D., Colloquium at the University of Warwick, England, 19.10.1971.

(122) Krempaský J. and Červenák J., Czech. J. Phys., B21 (1971) 285.

(123) Böer K.W., J. Non-Cryst. Solids, 4 (1970) 583.

(124) Henisch H. K. et al., Congres International sur les Couches Minces (Cannes, 1970) p. 437.

(125) Schmidlin F.W., Phys. Rev., B1 (1970) 1583.

(126) Osipov V.V. and Kholodnov V.A., Sov. Phys. - Semicond., September 1972.
Mizuschima Y. et al., Proc. I.E.E.E. (Correspondence) 53 (1965) 322.

(127) Coward L.A., reference (30) quoted in Chapter 4.

(128) Messier R. et al., J. Non-Cryst. Solids 8-10 (1972) 816.
also
Mott N.F. and Davis E.A., reference (10), p. 281.

(129) Perron J.C., J. Non-Cryst. Solids, 8-10 (1972) 272.
Perron J.C., Proc. Int. Conf. on "Conduction in Low Mobility Materials", Eilat, Israel, April 1971, p. 243.

(130) Minesota Mining and Manufg. Co., "Glass compositions and solid state switching devices using these compositions" Brit. Pat. 1,117,211 (1968).

(131) Carchano H. et al., Appl. Phys. Lett. 19 (1971) 414.

CHAPTER 3

THEORETICAL MODELS EMPLOYED IN THE PRESENT WORK

3.1 Introduction

During the first stage of the investigations of the switching effect the thermal model of switching was adopted as a working hypothesis (1). It was shown in (1) that a simple 1-D thermal model was capable of accounting for the quantitative aspects of the initiation of switching in bulk devices in a restricted temperature range and could even qualitatively account for several other features of the switching process. It was, however, shown in (1,2) that

(i) at low temperatures ($T \leq -70^{\circ}C$) the thermal model did not predict correct threshold voltages.

(ii) 1-D description of the "on"-state is inadequate and that 2-D or 3-D models should be considered

(iii) the switching resistance of the device changes after each switching operation. This could mean structural changes in the device and any further model of switching should take these changes into account.

The development of the theoretical models employed in the present work was influenced to a large extent by the above suggestions of the previous work.

Two 1-D models were considered which would explain the dependence of the threshold voltage on temperature below room temperature: the first of these follows suggestions by Böer[3], Owen[4] and calculations by Adam and Duchene[5] in which it is assumed that an initial temperature rise in the centre of the device causes the electric field at the electrodes to exceed a certain critical value which initiates the switching transition, i.e. the first model invoked was electrothermal model. The second model invoked

was, in some ways, analogous to the electrothermal model. In this second model it was assumed that a structural relaxation takes place when the temperature and/or electric field are sufficiently large, following a suggestion by Gupta[6]. Both models are discussed in the next section.

With respect to point (ii) above, a considerable effort has been made to produce 2-D solutions to the system (2.25 - 2.26 - Chapter 2), which presents certain mathematical difficulties. These are discussed together with the achievements in section 3.3.

A simple phenomenological model was developed in which the basic assumption of certain structural changes taking place in the threshold switching device during operation is used to permit the statistical analysis of the variability of the switching parameters. This model is discussed in detail in section 3.4.

3.2 Modified 1-D Thermal Models

3.2.1 Electrothermal Model

Adam and Duchene considered an electrothermal initiation of switching in sandwich structures[5]. The essential features of their model were used in the present calculations and are briefly summarized in the following paragraph.

It is assumed that the temperature profile in the sandwich device is given by

$$T(X) = T_a + \Theta_m \cos\left(\frac{\pi X}{d}\right) \tag{3.1}$$

where T_a is the ambient temperature, d is the device thickness and Θ_m is the maximum temperature rise in the device (see Fig. 3.1). The electrical conductivity[2.16.] is approximated by the expression

$$\sigma = \sigma_{oo} \exp(\beta\Theta) \tag{3.2}$$

where

$$\sigma_{oo} = \sigma_o \exp\left(-\frac{\Delta E}{2kT_a}\right) \tag{3.2a}$$

$$\beta = \frac{\Delta E}{2kT_a^2} \tag{3.2b}$$

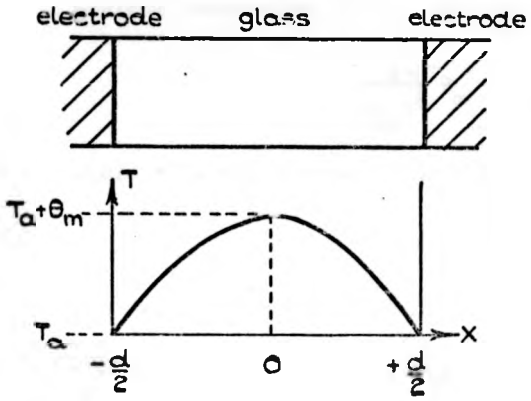

Fig. 3.1.

TEMPERATURE RISE IN A SANDWICH DEVICE.

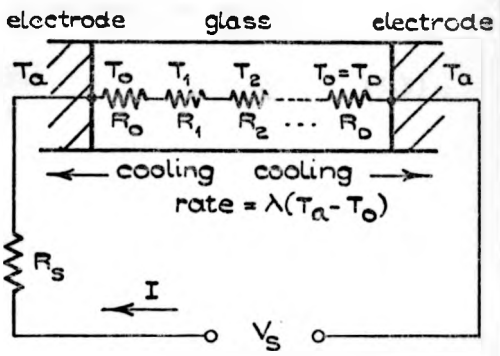

Fig. 3.3.

FINITE - DIFFERENCE APPROXIMATION.

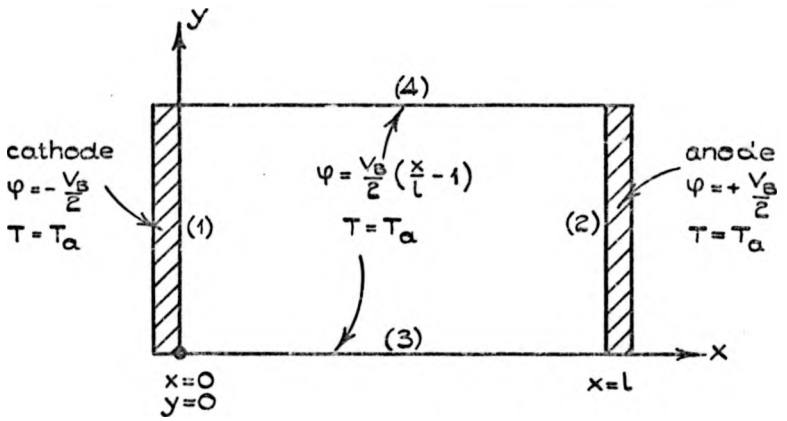

Fig. 3.5.

BOUNDARY CONDITIONS USED FOR THE 2-D SWITCHING PROBLEM.

For each voltage V applied to the device the corresponding maximum temperature rise θ_m is calculated by solving the equation:

$$\frac{4\kappa}{\sigma_{oo}V^2}\theta_m = \frac{\exp(-\beta\theta_m)}{I^2(\theta_m)} \tag{3.3}$$

where κ is the thermal conductivity and

$$I(\theta_m) = \int_0^{\frac{\pi}{2}} \exp(-\beta\theta_m \cos y)\, dy \tag{3.4}$$

and the field F at the electrodes, say at $X = \frac{d}{2}$ for definitness, is given by

$$F\left(\frac{d}{2}\right) = \frac{\pi V}{2dI(\theta_m)} \tag{3.5}$$

Adam and Duchene calculate for each ambient temperature T_a the critical value of $V = V_{th}$ at which the field at the electrodes $F_{(\frac{d}{2})}$ exceeds a critical value given by (2.28). In this way the threshold voltage V_{th} is calculated as a function of ambient temperature T_a.

In the present work the calculations have been repeated without approximating the conductivity by the relation (3.2) and the exact form (2.16) was used. In this case (3.3) and (3.4) are modified in the following way:

$$\frac{4\kappa\sigma_c}{\sigma_{oo}^2V^2}\theta_m = \frac{\exp\left(\frac{\beta T_a^2}{T_a+\theta_m}\right)}{IN^2(\theta_m)} \tag{3.6}$$

where

$$IN(\theta_m) = \frac{\sigma_{oo}}{\sigma_c}\int_0^{\frac{\pi}{2}} \exp\left(\frac{\beta\, T_a^2}{T_a+\theta_m\cos y}\right)dy \tag{3.7}$$

The relation (3.5) is also modified into

$$F\left(\frac{d}{2}\right) = \frac{\pi V}{2dIN(\theta_m)} \tag{3.8}$$

It was shown by computing $F_{(\frac{d}{2})}$ by using (3.5) and (3.8) that the results differed only slightly, by a few per cent, which means that the approximation (3.2) does not introduce an essential inaccuracy.

The new feature introduced in the present model was a new criterion for switching, which differs from that used by Adam and Duchene. It was assumed that the switching transition is initiated as soon as one of two competing conditions is fulfilled:

$$\text{(i)} \qquad \theta_m = \frac{2kT_a^2}{\Delta E} = \frac{1}{\beta} \tag{3.9}$$

$$\text{(ii)} \qquad F(\tfrac{d}{2}) = F_{crit.} \tag{3.10}$$

The first criterion corresponds to the relation for the temperature rise at the point of thermal runaway, it can be shown that $\theta_m = \frac{T_a^2}{\beta}$ corresponds to the maximum voltage V applied to the device[7], and thus represents the condition for thermal switching whilst the second criterion constitutes the condition for an electronic switching initiated by some mechanism occurring at the electrode $x = \frac{d}{2}$ when the electric field at that electrode exceeds the value of $F_{crit.}$

At sufficiently high ambient temperatures already a small applied voltage will cause a large rise in the device temperature because the average electrical conductivity of the switching material is large; thus it is expected that the condition (i) will be satisfied first. On the other hand, at sufficiently low ambient temperatures at which the electrical conductivity is decreased, a large voltage V would have to be applied in order to effect the temperature rise given by the condition (i), and such voltage V would be in excess of a voltage sufficient to give rise to the critical electric field F_{crit}. Therefore the criterion (ii) is expected to be operative at sufficiently low ambient temperatures. Thus at certain intermediate temperature a changeover from the thermal to the electrothermal initiation is expected as the ambient temperature is decreased.

The expected change in the mechanism of switching initiation is confirmed by the calculations which have been carried out. An example of such calculation is given in Table 3.1 which summarizes the results of a

calculation of switching voltage at various temperatures in the range 150°K to 500°K. Values of $F_{crit} = 1.43 \times 10^5$ V/cm and $\Delta E = 0.9$ eV were substituted in the critical conditions (3.9) and (3.10).

Table 3.1 Initiation of Switching in a Sandwich Device 150 μm Thick.

$\kappa = 1.64 \times 10^{-1}$ W°K^{-1}cm^{-1} (chosen to scale V_{th} with experiment)

$\sigma_o = 3 \times 10^3 \Omega^{-1}$ cm^{-1}

T_a (°K)	$10^3/T_a$ (°K^{-1})	V_{th} [V]	V at which $F(\frac{d}{2}) = F_{crit}$	V at which $\theta_m = \frac{1}{\beta}$
150	6.67	2146	2146	1.06×10^6
175	5.73	2146	2146	1.07×10^5
200	5.00	2130	2130	1.83×10^4
225	4.44	2030	2030	4860
250	4.00	1435	1435	1695
275*	3.64	727	727	727
300	3.33	360	**	360
325	3.08	200	**	200
350	2.86	122	**	122
375	2.67	80.0	**	80.0
400	2.50	54.6	**	54.6
425	2.35	40.2	**	40.2
450	2.22	31.7	**	31.7
475	2.11	23.7	**	23.7
500	2.00	18.9	**	18.9

* Transition temperature

** Condition (3.9) is fulfilled earlier than (3.10) when increasing the applied voltage.

It is seen that the transition from the electronic to the thermal mode of initiation of switching takes place at the ambient temperature of $T_a = 275\,^{\circ}K$. The values of the logarithm of the switching voltage are plotted against the reciprocal ambient temperature in Fig. 3.2. A comparison is made in the same Fig. 3.2 with the measured dependence of the threshold voltage on temperature. A better agreement would have been achieved by allowing F_{crit} to be temperature dependent, but this was not pursued in view of the lack of independent information about this dependence.

3.2.2 Model of Structural Relaxation

In this model it is assumed that the switching into the "on"-state takes place when the combined effect of the temperature and the electric field in the switching device is sufficient to produce some kind of structural relaxation; the type of the relaxation does not need to be specified in this phenomenological model, but is visualized as an ordering process by which the randomness of the amorphous structure is decreased thereby increasing the electrical conductivity of the material.

A number of experimental observations suggest that the threshold voltage decreases to zero as the ambient temperature approaches the glass transition temperature T_g[8]. Therefore this temperature can be regarded as one at which no electric field is necessary to effect the structural relaxation; at lower temperatures a certain electric field has to be applied to the device to cause the structural relaxation and switching. Following Gupta[6] the relaxation time for the structural change to occur is written as

$$\tau = \tau_o \exp\left(\frac{W(F)}{kT}\right) = \tau_o \exp(B) \qquad (3.11)$$

where $\tau_o \approx 10^{-12}$s. The activation energy W is certain decreasing function of the electric field F and in the first approximation it can be written as

$$W(F) = A\left(1 - \frac{F}{F_o}\right) \qquad (3.12)$$

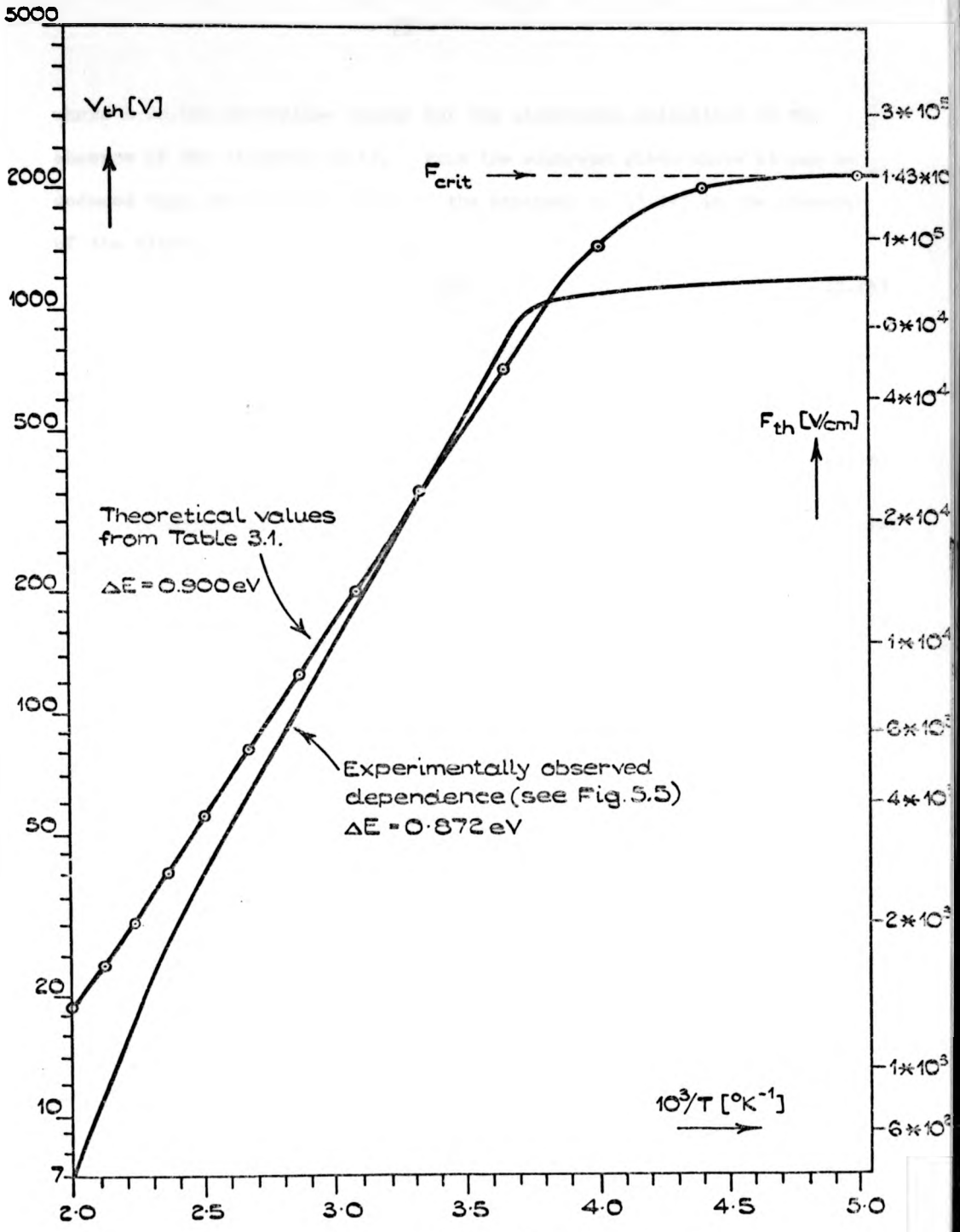

Fig. 3.2.

TEMPERATURE DEPENDENCE OF THRESHOLD VOLTAGE FOR A DEVICE 150 μm THICK. PREDICTION OF THE ELECTRO-THERMAL MODEL IS COMPARED WITH EXPERIMENT.

where A is the activation energy for the structural relaxation in the absence of the electric field. From the argument given above it can be deduced that the critical value of the exponent in (3.11) in the absence of the electric field is given by

$$B_{crit} = \frac{A}{kT_g} \tag{3.13}$$

In the presence of the electric field F and at temperature T (3.13) can be modified by using (3.12):

$$B_{crit} = \frac{A(1-\frac{F}{F_o})}{kT} \tag{3.14}$$

Comparison of (3.13) and (3.14) gives the condition for the structural relaxation at temperature $T<Tg$ in the presence of the electric field F:

$$\frac{T_g}{T}\left(1-\frac{F}{F_o}\right) = 1 \tag{3.15}$$

The constant F_o is interpreted as the intensity of electric field F sufficient to induce the structural relaxation at temperatures approaching absolute zero.

The criterion (3.15) was applied to a 1-D time-dependent solution of the heat equation

$$c\frac{\partial T}{\partial t} = \kappa\frac{\partial^2 T}{\partial X^2} + \sigma(T,F)F^2 \tag{3.16}$$

which was generated numerically by a finite-difference method. In this method the switching device is approximated by D regions in which the temperature and electric field are not changing with the coordinate and are denoted as T_i and F_i respectively ($i = 1,2,\ldots,D$) (Fig. 3.3). Electrically each of these regions represents a series resistor

$$R_i = \frac{S\cdot D}{d}\,\frac{1}{(T_i, F_i)} \tag{3.17}$$

where S and d are the area and the thickness of the switching device. The heat generated in the regions per unit time ($R_i I^2$) is dissipated by conduction, determined by a finite difference analog of the heat conduction

term in (3.16). At each time level new values of T_i and F_i are calculated by a method which is given in the appendix 2 (in the form of a computer programme). For each applied voltage V_s the time dependence of T_i and F_i can be calculated and the criterion (3.15) applied to each of the regions. The criterion will not be satisfied for values of the applied voltage V_s less than a certain threshold value V_{sth}; for values $V_s > V_{sth}$ the criterion will be satisfied at some region after a number of computational steps corresponding to the delay time for switching t_d. The case $V_s = V_{sth}$ corresponds to the limit $t_d \to \infty$.

By running the computer programme for different values of the applied voltage V_s and for different ambient temperatures it is possible to ascertain the dependence of V_{sth} on ambient temperature. This dependence, for a particular set of numerical values assigned to the constants in (3.16).

$$\kappa = 5_{10}{}^{-3} \quad W\,deg^{-1}cm^{-1} \qquad T_g = 550^{\circ}K$$

$$C = 2_{10}{}^{-2} \quad deg^{-1}g^{-1} \qquad F_o = 5 \times 10^5\ V/cm$$

and for the values

$$D = 10 \qquad d = 10^{-2}\ cm$$

$$R_s = 2 \times 10^3\ \Omega$$

$$\lambda = 0.7 \quad cm^{-2}s^{-1}\,deg^{-1}$$

and for the electrical conductivity of the form

$$\sigma(T_i, F_i) = \sigma_o \exp\left(\frac{F_i}{aT} - \frac{E}{2kT}\right) \qquad (3.18)$$

where $\sigma_o = 100\ \Omega^{-1}\ cm^{-1}$

$a = \infty$

$\frac{\Delta E}{2k} = 5000^{\circ}K$

is shown in Fig. 3.4. Within an intermediate temperature range the predicted dependence $V_{sth}(T_a)$ does not differ markedly from that predicted by a thermal model; in this temperature range the criterion (3.15) is first satisfied at the centre of the switching device ($i = D/2$). At low

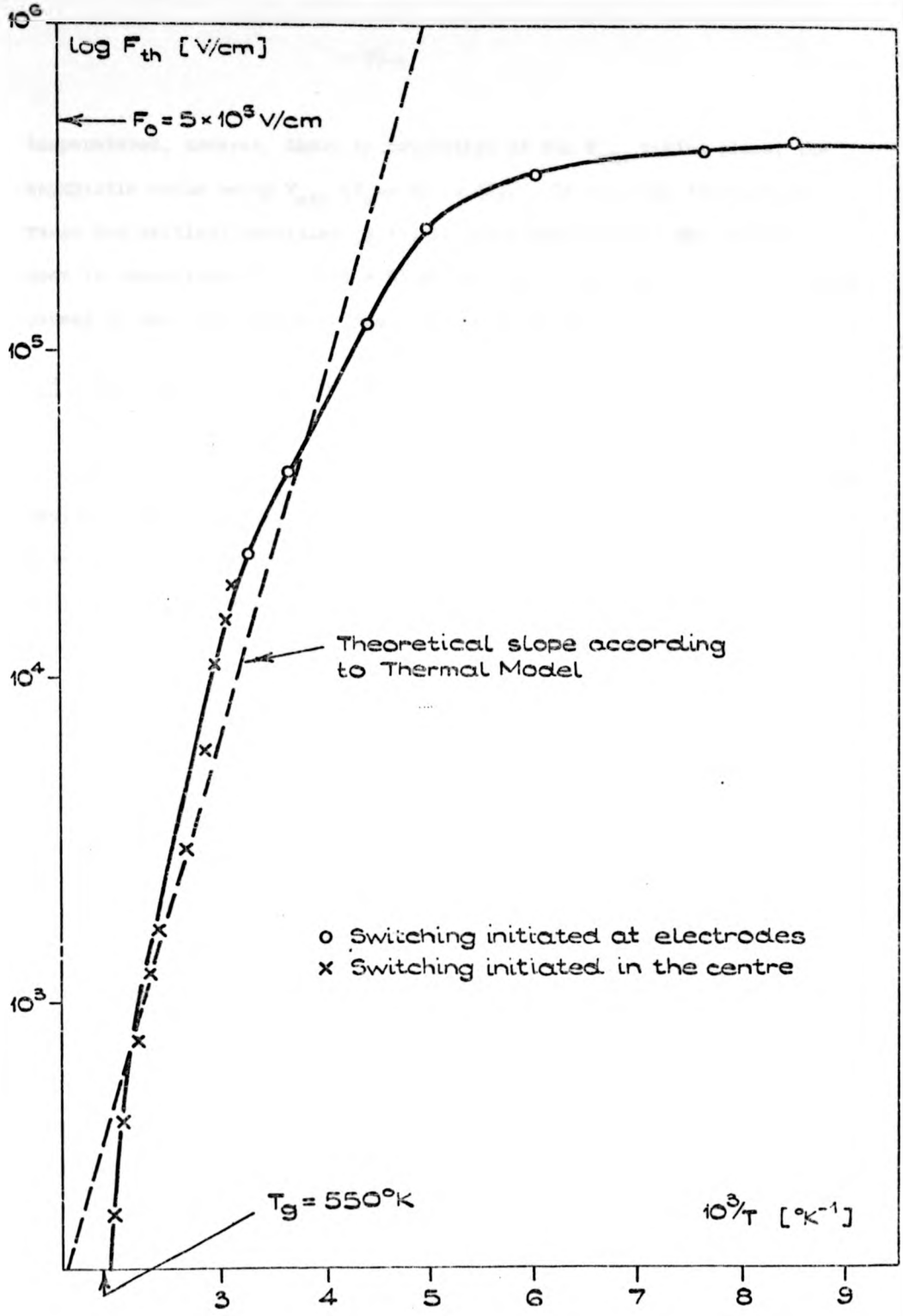

Fig. 3.4.

VARIATION OF THE LOGARITHM OF THRESHOLD VOLTAGE WITH RECIPROCAL TEMPERATURE ACCORDING TO THE MODEL OF

temperatures, however, there is saturation of the V_{sth} taking place, the asymptotic value being $V_{sth}\ (T_a \rightarrow 0) = dF_o$. In this low temperature range the critical condition (3.15) is first satisfied at the regions near the electrodes (i = 0, i = D) as the switching transition is primarily caused by the large value of the electric field at the electrodes.

3.3 Two Dimensional Thermal Model

A single dimensional thermal model of switching can only account adequately for the situations in which the current density in the switching device is uniform, i.e. in which no current constriction into a filament takes place. Therefore the 1-D model can only account satisfactorily for the initiation of switching. The subsequent transition into the "on"-state necessitates the use of, at least, a 2-D model and ideally a 3-D model should be used for description of the "on"-state. This is one of the reasons for a considerable effort which was directed towards the mathematical solution of the equations (2.25 - 2.26) with appropriate boundary conditions in two and three dimensions. Unfortunately, up to the present date this problem has not been solved in a satisfactory manner. It is appropriate therefore to discuss some of the difficulties encountered in solving the mathematical problem.

There is no known analytic method of solution of the system (2.25 - 2.26) with any realistic set of boundary conditions. Moreover, there is, to the author's knowledge, no known method of determining the qualitative features of the solution (e.g. existence, uniqueness), for a set of boundary conditions appropriate to the switching problem. When finite-difference methods of solution are employed there occur difficulties connected with

(i) designing the practical numerical technique which would yield a numerically stable solution

(ii) the questions of convergence of the approximate solution S(h) to the exact solution S as the mesh size h is decreased to zero.

The main reasons for the difficulties encountered in the use of finite-difference methods rest in the non-linearity of the equations (2.25 - 2.26). At the threshold of switching the heat generation term in (2.25) sharply increases and the character of the solution suddenly changes. If the computational scheme is not sufficiently stable then spurious solutions occur after the threshold value is exceeded. The tendency of the computational scheme towards instabilities is not only dependent on the character of the equations which it represents but also on the boundary conditions imposed. In general, boundary conditions in which values of the unknowns are specified on the boundary of the domain of integration (Dirichlet problem) will be less likely to render the finite-difference scheme susceptible to instabilities than the type of boundary conditions in which values of the unknowns and/or values of derivatives of the unknowns with respect to the normal to the boundary are specified on the boundary (mixed and von Neumann problem)[13]. Numerical instability in a finite difference scheme of a given kind is also generally more likely to occur if the scheme is applied to a system of equations rather than to one equation only.

Two- and three-dimensional switching problems were considered by several authors[9-12] who introduced various simplifications in the system (2.25 - 2.26) or in the boundary conditions. None of these authors describe their methods of solution and therefore critical consideration of their solutions is difficult: as explained earlier the considerations of the finite-difference scheme and its stability are important in order to ensure that the instability in the solution at the switching transition is of the physical (or "genuine") and not of the numerical nature, in other words that the "switching" is not caused by the divergence of the numerical method.

At the present time there is, to the author's knowledge, no method of numerical solution of the system (2.25 - 2.26) with any set of realistic

boundary conditions which is theoretically shown to be stable and convergent. Early attempts of the author of this thesis to solve the system (2.25 - 2.26) with mixed boundary conditions in two dimensions resulted in finite-difference schemes which numerically "exploded" at certain values of the applied electric potential although the schemes were unconditionally stable if applied to linear equations. It became therefore apparent that the speed of convergence of the numerical method is an important factor; search for schemes with rapid convergence was made and also the boundary conditions for the system (2.25 - 2.26) were limited to the Dirichlet type. A semi-explicit iterative scheme described by Gunn[13] proved to yield numerically stable solutions. Gunn used the scheme for the solution of the equation.

$$\nabla(a\nabla u) = f \tag{3.19}$$

(a,f are given functions, u is unknown) subjected to various boundary conditions. Based on the method of Gunn an iterative scheme was developed for the solution of the steady state form of the equation (2.26) with Dirichlet boundary conditions. For the solution of the heat equation (2.25) an iterative method described by Peaceman and Rachford[14] was used. The domain of integration was a rectangle and cartesian coordinates were employed. The potential φ and the temperature T were functions of x and y coordinates; thus the problem represented the problem of heating in a block infinite in the z-direction (Fig. 3.5) with electrodes applied to its two surfaces ((1) and (2)) and with all its surfaces held at ambient temperature T_a. The values of the potential φ on the parts (3) and (4) of the boundary were approximated by the function

$$\varphi(X) = \frac{V_p}{2}\left(\frac{X}{I} - 1\right) \tag{3.20}$$

(this expression is exact if there is a uniform temperature distribution in the integration domain). At the begining of the computation T and φ are approximated by linear distributions and with this zeroth approximation

the heat equation (2.25) is solved. The new temperature distribution given by the heat equation (2.25) is used in the equation (2.26), solution of which gives a new potential distribution used in turn in the heat equation. This outer iteration cycle is shown in the block diagram (Fig. 3.6).

A computer programme corresponding to the above block diagram appears in the Appendix 1. The rates of convergence achieved with this programme were comparable with those quoted by Gunn[13]. (If one operation is defined as one outer iteration cycle with the inner iterations performed 9 times then the initial error norm in the solution (resistance of the device) was reduced by the factor 10^{-2} (10^{-5},10^{-6}) in 7 (21,35) operations). The conductivity dependence on temperature was assumed of the form $\sigma = \sigma_o \exp(-\theta/T)$ (2.16). Using this programme, several "computer experiments" were performed in order to investigate the nature of the solution of the two-dimensional switching problem. The basic "experiment" aimed at ascertaining the qualitative features of the solution, namely the presence of

(i) a current filament,

(ii) a negative differential resistance of the "device",

(iii) a "hysteresis" effect in the solution.

The solutions $T(x,y)$ and $\varphi(x,y)$ were in all cases smooth "surfaces". (There were no points in which the solutions would have extreme or oscillatory values typical of numerically unstable solutions.) The temperature surface was always convex with no inflection points and no features which could be interpreted as the hot filament. In this experiment the applied potential difference $V_B = \varphi_a - \varphi_c$ (entering the boundary conditions) was varied whilst all the remaining parameters (e.g. ambient temperature, activation energy for conduction) were kept constant. It was found that the current through the "device" is always a strictly increasing function of the applied potential difference and in this sense there is no

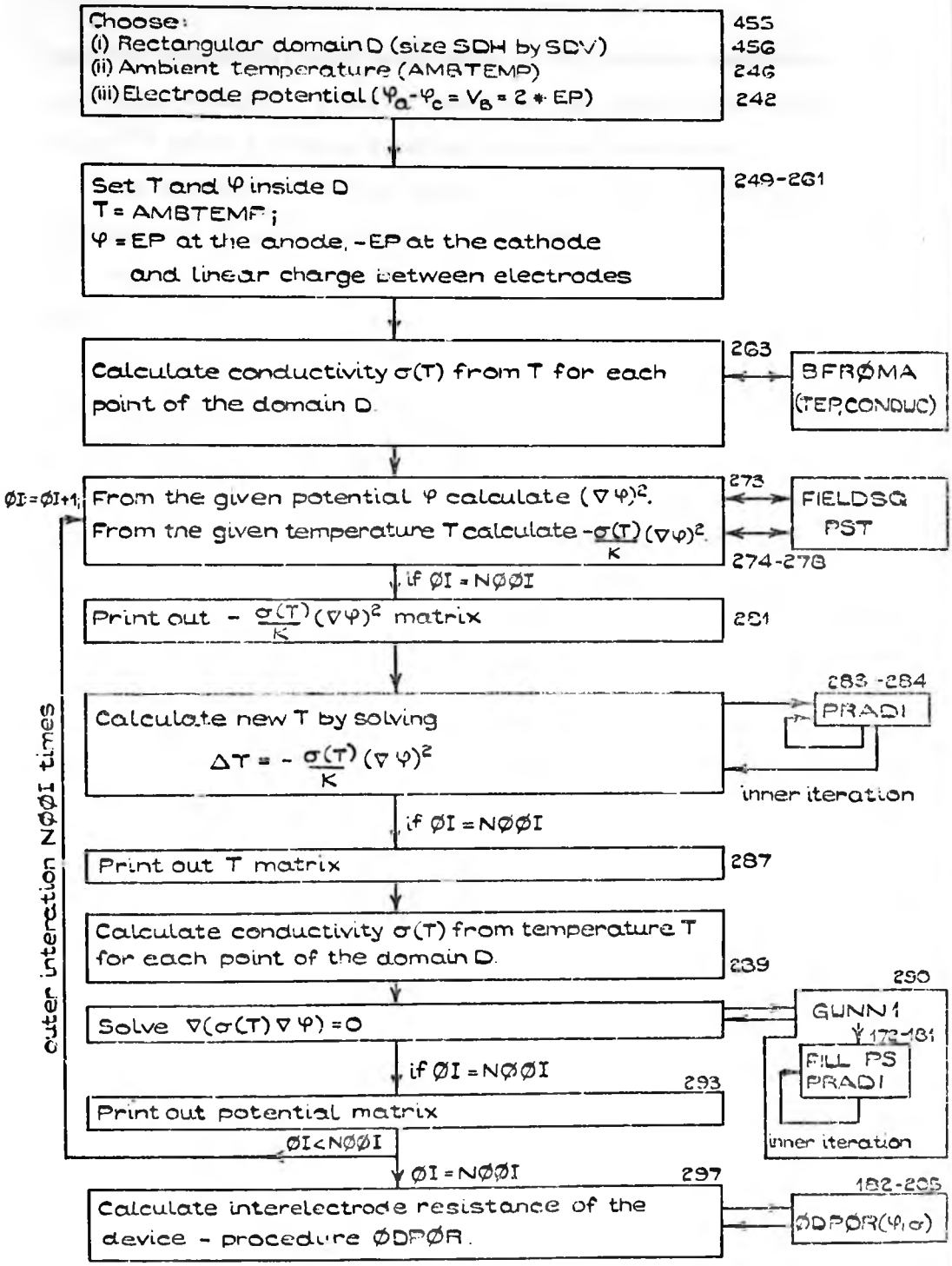

Fig.3.6.

COMPUTATIONAL METHOD FOR 2-D SWITCHING PROBLEM
Numbers by the blocks refer to the order number of

negative differential ressistance region on the simulated quasistatic I - V characteristic. A similar result has been found by Kaplan and Adler[12] for 2 - D problem solved in cylindrical coordinates.

An important new feature (which, to the author's knowledge has not been reported in the literature) is the existence of what can be described as a "hysteresis" effect in the solution of the 2 - D problem. The meaning of this effect can be seen from Fig. 3.7 where the current through the "device" is plotted against the applied potential difference V_B. As the voltage is increased from zero to a certain value $V_B = V_{th}$ there is a sharp increase in the current. Above the voltage $V_B = V_{th}$ the temperature in the "device" is very high and the resistance of the "device" R_{on} is much smaller than the "off"-state resistance ($V < V_{th}$) and is approximately constant as the voltage is further increased. If the applied voltage is now decreased and the initial temperature and potential distributions (zeroth iteration) for each calculation are taken as the final solutions of the previous calculation (computer programme cards 246 - 261) it is observed that the current through the device remains high for a range of voltages below $V = V_{th}$ and drops to the "off"-state value at some voltage $V_h < V_{th}$. Thus it is seen from Fig. 3.7 that for the values of the applied potential difference from the range (V_h, V_{th}) two solutions of the 2 - D finite-difference problem can exist: one "on" state solution and one "off"-state solution depending on the previous "history". The hysteresis effect was also observed if saturation into (2.16) was introduced at $T = 1000^{\circ}K$.

As a consequence of the hysteresis of the I - V characteristic of the device the load line $I = (V_B - V)/R_s$ can intersect the I - V curve at two points. Thus the hysteresis effect could explain the existence of the negative differential resistance in a real experimental situation where a resistor R_s is connected in series with the switching device and the supply of voltage V_B. If there is a discontinuity between points B and C then

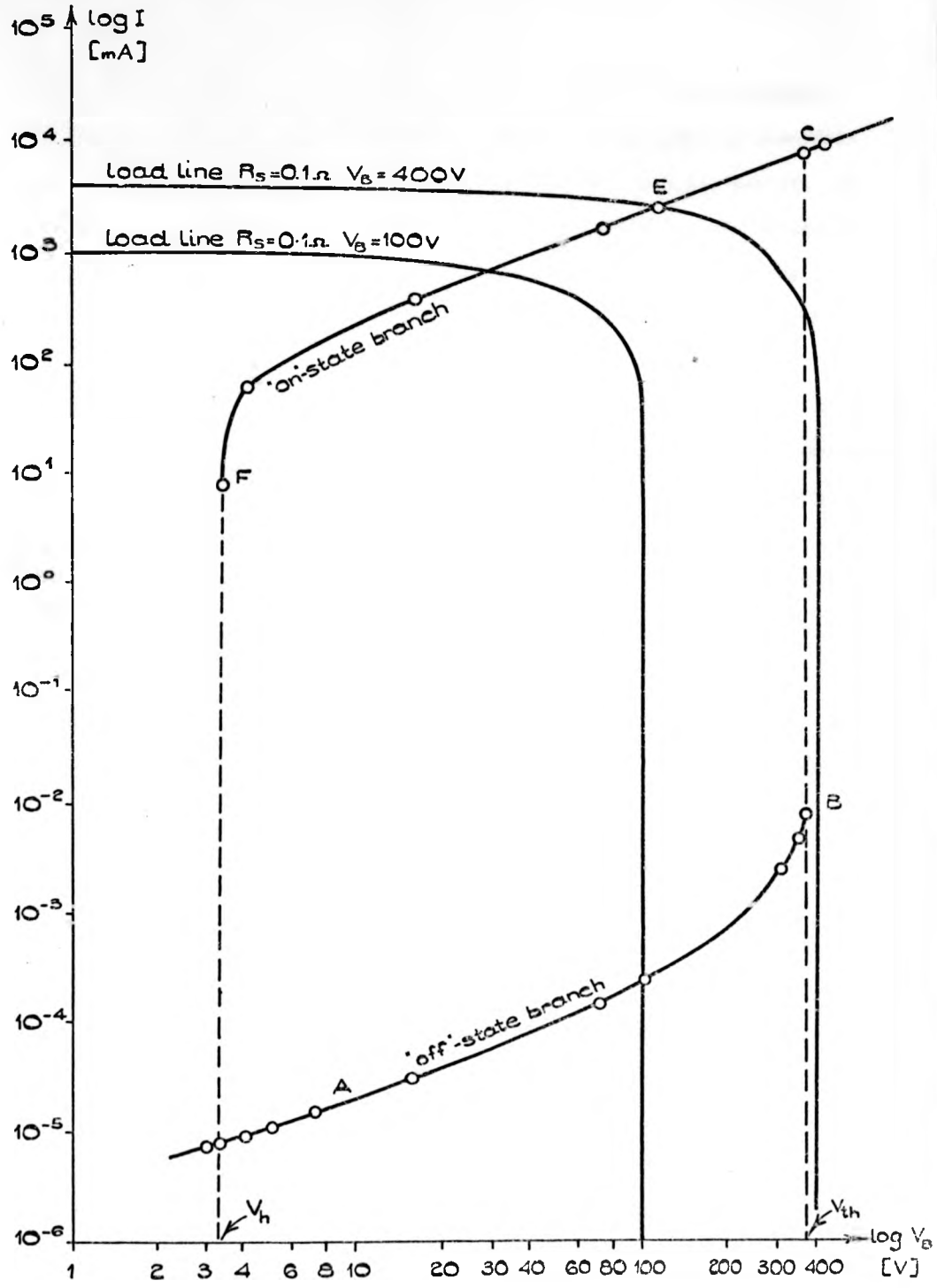

Fig.3.7.

HYSTERSIS EFFECT EXHIBITED BY COMPUTED I-V CHARACTERISTICS BASED ON THE 2-D THERMAL MODEL.

there will be a jump of the representative point from B to E when the voltage V_B is sufficiently increased. It was not possible to ascertain by the computer experiments whether the section BC, in fact, exists; it appears to be practically vertical: either "on"-state or "off"-state is obtained in the neighbourhood of the voltage V_{th}, attainment of any intermediate states did not seem possible even when the voltage V was increased by very small increments. Therefore the possibility of discontinuous I-V characteristic remains to be verified. For time-dependent solutions (which were not considered) the nature of the solutions corresponding to the section BC may be such that the representative point tends to move along the load line towards the intersection with the high current branch (E) as soon as the voltage V_B is increased to the extent that the load line intersects BC. This would constitute another explanation for the observed negative differential resistance region in terms of the thermal model.

It has been argued by several authors that the thermal mechanism cannot

(i) yield a negative differential resistance region[12]

or (ii) yields a negative differential resistance region in which the representative point can be stabilized (contrary to experimental observations)[16].

Such assertions may seem premature in the light of the results of the 2 - D analysis presented in this section. Above all it is possible that even the 2-D formulation of the problem is still too crude (2-D solutions can be qualitatively different from 3-D solutions[15], the boundary conditions imposed can also be of an essential importance, the Dirichlet type may be unrealistic).

Certain experimental evidence accumulated over the past two years seem to favour non-thermal interpretations of the switching phenomena and

this fact must be the ultimate measure of the usefulness of the thermal model of switching. The purpose of this section was, however, to show that the thermal model is not fully resolved mathematically and therefore it is not possible to discount the thermal theory on the basis of the failure of approximated models to account for experimental observations.

3.4 Model for the Time Variation in Switching Parameters

3.4.1 Variability of Switching Parameters

The performance of a switching device is often described in terms of the threshold voltage V_{th} and the delay time t_d (defined for a given overvoltage $V > V_{th}$). There are other important parameters (e.g. threshold and holding currents, "off"-state resistance of the device, etc.), but the following discussion will concern mainly these two basic switching parameters (V_{th} and t_d).

Any switching device has a certain finite lifetime during which the switching parameters are slowly changing from values which are satisfactory for the given purpose to values which are intolerable. Apart from this slow and irreversible change in the switching parameters there is in many cases observed a considerable variability on a much shorter scale. For example, the switching threshold voltage is found to vary from operation to operation, the changes being of positive and negative value around some average value and appearing to be random at first sight. The variation of the delay time t_d is best measured under the application of rectangular pulses. The variation is schematically shown in Fig. 3.8 for three applications of a rectangular pulse of length t_p. The variation in threshold voltage is more conveniently measured by using a sawtooth waveform (see section 3.4.3.); the threshold voltage V_{th} is then associated with the maximum voltage across the device. This also exhibits variation.

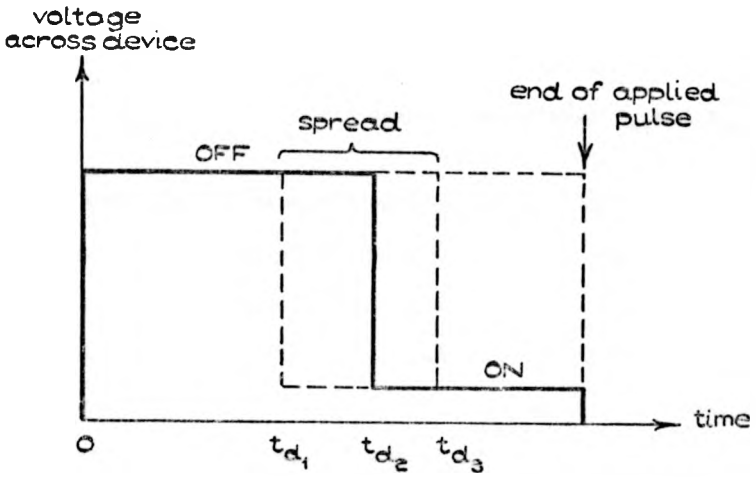

Fig. 3.8.

SCHEMATIC DIAGRAM OF THE DEVICE RESPONSE TO RECTANGULAR PULSES.

3.4.2 Analysis of Variability

The most obvious type of analysis of the variability of the switching parameter p ($p \equiv t_d$ or $p \equiv V_{th}$) is the determination of the distribution function $\varrho(p)$, which, when integrated between two values of its variable gives the probability of a switching effect occuring with the values of the parameter between the limits, eg.

$$\int_{t_{d1}}^{t_{d2}} \varrho(t_d)dt_d = \text{probability of switching event with delay time between } t_{d1} \text{ and } t_{d2}. \quad (3.21)$$

In this type of analysis the time sequencing of the data is not considered and therefore certain information is lost. Moreover, any correlation effects present cannot be revealed by this analysis.

When the time sequencing is considered, the switching parameter p is labeled by the order number of the switching operation n and a sequence of the switching parameters then constitues a discrete time series $\{p(n)\}$. The characterization of the time series is most conveniently achieved by constructing a correlogram[17,18], which is the graph of the quantity

$$R(m) = \frac{\langle X(n)X(n+m)\rangle}{\langle X^2(n)\rangle} \quad (3.22)$$

against the number m. In (3.22) R(m) denotes the normalized autocorrelation coefficient of a transformed quantity X (X is p (t_d or V_{th}) processed to have a zero mean) at lag m, brackets $\langle\ \rangle$ denote averaging over n.

The function R(m) has a maximum at m = 0 and decreases (or its envelope decreases) with increasing m. The rate of decrease is faster the smaller is the degree of correlation between subsequent events p(n). The value of $m = m_o$ at which R falls by 1/e can be related to a characteristic correlation time (for white noise $m_o = 0$, for completely correlated events $m_o = \infty$) and events X (or p) separated by m_o are (on statistical scale) correlated, i.e. have some causal connection. Thus the time series analysis can reveal an existing non-statistical (deterministic) component in the data which may appear random at first sight.

The Fourier transform of R(m) is denoted by G(k) and can be shown to give the spectral power density of the signal represented by the analysed sequence p(n) at discrete set of frequencies $f_k = \frac{k}{M}\frac{1}{2t}$ M = max (m) and t is the sampling interval (e.g. time between successive operations of the switching device). A completely random process has a flat spectrum (white noise), a periodic process with no random component gives a discrete spectrum ($G(k) \gg 0$ at the fundamental frequencies).

3.4.3 Results of the Analysis

Note: This section does not conform to the general layout of the thesis given in section 1.5 since the description of experiments and presentation of the results is concentrated in Chapter 5. The reason for discussing the results at this point is that the theoretical model described in the next section (3.4.4) is directly influenced by the results of the analysis and therefore for the sake of logical continuity the experimental results are described first.

The histograms of the delay times and the threshold voltages of a switching device, obtained in an experimental set up shown in Fig. 5.23 and Fig. 5.24 (in Chapter 5) have been found to change with time. The number of data points in any one histogram were chosen to be $2048 = 2^{11}$ (because of the construction details of the multichannel analyser used). After this number of measurements was completed the memory content was plotted out by a plotting facility, the memory erased and a new series of 2048 measurements was commenced.

The time taken to complete one histogram was about 2½ minutes and at the frequency used ($f_e = 25\,Hz$), the number of device operations to each measurement was ~ 4000 (the device was still operating during the plotting of the histogram). Fig. 3.9 shows a series of 4 histograms taken in succession and two features, which were found for both types of histograms ($\rho(V_{th})$ and $\rho(t_d)$) can be observed:

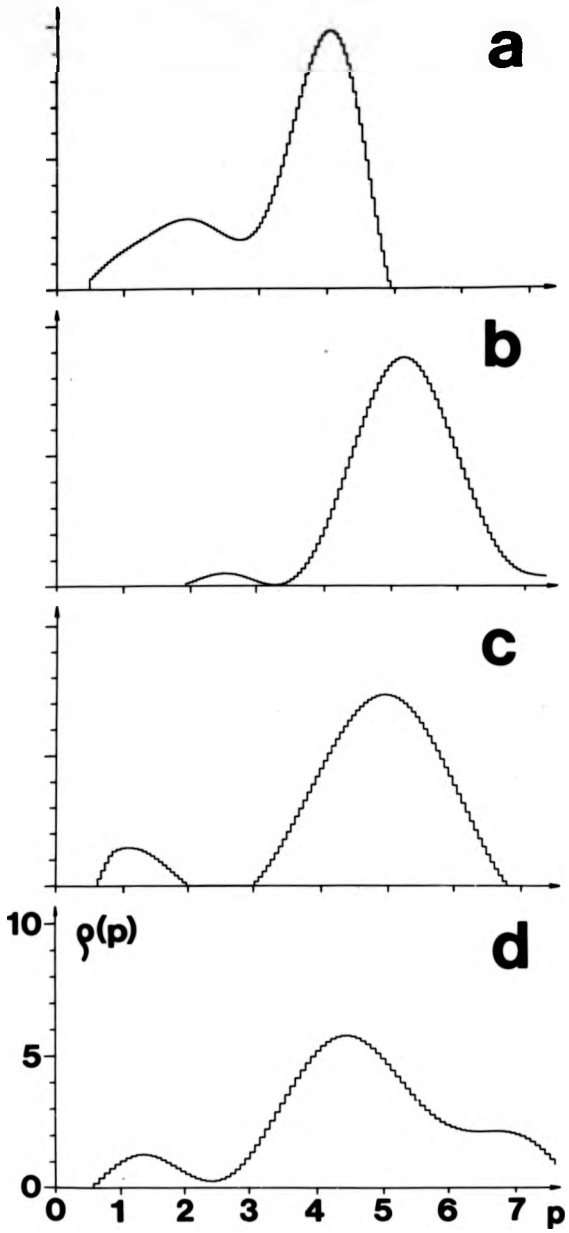

Fig.3.9.

CHANGES IN THE DISTRIBUTION OF SWITCHING PARAMETER p.

ORDINATE : arbitrary units.

ABSCISSA : 1V/unit if p relates to switching voltage
0·2m·s/unit if p relates to delay time.

(i) the existence of more than one maximum in the distribution; the side peaks started to grow suddenly during measurement

(ii) the position of the main maximum is changing with time (Fig. 3.9.a – 3.9.d).

The results in Fig. 3.9 indicate that a significant change in the distribution occurs over the period of ~10 minutes or over 1.5×10^4 device operations. Over much longer periods of operation (several hours) it was found in the case of the delay time histogram that the spread of the distribution diminished and also the average delay time shifted to lower values. This behaviour is interpreted as an ageing process present in the switching device. This means that the process of generating the statistical data is not a stationary process.

Over a short time interval, however, the trend in the data can be neglected (or removed by a mathematical transformation) and the process considered as a quasistationary. The number of pulses examined in the time series analysis was of the order of several hundreds. A typical record of the threshold voltage variation is shown in Fig. 3.10.a - d. together with the corresponding quantities R(m) and G(k). The rate at which the autocorrelation coefficients decrease with the time lag suggests that the switching operations spaced less than ~15 cycles are correlated.

In the next section we attempt to explain the observed behaviour using a model based upon a structural changes in the switching device.

3.4.4 Theoretical Model

From the experimental results presented in the previous section it is seen that there are two distinct variations in the switching parameters: the first one is a relatively slow gradual change or ageing occurring during the whole life of the device, the second is a rapid variation occurring from operation to operation.

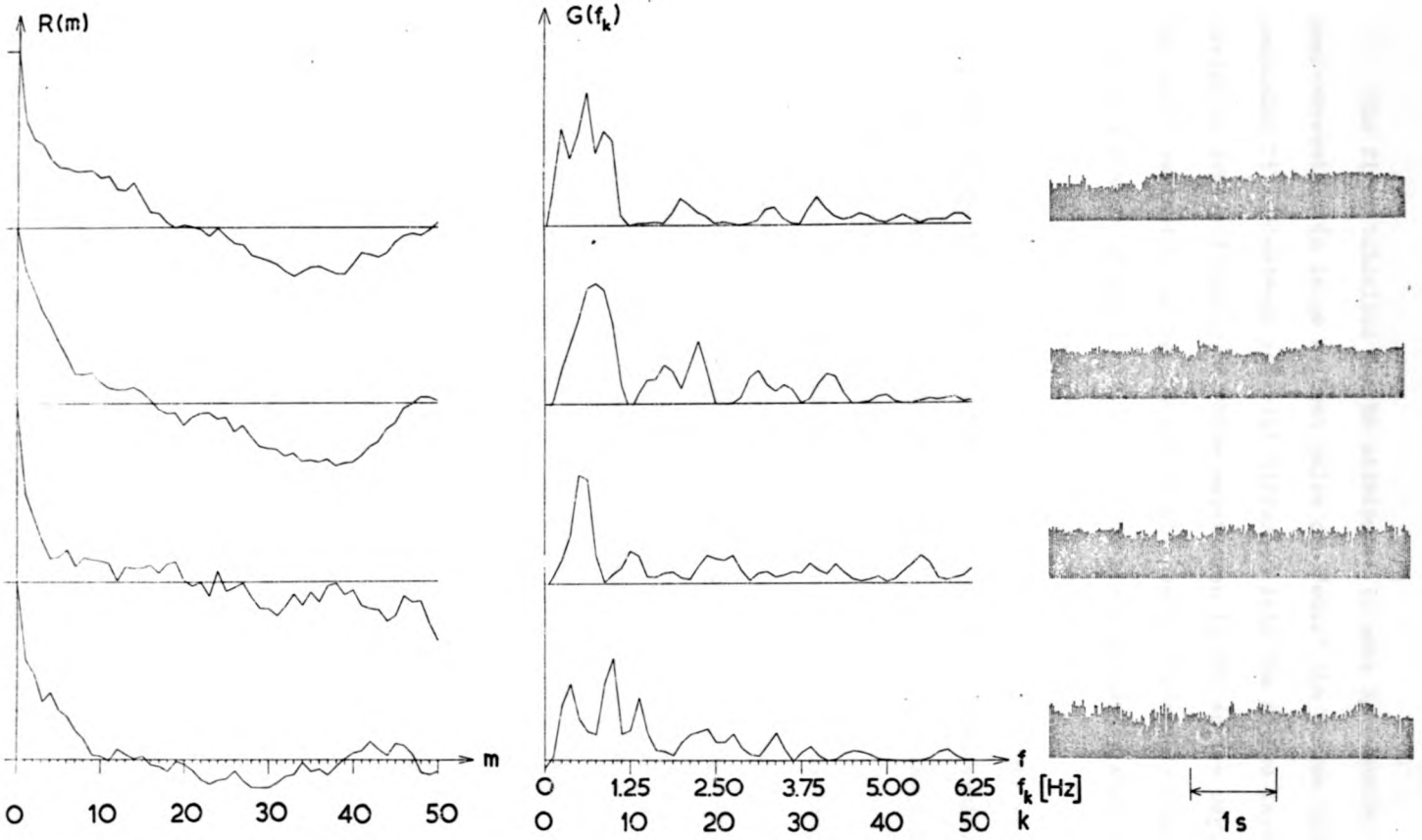

Fig. 3.10. a,b,c,d (from top to bottom)

EXAMPLES OF THE QUANTITIES R(m), G(k) AND OF THE RECORDS OF THE VARIATION OF THRESHOLD VOLTAGES.

The first behaviour can be attributed to some irreversible or semi-reversible (a large current pulse can "cure" the device temporarily) mechanism like electrode material diffusion into the active layer of the device or crystallization or phase separation in the active region, whereas the rapid variation can be associated with small reversible changes in the size or a number of small crystallites or phase separated regions. The plausibility of this assumption is supported by

(i) the existence of a forming process which always occurs when a virgin device is being operated for the first time, exhibiting a certain change (generally a decrease) in the switching parameters followed by a relative stabilization,

(ii) the experimental indication that there is no sharp division between the threshold and memory type of switching behaviour. Aged threshold devices often show behaviour resembling the memory action.

(iii) the experiments in which a memory device is operated as a threshold device using extremely short (ns) pulses for excitation (Thomas et al., ref. 8). Microcrystallites of needle-like shape have been observed in such devices. These devices also show about 10% scatter in their switching parameters[19].

(iv) the finding that the resistance of a threshold device changes slightly after each switching operation[1].

(v) the slow gradual ageing of bulk threshold devices (thicker devices age more readily) attributed to crystallization. A large current pulse can cure (temporarily) the device, similarly as a reset pulse applied to a memory device.

The autocorrelograms in Fig. 3.10 show a decay by a factor of 1/e in 5 - 10 steps of the lag m. This suggests a causal connection between subsequent fluctuations in the switching parameters of the device. In some cases (Fig. 3.10.a,b) the autocorrelograms seem to follow a kind of oscillatory

dependence, this will be discussed later. The natural question which now arises is what is the mechanism responsible for the causal connection between the fluctuations.

There are several tools of statistical inference[17] such as the method of trend and moving averages, the method of hidden periodicities, the functional approach or the approach involving autoregression analysis. The choice between these methods depends on the shape of the correlogram, on the nature of the expected mechanism responsible for the fluctuations and, to a certain extent, on intuition.

For the problem in hand, the assumption that an autoregressive process is responsible for the observed behaviour seemed to be the most plausible one. The autoregressive process is a representation of a system changing under its own internal forces which, being damped, are regenerated by a stream of random external perturbations[20]. If we assume that the state of the switching device after the n-th operation can be represented by x_n then the autoregressive process is formally characterized as

$$x_{n+1} = F(x_o, x_1, \ldots, x_s; r_o, r_1, \ldots, r_s, r_{s+1}) \cdot x_n \quad s < n \qquad (3.24)$$

where F is an operator and r represents a discrete random variable. Thus the (n + 1)-st value of the switching parameter x depends on its previous values (deterministic component of F) and a random variable r (non-deterministic component of F).

In most practical applications F is a linear form of the variables and then the values of x are said to be generated by a linear autoregressive system. If the linear function F is a function of only one variable, r_{n+1}, then the values of x will form a non-correlated time series. A physical example of such a situation is the statistical variation of the delay times in the occurence of an electrical discharge in gas after the application of a sufficiently high voltage to the electrodes. The variation is associated with the occurence of critically ionizing particles[21], which

is a random process, and the operation of the discharge tube is independent of the preceding operations. In the other extreme, if F depends on the deterministic component only, the performance of the system will be completely predictable, deterministic. It should be noted that F can represent a whole process, e.g. a solution of a differential equation, the variables of F acting as parameters in the initial or boundary conditions. However, the problem (3.24) has been solved in general only in the case where F is a linear function[17,22].

In particular, let us consider the linear autoregressive system

$$x_{n+1} = ax_n + x_{eq}(1 - a) + r_{n+1} \tag{3.25}$$

where $0 < a < 1$ is a number. If there are no random perturbations r on the right-hand-side of the recurrence formula (3.25) it is a matter of a simple calculation to show that the values of x will tend exponentially to the equilibrium value x_{eq}:

$$x_n = (x_o - x_{eq})\, a^n + x_{eq} \tag{3.26}$$

where x_o is the initial value of x. If there are random perturbations present in (3.25) it can be shown that the theoretical values of the autocorrelations of the series corrected for zero mean (subtract x_{eq} if $\langle r \rangle = 0$) are given by

$$R(m) = a^m \tag{3.27}$$

It is seen that R(m) falls by a factor of $1/e \approx 0.37$ in $m = n_o$ steps, where

$$a = \exp(-1/n_o) \tag{3.28}$$

Thus the correlation in the time series (3.25) increases as the rate of return of the system (3.26) to equilibrium (displaced by a single perturbation $(x_o - x_{eq})$) decreases.

It can be shown[23] that if (3.26) is replaced by the law of damped oscillations

$$x_n = (x_o - x_{eq}) \cos(\omega n) \exp(-n/n_o) + x_o \tag{3.29}$$

then the autocorrelogram of the time series with the random perturbations of the additive type (3.25) also exhibits a damped oscillation with very nearly the same frequency ω. This illustrates that the shape of the autocorrelogram is intimately connected with the properties of the generating autoregressive system.

Having introduced the basic concepts of regression analysis we now turn to the consideration of a possible mechanism by which a single perturbation in the state of a switching device would diminish over $n_o = 5 \sim 10$ switching operations and would show some kind of oscillation (not necessarily of the kind (3.29)), in order to explain the shape of the autocorrelograms in Fig. 3.10.

Let us assume that the state of the switching device can be characterized by a single scalar quantity: the volume fraction of conducting crystallites or phase-separated regions inside a semiconducting non-crystalline matrix of a switching device. The plausibility of such an assumption has been discussed to a certain extent at the begining of this section. The switching parameters t_d and V_{th} will depend on the volume fraction (denoted by x) in some way which we do not exactly specify. The behaviour of the switching device may, for instance, depend on one or more regions like that in Fig. 3.11. The current path is interrupted by the gaps between the conducting regions. There may exist a series or a parallel (or both) connections of these regions and we assume that the switching parameters t_d and V_{th} will depend on the volume fraction x of the conducting phase. As we are dealing only with small changes in x around the equilibrium value, the functions $t_d(x)$ and $V_{th}(x)^*$ can be replaced by linear relationships and thus the changes in t_d and V_{th} will be proportional to the changes in x. Now as the following regression analysis is invariant with respect to linear transformation, having determined the statistical behaviour of x we shall be able to apply the result directly to the behaviour of the switching parameters t_d and V_{th}.

* for a possible functional dependence see reference[24].

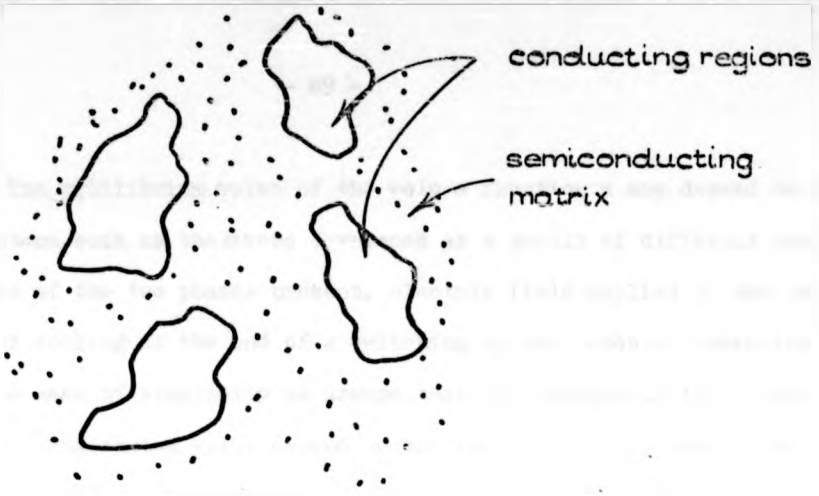

Fig. 3.11.

POSSIBLE STRUCTURAL CHANGES IN THE SWITCHING DEVICE.

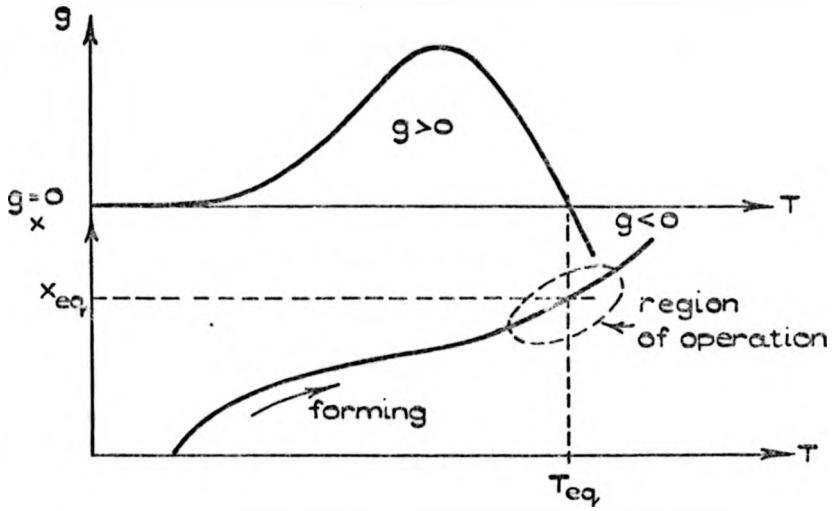

Fig. 3.12.

RELATIONSHIPS BETWEEN GROWTH RATE, g, VOLUME FRACTION, x, AND EFFECTIVE TEMPERATURE, T (SCHEMATIC).

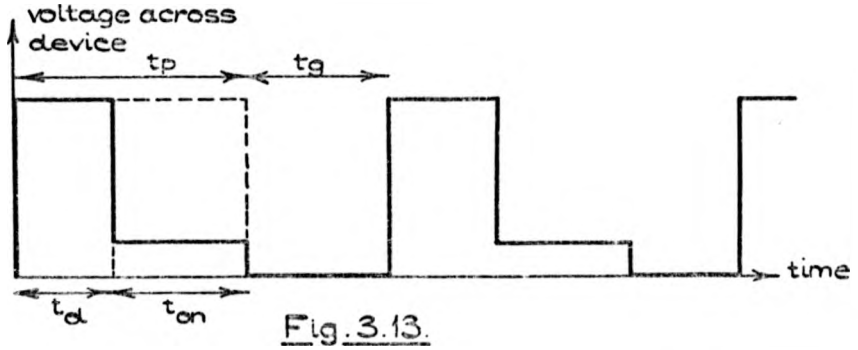

Fig. 3.13.

DEFINITION OF TIME INTERVALS DURING APPLICATION OF

The equilibrium value of the volume fraction x may depend on many parameters such as the stress developed as a result of different specific volumes of the two phases present, electric field applied to the device, rate of cooling at the end of a switching cycle; mode of operation, etc. For the sake of simplicity we assume that the changes in the volume fraction and its equilibrium value depend on one parameter only, namely the effective temperature T in the switching device during operation (T is not necessarily the physical temperature). We further assume that the dependence of the growth-rate g of the conducting phase on the effective temperature is given by Fig. 3.12., i.e. below some equilibrium temperature T_{eq} the growth-rate is positive and above this temperature the growth-rate is negative. The shape of the function g(T) in Fig. 3.12 schematically represents the relationship

$$g(T) = A \exp(-b/T)(T_{eq}-T) \qquad (3.30)$$

which holds in cases where the mass transfer is determined by thermally activated diffusion. The effective temperature T of the switching device during operation (i.e. when there is an applied voltage) is assumed to increase with the volume fraction x of the conducting phase as the heat dissipated in the device during the application of the switching pulse is proportional to the conductance of the device. The schematic graph of $T = T(x)$ is given in the lower part of Fig. 3.12.

Let us now calculate how the volume fraction x changes with time when a d.c. voltage is applied to the switching device with an initial volume fraction x_o ($x_o \approx x_{eq}$). We approximate the functions $g = g(T)$ and $T = T(x)$ by linear relationships for small changes of T and x around their equilibrium values

$$g(T) = c\,(T_{eq} - T) \qquad c > o \qquad (3.31)$$

and

$$T(x) = k(x - x_{eq}) + T_{eq} \qquad k > o \qquad (3.32)$$

Combining (3.31) and (3.32) one gets for the growth rate

$$g = \frac{dx}{dt} = - kc(x - x_{eq}) \tag{3.33}$$

Solving this for x with the initial condition $x(o) = x_o$ gives

$$x(t) = (x_o - x_{eq}) \exp(-kct) + x_{eq} \tag{3.34}$$

Thus an initial perturbation in the value of the volume fraction $(x_o - x_{eq})$ decreases exponentially to zero and x stabilizes at the value of x_{eq}. This stabilization can extend over many switching operations if $1/kc \gg t_{on}$, the length of time for which the device remains in the "on"-state at each application of the excitation pulse (see Fig. 3.13 for definition). If we denote by t_{oneq} the average time for which the device is in the "on"-state during a single operation (this time varies from operation to operation and it is the basis of a more refined analysis outlined below, see (3.44)), by x_n the volume fraction at the begining of the n-th "on"-state, then using (3.34) we can calculate the volume fraction at the end of the n-th "on"-state:

$$x_{n+1}' = \exp(-kct_{oneq})x_n + x_{eq}(1 - \exp(-kct_{oneq})) \tag{3.35}$$

During the subsequent n-th "cooling-off" period the volume fraction will somewhat increase from x_{n+1}' to the value of x_{n+1} because the effective temperature will decrease through the values for which the growth-rate is positive. This increase is given by

$$\Delta x_{n+1} = x_{n+1} - x_{n+1}' = \int_o^{\Delta t} g(T(t))\, dt \tag{3.36}$$

where T(t) is the function describing the change of temperature with time during the cooling-off period Δt. From Fig. 3.13 it is seen that $\Delta t = t_g + t_d(n + 1)$. The delay time of the (n + 1)-st switching pulse will depend on the volume fraction at the begining of the (n + 1)-st pulse

and so will the duration of the (n + 1)-st "on"-state, see relation (3.44); for the time being let us neglect this second order effect assuming that $t_g \gg t_d$ and regarding Δx to be constant. Then the volume fraction x_{n+1} at the begining of the (n + 1)-st "on"-state is given in terms of the volume fraction x_n at the begining of the n-th "on"-state (one operation earlier) by the relationship

$$x_{n+1} = A\,x_n + x_{eq}(1 - A) + \Delta x \qquad (3.37)$$

where

$$A = \exp(-k c t_{oneq}) \qquad (3.38)$$

If we now postulate the existence of random fluctuations in the volume fraction, occurring after each switching operation and being of the additive type (3.25), then introducing these fluctuations r_n into (3.37) gives

$$x_{n+1} = A\,x_n + x_{eq}(1 - A) + \Delta x + r_{n+1} \qquad (3.39)$$

which represents a linear autoregressive process.* The postulated random fluctuations in (3.39) can be physically interpreted by considering the statistical nature of mass transfer. The changes in the volume fraction are determined by the diffusion process which is a macroscopic aspect of the microscopic motion of atoms and this contains a certain degrec of randomness (Brownian motion). If short time intervals and small volumes of mass are involved in the mass transfer, then the randomness of the microscopic motion will be manifested in the random fluctuations of the macroscopic rate of mass transfer. The degree of manifestation of these effects in switching devices may be considerably increased if the shape of the conducting regions (Fig. 3.11) involves sharp tips or edges pointing in the direction of the applied electric field. In this case, which is likely to occur if the electric field enhances the diffusion process (c.f. references (26 - 30) in Chapter 2), small changes in the shape of the tips or edges can

* Note: (3.39) can be made formally identical with (3.25) by writing -

$$a = A \qquad (3.40a)$$

produce large effects on the switching parameters of the device (e.g. via field emission from the sharp edges). Thus the diffusion mass transfer can be considered as the cause of random fluctuations in the volume fraction of material transferred per unit time. (A diffusion process has been considered, albeit in a different context, as a cause of stochastic variation by Richardson[25]).

A possible competing model leading to an autoregressive scheme of the type (3.39) and not involving structural changes could be based on the observations reported by Lee et al[26]. These authors observed that the resistance of the switching device increases to a steady value for considerable periods of time (minutes) after a switching operation; the final resistance of the device can fluctuate by a few per cent. Lee et al attribute these fluctuations to the redistribution of residual charge in the traps (although they also admit the possibility of minor structural changes); the distribution of the charge in the traps influences the transport properties and therefore the resistance of the device. The random fluctuations in the resistance of the device are then the consequence of the stochastic nature of the diffusion and trapping of the residual charge after switching operations. It is possible that a combined structural and electronic effect could account for the existence of random fluctuations in the scheme (3.39) but this was not considered in the present work.

Let us now turn to the implications of equation (3.39). Comparison between (3.28), (3.38) and (3.40a) enables the lag number n_o (at which the value of the autocorrelation coefficient of the process (3.39) falls by 1/e) to be expressed in terms of the parameters of the model:

$$n_o = \frac{1}{k\ c\ t_{oneq}} \qquad (3.41)$$

By choosing the values $k = 100^{\circ}K$, $c = 1^{\circ}K^{-1}s^{-1}$ and $t_{oneq} = 2$ ms one

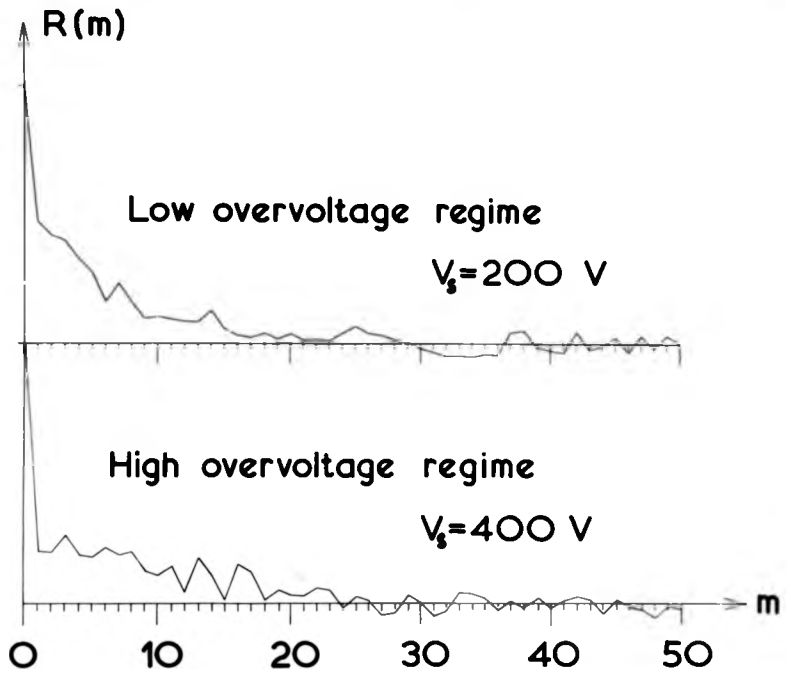

Fig.3.14.

EXPERIMENTAL AUTOCORRELOGRAMS OF THE TIME-SERIES OF THRESHOLD VOLTAGES FOR TWO REGIMES OF OPERATION.

obtains $n_o = 5$ in agreement with observation (Fig. 3.11), but in view of the uncertainty in the values of k, c, only qualitative conclusions can be drawn from (3.41). For example, as the average time of the "on"-state is increased, the degree of autocorrelation in the time series of switching parameters should decrease (faster return to equilibrium, smaller n_o; see note following (3.28)). In the regime of high overvoltage operation the delay times are small and therefore $t_{oneq} \rightarrow tp$ (Fig. 3.14); on the other hand in the regime of small overvoltages the delay times will be large and t_{oneq} will be small. Thus according to the relationship (3.41) a larger autocorrelation in the time series of switching parameters is expected in the regime of smaller overvoltages. This seems to be confirmed by experiment. In Fig. 3.15 two autocorrelograms are shown of the time series of threshold voltages for one device operated by a sinusoidal excitation waveform of the amplitude of $V_s = 200\,V$ and $V_s = 400\,V$. In the latter case (large overvoltage) it is seen that the correlation effects are absent (or much less pronounced). The mean square variation in the series is much smaller in the case of the large overvoltage regime; this is thought to be due to a greater heating of the switching device and therefore smaller "shunting" resistance which is "connected in parallel" to the resistance between the conducting regions of Fig. 3.12 (c.f. [16]). Other possible tests of the result (3.41) could be based on the variation of the constants k,c with ambient temperature. The constants are expected to increase with ambient temperature and therefore the correlation in the time series should decrease with ambient temperature. Experiments of this type, however, were not carried out.

3.4.5 Summary and Discussion

The theoretical model elaborated in the preceding section attempts to explain the experimentally observed correlation in the time series of switching

parameters in terms of a process involving structural changes in the switching device. A simple linear autoregressive scheme has been employed as the tool of statistical inference. Using this linear autoregressive model (3.37) it is possible to explain why the observed autocorrelogram R(m) decays by the factor of 1/e in n_o steps and this number of steps can be related to the model parameters by (3.41), which relation also permits an experimental test of the validity of the model.

The linear autoregressive scheme does not explain why R(m) should exhibit oscillations. In fact, no one term linear autoregressive scheme (3.25) with $0<a<1$ can yield an oscillating autocorrelogram. Two - or more (s-) term linear autoregressive scheme

$$x_{n+1} = a_1 x_n + a_2 x_{n-1} + a_3 x_{n-2} + \dots a_s x_{n-s+1} + a_{s+1} + r_{n+1} \qquad (3.42)$$

could yield an oscillatory autocorrelogram but employing such a scheme would mean admitting a direct causal connection between the behaviour of the device at a given (n + 1)-st operation and its state after two or more ($s \geq 2$) preceding operations. This is not possible in the framework of the simple model of structural change presented in this section, which assumes that the structure of the device does not change with time after completion of a switching operation (the model does not depend on t_g (Fig. 3.13) providing this is sufficiently large). If this assumption is relaxed then a linear (or non-linear) scheme with more than one variable ($s \geq 2$) could be elaborated; this line was not pursued in the present work. However, the possibility that the oscillatory behaviour of the autocorrelogram (Fig. 3.10.a,b) could be explained by a one-term non-linear autoregressive scheme of the type

$$x_{n+1} = f(x_n) + r_{n+1} \qquad (3.43)$$

f ... non-linear function of x_n

was considered in some detail. In the derivation of (3.37) the effect of the volume fraction x_n (n-th state of the device) on the delay time $t_{d(n)}$

and the duration $t_{on_{(n)}}$ of the "on"-state of the subsequent operation was neglected. We can take this effect into account by assuming a linear relationship

$$t_{on(n)} = t_{oneq} + d(x_n - x_{eq}) \tag{3.44}$$

where $d > o$, since the volume fraction $x_n > x_{eq}$ means a smaller resistance of the device and therefore greater heat dissipation during the delay period, shortening of the delay time (according to impulse thermal model of switching), and hence lengthening of the "on"-state duration. If (3.44) is substituted into (3.35) and the exponentials $\exp(-kcd(x_n - x_{eq}))$ approximated by $(1 - kcd(x_n - x_{eq}))$ then it is possible to show that the linear scheme (3.37) becomes a quadratic one

$$x_{n+1} = -A\,kcd\,x_n^2 + A(1 + 2\,kcd\,x_{eq})x_n + x(1 - A - kcd\,x_{eq}) + \Delta x \tag{3.45}$$

which reduces to (3.37) for $d = o$. This series will oscillate finitely if

$$1 \leq \sqrt{\left(\tfrac{1}{2} - \tfrac{A}{2}\right)^2 + A\,kcd\,\Delta x} \leq \tfrac{3}{2} \tag{3.46}$$

as shown by Chaundy and Phillips[22]. This oscillatory behaviour would be reflected in the autocorrelogram of the series (3.45) with random disturbances r_{n+1} added to its right hand side. There is, to the authors' knowledge, no theory which would predict the autocorrelogram directly from the quadratic autoregressive scheme, but it would be possible to use computer simulation of the series and determine the parameters in (3.45) which would give the best agreement between the simulated and observed autocorrelograms.

However, before going into such sophisticated analysis it should be made clear whether the oscillatory behaviour of the experimentally obtained autocorrelograms in Fig. 3.10. does not, in fact, arise from some trend in the time series of the switching parameters. In section 3.4.3 it was mentioned that such a trend was observed in the behaviour of the switching parameters

and this could be responsible for the oscillatory behaviour of the autocorrelograms or for any other features in the autocorrelograms extending over long ranges of the lag number m. (On the other hand this trend in the data would influence the behaviour of the spectral power density G(k) at small frequencies). The exponential decay of the autocorrelations is expected not to be affected very much by possible trends in the data and therefore the validity of the analysis made in this section should not be altered even if a slow trend is found in the data. Linear trend removal was performed on a number of experimental data and in some cases this affected the shape of the autocorrelograms, but a more detailed analysis would be required in order to ascertain the presence of a trend in the time series of switching parameters $\sim 10^3$ long. Apart from the analysis of a trend in the series the possible effect of the length of the series on the autocorrelogram should be investigated; longer samples (time series) may yield statistically more reliable autocorrelograms.

The presence of the structural changes of the type postulated in this section (Fig. 3.12) is not, or course, proved by the ability of the model to account for the experimental observations. It can be shown that the interaction between the glass transition temperature T_g and the rate of cooling of the device at the end of a switching operation (see relationship (2.2)) can constitute the basis of an autoregressive system (3.24). In this case it is again the structural changes in the device which cause variation and autocorrelation in the time series of switching parameters, but they are of a different kind than the structural changes postulated in the present model. An outline of a competing "non-structural" mechanism was given on page 92. It would be difficult to decide experimentally between the present model and the two models just mentioned, because the degree of correlation predicted by all three models would change with the experimental parameters (ambient temperature, overvoltage) in a similar manner. However, there are a number of independent observations suggesting the plausibility of the assumptions made in the present model and it is therefore preferred.

References Quoted in Chapter 3

(1) Nesvadba P., M.Sc. thesis, 1970, University of Warwick, England.

(2) McMillan P.W. and Nesvadba P., reference (30) quoted in Chapter 1.

(3) Böer K.W., reference (100) quoted in Chapter 2.

(4) Owen A.E., reference (101) quoted in Chapter 2.

(5) Adam G. and Duchene J., reference (68) quoted in Chapter 2.

(6) Cupta Y.P., J. Non-Cryst. Solids 3 (1970) 148.

(7) Stocker H.J. et al., reference (81) quoted in Chapter 2.

(8) Walsh P.J. et al., Phys. Rev. 178 (1969) 1274.
Thomas C.B. et al., Phil. Mag. 26 (1972) 617.

(9) Male J.C. and Warren A.C., contribution at the "Discussions on amorphous semiconductors", Chelsea College, London, December 1971.

(10) Thomas D.L. and Male J.C., reference (91) quoted in Chapter 2.

(11) Kroll D.M. and Cohen M.H., reference (87) quoted in Chapter 2.

(12) Kaplan T. and Adler D., reference (92) quoted in Chapter 2.

(13) Gunn J.E., J. Siam Numer. Anal. B4 (1964) 24.

(14) Peaceman D.W. and Rachford H.H., Jr., J. Soc. Indust. Appl. Math. 3 (1953) 28.

(15) Ladyzhenskaya O.A. and Ural'tseva N.N., "Linear and Quasilinear Elliptic Equations", (Academic Press, N.Y., 1968).

(16) Henish H.K., reference (12) quoted in Chapter 1.

(17) Wold H., "Analysis of Stationary Time Series", (Uppsala, 1954).

(18) Bendat J.S. and Piersol A.G., "Random Data : Analysis and Measurement Procedures" (Wiley-Interscience, 1971).

(19) Bosnell J.R., personal communication.

(20) Yule G.U., J. Roy. Stat. Soc. 108 (1921) 208.

(21) Meek J.M., "Dielectric Breakdown of Gases", (Oxford, 1953).

(22) Chaundy T.W. and Phillips E., Quart. J. Math. 7 (1936) 74

(23) Kendall M.G., Biometrika 33 (1944) 105.

(24) Cohen M.H. et al., J. Non-Cryst. Solids 8-10 (1972) 885.

(25) Richardson J.M., Bell System Tech. J. 29 (1950) 117.

(26) Lee S.H. et al., J. Non-Cryst. Solids 8-10 (1972) 422.

CHAPTER 4

MATERIAL AND DEVICE PREPARATION

4.1 Introduction

In principle, there are three basic methods of preparation of non-crystalline materials. In the first method (i) a film is deposited onto a substrate, i.e. the layer of material is built from zero thickness. In the other methods bulk quantities of the material are involved, usually employing some kind of melting procedure. Two possibilities can then arise; either (ii) the solidified ingot is non-crystalline and is then fabricated in the required way, or (iii) it is crystalline and has to be disordered by neutron bombardment or by shockwave treatment or by other means combined with some method of fabrication as in (ii). During this fabrication the thickness of the region of interest is reduced. The first two methods ((i) and (ii)) are the most commonly employed.

The geometry and other essential features of a switching device are thus intimately connected with the method of preparation. There are thin film devices with the thicknesses of the active region of the order of a micrometer as opposed to thick devices which employ a layer of fabricated bulk material more than 10μm thick. There appears to be a certain thickness 'gap' between the two classes which is difficult to bridge, and, what may be more important, the structures of the glasses on the two sides of the thickness gap may be different even for nominally the same composition due to the different methods of preparation[1]. Thus it is difficult at present to compare many aspects of the switching in thin and thick devices. This will be discussed further in Chapter 7. In the present section we briefly review the methods of preparation of non-crystalline materials.

4.1.1 Methods of Thin Film Preparation

These methods can be divided into two large classes

(i) physical methods

(ii) physico-chemical methods

The basic representative of a physical method is the simple evaporation technique in which the starting material in bulk form is melted in vacuo and the vapours of the material are condensed onto a substrate whose temperature is ideally controllable. This method requires modification if a multicomponent material is to be deposited, the components of which have different rates of evaporation. For example, during the preparation of a thin film of so-called Ovshinsky chalcogenide glass (or STAG (Si-Te-As-Ge) glass) containing silicon, As, Te and Ge, the rate of evaporation of Si is about half that of the rest of the components. Refinements are therefore needed to enable the final composition of the film to be controlled. This can be, in principle, achieved by evaporating each component from a different boat kept at different temperatures[4,5].

A different technique from boat evaporation is the flash evaporation technique where a rapid vaporization is achieved by dropping the bulk material onto a hot surface. Resulting vapours are condensed onto the substrate, the condensate having then a composition which is closer to the starting bulk material than in the case of slow heating.

In the third method belonging to group (i) drops of the molten starting material are dropped or projected onto a cold surface and thus cooled rapidly[6]. It was possible to prepare amorphous metals, substances most difficult to obtain of all, in an arrangement involving an electromagnetically operated jaws in which the flying droplet is squeezed[7]. Unfortunately the volume of the material produced by splat cooling is insufficient for use in device fabrication.

To the second group (ii) belongs a method of reactive sputtering[8,9]

where one or more components deposited on the substrate originate from a gas phase present in the evaporation chamber. The chemical reaction may be accomplished by causing a controlled r.f. discharge in the gas. (e.g. Si prepared from silane gas).

Finally a method of electrodeposition was used for the preparation of non-crystalline semiconductors in which the material is deposited on the cathode in a suitable electrolyte (solution of $GeCl_4$ in $C_3H_6(OH)_2$ in case of Ge[10].)

It is interesting to consider the rate of cooling in the method of thin film preparation. It can exceed the rates of cooling entailed in the fastest methods of melt quenching ($\sim 10^9$ °C/s) by several orders of magnitude[10,11]. A rough estimate of the rate of loss of kinetic energy $\frac{3}{2} kT_1$ of an atom of Ge (with mass $m = 72.59 \times 1.66_{10}{}^{-24}g = 1.23_{10}{}^{-22}g$) impinging onto a substrate at temperature T_2 can be made by assuming that the excess kinetic energy is lost during n collisions which are equally spaced (by λ) and take place every t_a seconds. Assuming that the average velocity v_a of the atom during collisions is given by $\sqrt{\frac{3k}{m}\left(\frac{T_1-T_2}{2}\right)}$ then by inserting numerical values $(T_1-T_2) = 600$°K and $\lambda = 10$Å, v_a is estimated at $\sim 3_{10}{}^{4} \text{ cms}^{-1}$ and $t_a = \frac{\lambda}{v_a} = 3.10^{-12}$s. If it is assumed that n = 10 the effective rate of cooling is then $\frac{T_1-T_2}{nt_a} \sim 2.10^{13}\ ^{\circ}\text{Ks}^{-1}$. (This can be by one or two orders of magnitude higher or lower principally due to the uncertainty in λ and n.) Therefore substances can be prepared in non-crystalline state which would never form a glass by melt quenching. These are, for example, amorphous Ge and Si. There are reports of properties of amorphous Ge and amorphous Si appearing in the literature which show an enormous variability and often contradictions between results of even one laboratory[12]. This irreproducibility of some materials in thin film form is undoubtedly connected with the method of preparation. Properties of materials prepared in bulk are much more easily reproducible.

4.1.2 General Remarks on Device Preparation

When the existing state and the trends of the development of the devices produced by the electronic industry are considered it is realised that the thin film devices play the primary role. If, therefore, the switching devices are ever to find their application in the way which would complement the conventional crystalline semiconductors of today, it will have to be in the thin film form to ensure production compatibility.

Also the possible application of non-crystalline semiconductors for information storage, which seems feasible and promising at the time of writing this thesis (see also section 1.4), would take place in the thin film form.

Having thus pointed out that the possible applications of the switching effect are most likely to occur in "thin film form", it needs to be emphasised that bulk devices are essential to the experimental physicists in order to carry out the basic research and gain understanding of the mechanisms of switching. Some of the reasons (reproducibility of the material) was discussed in the preceding section.

Both thin and thick switching devices employ materials having 3,4,5 or more components of: Te,As,Ge,Si,Se,S,In,Sb, etc.

In reviewing the development of the switching devices during the past 4 years one cannot avoid mentioning the products of the firm Energy Conversion Devices (Troy, Michigan)*, which are available commercially.

The first switching devices produced by ECD are called DO-7 and consist essentially of two carbon hemispheres coated with ~ 0.5 μm active layer of the six component glass and pressed together by a spring loaded mechanism. These devices are used now mainly for basic research.

In 1971 ECD introduced a first serious application of the memory effect in the RM-256 device. This is a "read mostly" memory array consisting of 16 x 16 = 256 switching devices accommodated on an area of

* S.R. Ovshinsky is a director of ECD.

0.1 cm^2 which can be electronically addressed and their state altered or read. Further similar devices are being currently developed by ECD (which in turn stimulates the interest in switching) and details can be found e.g. in (13,14). The section through a typical thin film switching device is in Fig. 4.1.a. The active area of the device is defined by a 20 μm pore in the alumina layer. The pore is produced by photofabrication (for details concerning photofabrication see section 4.5). The electrode material in contact with the active material was chosen as molybdenum which proved experimentally to be least diffusive in the chalcogenide glasses.

While the design of the thin film devices does not vary much from the one shown in Fig. 4.1.a the design of the switching devices reported in the literature employing bulk material shows much greater variability and flexibility. These are devices made simply by contacting the layer of the switching material by two wires from one (coplanar) or both sides[15], devices with large area electrodes prepared by evaporation[16,17] or combinations of the two methods (Fig. 4.2). Switching devices using transition metal oxide glasses were succesfully prepared by the following method. A platinum wire is heated and immersed into the molten glass so that it is covered with a layer of material. A second wire is then placed at right angles to the coated wire and a droplet of glass is applied to the crossing point so the net result is two wires immersed in a bead of active switching material (Fig. 4.2.d). A variation of this method is shown in Fig. 4.2.e where two wires separated by a gap (in the axial direction) were embedded in a drop of glass[18,19 for Selenium].

Both bulk and thin film devices can be classified according to the geometry into sandwich and coplanar structures.

The sandwich structures have the advantage of the possibility of defining exactly the active area of the device (window or pore) and of not introducing sharp edges which introduce an unknown factor in the

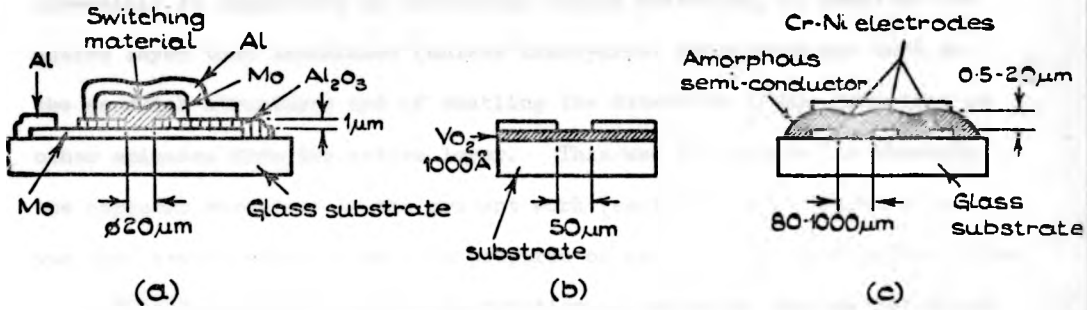

Fig. 4.1.

EXAMPLES OF SWITCHING DEVICES EMPLOYING THIN LAYERS.

a) ECD design
b) Duchene J. et. al., Phys. Stat. Solidi (a) 8 (1971) 459.
c) Croitoru N et. al., J. Non-Cryst. Solids 4 (1970) 493.

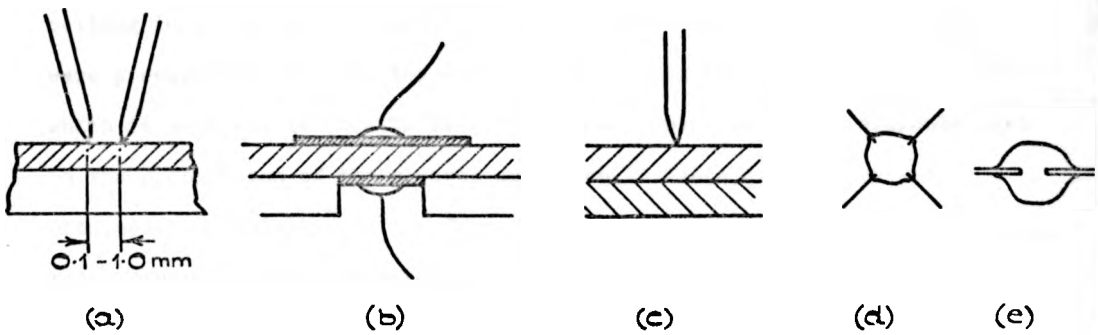

Fig. 4.2.

ELECTRODE GEOMETRIES USED IN BULK SWITCHING DEVICES.

strength of the electric field.

The coplanar structures have the advantage of rendering the device accessible to inspection by microscopy during switching, of enabling the active layer to be irradiated (unless transparent electrodes are used in the sandwich structure) and of enabling the detection of any radiation or other emission from the active layer. This was the reason for choosing the coplanar structure in the present work (section 4.5). Another reason was that several devices could be prepared on one disc of chalcogenide glass.

Finally a remark on the construction of switching devices employing liquid semiconductors can be made. These devices are most conveniently small cells (several cm^3) containing two electrodes immersed in the active liquid semiconductor[20]. The discussion of three terminal devices is limited to a short remark in Chapter 7.

4.2 Preparation of Chalcogenide Glasses

4.2.1 Method

The batches of 15 to 25 g of chalcogenide glasses were prepared by melting in sealed silica ampoules (Fig. 4.3). Several compositions were prepared but most of the work was done using the four component glass which is most stable (see Table 4.1). The properties of the elements used in the preparation of the glasses are given in Table 4.2. They were obtained commercially* in the form of powder, granules or lumps of purity better than 99.999%. After the original packages of the chemicals were opened, the containers were stored in a desiccator containing silicagel to reduce contamination of the chemicals by air and moisture. In some cases the raw materials had to be crushed to reduce the size of the grains or lumps which would not otherwise feed through the neck of the ampoule. This crushing took place in a mortar and could cause an increase in the impurity content owing to the particles ground off the mortar (porcelain)

* from Koch-Light Ltd., Colnbrook, Bucks, England.

and to exposure to the atmosphere. The former is probably less important than the second kind of contamination as the ceramic particles would be chemically inactive in the chalcogenide glass. The significance of oxygen contamination is not fully understood (a chalcogenide glass has been sucessfully prepared by using TeO_2 instead of Te[21]) and therefore the time of crushing and other necessary exposure to air was kept to a minimum.

Table 4.1 Glasses Prepared

	Atomic %	Weight %
Binary		
As-Te	40.0-60.0	28.1-71.9
Te-Si	80.0-20.0	94.8- 5.2
Te-P	95.0- 5.0	98.7- 1.3
Ternary		
As-Te-Ge	34.3-54.3-11.4	24.9-67.1-8.0
Quaternary		
As-Te-Ge-Fe	14.8-80.2- 4.0- 1.0	9.5-87.5- 2.5- 0.5
As-Te-Ge-Si*	30.0-47.4-10.0-12.6	23.9-64.5- 7.7- 3.8

* Ovshinsky composition or so called STAG.

Table 4.2 Properties of Elements used in Preparation of Chalcogenide Glasses

Element	At. No.	At. Weight	Valency	M.P. (°C)	Vap. pressure at 1000°C (atm)	B.P. (°C)	Density g/cm³	Allowed Toxicity level mg/m³
As	33	74.92	3,5	814	75		5.73	0.5
Si	14	28.10	4	1420	negligible	2355	2.33	-
Te	52	127.60	2,4,6	450	1.2	990	6.24	0.1
Ge	32	72.59	2,4	937	negligible	2830	5.32	-

The silica ampoules in which the elements were melted (see Fig. 4.3) were subjected to a multistage cleaning procedure. They were first cleaned with a solvent (acetone) followed by a short flush with 2% hydrofluoric acid and a thorough wash in distilled water. They were then dried in an electric furnace at a maximum temperature of 400°C and left to cool at the natural rate of the furnace to room temperature.

The weighing of the elements and their feeding into the ampoules took place in a nitrogen glove-box. The cleaned SiO_2 ampoules, starting elements, the balance and other accessories were placed into the glove box through which a flow of nitrogen was passed for 24 hours prior to and during weighing. The errors involved in the weighing out of the amounts of the elements were ± 5 mg.

The constituents were mixed thoroughly in a glass container before feeding through the neck into the ampoule. The nitrogen atmosphere in the filled ampoule was maintained by means of a vacuum valve. This also permitted connection of the ampoule to a pumping unit which had a facility of a controlled inlet of an inert gas (see Fig. 4.4).

The ampoule was evacuated 4 times to 10^{-4} torr, each time flushed with dry argon. During the final evacuation the ampoule was moderately heated (~120°C) to remove water vapour from the surfaces of the grains of raw materials. Finally the ampoule was filled with a reduced pressure of argon and sealed with an oxyacetylene torch. The presence of argon in the ampoule is believed to reduce the diffusion of oxygen through the silica wall of the ampoule during the period of melting.

The melting was carried out in a tube furnace (made by Carbolite Company) having a tube 40 cm long, 7.5 cm in diameter and a hot zone 20 cm long. The furnace was mounted on a trolley which was movable on a rail to enable withdrawal of the ampoule holder from the furnace. The ampoule was attached by Ni-Cr wire in a stainless steel tube attached at an angle

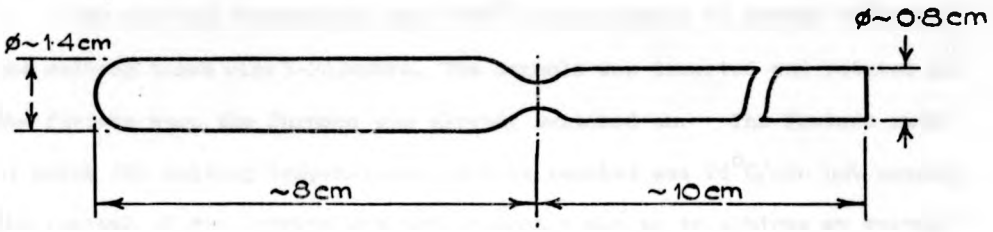

Fig. 4.3.

TYPICAL SILICA AMPOULE USED FOR MELTING.

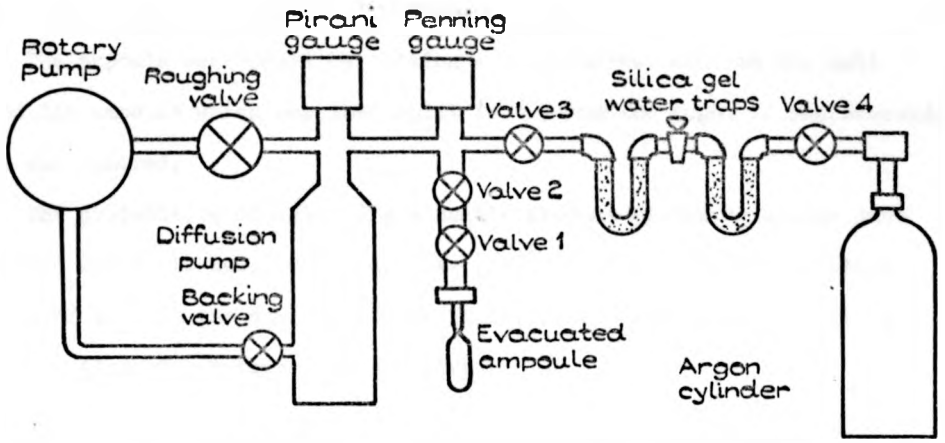

Fig. 4.4.

SYSTEM USED FOR EVACUATION AND FILLING THE AMPOULES WITH INERT GAS.

$\sim 15^{\circ}$ to a rotating shaft powered by an electric motor. This facilitated stiring of the ampoule contents during melting as the ampoule was subjected to a rotation about an axis not equal to its own.

The melting temperature was 1000°C controllable to within 10°C and the melting times were 3-24 hours. The ampoule was inserted and rotated in the furnace when the furnace was already switched on. The fastest rate at which the melting temperature could be reached was 24°C/min but usually the control of the furnace was set in such a way as to achieve an average temperature rise of approximately 8°C/min in order to dissolve the components without building up a large vapour pressure (this point is discussed later).

At the end of the melting stage the furnace was moved aside to expose the ampoule holder. The stirring was stopped and the stirring mechanism was tilted so as to bring the axis of the ampoule to the vertical position. A flow of compressed air was then directed onto the ampoule holder which was cooled to room temperature in several minutes.

The ampoule was opened by cutting a longitudinal slot in the wall around the ampoule which was then split in two and the ingot of chalcogenide glass was removed.

The probability of obtaining a usable product by the technique just described was quite low, something like 1/6. In the following sections methods of testing the quality of the ingot, problems in the preparation and suggestions for improvement are given.

4.2.2 Tests of the Quality of the Chalcogenide Glass. Problems.

The ingots of chalcogenide glass (Fig.4.5) were examined by several methods:

M1 visual inspection

M2 fracture and visual inspection of the fracture surface

M3 cutting a slice and examining its polished surface

M4 measuring the electrical resistance of the ingot (a rough informative measurement by two probes spaced ~ 1 cm)

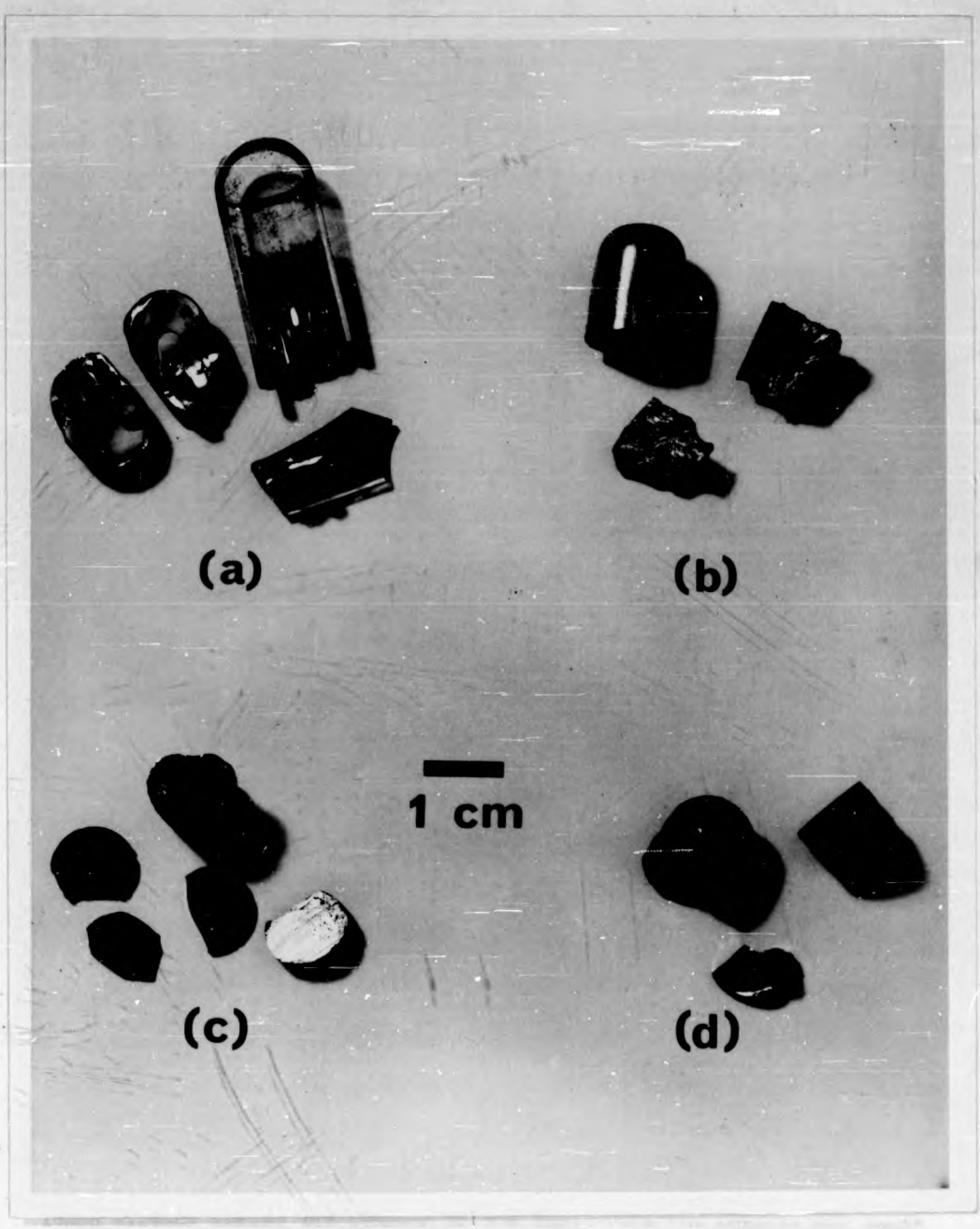

Fig. 4.5.

EXAMPLES OF AS-QUENCHED MATERIALS.

(a) Glass showing conchoidal fracture

(b) Polycrystalline material (defect D1, p. 108)

(c) Glassy material with internal bubbles (defect D4)

(d) Amorphous material with "mat" fracture surface

M5 x-ray powder analysis

M6 Electronic transmission microscopy and diffraction.

All the tests except for M6 were done as a matter of routine to ascertain whether the ingot was crystalline or amorphous and a degree of its quality. Already the first visual inspection could reveal the state of the ingot. Crystalline ingots had a typical metallic appearance, were ductile, difficult to fracture and had high electrical conductivity corresponding to metallic conduction. The fracture surface showed a typical polycrystalline morphology.

Apart from crystallinity which occured with the probability of ~1/10 there were other defects in the material encountered, given in the following list:

D1 Material Polycrystalline

D2 Material Amorphous but very weak mechanically

D3 Material had "mat" fracture surface

D4 Polished section revealed small bubbles in the material

D5 Surface of the ingot was not clean, some undissolved material free in the ampoule or trapped between the wall of the ampoule and the ingot ('slag' present).

The second defect occurred much more frequently; the degree of weakness was judged by the behaviour of the ingot during handling and preparation of specimen. For most measurements the ingots had to be cut into slices (as described later). During this procedure the brittleness was manifested to the greatest extent but some ingots broke up into small lumps already during the removal of the ingot from the ampoule and could not be used further. In some cases the mechanical weakness was demonstrated by the appearance of hair-line cracks in thin chalcogenide glass slices bonded to a substrate by the epoxy resin 'Araldite'. Although the manufacturer claims that no stresses are developed in the epoxy resin during its polymerization it was shown by an independent experiment[22]

that stress is developed during the setting of the glue and this caused cracking of very thin bonded slices.

The reasons for the defect D2 are seen in the finite rate of cooling of the ampoule after melting during which thermal stresses are set up in the ingot. Attempts to remove the stresses by annealing were described in (24) but this was not pursued in the present work.

The ingots which exhibited the mat fracture surface are thought to contain small regions of ordering, probably due to a partial phase separation or crystallization. The x-ray powder test showed sometimes sharp lines superimposed on a ring structure which was somewhat less diffuse than in the case of an "ideal" ingot. The electron diffraction in 100 kV microscope gave similar results, sometimes regions even in the "ideal" glass could be found which showed polycrystalline-like rings and diffraction spots. The glasses having a mat fracture surface had as large a resistivity as the 'ideal' glass and in switching experiments they did not differ from the behaviour of the 'ideal' glass.

Some problems in the preparation arose due to the large vapour pressure and the low boiling point of the main components used, namely tellurium and arsenic (see Table 4.2). It is difficult to estimate the vapour pressure of the four component glass As-Te-Ge-Si during melting because of the insufficient thermodynamic data available for the chalcogenide glasses. The total pressure will obviously be much lower than that of pure arsenic at the temperature of 1000°C because of the lowering of the vapour pressure due to mixing with the other components (Raolt's law). A crude estimate using the van't Hoff's law for the lowering of the freezing point of the mixture indicates that the vapour pressure during melting will be much less than the atmospheric pressure. This, on the other hand, is not true for the binary glass Te-Si (Table 4.1) for which the vapour pressure is probably very close to that of pure tellurium and which was demonstrated by an explosion of the ampoule in the course of preparation of this glass.

The defect D4 of the bubbles in the ingot is also attributed to the large volatility of the main components, it is not thought to be caused by the skrinkage of the ingot during solidification (this sometimes resulted in a large axial cavity starting at the top of the ingot and narrowing down). If the ampoule is quenched in such a way that the vapour pressure above the liquid glass is rapidly reduced, boiling of the melt will occur. The rate of ascent of vapour bubbles in a liquid is inversely proportional to the viscosity of the liquid and directly proportional to the $(\text{volume})^{2/3}$ of the bubbles. Large bubbles will therefore escape from the melt very quickly but small bubbles can be trapped in the solidifying melt as its viscosity increases. Small cavities in the ingot were found predominantly in the central region of the ingot. This indicates that the central core of the ingot starts boiling at an instant when the region near the walls of the ampoule is already sufficiently cold not to start boiling when the pressure above the melt drops to the critical value. The analysis of this effect could include more detailed study of the distribution of the bubbles in the ingot and also the dispersion of their sizes, which would probably confirm the above hypothesis. A practical consequence for the preparation technique therefore is to adopt a quenching procedure in which boiling of the melt is eliminated; this could be achieved by keeping the empty upper part of the ampoule hot and to start quenching from below.

The physical size of the grains of the materials used for melting was such that their specific volume decreased by about 60% on melting (ingot length $\sim 1/3$ of ampoule length) so the volume of the vapour in the ampoule is about 3/2 of that of the melt. The smaller the volume above the melt the more quickly the thermadynamic equilibrium between the melt and its vapour can be established during quenching and this could also serve as a basis for the improvement of the quenching procedure.

Frequently a case was encountered where the solution of the components of the glass was not apparently perfect as some powder material remained loosely in the ampoule (defect D5)[23]. This material was identified as silicon. The high melting temperature of this element which is, in fact, above the melting temperatures used suggests the cause for the defect. The silicon has to be dissolved by the rest of the liquid components without actual melting. Any contamination of the surface of the silicon powder can therefore drastically reduce this process or indeed prevent the dissolution at all. This is illustrated by the fact that the very fine powder obtained commercially was less readily dissolved than a powder prepared in the laboratory by crushing silicon lumps shortly before the glass preparation and therefore less liable to contamination by exposure to the atmosphere. It was suggested (25) that Si powder is more readily dissolved in the As_2Te_3 eutectic than in the As_{30} Te_{47} Ge_{10} fraction of the chalcogenide glass. The use of this idea for the preparation of chalcogenide glasses means, however, doubling the complexity of the process unless the As_2 Te_3 compound is obtained commercially. There is a large scope for possible improvements of the described method of preparation, some of which were already outlined in this section. The addition of a cold trap between the ampoule and the vacuum system is another possibility. The stirring rate also may need optimization. An opinion was expressed (26) that the diffusion of oxygen through or from the SiO_2 ampoules is a decisive factor. On several occasions an attempt was made to eliminate the first possibility by flowing nitrogen ("white spot") through the furnace during melting. Although the oxidation of the stainless steel holder, shaft and Ni-Cr wire was completely eliminated, the failure rate did not seem to decrease. Varying the stirring rate could test whether the contact between chalcogenide glass and SiO_2 is important.

In conclusion it is possible to say that the result of glass preparation could only be predicted in terms of probabilities as the effect of various stages of the preparation procedure on the resulting end product is not fully understood. The difficulty in tracing the steps which determine possibly the result is due to their large number: contamination of starting materials, their degree of mixing both in the solid and liquid states, condition of the surface of the silica ampoules, quality of the atmosphere in which the glasses are melted, method of quenching the ampoules, stirring rate, diffussion of oxygen into the ampoules. Each of these factors has to be varied and correlated with the changes in the produced glass. This can only be achieved by long experience.

4.3 Preparation of Switching Devices and other Experimental Specimens

The first stage in producing a specimen for any one of the experimental purposes involving electrical measurements was to produce a disc of the material which could then be thinned or polished as required. This was achieved by cutting the ingots (produced by the method described in the previous section) normal to their axes. The instrument used for cutting the ingots was a "Capco Q35 High Precision Cutting Machine" an essential feature of which was a thin (0.2 mm) anular blade, diamond impregnated on its inner edge, which rotated at ~1000 r.p.m. The ingots were glued by "Araldite" or fixed by wax ("Capco" mounting wax, Caplin Eng. Co.) to a horizontal table which could be moved parallel to and normal to the plane of the blade. The speed of the movement parallel to the blade (i.e. the cutting speed) was controlled by a hydraulic mechanism and was variable (usually 1 cm/20 minutes speed was used). In this way the ingots could be cut into parallel-sided discs of a thickness ~1 mm.

4.3.1 The Sandwich Switching Structures

The discs obtained by cutting the ingots as described above were polished on one side and glued by "Araldite" onto a microscope slide which had a circular hole ~5 mm in diameter. The discs covered the hole and thus the polished side was exposed through the hole so that an electrode could be prepared later on the exposed area. The microscope slide provided a sufficient mechanical support so that the disc could be thinned by grinding (600 mesh Carborundum, under water) to a thickness ~10 μm and its upper surface polished (Hypres Diamond Compound 1 μm or 1/4 um). Gold electrodes were then evaporated on both sides of the sample using a standard technique (Au wire on V-shaped W wire, 6 cm from the sample, vacuum 10^{-4} torr). The electrode thickness was estimated at 0.1 - 1 μm. Thin copper wires (s.w.g. 18) were then attached to the gold electrodes and secured by a conducting paint (Ag in methyl isobutyl ketone - silver 'dag').

4.3.2 The Coplanar Switching Structures

The starting point for the preparation of the coplanar devices were again slices of chalcogenide glass ~1 mm thick and 10 mm in diameter. They were bonded by one surface to a rectangular piece of glass obtained by cutting a microscope slide and the other surface was ground and polished by a similar procedure as in 4.3.1. Several switching devices could be produced on one disc by a photofabrication technique. The basis of the photofabrication are photosensitive resin solutions in organic solvents which are applied to the chosen material and dried. After exposure, the unwanted areas of the resist coating are removed by the developer, leaving a resist pattern which possesses extremely high chemical resistance to all commonly used etching solutions and electroplating solutions. In some cases a thick layer of photoresist will provide a satisfactory mark for airbrasion or sandblasting[27]. Kodak photoresist KPCR was used for the production of the etching in-contact masks. The stages of the process are given in Table 4.3.

Table 4.3 Stages of Fabrication of Switching Devices
(Refer to Fig. 4.6 - 4.8)

Stage	Description
Polishing	1/4 μm Hyprez Diamond Compound
Cleaning	Soap solution 'Teepol' and distilled H_2O compressed air drying.
Resist Coating	KPCR resist, undiluted, whirler coating at 8500 r.p.m.
Pre-bake	15 mins at R.T. 10 minutes at 110°C
Exposure	Vacuum frame with polythene membrane 25 cm from 100 W Hg lamp. 15 minutes exposure.
Developing	KPCR developer sprayed for 40-50 seconds.
Rinse	KFTR rinse; dried by compressed air of moderate pressure.
Post-baking	10 minutes at 120°C.
Etching	Solution: 34 ml H_2SO_4, 8 g $K_2Cr_2O_7$, 200 ml H_2O. Etching for 80 minutes. Cleaned by distilled water and dried by flow of air
Evaporation of electrodes	1) Molybdenum : stripe 4 mm wide and 0.07 mm thick, 20A, degassed for few minutes at red heat. 2) Aluminium : blob on W wire Vacuum 10^{-4} torr, specimen to source distance ~ 6 cm.
Polishing to remove excess metal	1/4 μm diamond compound on Hyprocel Pellon PAN-K discs.
Making contacts	Cu wire (s.w.g.40) secured by silver 'dag' to the device and suitable electrode base.

Fig 4.6.
VACUUM FRAME USED FOR EXPOSURE OF PHOTORESIST.

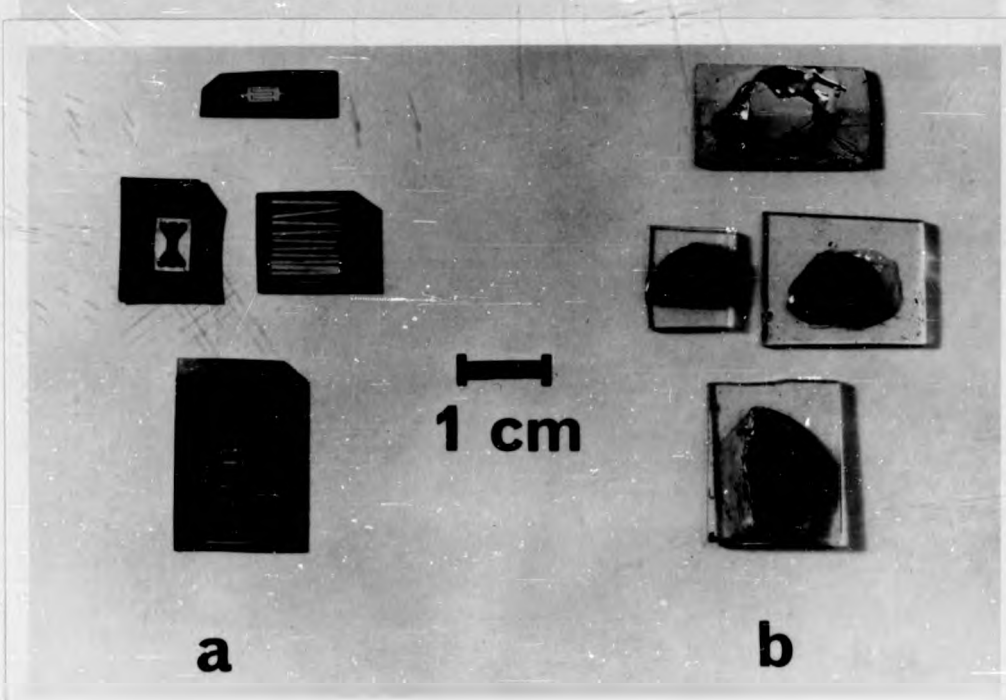

Fig. 4.7.
PHOTORESIST MASKS (a) AND DEVICES IN VARIOUS STAGES

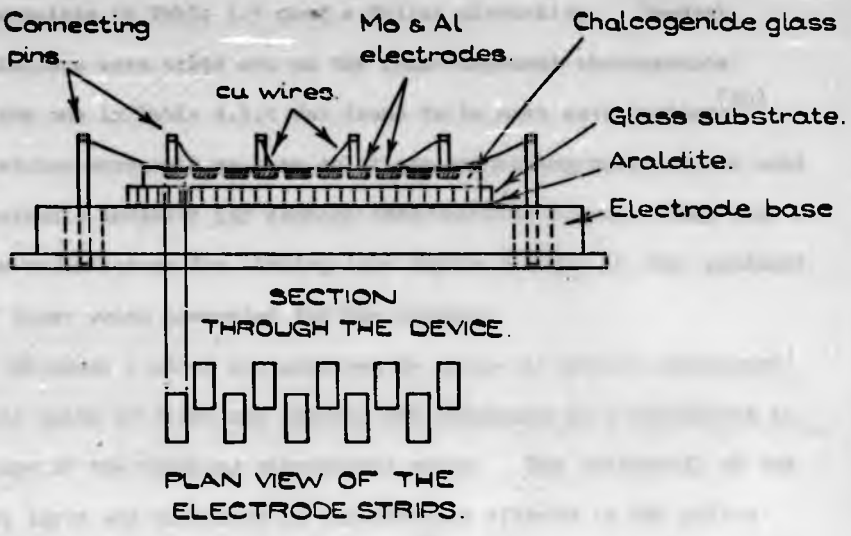

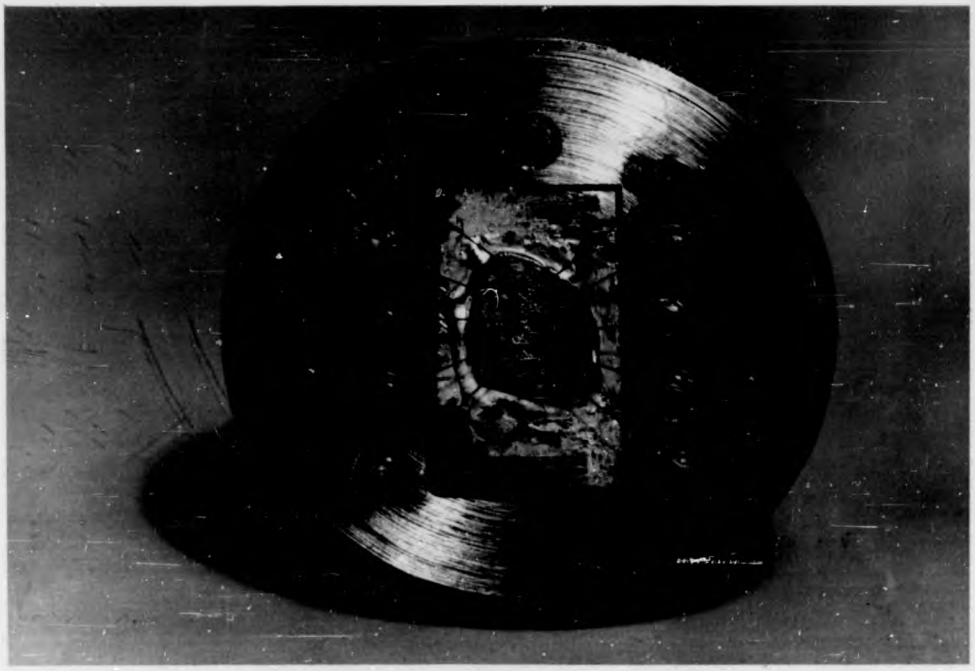

Fig. 48

SCHEMATIC DIAGRAM OF THE COPLANAR DEVICE AND ITS PHOTOGRAPH.

A few points in Table 4.3 need a fuller discussion. Several etching solutions were tried out on the four-component chalcogenide glass and the one in Table 4.3.1 was found to be most satisfactory[30]. The other etches were acid or base solutions containing halogens and used in the electronic industry for etching semiconductor films. They were not found to be satisfactory for etching into depths > 10 μm as they produced an "inert" layer which prevented further etching.

The thickness control was achieved by using an optical microscope with a small depth of focus and reading the thickness as a difference in the positions of the focusing micrometric screw. The uniformity of the photoresist layer was monitored by interference effects in the yellow Ilford safelight. A microscope with an interferometric attachment was available for more accurate measurements.

The evaporation of the molybdenum layer has a two-fold purpose. One is to aid the adhesion of the aluminium layer to the chalcogenide glass. Refractory metals are known to possess a good adhesion to glasses[28] (adhesion is related to the latent heat of evaporation[29]). The other reason is to prevent an excessive diffusion of the aluminium into the chalcogenide glass. Molybdenum was found to have a very low diffusion coefficient in these glasses.

The definition of the edges of the photoresist mask were determined mainly by the thickness of the photoresist layer, length of the exposure and developing. Generally the definition was not better than 3 μm but devices with thickness of 10 μm could be produced quite easily. Uncertainty in the thickness of the switching layer is mostly due to the undercutting factor caused by etching. In addition, the electric field near the electrodes can be concentrated on the weak spots which are probably present on the edges of electrodes. Therefore the switching effect as a function of thickness was not investigated.

4.3.3 Specimens for D.C. Conductivity

The discs obtained by cutting the ingots of chalcogenide glass were ground on 600 mesh carborundum under flowing water. Aluminium electrodes were evaporated on the flat surfaces of the discs: one bottom electrode and two top electrodes, one for high terminal and one guard ring.

4.3.4 Samples for x-ray Powder Camera

Powder obtained by scratching the chalcogenide glass with a diamond point cutter was fed into standard thin walled tubes which were then sealed by "Durofix".

4.3.5 Samples for Electron Diffraction

Powdered chalcogenide glass was dispersed ultrasonically in a very dilute solution of polymethacrylate in amylalcohol. A drop of this suspension was then transferred onto a thin carbon film supported by a standard "Polaron" grid.

4.3.6 Specimens for Scanning Electron Microscopy

The switching devices did not require any coating with metal (Pt/Pd alloy) as they were not liable to charging effects.

References Quoted in Chapter 4

(1) Kolomiets B.T. et al, Sov. Phys.-Semicond. 3 (1969) 267.

(2) Holland L., "Vacuum Deposition of Thin Films", Chapman & Hall, 1963.

(3) Chopra K.L., "Thin Film Phenomena", McGraw Hill, 1969.

(4) Howson R.P. and Malina V., J. Phys.D. (Applied Physics) 3 (1970) 871.

(5) Ferrier R.P. and Heller D.J., Phil. Mag. 19 (1969) 853.

(6) Duwez P. and Willens R.H., Trans. Met. Soc. A.I.M.E. 227 (1963) 362.

(7) Aho P., University of Turku, Finland, personal commun.

(8) Chittick R.C. et al, J. Electrochem. Soc. 116, (1969) 78.

(9) Sterling H.F. and Swan R.C., Solid State Electron. 8 (1969) 653.

(10) Szekely G., J. Electrochem. Soc. 98 (1951) 318.

(11) Sarjeant P.T. and Roy R., Mat. Res. Bull. 3 (1968) 265.
Owen A.E., contribution at the "Discussions on Amorphous and Liquid Semiconductors", Chelsea College, London, 17-18.12.1971.

(12) Results by Stuke J., J. Non-Cryst. Solids 4 (1970) 1
and Grigorovici R., et al, Phys.Stat.Solidi. 16 (1966) K143.
cited by Mott N.F. and Davis E.A. (ref. 6 of Chapter 1) p.281
also Connell G.A.N., J. Non-Cryst. Solids 8-10 (1972) 215.

(13) Neale R.G. and Cvshinsky S.R., 4th Int. Congress in Microelectronics, Munich, West Germany, November 1970.

(14) Fritzsche H., Proc. Conf. on Conduction in Low Mobility Materials, Eilat, Israel, April 1971.

(15) Haberland D.R., and Kehrer H.P., Solid State Electron, 13 (1970) 451.

(16) Neale R.G., J. Non-Cryst. Solids, 2 (1970) 558.

(17) Kolomiets B.T., et al, Sov. Phys.-Semicond. 6 (1972) 167.

(18) Drake C.F. et al., reference 10 of Chapter 1.

(19) Champness C.H., Armitage D., Proc. Conf. on Conduction in Low Mobility Materials, Eilat, Israel, April 1971, p.339.

(20) Andreev A.A. et al, Sov. Phys.-Semicond. 5 (1972) 1900.

(21) Savage J.A., J. Mater. Sci. 6 (1971) 964. (Chapter 2, ref. 20).

(22) Delchar T., University of Warwick, England, personal commun.

(23) also observed by Mathur B.P. and Arutz F.O., J. Non-Cryst. Solids 8-10 (1972) 445.

(24) Hulls K., Ph.D. thesis 1970, University of Warwick, England.
Červinka L., et al, J. Non-Cryst. Solids 4 (1970) 258.

(25) Robertson J.M., University of Edinburgh, Scotland, personal commun.

(26) Yoffe A.D., University of Cambridge, England, personal commun.

(27) "Kodak Photosensitive Resists: Photofabrication - application and processes". Kodak Ltd., 1970.
Dunham K.R., Solid State Technology 14 (1971) No. 6 (June) p.41.

(28) Holland L., "Thin Film Microelectronics", Chapman & Hall, London, 1965, p.38.

(29) Grosso P.F. and Heck R.F., IEEE Trans. ED17 (1970) 1083.
Anderson J.C., Thin Solid Films, 12 (1972) 1.

(30) Coward L.A., J. Non-Cryst. Solids 6 (1971) 107.

CHAPTER 5

EXPERIMENTS AND EXPERIMENTAL RESULTS

5.1 Temperature and Electric Field Dependence of Conductivity

The temperature and electric field dependence of the electrical conductivity of a switching material are of paramount importance to the switching process. The quantitative information about the electrical conductivity as a function of temperature and electric field enables a great deal to be inferred about the charge transport processes in the switching material which play an essential role in any theoretical model of switching, and the information also enables a particular model to be tested quantitatively. This is why special attention was devoted to the measurement of electrical conductivity of the chalcogenide glass $Si_{12}\ Ge_{10}\ As_{30}\ Te_{48}$, which was mostly used for switching experiments. The results of the measurements are presented in this section.

The measurements were carried out on two configurations of specimens:

(i) Sandwich configuration: slices 1 mm thick with guarded electrodes

(ii) Coplanar configuration: switching device 30 μm thick.

The samples were placed in a metal cryostat filled with helium gas whose temperature was measured by copper-constantan thermocouple. The measuring circuit consisted of a variable d.c. supply (bank of dry batteries) connected through an interchangeable normal resistor to the sample. The value of the normal resistor was chosen always to be at least a hundred times smaller than the sample resistance and therefore the voltage applied to the sample was considered to be sufficiently accurately the d.c. supply voltage measured by a moving coil voltmeter. The small voltage drop across the normal resistor, from which the current through the sample could

be determined, was measured by a vibrating reed electrometer (Vibron Precision Electrometer, Model 62A, Electronic Instruments Ltd., Richmond, Surrey, England.). The measuring apparatus was built by Hulls and its constructional details together with the method of measurement are described in detail in his thesis (Chap. 4, ref. 24).

The conductivity of the samples as a function of temperature (electric field kept constant) is given in Fig. 5.1 for various applied fields. At temperatures above $T \approx 250^{\circ}K$ there is a linear relationship between the logarithm of conductivity and the reciprocal temperature with corresponding activation energy of $E_g/2 = 0.56$ eV. At lower temperatures the conductivity ceases to depend on temperature, which behaviour resembles the transition between intrinsic and extrinsic conduction in crystalline semiconductors.

The current through the samples as a function of the applied field at constant temperatures (the I-V characteristic) is given in Fig. 5.2. It can be seen that the I-V characteristics are non-ohmic starting at very low fields (10^2 V/cm).

A considerable effort has been made to ascertain the functional form $I = f(V)$. Seven different functions which are frequently quoted as possible relationships between the current and the voltage applied to a non-crystalline material were considered. Each of the functions has two parameters; the value of the parameters was determined by using the least squares method to fit the set of experimental data. The results of least squares fit to the I-V characteristic taken at $T = 285^{\circ}K$ are given in Table 5.1 together with the results of fitting the same functions to the data which is known to result from heating effects (they were generated by a computer calculation based on the thermal model discussed in section 3.1).

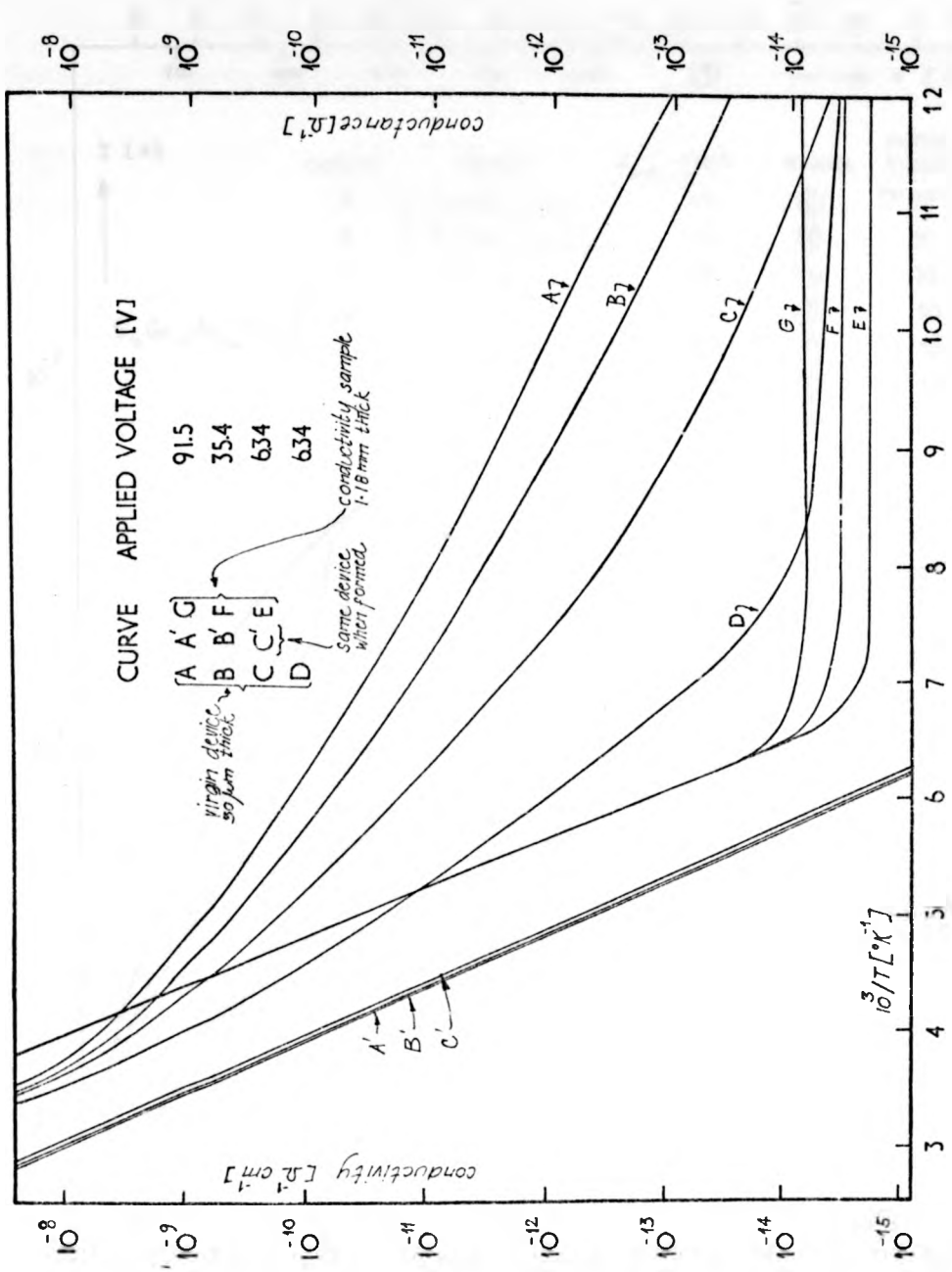

Fig.5.1.

D.C. CONDUCTIVITY AS A FUNCTION OF TEMPERATURE FOR VARIOUS DEVICES AND APPLIED ELECTRIC FIELDS.

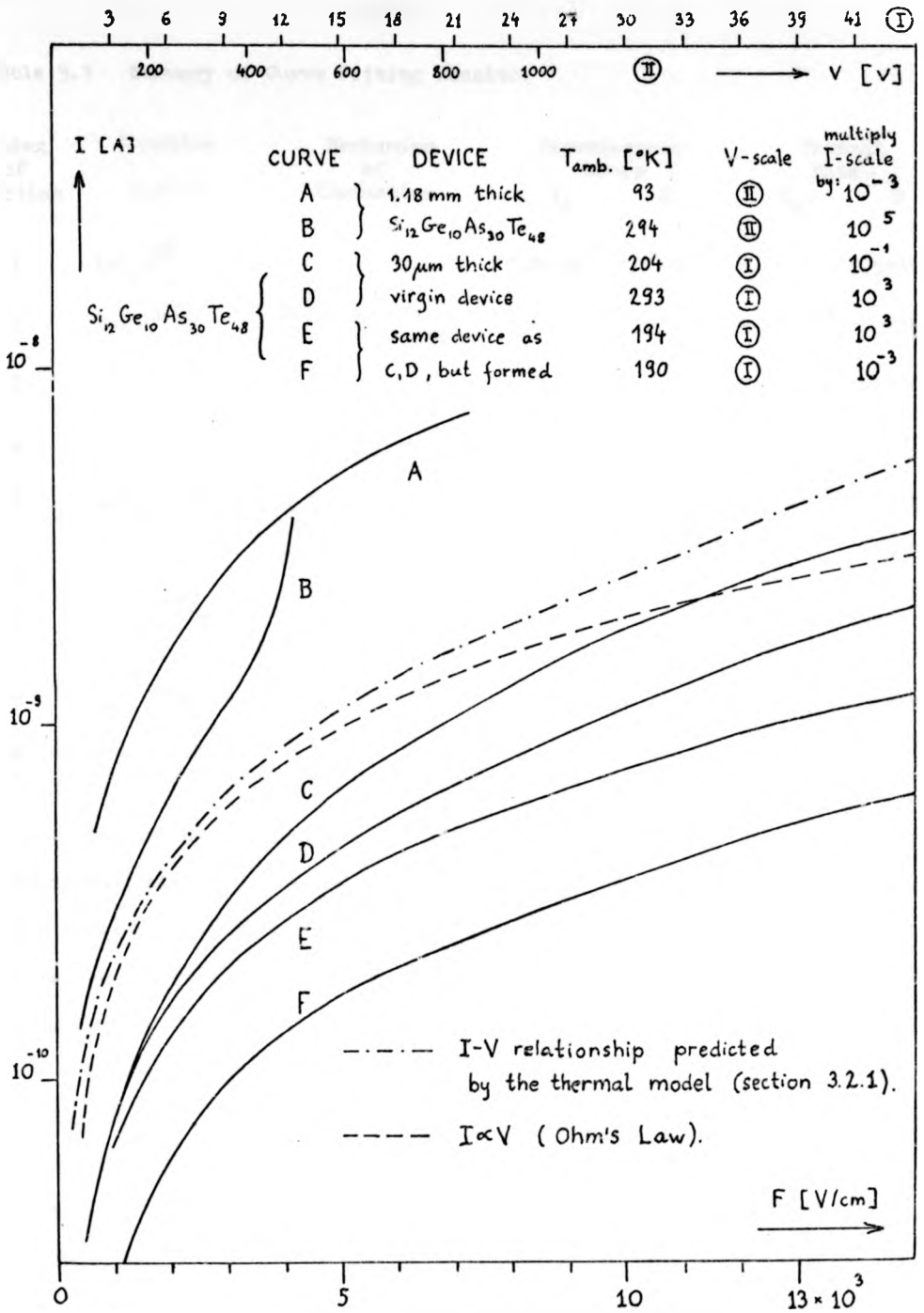

Fig. 5.2.

I-V CHARACTERISTICS FOR VARIOUS DEVICES AND AT VARIOUS AMBIENT TEMPERATURES.

Table 5.1 Summary of Curve Fitting Results.

Index of Function	Function I=f(V)	Mechanism of Conduction	Experimental Data * I_o	Experimental Data * B	Thermal Data + I_o	Thermal Data + B
1	$I=I_o e^{BV}$		$2.0*10^{-7}$	$2.9*10^{-2}$	$1.3*10^{-2}$	$7.5*10^{-2}$
2	$I=I_o e^{B\sqrt{V}}$	Poole-Frenkel or Schottky emission	$7.0*10^{-8}$	$3.9*10^{-1}$	$2.2*10^{-3}$	$8.0*10^{-1}$
3	$I=I_o V^B$	Space charge	$9.9*10^{-9}$	$1.2*10^{0}$	$3.4*10^{-3}$	$1.1*10^{0}$
4	$I=I_o(V+3)^B V$	Limited current	$8.9*10^{-9}$	$2.7*10^{-1}$	$2.4*10^{-3}$	$2.2*10^{-1}$
5	$I=I_o \sinh(BV)$	Conduction in inhomogeneous semiconductor	$1.2*10^{-6}$	$1.7*10^{-2}$	$2.2*10^{-2}$	$8.7*10^{-2}$
6	$I=I_o e^{B\sqrt{V}} V$	Poole-Frenkel or Schottky emission	$1.5*10^{-8}$	$7.6*10^{-2}$	$1.4*10^{-3}$	$8.3*10^{-1}$
7	$I=I_o e^{BV} V$		$1.9*10^{-8}$	$5.4*10^{-3}$	$7.3*10^{-4}$	$4.9*10^{-2}$

* device thickness = 30μm
\+ parameters assumed: $Eg/2 = 0.45eV$, $\sigma_o = 3*10^3 \Omega^{-1}cm$, $\kappa = 3*10^{-3} W deg^{-1} cm^{-1}$

The sum of least squares, which is a measure of how well the data is approximated by the particular function, is plotted in Fig. 5.3 against the index of the trial functions (ranging from 1 to 7). The results for both the experimental data and the theoretical thermal data are plotted out.

The best fit to the experimental data was obtained when the function $I = I_o \exp(V/V_o)V$ was used (function 6 in Table 5.1). The function $I = I_o \exp(V/V_o)$ fitted best to the thermal data but the fit was found to be poor (when plotted out). The fact that different functional dependencies $I = f(V)$ resulted in best fits to the experimental and theoretical thermal data indicates that the experimental I-V characteristic is not due to self-heating effects. This conclusion is also supported by the different behaviour of the graphs in Fig. 5.3.

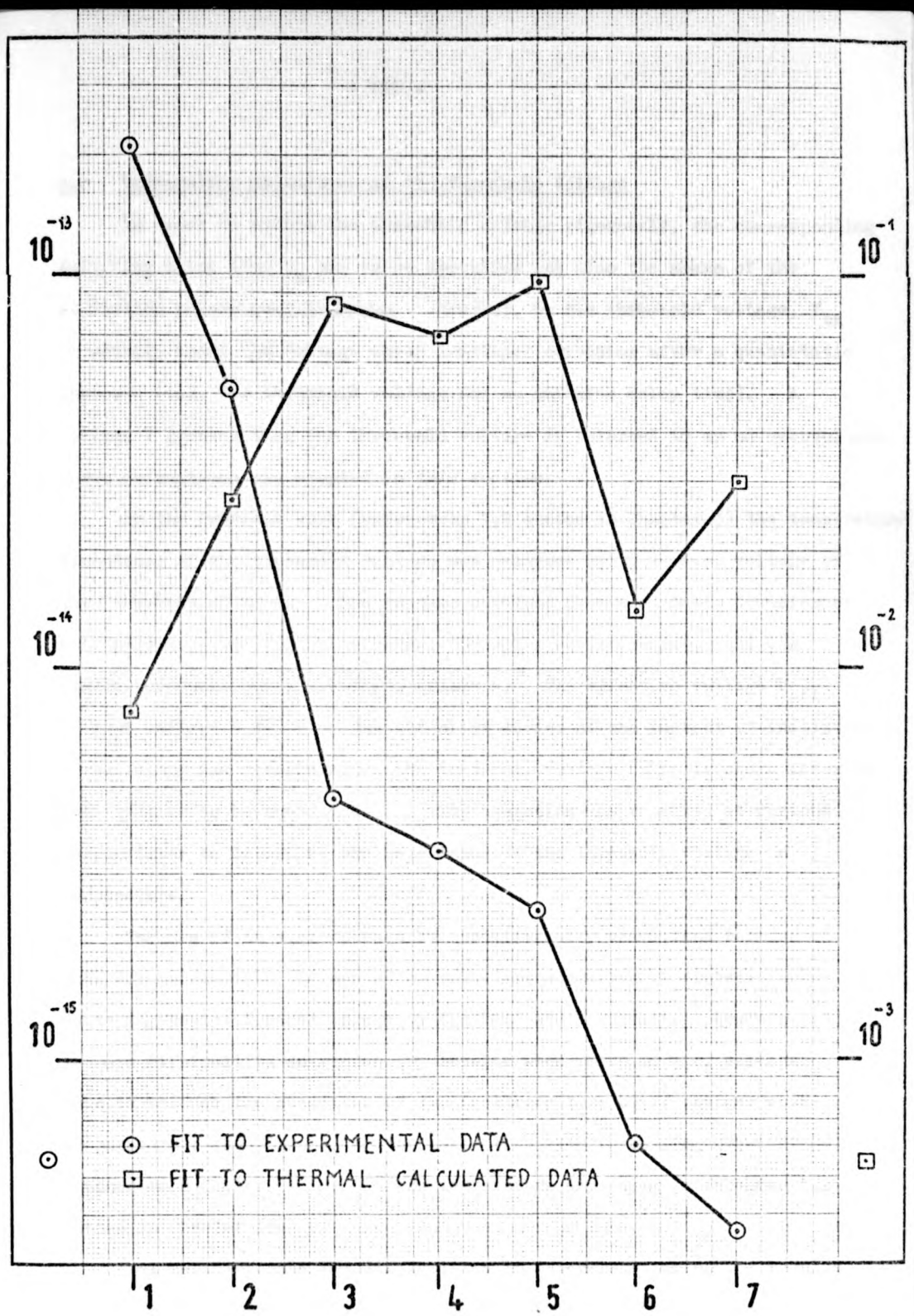

Fig.5.3.

PLOT OF THE SUM OF LEAST SQUARES AGAINST THE INDEX OF THE FUNCTION FITTED TO CONDUCTIVITY DATA.

5.2 Temperature Dependence of the Threshold Voltage

In order to define the threshold voltage rigorously, the corresponding switching delay time t_d has to be specified and also the shape of the excitation pulses must be known. However, by the threshold voltage, V_{th} is usually meant the voltage which initiates switching after a quasistatic increase (i.e. the threshold voltage for an infinite delay time). A voltage V greater than the threshold voltage is referred to as an overvoltage. These definitions are adopted in this section.

In the previous work (references 1,2 quoted in Chapter 3) the temperature dependence of the threshold voltage was measured using an a.c. voltage of the frequency of 50 Hz. The voltage obtained from a variable transformer was applied to the switching device through a series resistor and was slowly increased until switching occurred. The effective voltage V_{eff} (= peak voltage : $\sqrt{2}$) on the switching device at the instant of initiation of switching was designated as the threshold voltage (this is shown later in this section to be inaccurate). This operation was repeated at various temperatures to determine the dependence of the threshold voltage on temperature.

The use of an a.c. voltage is experimentally convenient because it does not necessitate the use of an auxiliary circuitry to protect the switching device against damage by the "on"-state current. However, it is more difficult to interpret the results when using an a.c. voltage. This is because the character of the isotherms $t_d = t_d(V)$ changes with temperature : the decrease of the delay time with increasing overvoltage becomes much faster as the ambient temperature decreases (references 1,2 quoted in Chapter 3).

Let us illustrate the difficulties in interpretation of the results of a measurement using an a.c. voltage by considering the response of a switching device to an a.c. sinusoidal voltage of frequency $^1/T$ in two

extreme regions of ambient temperature:

(i) At high temperatures the delay time only slowly decreases with overvoltage, the switching device can withstand large overvoltages V for a long time t_d, and therefore a sinewave with a peak value considerably in excess of the threshold voltage does not cause switching. Provided that the condition $T \ll t_d(V)$ is fulfilled, the switching device does not respond to individual a.c. cycles, but sees the a.c. voltage as a d.c. voltage of a magnitude lower than the peak a.c. voltage. In the case of a thermal mechanism of switching the equivalent value of the d.c. voltage is V_{eff}, i.e. the threshold voltage is correctly expressed in terms of the effective value of the a.c. voltage.

(ii) At low temperatures the delay time sharply decreases with overvoltage and thus the threshold voltage can be exceeded by a sinewave only by a small amount $V-V_{th}$, given implicitly by the condition $t_d(V) \leq T$. Therefore the peak value of an a.c. voltage just initiating switching is very closely equal to the threshold voltage.

These two examples show that at high temperatures the threshold voltage is given by the effective value of the applied a.c. voltage whereas at low temperatures it is given by the peak value. At intermediate temperatures the true threshold voltage lies between the effective and peak values of the a.c. voltage which just initiates switching and cannot be accurately determined without an additional information about the function $t_d(V)$.

To eliminate this ambiguity, the experiment was carried out using a d.c. voltage. The circuit diagram of the experimental arrangement is in Fig. 5.4. The damage to the switching device which would result during the "on"-state (low value of series resistor was used) was prevented by using a thyristor connected in parallel to the switching device. The thyristor switches on a few microseconds after the switching device and shunts the switching device.

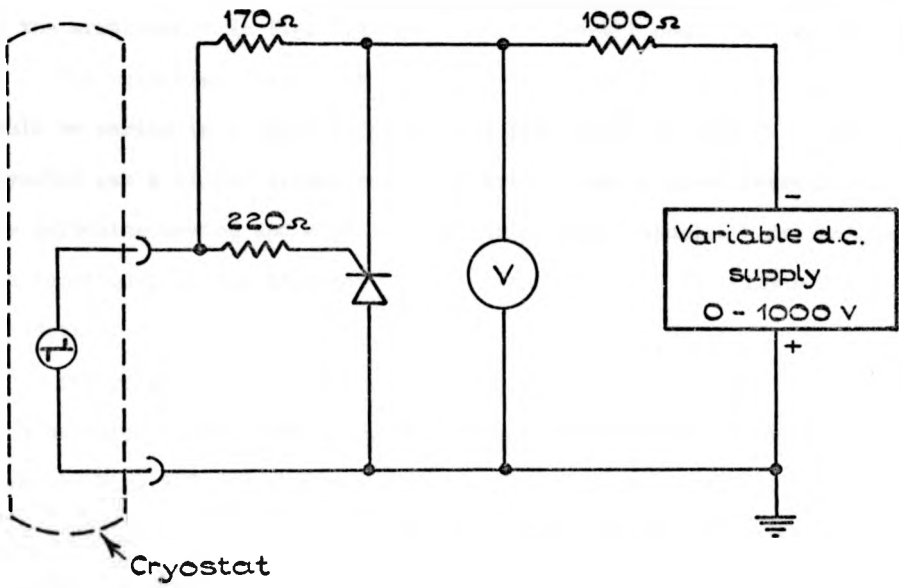

Fig. 5.4.

THE CIRCUIT DIAGRAM OF THE EXPERIMENTAL ARRANGEMENT FOR THE MEASUREMENT OF THRESHOLD VOLTAGES USING A d.c. VOLTAGE.

A measurement of the threshold voltage was carried out by slowly increasing the voltage of the d.c. supply (rates of about 6 V/s were employed) until the switching occurred - signalled by a drop in the voltmeter reading. The threshold voltage V_{th} was taken as the maximum voltage registered on the voltmeter before the drop. The voltage of the supply was then decreased until the thyristor switched off (to ~15 V in the arrangement in Fig. 5.4) and the measurement could be then repeated.

The switching device was placed into a cryostat whose temperature could be varied in a broad temperature range +200°C to -196°C. The cryostat was a closed silica container with a copper sheet housing for the switching device and a copper-constantan thermocouple. Helium gas was admitted into the cryostat during measurements to facilitate heat conduction.

The results of a measurement of the variation of threshold voltage of a sandwich device of $Si_{12}Ge_{10}As_{30}Te_{48}$ glass of thickness 150 μm are given in Fig. 5.5 and also re-plotted in Fig. 3.2 to provide a comparison with the theoretical prediction. It is seen that the logarithm of the threshold voltage plotted against the reciprocal temperature follows a straight line in a temperature region from 150°C to about -20°C. The slope of the straight line is very nearly equal to one half of the activation energy for electrical conductivity and thus a good agreement with the prediction of the thermal model is obtained. At temperatures above 150°C the switching transition is not well defined and it was difficult to obtain accurate data with the experimental arrangement in Fig. 5.5; it seems, however, that the switching voltage decreases in this region rather faster than predicted by the thermal model. It is not clear, if the threshold voltage extrapolates to zero at the glass transition temperature T_g of 230°C as is observed for some glasses.

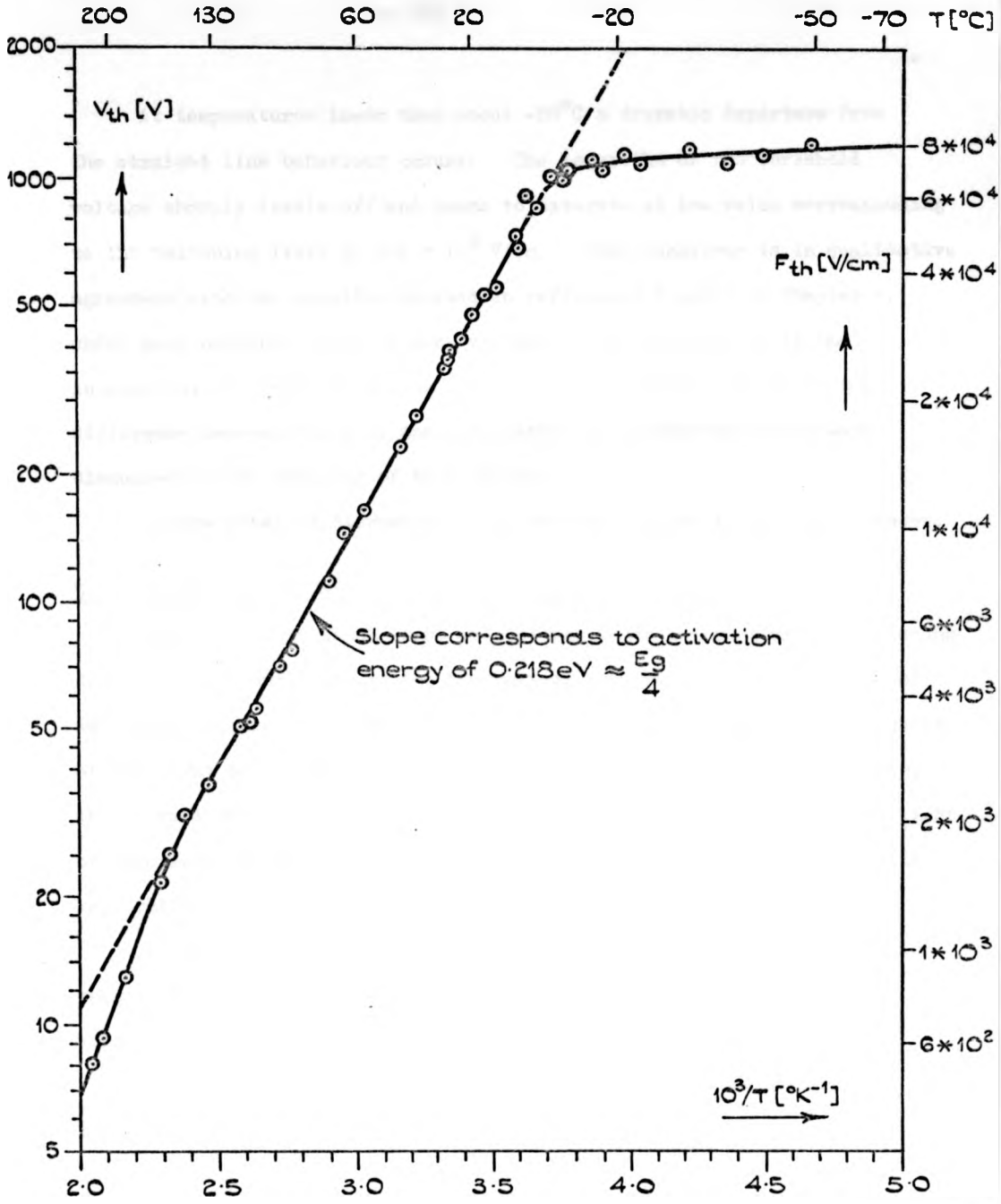

Fig. 5.5.

TEMPERATURE DEPENDENCE OF THRESHOLD VOLTAGE FOR $Si_{12}Ge_{10}As_{30}Te_{48}$ SANDWICH DEVICE 150 μm THICK (Note: Logarithmic and reciprocal scales are used).

At temperatures lower than about -20°C a dramatic departure from the straight line behaviour occurs. The logarithm of the threshold voltage sharply levels off and seems to saturate at the value corresponding to the switching field of $\sim 8 \times 10^4$ V/cm. This behaviour is in qualitative agreement with the results reported in references 1 and 2 in Chapter 3, which were obtained using an a.c. voltage. The differences in the intermediate temperature region seem to be explicable in terms of the difference between the d.c. and a.c. method of measurement which were discussed at the begining of this section.

A more detailed discussion of the results follows in the next Chapter.

5.3 Initiation of Switching by Light and Electron Beams

Experiments in which light or electron beams interact with a switching device should contribute to the theoretical insight into the mechanism of switching because different models of switching predict different influence of the light or electron beams on the switching process. In particular, the thermal mechanism of switching is not expected to be influenced by light or electrons as long as the heat dissipated by the beams per unit time is kept sufficiently small.

On the practical side, there would be an indisputable oportunity for technical applications if the switching parameters (e.g. the threshold voltage) could be varied by means of light or electron illumination.

There has been a considerable amount of work done and reported in the literature on the changes that light (laser) or electron beams can induce in the structure of chalcogenide glasses, i.e. on the aspects of memory switching (for review see section 2.1.2). Much less is known about the influence of light or electron beams on threshold switching. Shakovtseva[1] observed that the threshold voltage in CdS, CdSe devices is a function of light illumination and that light also influenced the

shape of the I-V characteristics. The fact that electrical breakdown in various substances can be activated by light was discussed by Klein[2].

In the present work two pilot experiments were carried out in order to ascertain whether switching in the threshold glass Si_{12} Ge_{10} As_{30} Te_{48} can be influenced by light and electron beams. The experiments are described in the following two sections.

5.3.1 Experiment with Light

Two basic geometries of devices were used: the sandwich and coplanar geometries. In the first case transparent tin oxide electrodes were used. The tin oxide layer was prepared by evaporating tin onto a silica window and oxidizing the tin in air at 400°C. The silica window was then placed in contact with a slice of polished chalcogenide glass which had a non-transparent counterelectrode prepared by evaporation of gold. In the coplanar arrangement zinc and silver electrodes were evaporated onto a polished surface of chalcogenide glass; the spacing between the electrodes was $\sim 5\,\mu m$. Platinum wires closely spaced ($\sim$ 0.1 mm) and touching the polished and lightly etched surface of the glass were also used as electrodes.

The experimental arrangement is shown in Fig. 5.6. Two kinds of experiments were carried out. In the first experiment a d.c. voltage supply connected between EB was set to give voltages just below the threshold voltage (onset of switching monitored by the voltmeter) and the shutter was then open to allow the light to shine on the device. Only a small increase in the "off"-state current was observed due to photoconductivity of the glass, however, and no evidence of the initiation of switching by the light was obtained. In the second experiment points A, B were connected to the vertical and horizontal inputs of an oscilloscope and an a.c. voltage supply was used. This enabled observation of the I-V characteristic of the switching device as a function of illumination, but similarly to the first experiment, no definite influence was observed.

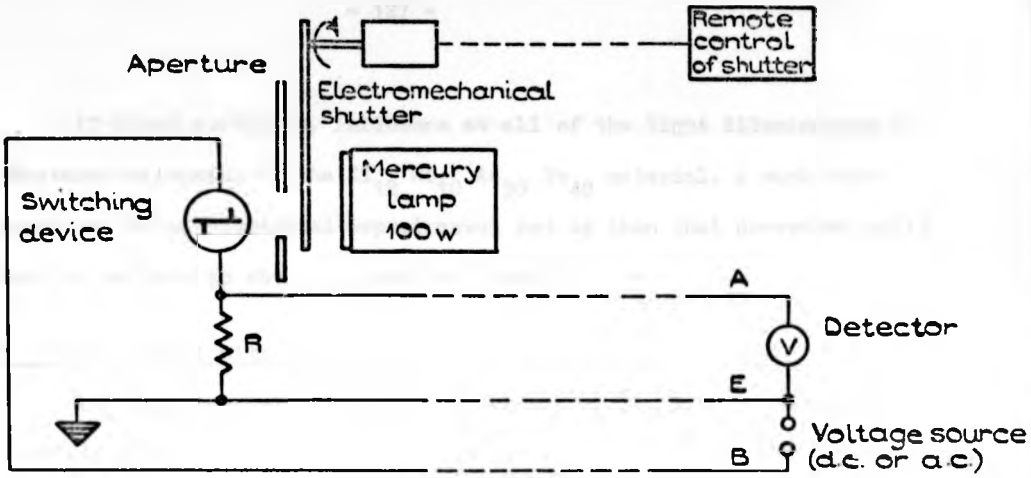

Fig. 5.6.

EXPERIMENTAL ARRANGEMENT FOR ASCERTAINING THE INFLUENCE OF LIGHT ON SWITCHING.

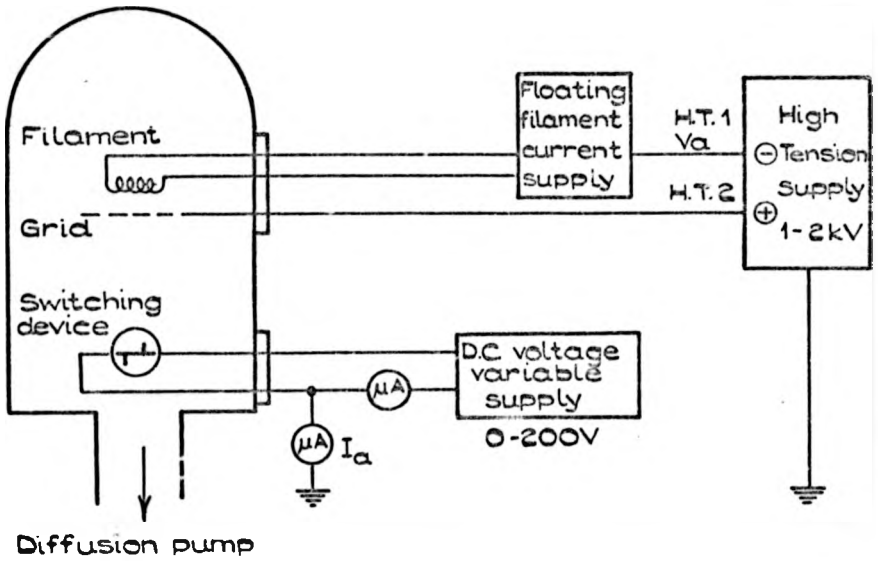

Fig. 5.7.

EXPERIMENTAL ARRANGEMENT FOR ASCERTAINING THE INFLUENCE OF ELECTRONS ON SWITCHING.

If there exists any influence at all of the light illumination on threshold switching in the Si_{12} Ge_{10} As_{30} Te_{48} material, a much more sensitive or sophisticated experimental set up than that described would have to be used to obtain a positive result.

5.3.2 Experiment with Electrons

The experimental arrangement is shown in Fig. 5.7. Devices of coplanar geometry were used in this experiment. The d.c. voltage in the device circuit was increased just below the threshold voltage and then the electron current was switched on. Initiation of switching was observed only when the power dissipated in the electron beam circuit $P = I_a V_a$ was 2 - 5 W and heating of the switching device resulted.

The experiment was later repeated in the specimen chamber of a scanning electron microscope (section 5.5) but no evidence of the electron beam influencing the switching mechanism could be found.

In conclusion it is possible to say that the electron beam initiated or influenced switching only when the power dissipated by the electron beam in the switching device was sufficient to initiate thermal switching.

5.4 Forming Process

The term "forming process" has so far been used only in section 3.4.4; therefore a brief account is given in this section together with the experimental results.

The forming process can be defined phenomenologically as a stabilisation of switching parameters of a new (unswitched or virgin) switching device. The forming process always takes place in thin oxide film devices prior to the occurrence of the voltage-controlled negative resistance ("N"-shaped I-V characteristic). It also seems to be a general requirement for the occurrence of the current-controlled negative resistance and switching ("S" - shaped I-V characteristic) in amorphous

semiconductors. Chopra[3] reviews some of the known aspects of the forming process.

The forming process in chalcogenide switching devices has not received very much attention in the literature so far, but it becomes increasingly apparent that the failure to explain switching effects satisfactorily by any of a number of theories may be due to not taking into account important changes in the device after the forming took place. (It is often observed that the thermal model correctly predicts thickness dependence of the threshold voltage only for the "first-fire" operations.)

The forming takes place in both memory and threshold devices. It is widely accepted that structural changes are responsible for the stabilization of switching parameters in the case of memory switching. This hypothesis has been extended in section 3.4.4 to the case of threshold switching. Fig. 3.12 depicts schematically how the volume fraction of the assumed highly conductive crystals developed during the forming process stabilizes and shows that the temperature inside the device during its operation is unable to rise when the crystals are fully developed. The discussion is taken up again in Chapter 6.

Let us now turn to the experimental results. Fig. 5.8 shows the changes in the threshold voltage of chalcogenide glass switching devices with the number of operations. An a.c. voltage of 50 Hz was used to switch the devices and by one operation is meant the application of a voltage causing switching for a number of cycles of the a.c. voltage (nomenclature of section 5.5 applies here).

It is seen from Fig. 5.8 that the threshold voltage of a sandwich device decreases from an initial high value and stabilizes after about 15 operations. The resistance of the device was measured after each operation and was found to decrease in a similar way as the threshold voltage. No damage of electrodes was observable on the device.

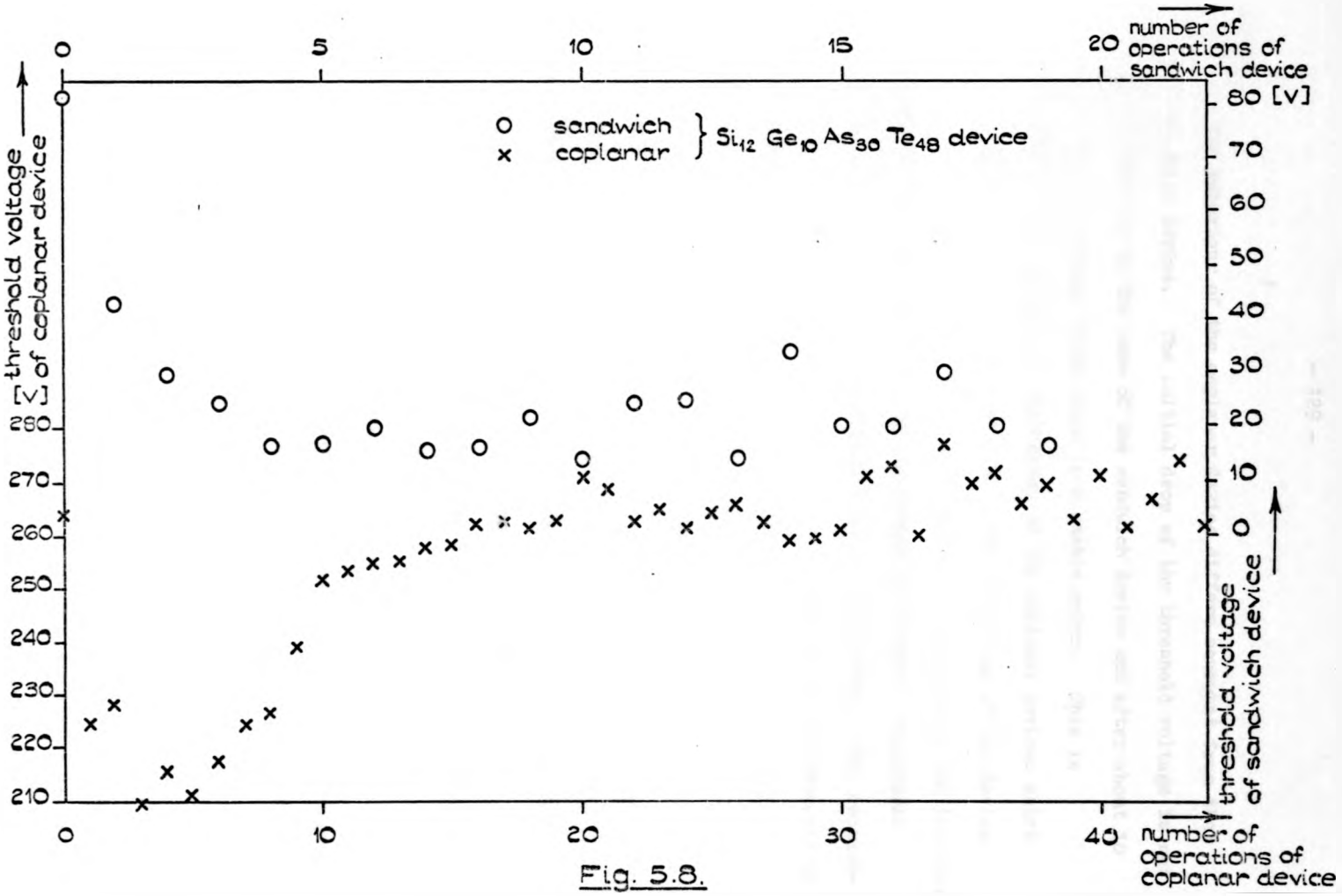

Fig. 5.8.

VARIATION OF THRESHOLD VOLTAGE DURING FORMING PROCESS FOR TWO DEVICES.

The behaviour of the coplanar device differs somewhat from that of a sandwich device. The initial drop of the threshold voltage is not as pronounced as in the case of the sandwich device and after about 10 operations the voltage rises again to a stable value. This is attributed to the changes in morphology of the coplanar devices which are discussed in the next section 5.5. The electrodes of the device were observed to "burn out" which resulted in the increase of the threshold voltage. Thus Fig. 5.8 shows two competing mechanisms: structural changes inside the material and changes in the electrodes. The measurements of the threshold voltage were again complemented by measurements of the resistance of the device after each operation; this was found to correlate with the changes in the threshold voltage.

After the stabilization of the threshold voltage there are still some seemingly random fluctuations in the voltage present from operation to operation. This aspect of variability is discussed in section 5.7, where additional evidence in favour of the interpretation of the forming process in terms of the structural changes is presented.

This section is concluded by a short description of an experiment in which a low resistance memory state was induced in a switching device employing the SMAG material. The device used was of sandwich geometry (thickness of 140 μm). After having been connected to a d.c. voltage of 400 V through a resistor of 82 kΩ, switching occurred after a few seconds. The voltage appearing across the switching device was then recorded. It is seen from the record (Fig. 5.9) that the voltage was of the order of 6 V and was fluctuating for about 7 minutes. Thereafter the voltage suddenly decreased to 4 V and the fluctuations decreased markedly. The resistance of the switching device was found at the end of this experiment to be 660 Ω (the initial resistance was 5.7 MΩ). This low resistance state was erased by an a.c. current of 6 mA (50 Hz) applied to the device through

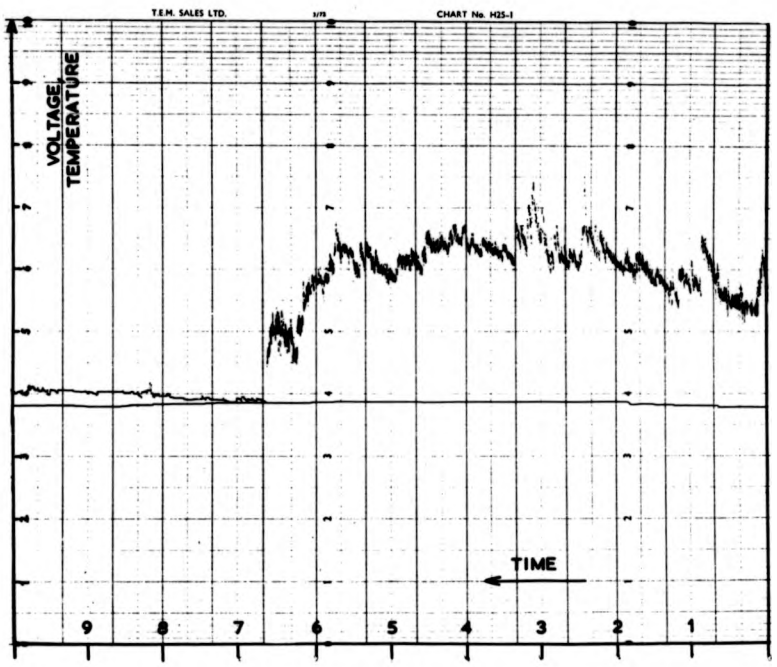

Fig.5.9.

UPPER TRACE: VOLTAGE ACROSS THE Si_{12} Ge_{10} As_{30} Te_{48} SWITCHING DEVICE IN THE 'ON'-STATE. MEMORY SETTING OCCURS AFTER $6^{2}/_{3}$ MINUTES.

LOWER TRACE: TEMPERATURE OF THE DEVICE.

SCALES: VERTICAL: VOLTAGE 1V/div.
TEMPERATURE 6·2°C/div.

HORIZONTAL: TIME 1 min./div.

9 kΩ resistor. The whole experiments could then be repeated several times with similar results.

This experiment provides additional evidence of structural changes in the STAG material. Its significance is discussed in section 6.3.2.

5.5 Scanning Electron Microscope Observations

The Scanning Electron Microscope (SEM) is a very powerful tool for investigation of semiconductor devices; it has been widely used for study of conventional crystalline semiconductor devices and in industrial laboratories for solving problems associated with the design of integrated circuits[4].

In SEM the specimen under study is scanned by a focused beam of electrons with energies up to several tens of keV[5]. In the emissive mode of operation the back-scattered electrons (here a further selection between reflected and secondary electrons is possible) are collected by a luminiscent target which in conjunction with a photomultiplier facilitates the measurement of the flux of the back-scattered electrons (Fig. 5.10a). The flux is a function of the properties of the specimen at the point of impact of the incident electron beam (e.g. topography, composition) and therefore by displaying the magnitude of the flux on a cathode ray tube (CRT) (e.g. in the way of modulating brightness) whose electron beam moves in synchronism with the beam directed at the specimen a "map" of the specimen is displayed on the CRT.

Apart from this emissive mode other modes of operation are possible depending on which physical quantity (a function of the position of the electron beam on the specimen surface) is used for display on the CRT. In the cathodoluminiscent mode the physical quantity is the flux of photons generated by the electron beam impinging on the specimen (Fig. 5.10b). If the current between the specimen and earth is used for display then the

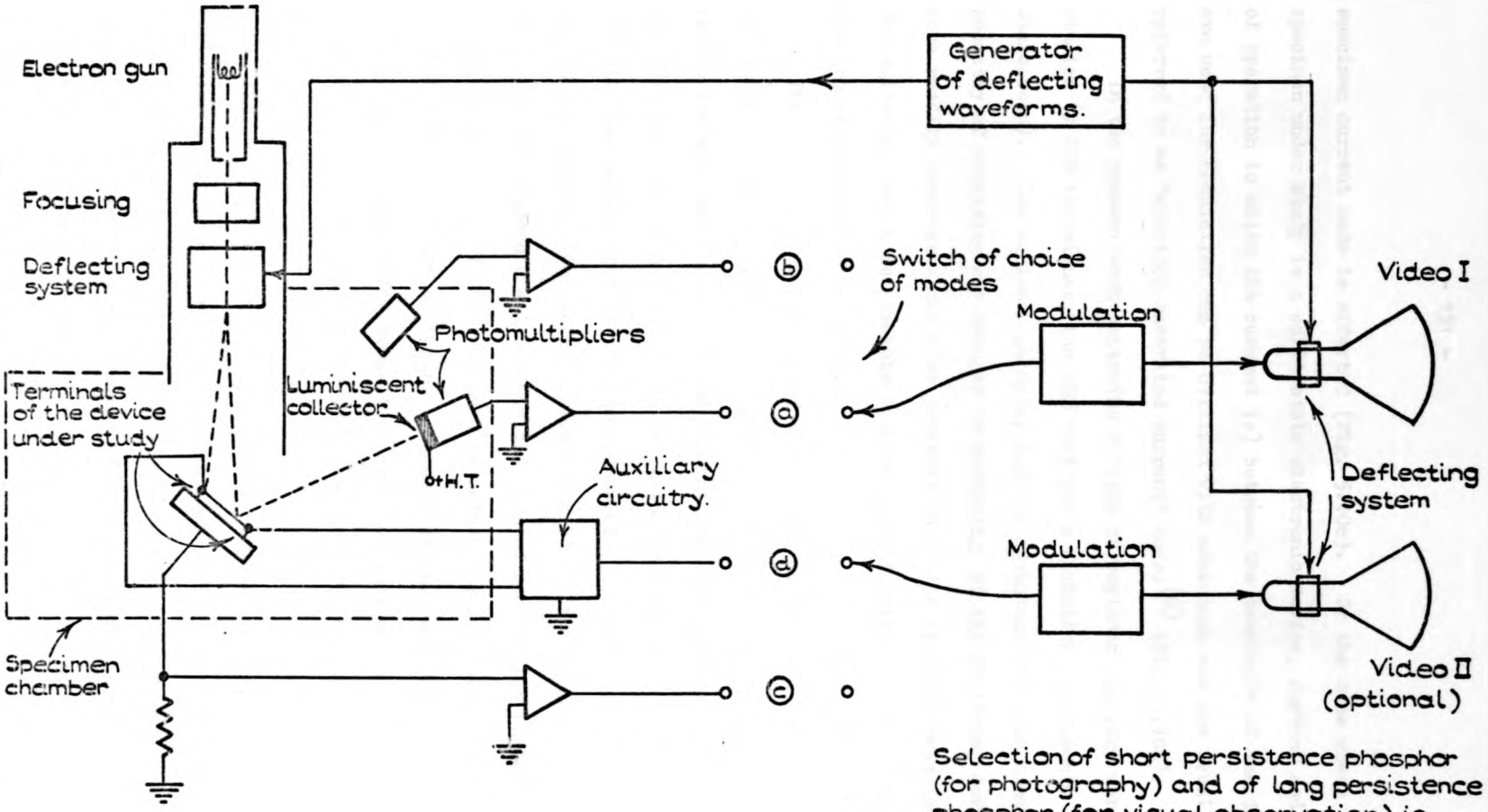

Selection of short persistence phosphor (for photography) and of long persistence phosphor (for visual observation) is available.

Fig. 5.10.

SCHEMATIC DIAGRAM OF SEM MODES OF OPERATION.

specimen current mode is effected (Fig. 5.10c). In the case where the specimen under study is a solid state electronic device, further modes of operation in which the current (s) between the terminals of the device are used for modulation can be utilized with advantage and are usually referred to as "electron generated current" modes[6] (Fig. 5.10d).

In the present work switching devices of coplanar geometry were studied by SEM techniques (the SEM used was a Cambridge Instruments Stereoscan). The coplanar geometry has the advantage over the sandwich geometry of rendering any changes in morphology of the switching device more readily observable and also penetration of the electron beam into the switching region is possible without necessitating the use of thin electron-transparent electrodes.

The changes in morphology of the devices were investigated using the emissive mode of operation. The switching devices could be operated inside the specimen chamber of the SEM and thus the process of damage to the switching device could be observed after each operation without removing the device from the specimen chamber. In the experiment carried out an a.c. voltage (variable between 0 and 500 V in the case of 50 Hz sine-wave and between 0 and 400 V in the case of rectangular pulses with frequency of 25 Hz - 7 kHz) was used to switch the device. The voltage was increased up to the switching threshold voltage and the device was then allowed to switch for some time (order of tens of seconds) until the voltage was removed; this cycle is hereafter in this section referred to as one operation.

Fig. 5.11 illustrated the changes in morphology of a coplanar switching device after a number of operations. The active region of the device is the step on the surface between its adjacent metal stripes clearly visible in the virgin device (there are several devices on one piece of chalcogenide glass). However, after only one or two operations

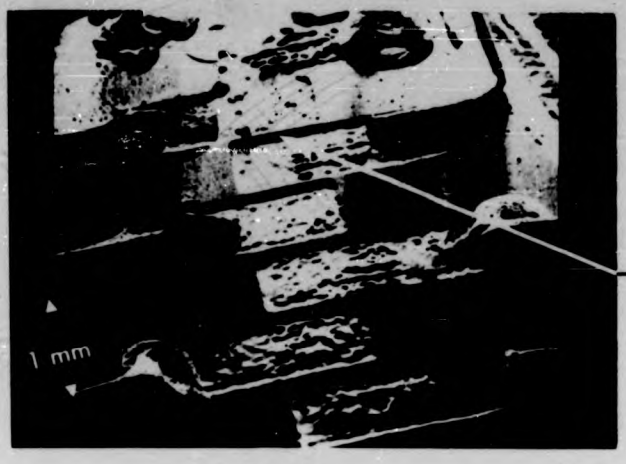

a

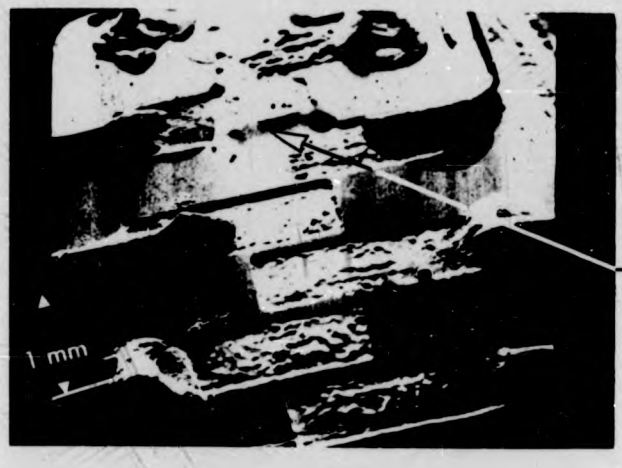

b

Fig. 5.11.

SCANNING ELECTRON MICROGRAPHS SHOWING CHANGES IN MORPHOLOGY OF A COPLANAR SWITCHING DEVICE.

of the device it could be observed that some changes in the morphology of the switching active region were taking place, apparently due to partial local melting of the chalcogenide glass in the active region. After the device had been operated for several times the initial sharp step on the surface between the adjacent electrode stripes was virtually smoothed out (Fig. 5.11b). The metal stripes were also affected by the operation of the device; in the vicinity of the switching region marks of "burning out" were apparent, probably due to alloying of the electrode metal with the chalcogenide glass or due to evaporation of the metal.

It was observed that the extent of the damage was related basically to the number of operations; the length of the operations was relatively unimportant. The progress of damage gradually slowed down after the first several operations during which most of the apparent change in morphology took place. The appearance of the active region was that of a smooth surface which resulted from the melting of the glass and was easily distinguished from the polished surface of the rest of the specimen (scratches caused by polishing disappeared after melting of the glass).

In the initial stages of the work with the SEM it was intended to study the conducting "on"-state of the switching device, particularly to search for the conducting channel which is expected to be present in the "on"-state according to the theoretical considerations (Chapter 2). The flux of the backscattered electrons is a strong function of the electrical conductivity of the material (the same applies to the specimen current) and therefore the SEM seemed to be an ideal instrument for monitoring and mapping conductivity changes in the switching device during its operation. However, several technical difficulties became immediately apparent. The a.c. voltage appearing across the switching device during its operation was sufficient to produce electric fields in the vicinity of the device which were high enough to disturb the flow of the electrons in the SEM;

this was manifested by stripes of changed contrast running across the CRT. (In this respect the coplanar geometry of the switching device is less suitable than the sandwich geometry).

The use of a d.c. voltage for the operation of the switching device was considered in order to achieve steady state electric fields around the device and eliminate the distracting changes in the contrast of the image. It was found, however, that if the "on"-state was sustained using a d.c. voltage for a period of even a short time (seconds) then the switching devices changed their properties markedly (the I-V characteristics degenerated into a non-linear resistance type of characteristics (no region of negative differential resistance)) and also pronounced changes in morphology occurred. The material between the electrodes became completely flattened, became black in appearance and at a magnification of 2000X droplets, presumed to be of dispersed metal, were clearly visible.

It would be possible to devise a method of a.c. operation of the device which would effectively be equivalent to the d.c. operation. This method would involve a suitable synchronization of the a.c. excitation waveform with the movement of the SEM electron beam (either a "stroboscopic" method or a method using advance of the SEM electron beam by finite increments) in conjunction with gating pulses applied to the modulation system (blanking pulses). In this way the SEM could be made to "see" the specimen only at short instances when the a.c. voltage appearing across the device were identical and steady (in the first approximation). A simple calculation shows that this method would necessitate the use of a long exposure photography (e.g. 10^6 dots per frame at 10^3 Hz a.c. excitation frequency gives 10^3 s exposure). Another disadvantage is the need for alterations to the SEM circuitry. As the preliminary experiments

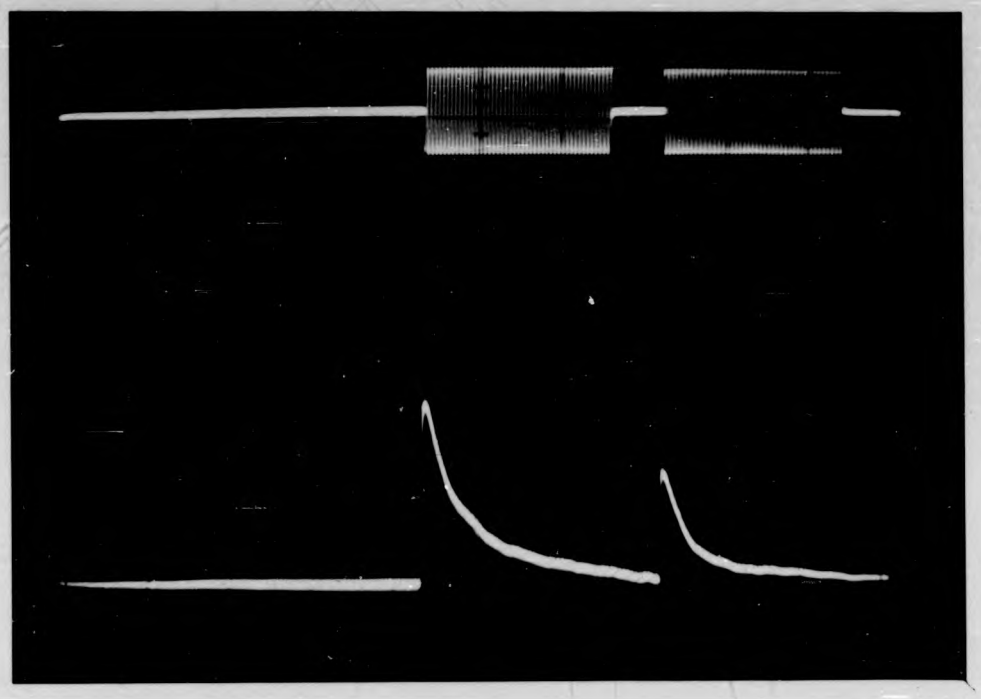

Fig. 5.12.

RECORDS OF THE CURRENT THROUGH THE SWITCHING DEVICE (UPPER TRACE) AND THE S.E.M. PHOTOMULTIPLIER SIGNAL (LOWER TRACE). HORIZONTAL SCALE : 0·3 s/div.

(employing emissive, specimen current and electron generated current modes) showed that the contrast associated with the formation of the "on"-state channel is very small (if observable at all without using a special detection system[7] suppressing compositional and topological contrast) it was decided to abandon further experimentation in this respect.

A phenomenon which was investigated experimentally and which is discussed in some detail in the following section 5.6 was first discovered during experimentation with the SEM. In this effect, a large signal is detected by the SEM at the begining of a switching operation and for some time afterwards. This is illustrated in Fig. 5.12 where the upper trace represents the current through the switching device and the lower trace is the record of the photomultiplier signal. At first this signal was thought to be due to spurious interaction between the circuit of the switching device and the sensitive photomultiplier amplifier input circuit at the instant of the onset of switching. Almost identical signals (signal levels of similar strength) were obtained in the emissive and in the cathodoluminiscent modes; in the latter case when the photomultiplier window was covered by an opaque lid the interception of the signal ceased thereby eliminating the possibility of a parasitic coupling between the circuits. The signals were also observed irrespective whether or not the SEM electron beam was incident on the switching device. It therefore became apparent that charged particles are produced by the switching device at the onset of switching, presumably resulting from the ionization of vapours of chalcogenide glass, electrode metal or residual atmosphere in the SEM and that at the same time a certain amount of light is also emitted. The quality of the vacuum inside the SEM specimen chamber (4×10^{-5} torr) was not sufficient to eliminate the possibility of ionization of the

residual gas by the high electric fields applied to the switching device. Therefore separate experiments were conducted using specially constructed device chambers and a good quality vacuum system; they are described in the following section.

5.6 Phenomena of Emission from the Switching Device

The preliminary experiments using the SEM which were described in the preceding section indicated that light quanta and charged particles were emitted from the switching device at the begining of its operation. In an attempt to ascertain the nature of these phenomena further experiments and observations were carried out; they are described in the following four sections.

5.6.1 Optical Microscope Observations

The switching devices of coplanar geometry were positioned on the table of an optical microscope and observed using a small magnification (x 10). The mode of operation of the devices was the same as described in section 5.5.

At the begining of each operation blue flashes of light were observed at various places across the active region. The duration of the flashes was too short to be estimated by a human observer (the SEM observations indicated a duration of ~0.2 s). During observations at atmospheric pressure it was noticeable that the shape of the flashes was needle-like (elongated) and that they started and ended at points on the electrodes a certain distance away from the edges (Fig. 5.13).

The flashes were still present when the device was housed in an enclosure which was evacuated to 2×10^{-5} torr or filled with argon under a pressure of 3×10^{-2} torr. The colour of the flashes was assessed as blue in all cases. If the flashes were due to the discharge in the surrounding gas, their colour would be expected to change from pink (or

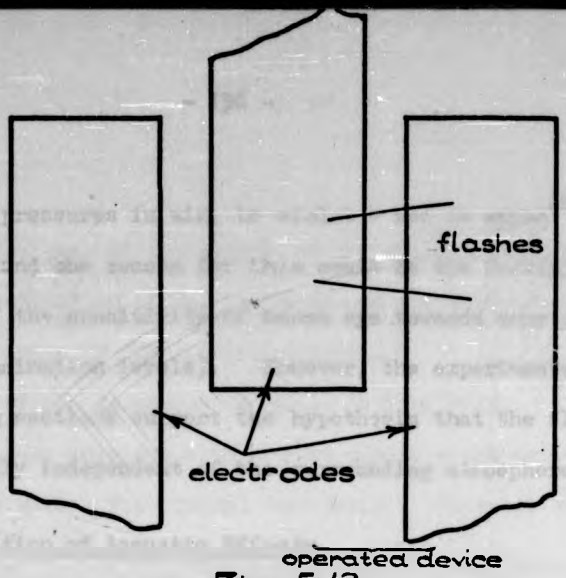

Fig. 5.13.
SCHEMATIC SITUATION DRAWING OF THE OBSERVED LIGHT FLASHES.

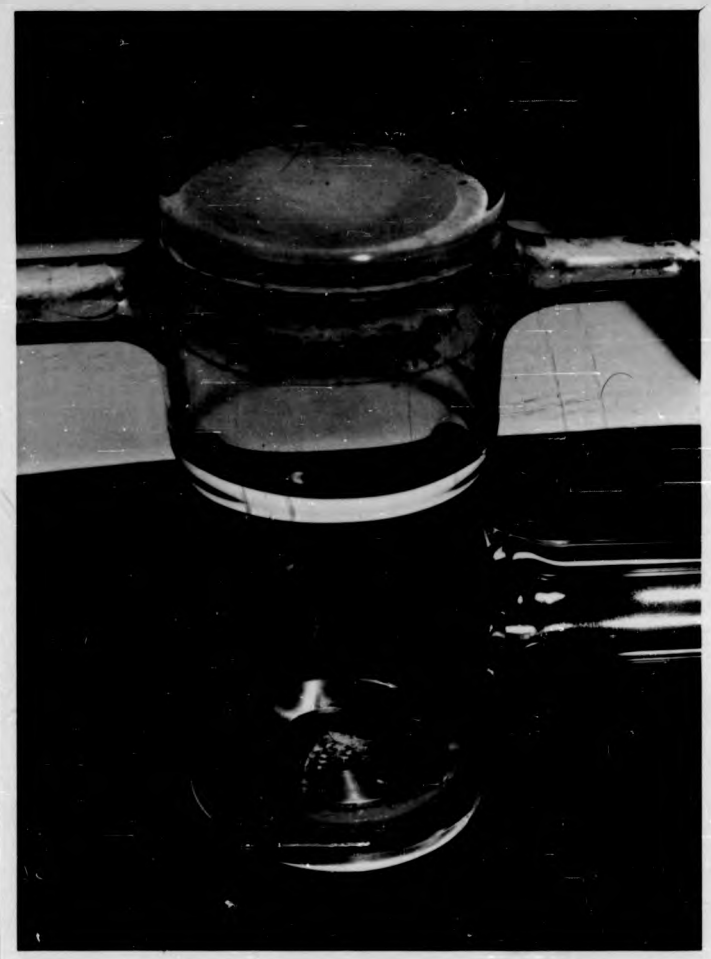

Fig. 5.14.
THE VACUUM TUBE HOUSING THE SWITCHING DEVICES WITH A

blue) at low pressures in air, to violet - red in argon[8]. This was not observed and one reason for this could be the Purkinje effect* (the shift of the sensitivity of human eye towards shorter wavelength at small illumination levels). However, the experiments described in the following sections support the hypothesis that the flashes observed are essentially independent of the surrounding atmosphere.

5.6.2 Observation of Acoustic Effects

During the observations carried out in air at atmospheric pressure a short sound whose occurrence coincided with the appearance of the light flash could be heard. The sound was similar to that produced by a capacitor discharge through a short circuit and its intensity at the distance of 50 cm from the switching device was assessed to be 10 dB. (From this follows a rough estimate of 10^{-11} W for the power dissipated by sound waves during the air impulse sound, which is negligible in comparison with the powers dissipated through light and heat emission[9]).

Acoustic effects of a similar description were observed by Stocker[10] during formation of a conducting path on the surface of a chalcogenide glass memory device. Stocker reports that a sharp click can often be heard as the path forms. It is not submitted that the effects described here are necessarily of the same nature as those observed by Stocker. A tentative explanation of the former is given in Chapter 6.

5.6.3 First High Vacuum Experiment

The aim of this experiment was to study the effect of the emission of charged particles from the switching device, which was first encountered during the SEM observations described in section 5.5. In order to obtain more reliable information about the effect it was necessary to carry out the experiment in high vacuum. An apparatus was designed which would

* J. E. Purkyně, Czech biologist.

enable

(i) analysis of the energy of the emitted charged particles

(ii) estimation of the location and the size of the emitting region of the switching device.

A photograph of the apparatus is given in Fig. 5.14. It comprises a cylindrical glass envelope with a flat window which is coated on its inner surface with a fluorescent substance. There is an electric connection to the fluorescent coating. The switching device is mounted on a base with lead-throughs (Fig. 4.3) and the base is sealed with low melting point wax (picein) to the end of the glass envelope opposite to the screen. A tungsten grid is provided above the switching device; the grid connection to an outside circuit is made also through the base leads. The envelope is evacuated through the side outlet. The minimum pressure obtained in the apparatus was 2×10^{-6} torr. This not very satisfactory pressure is partially due to the lack of a proper bake-out of the system. Only moderate heating to ~120°C could be applied because of the low melting point wax used in construction; the switching device itself would tolerate temperatures up to 230°C (T_g of the switching material).

With respect to the point (i) above, an experimental set up was tried out, the essence of which is the retarding potential method shown in Fig. 5.15. In the initial version of the equipment a negative ramp generator was used to produce the retarding potential (0 to -18 V) and a linear amplifier (Brookdeal LA350) as the current detector; a successful test run was made with a commercial diode (EZ80) substituted for the system switching device-grid in Fig. 5.15. The use of the analysing circuitry for the study of the emission from the chalcogenide switching device proved, however, to be much more difficult.

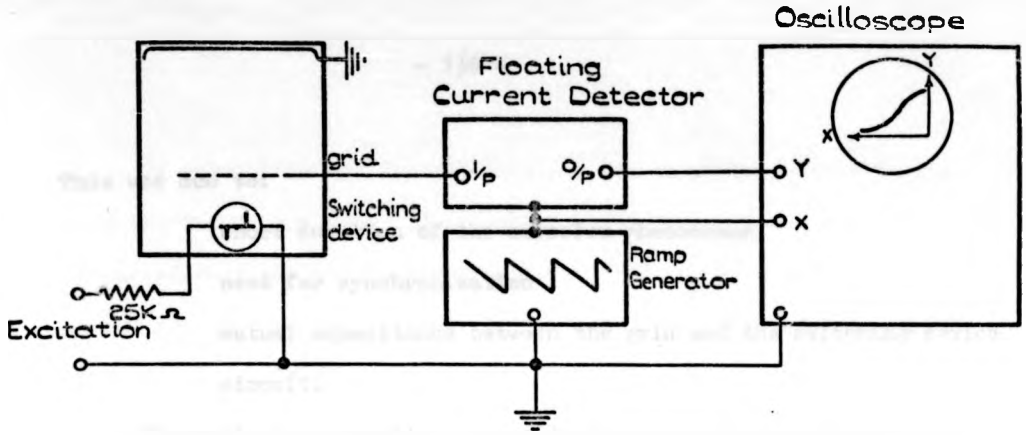

Fig. 5.15.

THE PRINCIPLE OF THE ANALYSIS OF THE ENERGY OF CHARGED EMITTED PARTICLES.

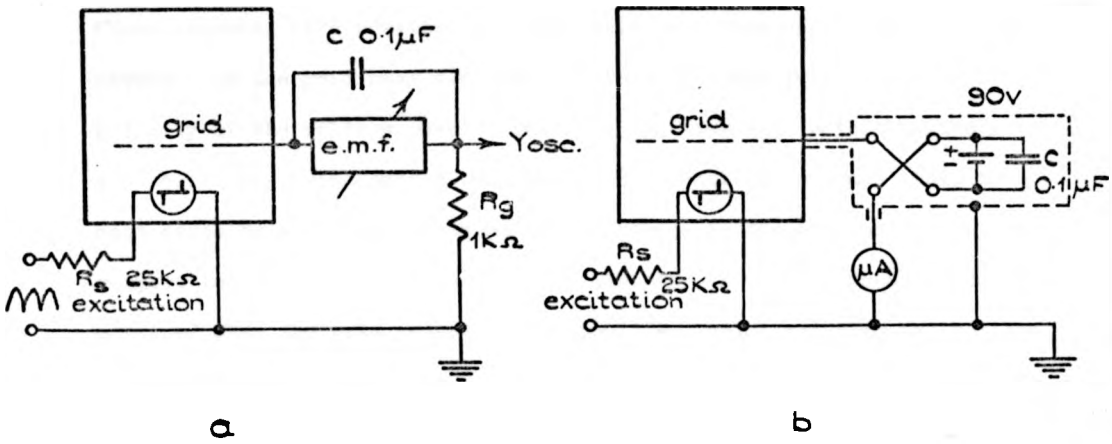

Fig. 5.16.

SIMPLIFIED VERSIONS OF THE PARTICLE ENERGY ANALYSER.

This was due to:

short duration of the emission phenomenon

need for synchronization

mutual capacitance between the grid and the switching device circuit.

The analysing circuitry was gradually reduced to mere detection circuits shown in Fig. 5.16a, b. In the first case the grid current developed a voltage drop on the resistor R_g which was observed on an oscilloscope; in the second case the detection was facilitated by a moving coil galvanometer. In both cases grid currents were detected if the grid was positively biased with respect to earth but only for a short time following the onset of switching. A voltage peak of less than 1 ms in duration was observed on the resistor R_g and similarly a ballistic deflection occurred on the galvanometer. When the polarity of the grid bias was reversed (negatively biased grid) no current was detected by the galvanometer in some cases, but in other cases deflections similar to those observed with positively biased grid were observed. The polarity reversal of the grid bias did not seem to affect systematically the polarity of the voltage peaks across the resistor R_g; both negatively and positively going pulses were observed. Their occurrence could in most cases be explained in terms of the change in the grid potential with respect to earth at the instant of switching; if the switching transition occurred when the grid potential was positive (negative) then the voltage peak was negative (positive).

The vacuum in the tube was maintained at 3.5×10^{-6} torr during these experiments. Later the experiments were repeated using an all-glass enclosure (Fig. 5.18) in which a better vacuum of 5×10^{-7} torr was achieved. The findings were similar to those obtained in the first experimental set up but with perhaps less ambiguity.

In summary it can be said that all the observed changes in the grid current at the onset of switching could be explained in terms of the changes in the mutual capacitance between the grid and the switching device and that no tangible evidence of charged particles being emitted from the switching device was produced by these experiments. The mutual capacitance could, in principle, be eliminated by including a second grid between the switching device and the existing grid and connecting it to a suitable potential; this was not, however, pursued at the time.

Another way of by-passing the unwanted influence of the mutual capacitances between the collecting electrode and the switching device is the use of the fluorescent screen which should convincingly show any genuine current of charged particles falling on it (no fluorescence is produced by displacement currents). When the fluorescent screen was connected in the circuit shown in Fig. 5.17 with R_a = 10 MΩ, there was no fluorescence observed, but with R_a = 1 kΩ an intense fluorescence of the screen took place at the begining of a switching operation. However the switching device was destroyed by this, showed an open circuit failure. The fluorescence of the screen was not localized but overall, so that this experiment did not yield information about the location of the emitting region and its size (point (ii) at the begining of this section).

It is possible that the fields between the collecting electrodes (grid and fluorescent screen) in the experiments above described were not sufficiently high to overcome the fields appearing across the switching device and thus failed to influence the flow of any charged particles which may be present.

The extent of experimentation was limited by the lifetime of the devices enclosed in the vacuum tubes and therefore a definite conclusion regarding various point mentioned in this section could not be reached.

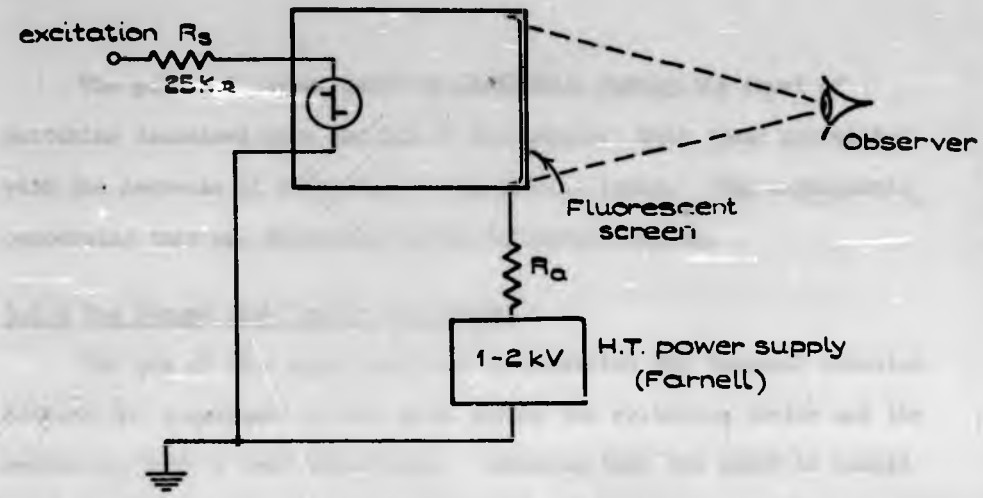

Fig. 5.17.

USE OF THE FLUORESCENT SCREEN FOR DETECTION OF CHARGED PARTICLES.

Fig. 5.18.

ALL-GLASS SWITCHING DEVICE HOUSING USED IN THE SECOND H.V. EXPERIMENT

The grid and screen currents registered during the onset of switching decreased with the age of the device; this trend correlates with the decrease of intensity of the emitted light. The experiments concerning this are described in the following section.

5.6.4 The Second High Vacuum Experiment

The aim of this experiment was to establish the temporal relation between the appearance of the spark across the switching device and the switching "off" - "on" transition. Assuming that the spark is caused by electric field excitation of vaporized material from the device at the begining of a switching operation, it should, in principle, be possible to ascertain at what instant of time the vaporization (i.e. the heating of the switching device) takes place by carrying out the present experiment.

There are two possible causes for the vaporization. It seemed most likely that an intense heating of the device could be due to the discharge of energy stored in the capacitance of the device and its leads ($\frac{1}{2}CV^2$) at the begining of the "off" - "on" transition. In such a case the vaporization would take place within a time comparable with the time constant of the discharging circuit following the "off" - "on" transition. This time would be less than a microsecond in most experimental situations ($R_{on} \lesssim 1\,k\Omega$, $C(\text{device + leads}) \lesssim 1\,nF$) and there would be very little difference between the behaviour in cases of an electronic and a thermal mechanism of switching.

The second possibility is that the heat dissipated by the current through the device in the "on"-state causes the vaporization (the fact that the spark occurs only during the first switching cycle of a switching operation could be accounted for by a spread of the current channel during subsequent cycles). Referring to the remark in section 2.2.1 (p. 43) concerning the temporal relation between the switching current and the

temperature distribution in the device it is expected in the case of a thermal mechanism of switching that the spark occurs during the increase of the device current. If the origin of the switching phenomenon is an electronic one then the heating and vaporization due to the device "on"-state current take place after the voltage across the device has dropped to the "on"-state value (which also may be insufficient to excite the spark in the vapour). Thus the temporal relation between the occurrence of the spark and the switching transition is expected to be different in the cases of thermal and electronic switching (in the framework of the hypothesis). Fig. 5.18 shows the position of the switching device in a vacuum system and the principle of the method of measurement, is indicated in Fig. 5.19. The current flowing through the switching device and the photometer signal are displayed simultaneously on the dual trace oscilloscope. The experimental accurracy with which the temporal relation between the two traces could be determined was about 1 μs. This limit was obtained by using a testing set-up in which the chalcogenide device was replaced by a neon tube operated by a voltage much greater than its ignition voltage.

The result of the experiment in which the appearance of the spark across the switching device was being measured against the occurrence of the switching transition is shown in Fig. 5.20; the oscillogram sets an upper limit of 4 μs on the time between the "off"-"on" transition and occurrence of the spark. The variations in the performance of the reed relay and in the device delay time prevented improvement of the time resolution of the experiment. (It was difficult to capture the event on the screen when the sweep time was much less than the variations in the delays). The result of this experiment is discussed further in section 6.3.

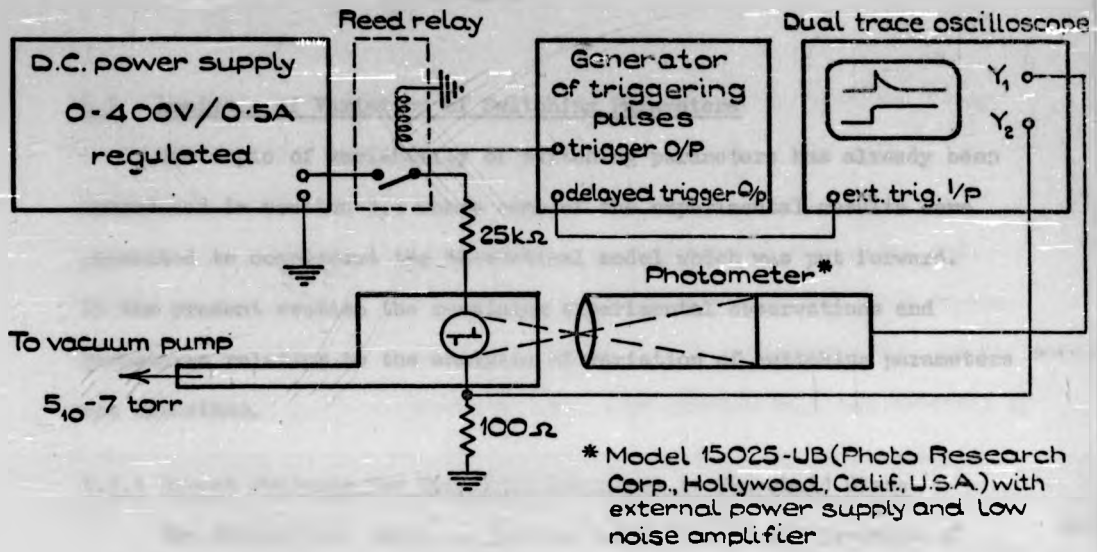

Fig. 5.19.

BLOCK DIAGRAM OF THE EXPERIMENT DESCRIBED IN SECTION 5.7.3.

Fig. 5.20.

TEMPORAL RELATION BETWEEN THE INTENSITY OF THE EMITTED LIGHT (UPPER TRACE) AND THE DEVICE CURRENT (LOWER TRACE).

5.7 Analysis of Variation of Switching Parameters

The topic of variability of switching parameters has already been introduced in section 3.4 where some of the experimental results were presented to complement the theoretical model which was put forward. In the present section the remaining experimental observations and procedures relating to the analysis of variation of switching parameters are described.

5.7.1 Direct Evidence for Two Phase Structure in Threshold Glass

The theoretical model in section 3.4 relies on the presence of highly conducting regions inside the semiconducting matrix of the switching material. These regions are most likely small crystallites which should be detectable by diffraction techniques.

X-ray diffraction, electron diffraction and transmission microscopy on the threshold type glass of composition Si_{12} Ge_{10} As_{30} Te_{48} atomic per cent (Ovshinsky composition) were carried out and are described in the following two sections.

5.7.1.1 X-ray Diffraction

Samples for X-ray powder diffraction were prepared by the technique described in section 4.3.4 from

(i) as made chalcogenide glass

(ii) material removed from the active region of a switching device

The X-ray powder diffraction technique with Cu K_α filtered radiation ($\lambda = 1.54$ Å) did not reveal any crystallinity in either of the two cases above, except when the as made material was obviously crystalline (detected by tests discussed in section 4.2.2). In that case analysis showed that the crystalline phase was As_2 Te_3; the diffraction pattern is in Fig. 2.4 (bottom).

The Laue back-reflection method was also employed, with the X-ray beam directed onto the switched region of the device. The only crystalline material detected was the electrode material. This was probably due to the beam being incident on part of the electrodes and not due to diffusion of the electrode material into the switching region; removal of the electrodes by etching could decide between the two possibilities.

There may be two reasons why small crystallites were not detected by X-ray difraction. Firstly, as already mentioned in the review chapter (section 2.1.1, p. 21) X-ray diffraction does not reveal very small crystallites of the size of the order $10^2 - 10^3\lambda$. Secondly, the intensity of the diffracted beam is proportional to the volume of the appropriate phase. Thus if the volume fraction of a crystalline phase in an amorphous matrix is very small then its diffraction pattern may not be resolved on the background resulting from the amorphous phase.

5.7.1.2 Electron Diffraction

Electron diffraction is superior to X-ray diffraction with respect to the two points above. Electrons with energy of 200 keV have about 60 times shorter wavelength than the CuK_α line and also somewhat smaller diffraction angles are used in electron diffraction than in X-ray diffraction; therefore much smaller crystals can be detected. The cross-sectional area of the electron beam can easily be made much smaller than that of an X-ray beam and therefore much better spatial selectivity is achieved which also facilitates detection of small crystallites.

One danger present in electron microscopy of chalcogenide glasses is the possibility of causing devitrification or even melting of the material by the electron beam[11,12]. The observations described in this section were made by using 200 keV electron microscope (JEM 200) and a "safe" level of the current density of the electron beam was determined

by observing a diffraction pattern of an amorphous region (rings) of the chalcogenide glass for about 15 minutes and determining that the diffraction pattern did not change.

The current density of 0.1 $\mu A/um^2$ was considered as one not causing structural changes in the chalcogenide glass and values less than this were used in the observations. For more energetic electrons the beam current density could be greater because less energy is dissipated by the electron beam.

Samples for electron microscopy were prepared by the method described in section 4.3.5. A transmission micrograph in Fig. 5.21 shows the distribution of fragments of the chalcogenide glass. The electron transparent fragment in the centre of the field shows regularity in its features - shadows running parallel, resembling a layer-like structure. A selected area diffraction pattern given by the fragment is in Fig. 5.22, the pattern was identified as crystalline tellurium.

In other cases the diffraction patterns obtained from the fragments of material were rather sharply defined rings which sometimes contained spots resembling polycrystalline-like patterns. It was not possible to identify positively the phases present and only a limited degree of similarity with the electron diffraction patterns obtained from thin films of the same glass (11 - 17) was found.

The microcrystallites were detected in both as made material and material removed from the switched region of a device. It was not possible to conclude whether the incidence of crystallinity differed in the two cases.

In summary, it can be concluded that a chalcogenide glass can be stable in the sense that it exhibits threshold switching as distinct from memory switching, and at the same time contain microcrystallites.

Fig. 5.21. TRANSMISSION ELECTRON MICROGRAPH OF FRAGMENTS OF $Si_{12}Ge_{10}As_{30}Te_{48}$ GLASS. MAGNIFICATION × 28,000.

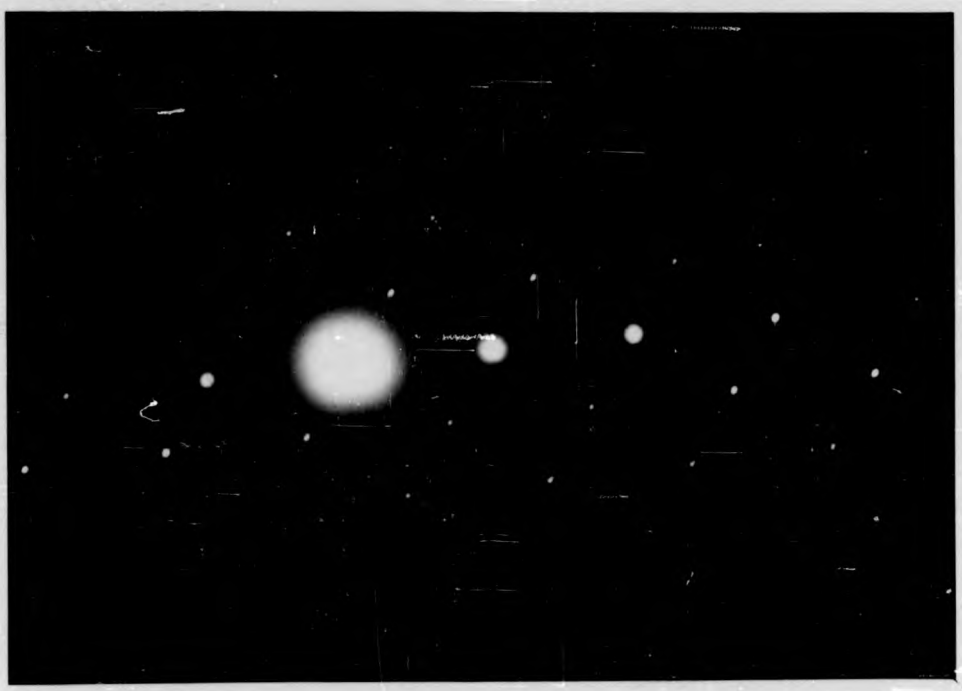

Fig. 5.22. ELECTRON DIFFRACTION PATTERN FROM THE FRAGMENT SHOWN IN THE CENTRE OF FIG. 5.21,

5.7.2 Techniques for Analysis of Variability of Switching Parameters

5.7.2.1 The Distribution Function

The distribution function of the delay times $\varrho(t_d)$ was obtained directly by using a multichannel analyser (Northern Scientific with 1024 channels). The block diagram of the experimental set up is in Fig. 5.23. The address advance of the multichannel analyser is initiated by a start pulse at $t = 0$ and stopped at the time $t = t_d$ at an address $N_d = k.t_d$ (nearest integer), where k is the rate of advance. The memory content of the N_d -th channel is increased by 1 bit and then the advance scaler is reset to $N = 0$. Thus if the whole cycle is repeated many times the memory content $M = M(N)$ as a function of N gives directly a histogram approximating the distribution function $\varrho(t_d)$ defined by (3.21).

The measurement of the distribution of the threshold voltages represented a slightly more difficult problem. The analyser used did not have a suitable digitizer and therefore a simple (but less efficient) method involving the use of an external discriminator was employed. Fig. 5.24 shows the block diagram of the experimental arrangement in which the first order distribution function was directly displayed on the screen of the analyser. The second order distribution function $\varrho(V_{th})$ was obtained by differentiating the memory content

$$\frac{d\,M(N)}{dN} \propto \varrho(V_{th})$$

this was carried out on a digital computer.

5.7.2.2 The Autocorrelation Coefficients

The basic requirement in the time series analysis is to record a sufficiently long series (preferably more than a thousand) of switching parameters for further processing. In the present work the time series

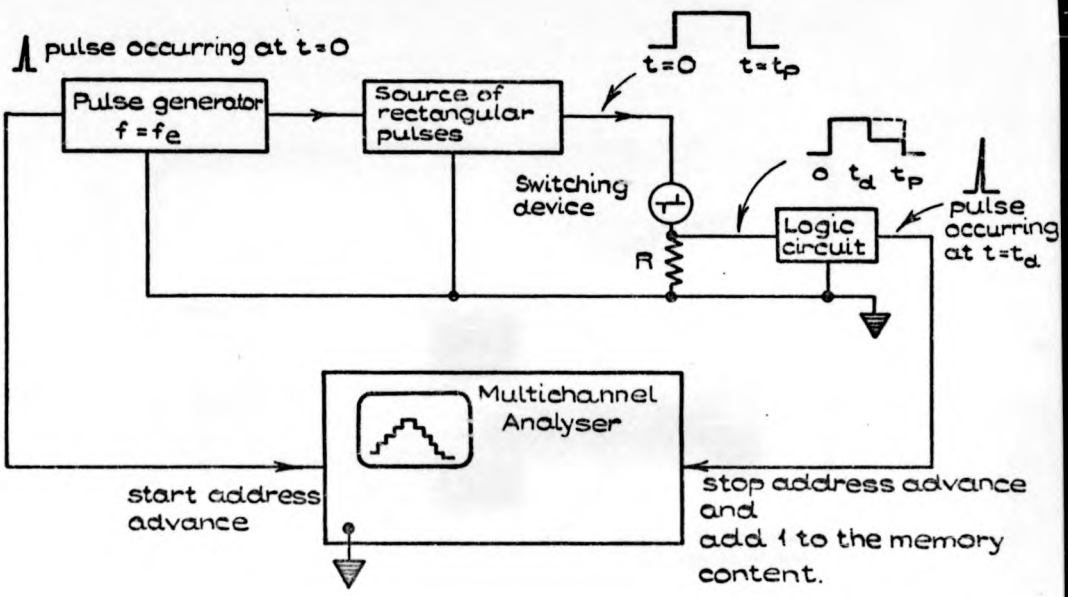

Fig. 5.23

STATISTICAL ANALYSIS OF SWITCHING DELAY TIMES EMPLOYING A MULTICHANNEL ANALYSER IN THE TIME HISTOGRAM MODE.

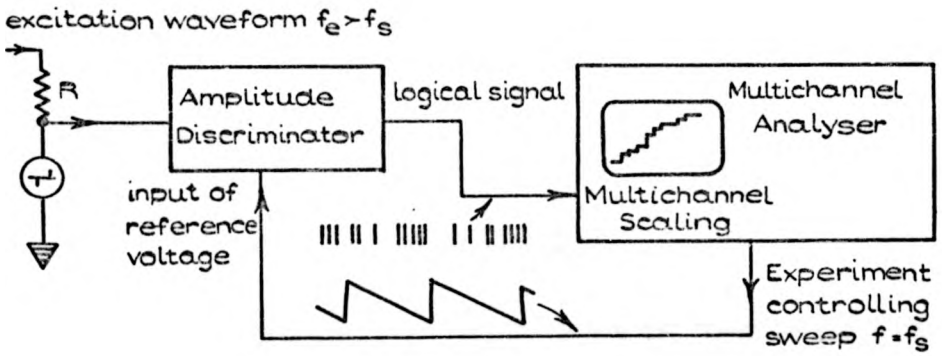

Fig. 5.24.

STATISTICAL ANALYSIS OF THE VARIATION IN THRESHOLD VOLTAGES.

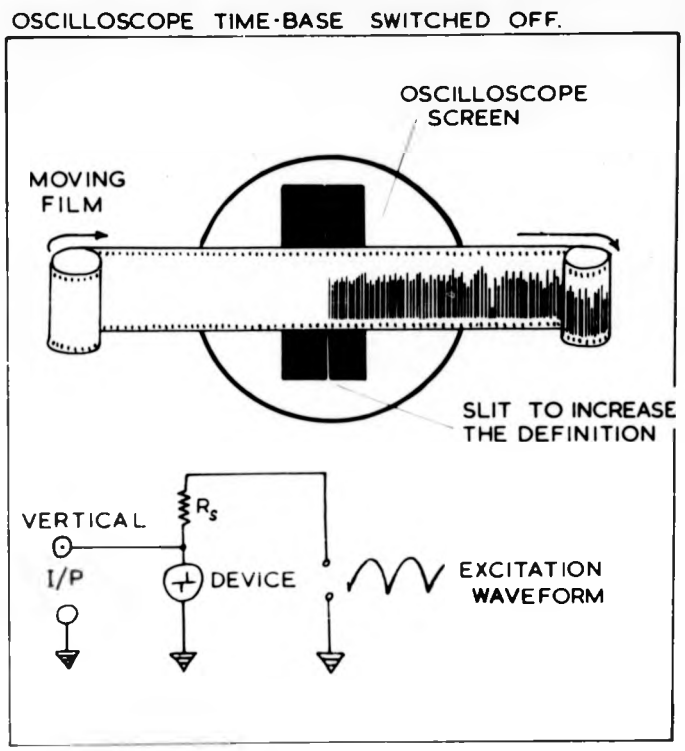

Fig. 5.25.

METHOD OF THE RECORDING OF THE TIME-SERIES OF THRESHOLD VOLTAGES.

of threshold voltages has been recorded by the method schematically illustrated in Fig. 5.25. The periodic excitation waveform (a rectified sine-wave) was applied to the device through a series resistor and the voltage appearing across the switching device was applied to the vertical deflection system of an oscilloscope with no time-base operating. The image of the resulting bright section of oscillating length was projected on a moving film using an adapted oscilloscope camera. After the film was developed and printed the sequence of threshold voltages $V_{th}(n)$ was obtained by measuring the maxima of the curve on the print. The data were processed by a computer to obtain the autocorrelation coefficients R(m) and their Fourier transform G(k). The mathematical procedures involved are described in a book by Bendat and Piersol[18].

The computer program had 3 main parts

(i) Data transformation (including an optional trend removal by least square method)

(ii) Calculation of the coefficients R(m)

(iii) Calculation of the spectral power density coefficients G(k).

and is given in the Appendix.

References Quoted in Chapter 5

(1) Shakovtseva S.I., Sov. Phys. Sol. State 6 (1965) 2022.

(2) Klein N., Advances in Electronics and Electron Physics 26 (1969) 309.

(3) Chopra K.L., "Conduction Instabilities in Thin Oxide Films - A Review". Conference on thin film devices, Cannes, France 1970 p.351

(4) Thornton R.E. et al, Microel. Rel. 5 (1966) 291, 299.

(5) Nixon C.W., Contemp. Phys. 10 (1969) 71.

(6) Everhart T.E. et al., Proc. IEEE 52 (1964) 1642.
Sie C.H., Proc. 5th Annual SEM Symposium, part I and II, Chicago, Ill., U.S.A., 25-27 April 1972, p. 193.

(7) Luginbuhl H.W., Purdue Univ., Lafayetle, Ind., U.S.A., Thesis 1971.

(8) Yarwood J., "High Vacuum Technique" Chapman & Hall, 1961, p.75.

(9) Weber W., Z. Akustik 4 (1939) 373.
McFarlane W., Phil. Mag. 18 (1934) 29.

(10) Stocker H.J., J. Non-Cryst. Solids 2 (1970) 371.

(11) Bagley B.G. and Northover W.R., ibid., 2 (1970) 161.

(12) Suntola T., Acta Physica Scandinavica Ph. 83, p.12.

(13) Bosnell J.R. and Savage J.A., J. Mater. Sci. 7 (1972) 1235.

(14) Bosnell J.R. and Thomas C.B., Phil. Mag., to be published 1973.

(15) Uttecht R. et al., J. Non-Cryst. Solids 2 (1970) 358.

(16) Bagley B.G. and Bair H.E., ibid., 2 (1970) 155.

(17) Fritzsche H. and Ovshinsky S.R., ibid., 2 (1970) 148.

(18) Bendat J.S. and Piersol A.G., "Random Data: Analysis and Measurement Procedures" Wiley-Interscience 1971. (Chapter 3, ref. 18).

CHAPTER 6

DISCUSSION OF EXPERIMENTAL RESULTS

In this Chapter the experimental results reported in this thesis are discussed in the light of theoretical models presented in Chapter 3. Theoretical and experimental results of other investigators are also brought into the discussion.

The implications of this discussion and comparison are presented in a separate Chapter 7.

In the first section of the present Chapter the electrical conductivity of the switching material and its dependence on temperature and electric field is discussed before going on to consider experimental results more directly concerned with the switching effect.

6.1 Temperature and Field Dependence of Conductivity

The results of conductivity measurements on the Si_{12} Ge_{10} As_{30} Te_{48} glass were given in section 5.1. The central result concerning the temperature dependence of electrical conductivity is that the conduction process is thermally activated over a broad temperature range. The corresponding activation energy was found to vary slightly between different batches of glass (from 0.42 eV to 0.56 eV) and also a small decrease in the activation energy was observed on one glass after it was "switched".

These results suggest that the preparation of the chalcogenide glass influences its electrical conductivity to some extent. In the present method of preparation described in Chapter 4 certain difficulties were encountered in incorporating all of the silicon into the melt; this could be one reason for the variation in the activation energy. Another cause, which is thought to be more likely, is the probable contamination of the chalcogenide glass with minute traces of oxygen. It is known that

proportions less than 1% of oxygen in chalcogenide glass can alter significantly its structural and other properties[1].

It is appropriate to mention here also the dependence of properties of amorphous semiconductors on the rate of quenching during different methods of preparation (discussed in Chapter 4). When comparing data on the Si_{12} Ge_{10} As_{30} Te_{48} material quoted in the literature there are differencies found between the values of the activation energies of conduction in evaporated materials and in bulk (e.g. Croitoru et al 0.47 eV on films[2], Phillips et al[3] 0.6 eV on bulk), which document the important differencies between evaporated films and glasses.

The change in the activation energy after "switching" the material which was observed is likely to be associated with the changes in structure of the glass induced by heating and possibly also electric field. The aspects of structural changes during switching are dealt with in a later section 6.3.2.

At low temperatures the conductivity exhibits an extrinsic-like character, which may also be associated with the presence of structural changes in the material. It was observed that the temperature at which the extrinsic type of conduction sets in depends on the applied field and also changes after the switching device has been operated. These observations could be explained by assuming, for instance, that the transport at low temperatures takes place by field emission from highly conducting microcrystallites or phase separated regions in the semiconducting matrix. However, further investigations are required before drawing more specific conclusions.

The results on the field dependence of conductivity are summarized in a graphical form in Fig. 5.2. The field dependence of electrical conductivity is a difficult phenomenon to analyse because of the possibility of temperature rise in the sample due to Joule heating. The thinner the

sample the greater the electric field that may be safely applied without causing the sample temperature to rise. The power dissipation levels in bulk samples were less than 120 mW (at this level of dissipation the thermal runaway commenced) and in switching devices used for measurement less than 1 mW.

The functional form of the I-V characteristics seems to be the same in both virgin and formed devices and also in a thick bulk sample at low fields. The independence of the I-V characteristic of forming is rather surprising in view of what has been said about the change of activation energy of conduction. However, it is possible that a difference in behaviour of virgin and formed devices could be detected at higher applied fields than those employed in the present measurements.

The computer analysis showed that several functional dependencies $I = f(V)$ fit the experimental data quite satisfactorily and it would have been extremely difficult to detect differencies between the laws merely by plotting the data. This can explain to some extent the "variety" of laws $I = f(V)$ reported in the literature.

The best fit to the experimental data was obtained using the law $I = I_o \exp(V/V_o)$ V. It was assumed that a single function can apply to the whole of the measuring interval, unlike, for instance, Hall[4] who used the sum of two different functions to fit the data.

The best fit to the set of I-V values obtained by numerical solution of the problem of Joule heating in the switching device (see sections 5.1 and 3.2.1) was achieved for the law $I = I_o \exp(V/V_o)$, i.e. a different law from that for the experimental data. This result therefore suggests that the experimentally observed I-V characteristics are not due to heating effects.

The possibility of space charge limited current is considered to

be real in the thinner samples ($\lesssim 30$ μm). Support is lent to this hypothesis by the apparent time dependence of the currents through the device observed during conductivity measurements. A slow decrease of current through the device was observed (when a constant d.c. voltage was applied), the decrease taking place over many minutes. The plot of the logarithm of current against the logarithm of time was not linear as observed by Polanco et al[5].

The form of the law $I = f(V)$ for the case of the space charge limited current depends on the assumed distribution of traps (density of traps at various energy levels) in the semiconductor.

Only the law corresponding to the exponential distribution of traps in energy was considered here and it is not ruled out that a better agreement could be found using a different law.

6.2 Threshold Voltage as a Function of Temperature

The threshold voltage was found to be strongly dependent on the ambient temperature (section 5.2); in the range of temperatures above room temperature and a little below, the logarithm of the threshold voltage plots linearly against the reciprocal temperature. The corresponding activation energy was found to be one half of that of electrical conduction, which result suggests that the switching is thermally initiated.

At lower temperatures than about -20°C the threshold voltage becomes much less dependent on the ambient temperature than expected on the basis of the thermal model. However, a semi-quantitative agreement with experiment can be achieved by modifying the thermal model by incorporating into it additional assumptions. Two different modifications of the thermal model were discussed in Chapter 3. In the first model the additional assumption was that the switching may be initiated by an electronic mechanism which becomes operative at a sufficiently high electric field. In the second

model it was assumed that a highly conducting phase occurs in the switching material when a high electric field and/or elevated temperature are present in the material. The two models have a common feature in that a transition from a thermal to a non-thermal mechanism occurs at intermediate temperatures, providing thereby two possible phenomenological explanations for the experimental result.

There are other ways in which a qualitatively similar result could be obtained. One obvious suggestion is to include the field dependence of electrical conductivity in the equations of the thermal model (equations 2.25 - 2.26). This in fact was carried out in the present work in the one dimensional form of the model but it was found that even in one dimension it represents a considerable mathematical complication (the need for an inner iterative process associated with the redistribution of electric field due to the change in electrical conductivity). At that time the main interest was in the dynamical aspects of the electro-thermal model, namely the dependence of the delay time on overvoltage at various temperatures and simulation of switching characteristics. The results of the model were not satisfactory on those counts and therefore it was concluded that if it is possible to obtain an agreement with experiment by introducing the field dependence of conductivity into the thermal model then a more realistic spatial domain of the problem must be considered, possibly the two dimensional problem. This would be a major mathematical task in itself.

One objection to incorporating the field dependence of conductivity is that it is necessary to understand the cause of the field dependence before proceeding further; this is because the different spatial regions of the sample (or the switching device) may contribute differently to the total conductivity which is measured and a simple phenomenological description is not possible. Several authors (for references see

section 2.2.3) have used the field dependence of conductivity as a modification of the assumptions of the thermal model. This is speculative at the present stage of understanding of the transport processes in amorphous semiconductors.

An example of a modification of the thermal model in which microscopic processes in designated spatial regions of the switching device are taken into consideration is the model of Kolomiets et al[6], in which the thermal model is modified by taking into account the space charge limited current in order to explain the temperature dependence of threshold voltage in thin film devices.

This section has so far been concerned only with the aspects of the dependence of the threshold voltage on temperature. We conclude this section by discussing the dependence of threshold voltage on other experimental parameters which were considered, namely: illumination by light and electron beams (section 5.3). No dependence of the threshold voltage on these experimental parameters was found in the devices employing the Si_{12} Ge_{10} As_{30} Te_{48} glass, except in cases where the heat dissipation was sufficient to initiate switching thermally. If such a dependence can be detected at all, it is likely to be manifested more strongly at low temperatures where switching may be electronic in character and heating is suppressed.

6.3 Structural Changes in the Switching Device

6.3.1 Macroscopic Changes in Morphology

The observations made by the optical microscope and examination of the switched devices by the scanning electron microscope (section 5.5) reveal that coplanar switching devices change their morphology due to evaporation of the electrodes and melting of the chalcogenide glass during switching operations. It was observed that the extent of the

damage depends on the number of switching operations (nomenclature of section 5.5 applies here) not on their length. It is therefore concluded that the damage to the switching device is caused by the discharge of the energy stored in the capacitance of the switching device and the associated circuit at the instant of switching. The "on"-state current which was limited by using a series resistor is not thought to contribute significantly to the damage.

The observations show that a coplanar switching device with aluminium electrodes 0.4 μm thick operated at the threshold voltage of 400 V, sustains damage in an area of about 10^{-2} mm^2 of the electrodes during one operation. A short calculation shows that the amount of energy needed to vaporize the aluminium from the area of the damage is compatible with the amount of energy stored in a capacitor of 100 pF charged at 400 V (latent heat of vaporization for aluminium is 68 kcal/mole). The capacitance of the switching devices used in these experiments was about 10 pF and that of the connecting coaxial cable was 60 pF which gives an order of magnitude agreement with the calculated value of 100 pF. When a parallel capacitance of 33 nF was connected to the switching device the damage rate was extremely high - the device was virtually destroyed during 5 switching operations; its resistance changed from 30 MΩ to 170 MΩ.

The vaporization of the electrode material is accompanied by the vaporization of the chalcogenide glass. This is concluded from the change in appearance of the active region of the switching device, indicating some loss of material.

The effective discharge time of the capacitively stored energy is expected to be of the order of $R_{on}\ C_{d+l}$, where $R_{on} \approx 100$ is the "on"-state resistance of the switching device and $C_{d+l} \approx 70$ pF is the capacitance of the device and the associated circuit, which is of the order of nanoseconds. This agrees with the high temperature transients observed.

The fact that the vaporization takes place in a very short time interval is also demonstrated by the acoustic effects observed when the device is operated in air at atmospheric pressure (section 5.6) which are interpreted as a sound pulse produced by the expansion of hot vapours.

The emission of light from the switching device is interpreted as a spark discharge in the vaporized species, (similar sparks have been observed by other investigators[7]). It would be extremely helpful to analyse the spectrum of the emitted light spectrographically. It is expected that the spectrum would show mainly lines belonging to aluminium used for electrodes because it has the lowest ionization potential, but possibly some of the components of the chalcogenide glass (Te) would also be detected.

Damage in coplanar switching devices was studied by Adam and Duchene[8] and by Armitage et al[9]. These authors associated the cause of damage also with the capacitive discharge. Armitage et al report that the damage was polarity dependent, the anode being more damaged than the cathode.

The sandwich devices seem to be much less affected by the capacitive discharge. This is apparently due to a much better heat conduction from the area of localized heating arising at the instant of switching; in the sandwich structures the heat is conducted away from a point inside the electrode area radially outwards across the electrodes, whereas in the coplanar devices the heating takes place at the edge of the electrodes and the solid angle in which the heat can be dissipated is effectively more than halved.

Although the external surface damage of sandwich devices is negligible it is possible that internal structural changes can be induced by the capacitive discharge in the sandwich devices. The next section deals with some aspects of the internal structural changes.

6.3.2 Microstructural Changes in the Switching Material

Direct experimental evidence for the existence of tellurium microcrystallites in the Si_{12} Te_{48} As_{30} Ge_{10} (STAG) material was obtained by electron diffraction (section 5.7.1.2). Indirect evidence for the structural changes taking place in the switching devices is obtained by monitoring their switching parameters, in particular the threshold voltage. The changes in the threshold voltage have two components:

There is a gradual slow change in the threshold voltage observed throughout the life of the switching device. This change is illustrated by the shift in the maximum of the distribution of threshold voltages and change in the shape of the distribution curve (section 3.4.3). The threshold voltage generally decreases during prolonged periods of operation; an aged device can be temporarily revived by the application of suitable "curing" pulses. In this sense the slow change in the threshold voltage is semi-reversible.

The second component of the changes is a fast fluctuation of the threshold voltage observed during a.c. operation. The theoretical model presented in section 3.4.4 suggests that these fast fluctuations in the switching parameters are associated with fluctuations in the size or shape of the microscopic crystallites dispersed in the chalcogenide glass matrix. The state of the crystallites is described in the model by a single scalar variable, x, which is interpreted as the volume fraction of the crystallites. The growth-rate $\frac{dx}{dt}$ of the crystallites is assumed to depend only on the effective temperature in the switching device and no explicit dependence on the electric field or other quantities which are likely to influence the growth, such as mechanical stress, was taken into account. In spite of these simplifications the model is capable of explaining the observed phenomena:

(i) the fast fluctuations in the switching parameters are not random but correlation exists between sequential fluctuations,

(ii) the degree of correlation depends on the operating regime; a decrease in correlation is observed when the applied voltage during a.c. operation is increased.

The correlation between sequential fluctuations of the threshold voltage is explained in terms of the interaction between the growth of the crystallites and the temperature which is reached in the switching device during operation. Mathematically this interaction leads to an autoregressive process. In this connection it is possible to mention that a mathematically identical mechanism could be obtained by considering other physical models for the variability of switching parameters, which do not involve the assumption of the existence of highly conducting crystallites in the switching material. For example, the dependence of the properties of the glassy switching material on the rate of cooling of a molten channel after the end of a switching operation (expressed in terms of the glass transition temperature by the relation 2.2) can be shown to be a possible basis for an autoregressive process. A completely non-structural explanation for the variation of switching parameters has been put forward by Lee et al[13]. They suggest that the variation of threshold voltage is caused by the variation in the quantity of the residual charges trapped in the switching material at the end of each operation. This model could also be developed into one having auto-regressive properties. However, in the light of the experimental evidence in favour of the existence of the crystallites the last two models above are thought to be unrealistic and the model put forward in section 3.4.4 is preferred.

By changing some of the assumptions of the present model (relaxing the assumption of random perturbations in growth and introducing an

assumption of a limiting mechanism for growth of the crystallites) it would be possible to change the autoregressive nature of the model into an oscillatory one. This would then explain the unusual periodic variation in the threshold voltage reported by Suntola[16].

The capability of the theoretical model to account semi-quantitatively for the correlation in the time-series of switching parameters and its changes with the regime of operation reinforces the argument that microscopic structural changes in the threshold switching material are an important factor in the switching mechanism. It can be further argued that there is no sharp division between threshold and memory switching materials; this is supported by the experiment described in section 5.4, in which a reversible memory state has been induced in a device employing the stable STAG material.

The forming process is interpreted in terms of the model as a stage during which the microcrystallites develop to a state that is compatible with the operating conditions (Fig. 3.12). The change of switching parameters (threshold voltages) during the forming stage has been discussed in section 5.4. It was shown that in the case of coplanar switching devices it is not possible to interpret the changes in switching parameters solely in terms of the internal structural changes in the device because changes in the properties of the electrodes make a significant contribution. The decrease in the threshold voltage of sandwich devices after forming is probably more directly associated with the internal changes in microstructure. Experiments conducted by Coward[10] on the STAG material show that a filament with a much higher conductivity than the as-deposited thin film is produced during the forming process. Bosnell and Thomas[12] showed recently that this filament consists of small needle-shaped tellurium crystals embedded in a glassy matrix and oriented with their c-axis parallel to the direction of switching field.

The ability of switching materials to precipitate a highly conducting phase when an electric field is applied to them may be considered to be the factor which distinguishes between switching and destructive breakdown. (This view has been also expressed by Bosnell and Thomas[12]). In this context it is possible to mention the result of Yurlova[11] who observed that the "on"-state can be withstood for long periods on d.c. operation of thin STAG film devices only when the forming stage is completed.

Another argument in favour of the general importance of the structural changes in switching materials is that the variability of switching parameters is observed in devices employing materials of different nature. The variability of switching parameters in chalcogenide based devices[13 - 17] as well as in completely different transition metal oxide devices[18 - 20] has been reported. It is likely that the variability is caused by structural changes in all cases. Thus in the light of the foregoing discussion it may be concluded that the structural changes in switching materials are an important and universal part of the switching process.

References Quoted in Chapter 6

(1) Takamori T. and Roy R., J. Mater. Sci. 8 (1973) 415.

(2) Croitoru N., Vescan L., Popescu C and Lăzărescu M., J. Non-Cryst. Solids 4 (1970) 493. (Chapter 2, reference 50).

(3) Phillips S.V., Booth R.E. and McMillan P.W., ibid., 4 (1970) 510. (Chapter 2, reference 79).

(4) Hall J.E., ibid., 2 (1970) 125.

(5) Polanco J.I., Roberts G.G. and Myers M.B., Phil. Mag. 25 (1972) 117.

(6) Kolomiets B.T., Lebedev B.A. and Tsendin K.D., Sov. Phys. - Semicond. 5 (1972) 1369.

(7) Carchano H., Lacoste R. and Segui Y., Appl. Phys. Lett. 19 (1971) 414 and references therein:
Argall F., Electron. Lett. 2 (1966) 282,
Sliva P.O., Dir G. and Griffiths C., J. Non-Cryst. Solids 2 (1970) 316.

(8) Adam G. and Duchene J., Solid State Commun. 10 (1972) 1277.

(9) Armitage D., Brodie D.E. and Eastman P.C., Canad. J. Phys. 49 (1971) 1662.

(10) Coward L.A., J. Non-Cryst. Solids 6 (1971) 107. (Chapter 4, reference 30).

(11) Yurlova G.A., Sov. Phys.-Semicond. 4 (1971) 1401.

(12) Bosnell J.R. and Thomas C.B., Phil. Mag. to be published.

(13) Lee S.H., Henisch H.K. and Burgess W.D., J. Non-Cryst. Solids 8-10 (1972) 422. (Chapter 3, reference 26).

(14) Cohen M.H., Neale R.G. and Paskin A., ibid., 8-10 (1972) 885.

(15) Luby Š., Červenák J., Kubek J., Marcin M. and Schilder J., Czech. J. Phys. B21 (1971) 878.

(16) Suntola T., Solid State Electron. 14 (1971) 933.

(17) Kolomiets B.T., Zhurakovskii L.A. and Zeinally A.Kh., Sov. Phys. Semicond. 5 (1971) 232.

(18) Drake C.F., contribution at IEE meeting, Savoy Place, London, 8.5.1972.

(19) Regan M., contribution at the Discussion on Amorphous Semiconductors, Chelsea College, London, 17 - 18.12.1971.

(20) Murawski L., Nakonieczny W. and Gzowski O., Acta Physica Polonica A40 (1971) 93.

CHAPTER 7

SUMMARY AND CONCLUSIONS

The initial work (Chap. 3, ref. 1 and Chap. 1, ref. 30), continuation of which is the work described in this thesis, was based on the thermal model of switching. The thermal model, however, was inadequate to explain some of the observed phenomena (e.g. variation of the threshold voltage with temperature, change of the character of $t_d(V)$ isotherms with temperature) and therefore modifications of this model were necessary.

7.1 Modifications of the Thermal Model

The two different modifications which were considered have a common feature in that in both models an independent condition for switching to occur is added to the purely thermal model.

In the first model (section 3.3.1) it was postulated that heating together with an electronic effect taking place at a critical electric field is causing the initiation of switching. The nature of the electronic effect was not specified in the model, however, in the light of further investigations (structural changes) it is thought that field emission of carriers from sharp microcrystallites could be operative.

In the second model the key assumption was that the switching "off"-"on" transition is caused by a structural relaxation which takes place at a critical temperature and/or a critical electric field (section 3.2.2). This relaxation results in a highly conducting phase and vanishes when the applied electric field is removed.

Both models explain qualitatively the observed variation of threshold voltage with temperature, i.e. lower values of the threshold voltage than those predicted by purely thermal model and also the fact

that the threshold voltage tends to a constant value at low temperatures.

The models considered were one-dimensional. The restriction to one dimension is a realistic simplification only if the initiation of switching is modelled (this is the case in the present models) and the constriction of current into a channel does not take place (this assumes that no structural changes have taken place contrary to later experimental observations). If these conditions are not fulfilled then at least a two dimensional model is necessary and its predictions can be fundamentally different from those of a one-dimensional model and in better agreement with experiment. This was shown by solving the equations of the purely thermal model in two dimensions using a digital computer (section 3.3).

Moreover, the models considered did not include any modifications due to the presence of structural changes in the threshold switching material and therefore could not account for the observed variation in switching parameters. It was concluded that these structural changes have to be studied and understood before any attempt to develop a realistic quantitative model of the threshold switching.

7.2 Structural Changes in the Threshold Switching Devices

It was possible to classify the structural changes into macroscopic and microscopic. The phenomenon of damage of the switching device which was observed when coplanar geometry was used falls into the first category. It was concluded that the damage (evaporation of electrode and switching materials) is caused by the discharge of electrostatic energy stored in the device and circuit capacitance.

The microscopic structural changes evidence of which was seen in threshold devices of all geometries used are of fundamental importance. The experimental evidence of the microstructural changes in the switching material $Si_{12}\ Ge_{10}\ As_{30}\ Te_{48}$ was based upon the following experiments:

(i) Direct observation of the microcrystallites in threshold chalcogenide glass by the use of electron microscopy and electron diffraction. The crystals, identified as tellurium, were shown to be present already in the unswitched material.

(ii) Observation of the changes in the properties of the switching device during the forming process. The threshold voltage of the switching device and the resistance of the device change during the forming process and also the activation energy of conduction was found to decrease slightly after the first-fire operation.

(iii) Aged threshold switches which showed degenerate I-V characteristics with no negative differential resistance region could be regenerated by applying short high current pulses to them. A memory state could be induced in the threshold glass Si_{12} Ge_{10} As_{30} Te_{48} by the application of a d.c. current of several tens of milliamperes for a few minutes and erased by a short high current pulse.

(iv) Observation of the variation in switching parameters of formed devices with the number of operations. Experimental analysis revealed that the variation has two main components:

(a) Slow variation taking place throughout the life of the device,

(b) Fast fluctuations occurring from operation to operation.

It was further shown that the latter variation is not random but that correlation exists between sequential switching operations.

A semi-quantitative theoretical model was presented to explain the observed phenomena in terms of microstructural changes in the glass during threshold switching (section 3.4.4). This model incorporates some simplifying assumptions but nevertheless it is capable of satisfactorily predicting the experimental observations and of suggesting areas for further research.

7.3 Mechanism of Switching

It was indicated in the preceding sections that the presence of structural changes in the switching material makes it difficult to elucidate the switching mechanism by comparing available theoretical models with experiment. Therefore direct experimental steps were taken towards the elucidation of the mechanism initiating switching.

In the first set of experiments light and electron beams were interacting with the switching device in an attempt to initiate the threshold switching. The results of these experiments were negative except in cases where the power dissipation by the beam was causing a significant temperature rise in the switching device (section 5.3).

In the second experiment (described in section 5.6) a spark across the coplanar switching device was observed. The spark was interpreted as a discharge in the vaporized device material. The occurrence of the spark coincides (within the resolution of the experiment) with the switching "off"-"on" transition. This result means that a high temperature rise is associated with the switching transition and thus favours the thermal mechanism of switching.

No more definite conclusions with regard to the mechanism of switching could be drawn from these experimental results. However, the overall results indicate that the thermal model, when modified by the introduction of the aspects of structural changes and electric field enhanced conduction, is capable of explaining the observed features of the switching effect.

CHAPTER 8

SUGGESTIONS FOR FUTURE WORK

The results of the present work indicate the major importance of structural changes in the threshold switching material and therefore the design of new experiments is seen mainly in the direction of more complete investigation of these changes.

The chalcogenide glass Si_{12} Ge_{10} As_{30} Te_{48} used in the present work has two disadvantages: it is fairly complex and therefore the role of individual constituents in the structural changes may be difficult to follow; it is also relatively stable so that it does not exhibit a large amount of structural change. It is therefore suggested that future work on a simpler threshold material would be profitable, since this would be more prone to structural changes.

It is thought that the following aspects of the structural changes ought to be studied:

(i) Characterization of the switching material

(ii) Relationship between the structural changes and switching behaviour.

The experiments belonging into the first category could be concerned with ascertaining of the importance of the method of preparation with regard to the structural properties of chalcogenide glass (the role of oxygen impurities, speed of cooling and possible fundamental difference between thin film and bulk materials). The influence of the previous history of the switching material on its properties, in particular the influence of thermal treatment on the electrical conductivity and its temperature and field dependence should be investigated. A quantitative use of electron microscopy should be made to obtain fuller information about the phases in the switching material.

The second category comprises experiments which are more closely concerned with the actual switching behaviour. In the light of the present research programme it is considered that the following aspects of the forming process are in need of further analysis:

(a) The dependence of the decrease in the threshold voltage with the number of switching operations on ambient temperature, switching regime and composition of the chalcogenide glass.

(b) The relationship (if any) between the decrease of threshold voltage during the forming stage and the decrease of the autocorrelation coefficients with the lag number, suggested in section 3.4.4.

The voltage appearing across the switching device in the "on"-state during d.c. operation before the memory state is set is very noisy. The relation between the spectrum of the noise and the spectrum of the discrete time-series of switching parameters obtained during a.c. operation could be investigated.

The character of the damage of switching devices should also be investigated more fully than in the present work, e.g. by spectrography of the light emitted from the switching region or scanning electron microscopy of the damaged area. This would provide information for the construction of devices with improved damage resistance.

The range of scanning electron microscopy techniques could be extended by introducing a special detection system to yield more information about the temperature and electric potential distribution in coplanar switching devices. The distribution is likely to be modified by the microstructural changes and this aspect could also be investigated.

The results of the experiments from the categories (i) and (ii) above would enable the development of a realistic theoretical model of the switching effect.

In addition to the specific experiments outlined above it is clear that further research is necessary into the more fundamental properties of amorphous semiconductors, e.g. structure and aspects of disorder, thermodynamic properties, energy states and transport of charge carriers. Increased knowledge in these areas would provide a better basis for understanding the switching processes.

APPENDICES

Appendix 1. 2-D Thermal Model. Computer Programme.

Appendix 2. Structural Relaxation Model of Switching. Computer Programme.

Appendix 3. Computer Programme for Time-Series Analysis.

Appendix 4. Computer Programme for I-V Curve Fitting.

Appendix 5. Reprint of Paper Quoted in Chap. 1 (ref. 30), Chap. 5 (section 5.2) and Chap. 7. This paper was based on the author's M.Sc. work, but was completed during the first term of the present Ph.D. course.

```
** ICL 4130 DEC2 SYSTEM  :  SLAVE BACK      :  CORE 64K  :  VOL  9                         DATE  29 11 72    :  TIME  11.47.23

&JOB;     PH/R022/YD; Y D SWITCHING PROBLEM;

&ALGOL;         L;                                                                          CPU TIME =  0000  00.061

&TIME;     181;                                                                             CPU TIME =  0000  00.130

&LINES;    79001;                                                                           CPU TIME =  0000  00.149

&LIST;                                                                                      CPU TIME =  0000  00.197

ZKOUSKA PROCEDURY TISKN; 'BEGIN'                                                                              BLOCK1
        'PROCEDURE' TISKN (A);                                                   TISKN100
        'ARRAY'A;                                                                TISKN101                     BLOCK2
'BEGIN''INTEGER'I,J,E;'SWITCH'SS:=S0,S1,S2,S3,S4,S5,S6,S7,S8,S9,S10,S11,         TISKN102
        S12,S13,S14,S15,S16,S17,S18,S19,S20,S21,S22,S23,S24,S25,S26,S27,         TISKN103
        S28,S29,S30,S31,S32 ;  'REAL'AMAX,AMIN;'INTEGER'L1,L2,U1,U2;             TISKN104
        'BOOLEAN' STRAIGHT,TAB; STRAIGHT:='TRUE';                                TISKN104
        L1:=LOWBOUND(A,1); L2:=LOWBOUND(A,2);                                    TISKN105
        U1:=L1-1+RANGE(A,1);     U2:=L2-1+RANGE(A,2);                            TISKN106
        AMAX:=AMIN:=0;                                                           TISKN107
        'FOR'I:=L1'STEP'1'UNTIL'U1'DO'                                           TISKN108
        'FOR'J:=L2'STEP'1'UNTIL'U2'DO'                                           TISKN109
        'IF' A[I,J]>AMAX 'THEN' AMAX:=A[I,J];                                    TISKN110
        AMIN:=AMAX;                                                              TISKN111
        'FOR'I:=L1'STEP'1'UNTIL'U1'DO'                                           TISKN108
        'FOR'J:=L2'STEP'1'UNTIL'U2'DO'                                           TISKN109
        'IF' A[I,J]<AMIN 'THEN' AMIN:=A[I,J];                                    TISKN110
        AMAX:=AMIN;                                                              TISKN111
        'FOR'I:=L1'STEP'1'UNTIL'U1'DO'                                           TISKN108
        'FOR'J:=L2'STEP'1'UNTIL'U2'DO'                                           TISKN109
        'IF' A[I,J]>AMAX 'THEN' AMAX:=A[I,J];                                    TISKN110
        'IF'AMAX=AMIN'THEN'                                                      TISKN611
'BEGIN''PRINT'''L'CONSTANT'S'MATRIX',SAMELINE,AMAX;                              TISKN611
        'GOTO' ENDTISK;                                                          TISKN611
'END';                                                                           TISKN611
        TAB:='TRUE';                                                             TISKN112
        'PRINT'''P''; SPECIAL(5);   I:=-1;                                       TISKN112
Z:      I:=I+1;  'PRINT'''L'';  'GOTO'SS[I+1];                                   TISKN112
Y:      'PRINT' SAMELINE,I+1,''S'',AMIN+I*(AMAX-AMIN)/30;                        TISKN112
        'IF'I'LE'30'THEN''GOTO'Z;  'PRINT'''L'';     TAB:='FALSE';               TISKN112
        'IF'U1>130'AND'U2>130'THEN'                                              TISKN113
'BEGIN''PRINT'''L'TOOBIGFORPRINTING';'GOTO'ENDTISK;                              TISKN114
'END';                                                                           TISKN115
        'IF'U1>130'OR'U2>130'THEN'                                               TISKN116
'BEGIN'    'IF'U1>U2'THEN'                                                       TISKN117
'BEGIN' STRAIGHT:='FALSE';  'GOTO'NEPRINO;                                       TISKN118
'END';                                                                           TISKN118
'END';                                                                           TISKN119


        J:=L2-1;'PRINT'''L'ROWS'S'OF'S'MATRIX'S'PRINTED'S'VERTICALLY'';          TISKN420
LA1:    J:=J+1;'IF'J>U2'THEN''GOTO'ENDTISK;'PRINT'''L'';I:=L1-1;                 TISKN121
LA2:    I:=I+1;   'GOTO' PRINO;                                                  TISKN122
NEPRINO:I:=L1-1;'PRINT'''L'ROWS'S'OF'S'MATRIX'S'PRINTED'S'HORIZONTALLY'';        TISKN123
LA3:    I:=I+1;'IF'I>U1'THEN''GOTO'ENDTISK;'PRINT'''L''; J:=L2-1;                TISKN124
LA4:    J:=J+1;                                                                  TISKN125
PRINO:'BEGIN'                                                                    TISKN126
        B:=ENTIER(30*(A[I,J]-AMIN)/(AMAX-AMIN)+1);                               TISKN127
        'GOTO'SS[B+1];                                                           TISKN128
        S0 :'PRINT''Z';'GOTO'X;          S1 :'PRINT''*';'GOTO'X;                 TISKN129
        S2 :'PRINT''+';'GOTO'X;          S3 :'PRINT''@';'GOTO'X;                 TISKN130
        S4 :'PRINT''&';'GOTO'X;          S5 :'PRINT''Z';'GOTO'X;                 TISKN131
        S6 :'PRINT''Y';'GOTO'X;          S7 :'PRINT''X';'GOTO'X;                 TISKN132
        S8 :'PRINT''W';'GOTO'X;          S9 :'PRINT''V';'GOTO'X;                 TISKN133
        S10:'PRINT''U';'GOTO'X;          S11:'PRINT''T';'GOTO'X;                 TISKN134
        S12:'PRINT''S';'GOTO'X;          S13:'PRINT''R';'GOTO'X;                 TISKN135
        S14:'PRINT''Q';'GOTO'X;          S15:'PRINT''P';'GOTO'X;                 TISKN136
        S16:'PRINT''O';'GOTO'X;          S17:'PRINT''N';'GOTO'X;                 TISKN137
        S18:'PRINT''M';'GOTO'X;          S19:'PRINT''L';'GOTO'X;                 TISKN138
        S20:'PRINT''K';'GOTO'X;          S21:'PRINT''J';'GOTO'X;                 TISKN139
        S22:'PRINT''I';'GOTO'X;          S23:'PRINT''H';'GOTO'X;                 TISKN140
        S24:'PRINT''G';'GOTO'X;          S25:'PRINT''F';'GOTO'X;                 TISKN141
        S26:'PRINT''E';'GOTO'X;          S27:'PRINT''D';'GOTO'X;                 TISKN142
        S28:'PRINT''C';'GOTO'X;          S29:'PRINT''B';'GOTO'X;                 TISKN143
        S30:'PRINT''A';'GOTO'X;          S31:'PRINT''£';'GOTO'X;                 TISKN144
        S32:'PRINT''$';'GOTO'X;                                                  TISKN145
X:      'IF' TAB 'THEN''GOTO'Y; 'END'; 'IF'STRAIGHT'THEN'                        TISKN146
'BEGIN''IF'I<U1'THEN''GOTO'LA2'ELSE''GOTO'LA1;                                   TISKN147
'END'; 'IF'J<L2'THEN''GOTO'LA4'ELSE''GOTO'LA3;                                   TISKN148                     BLOCK END
ENDTISK: 'PRINT'''L5'PRINTING'S'COMPLETED';        'END' OF TISKN;               TISKN146
        'PROCEDURE' FIELD B (A,B,DX,DY);                                         FIELDB00
        'VALUE'DX,DY; 'INTEGER'DX,DY;                                            FIELDB01
        'ARRAY'A,B;                                                              FIELDB01                     BLOCK4
'BEGIN''INTEGER'I,J;                                                             FIELDB02
        'FOR'J:=2'STEP'1'UNTIL'DY-1'DO'                                          FIELDB03
        'FOR'I:=1'STEP'1'UNTIL'DX-1'DO' B[I,J]:=  (A[I,J]+A[I+1,J])/2;           FIELDB04                     BLOCK END
'END' OF PROC FIELDB;                                                            FIELDB05
        'PROCEDURE' FIELD C  (A,C,DX,DY);                                        FIELDC00
        'VALUE'DX,DY; 'INTEGER'DX,DY;                                            FIELDC01
        'ARRAY'A,C;                                                              FIELDC01                     BLOCK5
'BEGIN''INTEGER'I,J;                                                             FIELDC02
        'FOR'I:=2'STEP'1'UNTIL'DX-1'DO'                                          FIELDC03
        'FOR'J:=1'STEP'1'UNTIL'DY-1'DO' C[I,J]:=  (A[I,J]+A[I,J+1])/2;           FIELDC04                     BLOCK END
'END' OF PROC FIELDC ;                                                           FIELDC05
        'PROCEDURE' FILL PS (U,ALPHA,F,DX,DY,PS,RO,MESH);                        FILLPS01
        'VALUE'DX,DY;'INTEGER'DX,DY;'ARRAY'U,ALPHA,F,PS;'REAL'RO,MESH;           FILLPS02                     BLOCK6
'BEGIN''ARRAY'BETA[1:DX-1,2:DY-1],GAMA[2:DX-1,1:DY-1];                           FILLPS03
        'INTEGER'K,L;                                                            FILLPS04
        FIELD B (ALPHA,BETA,DX,DY);                                              FILLPS05
        FIELD C (ALPHA,GAMA,DX,DY);                                              FILLPS06
        'FOR'L:=2'STEP'1'UNTIL'DY-1'DO'                                          FILLPS09
        'FOR'K:=2'STEP'1'UNTIL'DX-1'DO'                                          FILLPS10
    PS[K,L]:=((U[K+1,L]+U[K-1,L]+U[K,L-1]+U[K,L+1]-4*U[K,L])                     FILLPS11
        -RO*(BETA[K,L]*(U[K+1,L]-U[K,L])-BETA[K-1,L]*(U[K,L]-U[K-1,L]))          FILLPS12
        -RO*(GAMA[K,L]*(U[K,L+1]-U[K,L])-GAMA[K,L-1]*(U[K,L]-U[K,L-1])))         FILLPS13
        /MESH/MESH+40*F[K,L];                                                    FILLPS14                     BLOCK END
'END' OF PROCEDURE FILL PS ;
        'PROCEDURE' FIELD S2 (POT,PRAV,DX,DY,MESH);                              FIELDS00
        'VALUE'DX,DY,MESH;'INTEGER'DX,DY;'REAL'MESH;'ARRAY'POT,PRAV;             FIELDS01                     BLOCK7
'BEGIN''INTEGER'K,L;                                                             FIELDS02
```

```
99          *FOR*K:=2*STEP*1*UNTIL*DX-1*DO*                                                  F|GLOB03
100         *FOR*L:=2*STEP*1*UNTIL*DY-1*DO*                                                  F|GLOB04
101         ARRAY[K,L]:=(POT[K,L+1]-POT[K,L-1])*2+(POT[K+1,L]-POT[K-1,L])*B  F|GLOB05
102           /4/MESH/MESH;                                                                  F|GLOB06   BLOCK END
103 *END* OF FIELD 33 ;                                                                     F|GLOB07
104         *PROCEDURE* NULUJ(A);                                                            NULUJ  0
105         *ARRAY*A;                                                                        NULUJ  1   BLOCK8
106 *BEGIN**INTEGER*K,L,L1,L2,U1,U2;                                                         NULUJ  2
107         L1:=LOWBOUND(A,1);   L2:=LOWBOUND(A,2);                                          NULUJ  3
108         U1:=L1-1+RANGE(A,1);   U2:=L2-1+RANGE(A,2);                                      NULUJ  4
109         *FOR*K:=L1*STEP*1*UNTIL*U1*DO*                                                   NULUJ  5
110         *FOR*L:=L2*STEP*1*UNTIL*U2*DO* A[K,L]:=0;                                        NULUJ  6   BLOCK END
111 *END* NULUJ ;                                                                           NULUJ  7
112         *PROCEDURE* PRAD(U,P,DX,DY,IP,MESH);                                             PRADI700
113         *VALUE*DX,DY,IP,MESH;*INTEGER*DX,DY;*REAL*IP,MESH;*ARRAY*P,U;                    PRADI701   BLOCK9
114 *BEGIN**INTEGER*K,L,L1,L2,U1,U2;                                                         PRADI702
115         *REAL*H2,R;   *ARRAY*D[2:DX-1,2:DY-1];                                           PRADI703
116           H:=1/IP;                                                                       PRADI704
117 *BEGIN*                                                                                  PRADI705   BLOCK16
118         *PROCEDURE*THOMCOL(I);   *VALUE*I;*INTEGER*I;                                    THOMCOL0   BLOCK11
119 *BEGIN**INTEGER*K;   *ARRAY*C[L1:U1];                                                    THOMCOL1
120           C[L1]:=-2-R;   U[L1,I]:=D[L1,I]/(-2-R);                                        THOMCOL2
121         *FOR*K:=L1+1*STEP*1*UNTIL*U1*DO*                                                 THOMCOL3
122 *BEGIN* C[K]:=-2-R+1/C[K-1];                                                             THOMCOL4
123           U[K,I]:=(D[K,I]-U[K-1,I])/C[K]                                                 THOMCOL5
124 *END*;                                                                                  THOMCOL6
125         *FOR*K:=U1-1*STEP*-1*UNTIL*L1*DO*U[K,I]:=U[K,I]-U[K+1,I]/C[K];                   THOMCOL7   BLOCK END
126 *END* OF THOMCOL;                                                                       THOMCOL8
127         *PROCEDURE* THOMROW(I);   *VALUE*I; *INTEGER*I;                                  THOMROW0   BLOCK42
128 *BEGIN**INTEGER*K;*ARRAY*C[L2:U2];                                                       THOMROW1
129           C[L2]:=-(2+R);   U[I,L2]:=D[I,L2]/(-2-R);                                      THOMROW2
130         *FOR*K:=L2+1*STEP*1*UNTIL*U2*DO*                                                 THOMROW3
131 *BEGIN* C[K]:=-2-R+1/C[K-1];                                                            THOMROW4
132           U[I,K]:=(D[I,K]-U[I,K-1])/C[K];                                                THOMROW5
133 *END* ;                                                                                 THOMROW6
134         *FOR*K:=U2-1*STEP*-1*UNTIL*L2*DO*U[I,K]:=U[I,K]-U[I,K+1]/C[K];                   THOMROW7   BLOCK END
135 *END* OF THOMROW;                                                                       THOMROW8
136           L1:=L2:=2;   U1:=DX-1;   U2:=DY-1;    H2:=MESH*MESH;                           PRADIT09
137         *FOR*K:=2*STEP*1*UNTIL*DX-1*DO*                                                  PRADI  0
138 *BEGIN* T[K,2]:=U[K,1]-U[K-1,2]*(2-R)*U[K,2]-U[K+1,2]*H2*P[K,2];                        PRADIT11
139           *FOR*L:=3*STEP*1*UNTIL*DY-2*DO*                                                PRADIT12
140           T[K,L]:=U[K-1,L]*(2-R)*U[K,L]-U[K+1,L]*H2*P[K,L];                              PRADIT13
141           T[K,DY-1]:=U[K,DY]-U[K-1,DY-1]*(2-R)*U[K,DY-1]-U[K+1,DY-1]                     PRADIT14
142           *H2*P[K,DY-1];                                                                 PRADIT15
143 *END*;                                                                                  PRADIT16
144         *FOR*K:=2*STEP*1*UNTIL*DX-1*DO* THOMROW(K);                                      PRADIT17
145         *FOR*L:=2*STEP*1*UNTIL*DY-1*DO*                                                  PRADIT18
146 *BEGIN* T[2,L]:=U[1,L]-U[2,L-1]*(2-R)*U[2,L]-U[2,L+1]*H2*P[2,L];                        PRADIT19
147         *FOR*K:=3*STEP*1*UNTIL*DX-2*DO*                                                  PRADIT20
148           T[K,L]:=U[K,L-1]*(2-R)*U[K,L]-U[K,L+1]*H2*P[K,L];                              PRADIT21
149           T[DX-1,L]:=U[DX,L]-U[DX-1,L-1]*(2-R)*U[DX-1,L]-U[DX-1,L+1]                     PRADIT22
150           *H2*P[DX-1,L];                                                                 PRADIT23
151 *END*; *FOR*L:=2*STEP*1*UNTIL*DY-1*DO* THOMCOL(L);                                     PRADIT24
152 *END*                                                                                  PRADIT25   BLOCK END
153 *END* OF PRAD|T|                                                                       PRADIT26
154         *INTEGER* DX,DY,SDX,SDY;USER M;USER V;
155           DX:=30;  DY:=30;   SDX:=13;  SDY:=9;                                                    BLOCK13
156 *BEGIN**ARRAY*TE=,PCY,COXDUCC[1:SDX,1:SDY],PST,PSPC[2:SDX-1,2:SDY-1],   PROGRAM1
157           TYPAR[1:9];                                                                    PROGRAM2
158         *ARRAY* PRAVSTPAN[2:SDX-1,2:SDY-1];                                              PROGRAM3
```

```
159         *REAL*EP,MS;  *INTEGER*KO;                                                       PROGRAM4
160         *REAL* SO,SOSOO,KINO;                                                            DECLARE*
161         *REAL*AMBTEMP;                                                                   DECLARE*
162         *INTEGER*NO3;                                                                    DECLARE*
163         *PROCEDURE*BFROMA(A,B);                                                          BFROMA00
164         *ARRAY*A, B;                                                                     BFROMA01   BLOCK14
165 *BEGIN**INTEGER*K,L,L1,L2,U1,U2;                                                        BFROMA02
166           L1:=LOWBOUND(A,1);   L2:=LOWBOUND(A,2);                                        BFROMA03
167           U1:=L1-1+RANGE(A,1);   U2:=L2-1+RANGE(A,2);                                    BFROMA04
168         *FOR*K:=L1*STEP*1*UNTIL*U1*DO*                                                   BFROMA05
169         *FOR*L:=L2*STEP*1*UNTIL*U2*DO*                                                   BFROMA06
170                                   B[K,L]:=80-6*P(-45000/ACK,L);                          BFROMA07   BLOCK END
171 *END* A TFROMA;                                                                        BFROMA07
172         *PROCEDURE* QUNN1 (KNOWN,UNKNOWN,RHS,SDX,SDY,ITNO,RO,MSIZE);                     QUNNS  0
173         *VALUE*ITNO,RO,MSIZE;                                                            QUNNS  0
174         *ARRAY*KNOWN,UNKNOWN,RHS;*INTEGER*SDX,SDY,ITNO;*REAL*RO,MSIZE;                   QUNNS  1   BLOCK19
175 *BEGIN* *INTEGER*N;                                                                     QUNNS  1
176         *FOR*N:=1*STEP*1*UNTIL*ITNO*DO*                                                  QUNNS  2
177 *BEGIN*                                                                                 QUNNS  3
178           FILL PB (UNKNOWN,KNOWN,RHS,SDX,SDY,PRAVB*RAN,RO,MSIZE);                       QUNNS  3
179           PRAD(UNKNOWN,PRAVB*RAN,SDX,SDY,1/2/MIN(3,14/SDY),MSIZE);                       QUNNS  3
180 *END* FOR N;                                                                           QUNNS  3   BLOCK END
181 *END* QUVN ;                                                                           QUNNS  4
182         *REAL*RESIST,RELC=R;        *PROCEDURE* QDPOR(V,SIGMA);                        QDPOR  0
183         *ARRAY*V,SIGMA;                                                                QDPOR  1   BLOCK16
184 *BEGIN**INTEGER*K,L,L1,L2,U1,U2;  *REAL*VPOS,VNEG,SUM,AVERAGE,SOQ,ERROR;              QDPOR  2
185           L1:=LOWBOUND(V,1);              L2:=LOWBOUND(V,2);                           QDPOR  3
186           U1:=L1-1+RANGE(V,1);            U2:=L2-1+RANGE(V,2);                         QDPOR  4   BLOCK17
187 *BEGIN**ARRAY* T[L1-1:U1+1];                                                           QDPOR  5
188         *FOR*K:=L1-1*STEP*1*UNTIL*U1+1*DO*                                             QDPOR  6
189 *BEGIN* T[K]:=0;          *FOR*L:=L2*STEP*1*UNTIL*U2*DO*                               QDPOR  7
190           T[K]:=T[K]+SIGMA[K,L]*(V[K-1,L]-V[K+1,L])/2;                                 QDPOR  8
191 *END* K;          SUM:=0;                                                            QDPOR  9
192         *FOR*K:=L1+1*STEP*1*UNTIL*U1-1*DO*  SUM:=SUM+T[K];                             QDPOR  0
193           AVERAGE:=SUM/(U1-L1-1);     SOQ:=0;                                        QDPOR  1
194         *FOR*K:=L1+1*STEP*1*UNTIL*U1-1*DO*  SOQ:=SOQ+(T[K]-AVERAGE)*2;               QDPOR  2
195           ERROR:=SOQ/(U1-L1-1)/(U1-L1-2)*0.5;                                          QDPOR  3
196         **PRINT** ''L'CURRENT'L';                                                      QDPOR  4
197         *FOR*K:=L1+1*STEP*1*UNTIL*U1-1*DO***PRINT*ALIGNED(3,0),T[K];                   QDPOR  5
198         **PRINT***''L'RESULTI'B4'',SAMELINE,AVERAGE,''B1''='B1'',ERROR;                QDPOR  6
199         **PRINT***''L'NUMBER'B'OF'B'OBSERVATIONS='B',SAMELINE,U1-L1+1;                 QDPOR  7
200           RELCKR:=ERROR*100/AVERAGE;                                                   QDPOR  8
201         **PRINT**''L'REL.'B'ERR.=',SAMELINE,RELCKR;                                    QDPOR  9
202           VPOS:=VEU1,U2]; VNEG:=V[L1,L2];    RESIST:=(VPOS-VNEG)/AVERAGE;              QDPOR  0
203         **PRINT***''L3'RESISTANCE=',SAMELINE,RESIST;                                   QDPOR  1   BLOCK END
204 *END*;                                                                                 QDPOR  2   BLOCK END
205 *END* OF QDPOR;                                                                       QDPOR  3
206         **REAL**PROCEDURE* RADIUS(A);                                                  RADIUS00
207         *ARRAY*A;                                                                      RADIUS01   BLOCK18
208 *BEGIN**INTEGER*I,J,L1,L2,U1,U2; *REAL*AMIN,AMAX;                                      RADIUS02
209           L1:=LOWBOUND(A,1); L2:=LOWBOUND(A,2);                                        RADIUS03
210           U1:=L1-1+RANGE(A,1);     U2:=L2-1+RANGE(A,2);                                T|SKN106
211           AMAX:=AMIN:=A[0];                                                            T|SKN107
212         *FOR*I:=L1*STEP*1*UNTIL*U1*DO*                                                 T|SKN40
213         *FOR*J:=L2*STEP*1*UNTIL*U2*DO*                                                 T|SKN40
214         *IF* A[I,J]>AMAX *THEN* AMAX:=A[I,J];                                          T|SKN410
215           AMIN:=AMAX;                                                                  T|SKN411
216         *FOR*I:=L1*STEP*1*UNTIL*U1*DO*                                                 T|SKN408
217         *FOR*J:=L2*STEP*1*UNTIL*U2*DO*                                                 T|SKN409
218         *IF* A[I,J]<AMIN *THEN* AMIN:=A[I,J];                                          T|SKN40.0
```

```
        AMAX:=AMIN;                                                   TISKN411
        'FOR'I:=L1'STEP'1'UNTIL'U1'DO'                                TISKN108
        'FOR'J:=L2'STEP'1'UNTIL'U2'DO'                                TISKN409
        'IF' A[I,J]>AMAX 'THEN' AMAX:=A[I,J];                         TISKN410
        RADIUS:=1/(AMAX-AMIN);                                        RADIUS04
'END' OF RADIUS;                                                      RADIUS09      BLOCK END
        'INTEGER'K,L;                                                 DECLAR**
        'INTEGER'    O ;                                              DECLAR**
        'REAL' SCALE;                                                 DECLAR**
        S0:=S0;         S0300:=S0*EXP(-5000/300);                     ASSIGN**
        KOND:=4,-3;                                                   ASSIGNSS
        USER H (= (DH-SDH+1)/2;  USER V (= (DV-SDV+1)/2;
        ITPAR[1]:=0,25159;                                            ASSIGNIT
        ITPAR[2]:=0,47492;                                            ASSIGNIT
        ITPAR[3]:=0,89666;                                            ASSIGNIT
        ITPAR[4]:=1,69291;                                            ASSIGNAT
        ITPAR[5]:=3,19423;                                            ASSIGNAT
        ITPAR[6]:=6,03450;                                            ASSIGNAT
        ITPAR[7]:=11,39320;                                           ASSIGNAT
        ITPAR[8]:=21,51049;                                           ASSIGNAT
        ITPAR[9]:=40,61195;                                           ASSIGNIT
        EP:=1;                                                        PROGRAM4
        HS:=0,1;                                                      PROGRAM4
        AMBTEMP:=300;                                                 ASSINGAT
        NOOI:=7;                                                      ASSINGNI
        'FOR'O:=1'STEP'1'UNTIL'7'DO'                                  PROGRAM1
'BEGIN'                                                               P-OG-AM2
        'READ' EP;                                                    PROGRAM2
        'IF'O=1'THEN'                                                 P-OG-AM3
'BEGIN'                                                               P-OG-AM4
        'FOR'K:=1'STEP'1'UNTIL'SDH'DO'                                PROGRAM5
        'FOR'L:=1'STEP'1'UNTIL'SDV'DO'                                PROGRAM5
'BEGIN' TEP[K,L]:=AMBTEMP;                                            PROGRAM7
        POT[K,L]:=2*EP*(K-1)/(SDH-1)-EP;                              PROGRAM*
'END';                                                                PROGRAM*
        'GOTO' CYCLE;                                                 P-OG-A10
'END';                                                                P-OG-A11
        SCALE:=EP/POT[SDH,1];                                         PROGRA11
        'FOR'K:=1'STEP'1'UNTIL'SDH'DO'                                PROGRA14
        'FOR' L:=1 'STEP' 1 'UNTIL' SDV 'DO'                          P-OG-A15
'BEGIN'                                                               P-OG-A16
        POT[K,L]:=POT[K,L]*SCALE;                                     PROGRA16
'END';                                                                P-OG-A20
CYCLE:                                                                P-OG-A21
        TPROMA(TEP,CONDUC);                                           PROGRA14
        NULUJ(PSP);                                                   PROGRA**
        'PRINT'''P'';                                                 PRINTING
        'PRINT'''L'SO=',SAMELINE,SO;                                  RINTING1
        'PRINT'''L'KOND=',SAMELINE,SCALED(4),KOND;                    PRINTING
        'PRINT'''L'RATIO'S'S(300)/KOND'S'=',SAMELINE,SCALED(4),S0300/KOND  PRINTING
           ;                                                          PRINTING
        'PRINT'''L'ELECTRODE'S'POTENTIAL'S'=',SAMELINE,EP;                  IN
        'PRINT'''L'AMBIENT'S'TEMPERATURE'S'=',SAMELINE,AMBTEMP;         RINTIN
        'FOR'OI:=1'STEP'1'UNTIL'NOOI'DO'                              PROGRA12
'BEGIN' FIELD SQ (POT,PST,SDH,SDV,HS);                                PROGRA13
        'FOR'K:=2'STEP'1'UNTIL'SDH-1'DO'                              PROGRA15
        'FOR'L:=2'STEP'1'UNTIL'SDV-1'DO'                              PROGRA16
'BEGIN'
        PST[K,L]:=PST[K,L]*CONDUC[K,L]/KOND;                          PROGRA17
'END';


        'IF'OI=NOOI'THEN'                                             PROGTAM*
'BEGIN'                                                               PROGRAM*
        TISKNI(PST);        'PRINT'''L'PST'';                         PROGRA18
'END';                                                                PROGRAM*
        'FOR'K:=1'STEP'1'UNTIL'9'DO'                                  PROGRA19
        TRADI(TEP,PST,SDH,SDV,ITPAR[K],HS);                           PROGRA20
        'IF'OI=NOOI'THEN'                                             PROGTAM*
'BEGIN'                                                               PROGRAM*
        TISKNI(TEP);        'PRINT'''L'TEP(1)'';                      PROGRA21
'END';                                                                PROGRAM*
        TPROMA(TEP,CONDUC);                                           PROGRA22
        SUKNI(CONDUC,POT,PSP,SDH,SDV,10,RADIUS(CONDUC),HS);           PROG-A25
        'IF'OI=NOOI'THEN'                                             PROGTAM*
'BEGIN'                                                               PROGRAM*
        TISKNI(POT);        'PRINT'''L'POT(1)'';                      PROGRA24
'END';                                                                PROGRAM*
        'PRINT'''L'OUTER'S'ITERATION',SAMELINE,OI;                    PROGRA27
'END'   FOR OI;                                                       PROGRA28
        ODPOR(POT,CONDUC);
'END';                                                                              BLOCK END
'END';                                                                PROGRAM*      BLOCK END
'END';
   986  MC
  3144  CODE
  4132  TOTAL


 @DIAG;                                                  CPU TIME = 0000  33,531
DIAG


 @RUN;                                                   CPU TIME = 0000  33,955
ZKOUSKAP
DRO
```

```
&END;
 ** ICL 4130 DE92 SYSTEM  :  SLAVE BIG       :  CORE 70K  :  VOL  4                DATE  21 08 73    :  TIME  00,23,43

&JOB; PH/R022/20; MODEL OF STRUCTURAL RELAXATION;

&ALGOL;
LIBRARY                                                                  CPU TIME =  0000  00,063
ALGOL

&LINES;              2500;                                               CPU TIME =  0000  03,497

&LIST;                                                                   CPU TIME =  0000  03,526

    1   TRIAL FOR GAUSS;
    2   "BEGIN""INTEGER"DIM;
    3           "REAL" AEFO, TGT,EM1;                                    ELECTH34
    4            TGT:=590;  EM1:=2,-6;                                   ELECTH69
    5            DIM:=10;                                                ********
    6   "BEGIN""ARRAY"ASOL[0:DIM];
    7           "ARRAY"APOT[0:DIM];                                      ELECTHER
    8           "PROCEDURE"GAUSS(AA,AB,AC,AD,D);                            USC0
    9           "ARRAY"AA,AB,AC,AD;                                         USC1
   10           "INTEGER"D;                                                 USC2
   11   "BEGIN""INTEGER"I;"ARRAY"S[0:DIM],ALPHA[0:DIM];                     USC3
   12            ALPHA[0]:=AB[0];                                           USC4
   13                S[0]:=AD[0];                                           USC4
   14           "FOR"I:=1"STEP"1"UNTIL"D"DO"                               USC5
   15   "BEGIN" ALPHA[I]:=AB[I]-AA[I]*AC[I-1]/ALPHA[I-1];                  USC6
   16                S[I]:=AD[I]*AA[I]*S[I-1]/ALPHA[I-1];                   USC7
   17   "END" FOR I ;                                                       USC8
   18            ASOL[D]:=S[D]/ALPHA[D];                                    USC9
   19           "FOR"I:=D-1"STEP"-1"UNTIL"0"DO"                            USC10
   20            ASOL[I]:=(S[I]*AC[I]*ASOL[I+1])/ALPHA[I];                 USC11
   21   "END" OF GAUSS ;                                                    USC12
   22           "REAL"DX;                                                   USC13
   23           "REAL" VOLTAGE,WC;                                      ELECT021
   24           "REAL" THETA;                                             LECTHE
   25           "REAL" SO,CS,TCOND;                                     ELECTHER
   26           "REAL""PROCEDURE"TOCO(A,P);"ARRAY"A,P;                  ELECTHER
   27   'BEGIN""INTEGER"W;"REAL"TC; TC:=0;                                  C000
   28          "FOR" W:=0 "STEP" 1 "UNTIL" DIM "DO"                          C001
   29           TC:=TC+EXP((THETA-P[W])/WC)/A[W];                            C002
   30           TOCO:=SO/DX/TC;                                              C003
   31   "END" OF TOCO;                                                       C004
   32           "REAL" SHUV,RTIME;                                          C005
   33           "REAL""PROCEDURE"F(K); "INTEGER"K;                      ELECTHER
   34            F:=SO*EXP((APOT[K]/WC-THETA)/ASOL[K])/SHUV;            ETMFFF00
   35           "ARRAY"A[0:DIM],B[0:DIM],C[0:DIM],D[0:DIM];            ETMFFF01
   36           "INTEGER"K;                                                 NI00
                                                                            NI01
```

```
37          "INTEGER"N;                                                    NIC
38          "REAL" R,DT,JOU,LAMBDA,TO;                                     NIC
39          "REAL" CURRENT,CG,VO,FRQCY;                                    ELECTHE
40          "REAL" VOINITIAL;                                              ELECTH4
41          "BOOLEAN" PRESWI, PREECR, SWIPOS;                              ELECTH5
42          "REAL" AREA;                                                   ELECTH3
43          "PROCEDURE" DELT(UO);                                          LTO
44          "REAL"UO;                                                      LTO
45  "BEGIN"                                                                LTO
46          "REAL""PROCEDURE"VNLOR(TEPROZ,PRINT);"VALUE"PRINT;"BOOLEAN"    VNLOR=0
47          PRINT; "ARRAY" TEPROZ;                                         VNLOR=0
48  "BEGIN""INTEGER"K,L,M;                                                 VNLOR=0
49          "INTEGER"N;                                                    VNLOR0=
50          "REAL"F,FD,EPS,SUMRESQ,RES,SUM1,SUM2;                          VNLOR=0
51          "REAL" PVNLOR;                                                 VNLOR=0
52          "ARRAY"V[0:DIM];                                               VNLOR=0
53           "FOR"K:=0"STEP"1"UNTIL"DIM"DO" V[K]:=APOT[K]*DX;              VNLOR=0
54           EPS:=DIM*V[DIM]**2/*10;                                       VNLOR06
55           SUM2:=AREA*SO/CS/DX;                                          VNLOR=0
56           N:=0;                                                         VNLOR=0
57  RET:     N:=N+1;                                                       VNLOR=0
58           SUMRESQ:=0;                                                   VNLOR=0
59          "FOR"K:=0"STEP"1"UNTIL"DIM"DO"                                 VNLOR=0
60  "BEGIN" SUM1:=0;                                                       VNLOR=1
61          "FOR"M:=0"STEP"1"UNTIL"DIM"DO"                                 VNLOR=1
62           SUM1:=SUM1+EXP((THETA-V[M])/WC)/TEPROZ[M]);                   VNLOR=1
63           F:=UO*(DIM+1)/DIM*                                            VNLOR=16
64                 EXP((THETA-V[K])/WC)/TEPROZ[K])/(SUM1+SUM2)-V[K];       VNLOR=1
65           FD:=-UO*(DIM+1)/DIM*                                          VNLOR=1
66                   EXP((THETA-V[K])/WC)/TEPROZ[K])*(SUM1+SUM2-           VNLOR=1
67               EXP((THETA-V[K])/WC)/TEPROZ[K]))/WC/TEPROZ[K]/(SUM1+SUM2)**2  VNLOR=1
68           -1;                                                           VNLOR=1
69           RES:=-F/FD;                                                   VNLOR=1
70           SUMRESQ:=SUMRESQ+RES**2;                                      VNLOR=2
71          V[K]:=V[K]+RES;                                                VNLOR=2
72  "END";                                                                 VNLOR=2
73          "IF"SUMRESQ>EPS"AND"N<200"THEN"                                VNLOR=2
74          "GOTO" RET;                                                    VNLOR=2
75           PVNLOR:=0;                                                    VNLOR=2
76          "FOR"K:=0"STEP"1"UNTIL"DIM"DO"                                 VNLOR=2
77  "BEGIN" APOT[K]:=V[K]/DX;                                              VNLOR=3
78           PVNLOR:=PVNLOR+V[K];                                          VNLOR=3
79  "END";                                                                 VNLOR=3
80          "IF"PRINT"THEN"                                                VNLOR=3
81  "BEGIN"                                                                VNLOR=3
82          "PRINT"//(5X),"FOR"K:=0"STEP"1"UNTIL"DIM"DO""PRINT"//S2X,
83              SAMELINE,TEPROZ[K];
84  "BEGIN""PRINT"//(X);                                                   VNLOR=2
85          "FOR"M:=0"STEP"1"UNTIL"DIM"DO""PRINT"SAMELINE,//S2X,V[M];      VNLOR=2
86  "END";                                                                 VNLOR=2
87          "PRINT"SAMELINE,//S3X"PVNLOR=",PVNLOR;                         VNLOR=3
88          "PRINT"//UO=",SAMELINE,UO;                                     VNLOR=3
89          "PRINT" SAMELINE,N;                                            VNLOR=3
90  "END";                                                                 VNLOR=3
91           VNLOR:=PVNLOR;                                                VNLOR=3
92  "END" OF VNLOR;                                                        VNLOR=3
93          "INTEGER"J,KMAX;    "ARRAY" VSTORE[1:10];                      ELECTHE
94           "ARRAY"TSTORO,TSTORD,PSTORO,PSTORD[1:10];                     ELECTHE
95          "ARRAY" TTS[1:10];                                             ELECTHE
96          "INTEGER"KOBS;                                                 ELECTHE
```

```
97          KMAX:=100;
98          KORS:=60;
99          PRESW:="TRUE";
100         PREPOR:="TRUE";
101         "PRINT"(/L10);
102         "FOR"N:=0"STEP"1"UNTIL"DIM"DO" APOT[N]:=V0/DIM/DX;
103         "FOR"N:=0"STEP"1"UNTIL"DIM"DO" ASOL[N]:=T0;
104         "FOR"J:=1"STEP"1"UNTIL"9"DO" VSTORE[J]:=U0;
105         "FOR"J:=1"STEP"1"UNTIL"9"DO"
106   "BEGIN" TSTORO[J]:=TSTORD[J]:=T0;
107         PSTORO[J]:=PSTORD[J]:=U0/DIM/DX;
108         TTS[J]:=0;
109   "END";
110         TTS[10]:=0;
111         K:=1;
112   L1:
113         VOLTAGE:=VALOR(ASOL,0>1);
114         VSTORE[10]:=VOLTAGE;
115         TSTORO[10]:=ASOL[0];
116         TSTORD[10]:=ASOL[DIM];
117         PSTORO[10]:=APOT[0];
118         PSTORD[10]:=APOT[DIM];
119         TTS[10]:=TTS[10]+DT;
120        "FOR"J:=1"STEP"1"UNTIL"9"DO" VSTORE[J]:=VSTORE[J+1];
121        "FOR"J:=1"STEP"1"UNTIL"9"DO"
122   "BEGIN" TSTORO[J]:=TSTORO[J+1];
123         TSTORD[J]:=TSTORD[J+1];
124         PSTORO[J]:=PSTORO[J+1];
125         PSTORD[J]:=PSTORD[J+1];
126         TTS[J]:=TTS[J+1];
127   "END";
128         "IF" (TSTORD[9]-TSTORD[8])<3"AND" R<1.2*-4 "AND" K>40 "THEN"
129   "BEGIN" DT:=2*DT;
130         R:=2*R;
131         A[0]:=0;   B[0]:=1+R*(1+DX*LAMBDA/TCOND);   C[0]:=R;
132        "FOR"N:=1"STEP"1"UNTIL"DIM-1"DO"
133   "BEGIN" A[N]:=R;
134         B[N]:=2+2*R;
135         C[N]:=R;
136   "END"  FOR N ;
137         A[DIM]:=2*R;    B[DIM]:=2+2*R;     C[DIM]:=0;
138   "END";
139         "IF" (TSTORD[9]-TSTORD[8])>10 "THEN"
140   "BEGIN" DT:=DT/2;
141         R:=R/2;
142         A[0]:=0;   B[0]:=1+R*(1+DX*LAMBDA/TCOND);   C[0]:=R;
143        "FOR"N:=1"STEP"1"UNTIL"DIM-1"DO"
144   "BEGIN" A[N]:=R;
145         B[N]:=2+2*R;
146         C[N]:=R;
147   "END"  FOR N ;
148         A[DIM]:=2*R;    B[DIM]:=2+2*R;     C[DIM]:=0;
149   "END";
150         "BEGIN"
151         AEF0:=TGT*(1-EM1*APOT[0])/ASOL[0];
152        "PRINT"(/L,SAMELINE,K,''S2'',ASOL[0],''S'',ASOL[DIM]-ASOL[0],
153        ''S3'',APOT[0],''S'',APOT[DIM],''S2'',SCALED(4),TTS[10],
154         FREEPOINT(4),''S2'',AEF0,''S'',TGT*(1-EM1*APOT[DIM])/ASOL[DIM];
155        "IF" AEF0<1 "THEN""GOTO" ENDDELT;
156   "END";
```

```
157           CG;=TOCO(ASOL,APOT);                                                ELECTHO!
158           CURRENT;=UO*CS*CG/(CG+CS);                                          ELECTHER
159           B[0]:=R*ASOL[1]*(1=R*(1=DX*LAMBDA/TCOND))*ASOL[0]*2*R*DX*           ELECT115
160            LAMBDA*TO/TCOND*DT*APOT[0]*2*F(0)/2;                               ELECT116
161           "FOR"N:=1"STEP"1"UNTIL"DIM=1"DO"                                    ELECT100
162            B[N]:=R*ASOL[N=1]*(2=2*R)*ASOL[N]*R*ASOL[N+1]                      ELECT101
163                  +DT*APOT[N]*2*F(N);                                          ELECT102
164            B[DIM]:=2*R*ASOL[DIM=1]*(2=2*R)*ASOL[DIM]*DT*APOT[DIM]*2*F(DIM);   ELECT103
165            PASS(A,B,C,D,DIM);
166            K:=K+1;                                                                Nl**
167           "IF"KKKMAX"THEN""GOTO"L1;                                               DGAU
168           "FOR"N:=0"STEP"1"UNTIL"DIM"DO""PRINT" ASOL[N],                  ********
169             //S3\\,SAMELINE,TGT*(1=EM1*APOT[N])/ASOL[N];                  ********
170           "IF" K=150 "THEN"                                                   ELECT149
171   "BEGIN" SWIPOS:="FALSE";                                                    ELECTHKO
172           "PRINT"K,SAMELINE,'/S3\\,UO,'/S3\\,TO,'/S3\\,LAMBDA,'/S5\RUNOUT\          LT**
173   "END"                                                                       ELECTHKO
174           "ELSE"                                                                 LT**
175           "PRINT"K=KOBS      ,SAMELINE,'/S3\\,UO,'/S3\\,TO,'/S3\\,'RESULT\;   ELECT154
176            DT:=RTIME[1]     R1:=DT*TCOND/SHUV/DX/DX;                          ELECT155
177            A[0]:=0;   B[0]:=1+R*(1=DX*LAMBDA/TCOND);   C[0]:=R;               ELECT156
178           "FOR"N:=1"STEP"1"UNTIL"DIM=1"DO"                                    ELECT157
179   "BEGIN" A[N]:=R;                                                            ELECT157
180            B[N]:=2+2*R;                                                       ELECT157
181            C[N]:=R;                                                           ELECT157
182   "END"  FOR N ;                                                              ELECT157
183            A[DIM]:=2*R;     B[DIM]:=2+2*R;      C[DIM]:=0;                    ELECT157
184    ENDDELT;                                                                   ELECT157
185   "END" OF DELT;
186
187           "REAL"RECTEMP;
188           "REAL"OLDUD,KROK,KAM;
189           "REAL" RC,SOBULK;                                                   ELECTHER
190           "REAL" THICKNESS;                                                   ELECT157
191           "REAL"EGAP;                                                         ELECT158
192            THICKNESS:=,=2;                                                    ELECT158
193            JOI:=0;                                                            ELECT159
194            DX:=THICKNESS/DIM;                                                 ELECT160
195            LAMBDA:=,=3;                                                    ********
196            EGAP:=0,45*1,6,=12;                                                ELECT163
197            THETA:=EGAP/1,38,=16;                                              ELECT164
198            CS:=,=7;                                                        ********
199            SOBULK:=3,=3;                                                      ELECT173
200            SHUV:=2,=2;                                                        ELECTDAT
201            RC:=2,=2;                                                          ELECTHER
202            TCOND:=3,=3;                                                       ELECT176
203            AREA:=1;                                                           ELECT174
204            RTIME[1]:=,=7;
205                                                                               ELECTHER
206            DT:=RTIME[1];                                                      ELECT173
207            R1:=DT*TCOND/SHUV/DX/DX;                                           ELECT174
208            RC:=RC;                                                            ELECT175
209            S01:=SOBULK/DX;                                                    ELECT134
210            A[0]:=0;   B[0]:=1+R*(1=DX*LAMBDA/TCOND);   C[0]:=R;                  N106
211           "FOR"N:=1"STEP"1"UNTIL"DIM=1"DO"                                       N107
212   "BEGIN" A[N]:=R;                                                               N108
213            B[N]:=2+2*R;                                                          N109
214            C[N]:=R;                                                              N109
215   "END"  FOR N ;                                                                 N110
216            A[DIM]:=2*R;     B[DIM]:=2+2*R;      C[DIM]:=0;                        N111
217           "PRINT"'SIGMA='S\\,SAMELINE,S0,/*\,'EXP((V/\,WC,=THETA, ')/T)\;
218           "PRINT"//[\EGAP='S\\,SCALED(3),SAMELINE,EGAP/1,6=12;                ELECT183
219           "PRINT"//[\TCOND='S\\,SAMELINE,TCOND;                               ELECT183
220           "PRINT"//[\THICKNESS='\,SAMELINE,SCALED(3),THICKNESS;               ELECT183
221           "PRINT"//[\DIM='S\\,SAMELINE,DIM;                                   ELECT183
222           "PRINT"//[\DX='\,SAMELINE,DX;                                       ELECT184
223           "PRINT"//[\DT='\, SCALED(3),SAMELINE,DT;                            ELECT185
224           "PRINT"//[\R='\,SAMELINE,R;                                         ELECT183
225           "PRINT"//[\WC='\,SAMELINE,WC;                                       ELECT186
226           "PRINT"//[\AREA='\,SAMELINE,AREA;
227           "PRINT"//[\SOBULK',SAMELINE,SOBULK;                                 ELECTHER
228           "PRINT"//[\CS='\,SAMELINE,CS;                                       ELECTHER
229           "PRINT"//[\LAMBDA='\,SAMELINE,SCALED(3),LAMBDA;                     ELECT190
230           "PRINT"//[\TGT='\,SAMELINE,TGT;                                     ELECT191
231           "PRINT"//[\EM1='\,SAMELINE,EM1;                                     ELECT192
232            RECTEMP:=1000/270;                                                 ********
233           "READ" TO,VOINITIAL;
234   "BEGIN""PRINT"//[10\\]  PRESV:="TRUE";                                      ELECT205
235           "PRINT"//[\TO='\,SAMELINE,TO;                                       ELECT206
236            SWIPOS:="TRUE";                                                    ELECT--C
237           KROK:=VOINITIAL*(1,47=1/1,47)/4;                                    ********
238            "FOR"VO:=VOINITIAL/1,47"STEP"KROK"UNTIL"VOINITIAL*1,47"DO"         ********
239                  DELT(VO);                                                    ********
240   "END" FOR RECTEMP;
241   "END";"END" OF PROGRAMME;
  650     MC
 2182   CODE
 2832  TOTAL
```

```
** ICL 4130 DE92 SYSTEM  :  SLAVE BACK      :  CORE 48K  :  VOL  0                    DATE  18 05 73    :  TIME  13,05,47

&JOB(PH/R002/73)

&TIME(10)                                                                  CPU TIME =  0000  00,067

&ALGOL(L)                                                                  CPU TIME =  0000  00,102
LIBRARY
ALGOL

&LINES(     2500)                                                          CPU TIME =  0000  03,769

&LIST)                                                                     CPU TIME =  0000  03,801

    1   STUDY OF CORRELATION EFFECTS)                                      SOCE=000
    2   "BEGIN"                                                            SOCE=001                              BLOCK1
    3         "PROCEDURE" CORF(A,N,M)                                      CORF=00
    4         "VALUE"M)                                                    CORF=01
    5         "INTEGER"N,M;    "ARRAY"A)                                   CORF=02                               BLOCK2
    6   "BEGIN""INTEGER"K,LAG)                                             CORF=03
    7         "REAL"MEAN,MEANSQUARE,SQUAREDMEAN,  P)                       CORF=04
    8         "REAL"SUM,MI "INTEGER"LI                                     CORF=05
    9          "ARRAY"R,AC,D,D[0(M)                                        CORF=06
   10         "ARRAY"E[1(N)]                                               CORF=07
   11         "PROCEDURE" PLOT(A,N1,N2)I  "VALUE"N1,N2I  "ARRAY"AI "INTEGER"  PLOT=00
   12          N1,N2)                                                      PLOT=01                               BLOCK3
   13   "BEGIN""INTEGER"K)                                                PLOT=02
   14          MOVEPEN(0,6000)) SETORIGIN(1500,0)) DRAWLINE(0,50*(N2-N1))) PLOT=04
   15          MOVEPEN(-1000,0)) DRAWLINE(1000,0)) MOVEPEN(-1000*A[N1],0)) PLOT=05
   16          MOVEPEN(0,0)) "FOR" K:=N1*STEP*1"UNTIL" N2 "DO"            PLOT=05
   17   "BEGIN" DRAWLINE(20, 50*(K-N1)))  MOVEPEN(0,50*(K+1-N1)))         PLOT=05
   18   "END"I  MOVEPEN(-1000*A[N1],0))                                    PLOT=05
   19         "FOR"K:=N1+1"STEP"1"UNTIL"N2"DO" DRAWLINE(-1000*A[K],50*(K-N1)))  PLOT=06                           BLOCK END
   20   "END" OF PLOTI                                                     PLOT=07
   21         "REAL"S0,S1,S2,S3,S4,P0,P1,P2)                               TREND=00
   22         "REAL"B2,D5,B6,B1)                                           TREND=01
   23         "REAL" MI                                                    TREND=01
   24         "REAL""PROCEDURE"D3(A,B,C,D,E,F,G,H,I)                       TREND=02
   25               "REAL"A,B,C,D,E,F,G,H,I)                               TREND=03                              BLOCK4
   26                D3:=A*(E-I)+F*H)-B*(D-I)+F*G)+C*(D*H-E*G))           TREND=04                              BLOCK END
   27          M:=1/50)
   28          PI:=3,14159265351                                          CORF=05
   29          MEAN:=0)                                                   CORF=05
   30         "FOR"K:=1"STEP"1"UNTIL"N"DO" MEAN:=MEAN+A[K])               CORF=06
   31          MEAN:=MEAN/NI SQUAREDMEAN:=MEAN*2)                         CORF=07
   32         "PRINT"(//L5)MEAN=',SAMELINE,MEAN,//L3'))                   CORF=08

   33          "PRINT"(//L2)SQUAREDMEAN=',SAMELINE,SQUAREDMEAN)           CORF=09
   34           P0:=P1:=P2:=0)                                            TREND=10
   35          "FOR"K:=1"STEP"1"UNTIL"N"DO"                               TREND=05
   36   "BEGIN" P0:=P0+A[K]) P1:=P1+K*A[K]) P2:=P2+K*K*A[K])              TREND=06
   37   "END")                                                            TREND=07
   38           P1:=P1*M)                                                 TREND=08
   39           P2:=P2*M*M)                                               TREND=09
   40           W1:=N)                                                    TREND=09
   41           S0:=N)                                                    TREND=10
   42           S1:=N*(N+1)/2*M)                                          TREND=11
   43           S2:=N*(N+1)*(2*N+1)/6*M*M)                                TREND=12
   44           S3:=N*N*(N+1)*(N+1)/4*M*M*M)                              TREND=13
   45           S4:=N*(N+1)*(2*N+1)*(3*N*N+3*N-1)/30*M*M*M*M)             TREND=14
   46           D5:=D3(S0,S1,S2,S1,S2,S3,S2,S3,S4))                       TREND=15
   47           B0:=D3(P0,S1,S2,P1,S2,S3,P2,S3,S4)/D5)                    TREND=16
   48           B1:=D3(S3,P0,S2,S1,P1,S3,S2,P2,S4)/D5)                    TREND=17
   49           B2:=D3(S0,S1,P0,S1,S2,P1,S2,S3,P2)/D5)                    TREND=18
   50          "PRINT"(//L1)B0=',SAMELINE,B0,//'S3'B1=',B1,//'S3'B2=',B2) TREND=20
   51          "FOR"K:=1"STEP"1"UNTIL"N"DO"T[K]:=A[K]-B0-B1*K-B2*K*K)     TREND=21
   52           R[0]:=0)                                                  CORF=007
   53          LAG:=0) "FOR"K:=1"STEP"1"UNTIL"N"DO"R[0]:=R[0]+T[K]*2)     CORF=107
   54           R[0]:=R[0]/N) MEANSQUARE:=R[0]) "PRINT"(//L1)MEANSQUARE=',SAMELINE  CORF=207
   55                 ,MEANSQUARE,//L3'))                                 CORF=307
   56            AC[LAG]:=R[LAG]/MEANSQUARE)                              CORF=407
   57              "FOR"LAG:=1"STEP"1"UNTIL"M"DO"                         CORF=10
   58   "BEGIN" R[LAG]:=0)                                                CORF=11
   59          "FOR"K:=1"STEP"1"UNTIL"N-LAG"DO"R[LAG]:=R[LAG]+T[K]*T[K+LAG])  CORF=12
   60           R[LAG]:=R[LAG]/(N-LAG))                                   CORF=12
   61            AC[LAG]:=R[LAG]/MEANSQUARE)                              CORF=407
   62   "END" LAG)                                                        CORF=15
   63          "FOR"K:=0"STEP"1"UNTIL"M"DO"D[K]:=(1+COS(P[*K/M))/2)       CORF=16
   64           "FOR"K:=0"STEP"1"UNTIL"M"DO"                              CORF=17
   65   "BEGIN" SUM:=0)                                                   CORF=18
   66          "FOR"L:=1"STEP"1"UNTIL"M-1"DO"SUM:=SUM+D[L]*AC[L] +COS(P[*L*K/M))  CORF=19
   67           T[K]:=2*+*(AC[0]+2*SUM))                                 CORF=20
   68   "END")                                                            CORF=21
   69          "FOR"K:=0"STEP"1"UNTIL"M"DO"                              CORF=22
   70           "PRINT"(//L1)LAG=',SAMELINE,K,//'S3'R=',R[K],//'S3'AC=',AC[K],  CORF=23
   71                  //'S3'G=',G[K])                                    CORF=24
   72          PLOT(AC[0, 50)) PLOT(G,0, 50))                            PLOTINC=
   73          "PRINT"(/L5)',SAMELINE,N,//'S1',MI                        CORF=16                               BLOCK END
   74   "END" OF CORFI                                                    CORF=17
   75          "ARRAY"X[1(10000)                                         SOCE=002
   76          "INTEGER" N,NO)                                           SOCE=003
   77          "REAL"I                                                   PODDAT00
   78   RET:    N:=N+1;   "READ" X[N);                                   PODDAT01
   79          "IF" ABS(X[N]-333)>=0 "THEN""GOTO" RET)                   PODDAT02
   80                                                  CORF(X,NO,200))   PODDAT03
   81           NO:=N-1)                                                 SOCE=010
   82           MOVEPEN(0,6000)) SETORIGIN( 400,0))                      SOCE=011
   83          "FOR"N1:=1"STEP"1"UNTIL" NO "DO"                          SOCE=012
   84   "BEGIN"DRAWLINE(200*5* X[N], 10*N))  MOVEPEN(0,10*(N+1)))        SOCE=012                              BLOCK END
   85   "END")
   86   "END" OF PROGRAMME STUDY)
  446     MC
 1200  CODE
 1646 TOTAL

                                                                           CPU TIME =  0000  12,011
```

```
** ICL 4130 DOS2 SYSTEM  :  SLAVE HACK      :  CORE 48K  :  VOL  0                    DATE  13 06 73    :  TIME  11.29.56

&JOB: PW/R022/24:  LEAST SQUARES FIT:


&LINES:   2400:                                                          CPU TIME =  0010  00.042


&ALGOL:   L1                                                             CPU TIME =  0000  00.083
LIBRARY
ALGOL


&LIST:                                                                   CPU TIME =  0000  03.381
    1   LEAST SQUARES FIT:                                                          LSF1T000
    2   'BEGIN'                                                                     LSF1T001                                BLOCK1
    3         'REAL''PROCEDURE'LSF1T(A1,A2,A3,H2);                                  LSF1T002                                BLOCK2
    4               'REAL'A1,A2,A3,H2;  IF12:A3:=A2-H2;                            LSF1T003                                BLOCK E D
    5         'REAL'A;R;                                                           LSF1T004
    6         'PROCEDURE' LSF1T(X,Y,M);                                            LSF1T005
    7               'VALUE'M;'INTEGER'M;'ARRAY'X,Y;                                LSF1T006                                BLOCK3
    8   'BEGIN'                                                                    LSF1T007
    9         'REAL''PROCEDURE'F(X);                                               LSF1T008
   10               'REAL'X;                                                      LSF1T009                                BLOCK4
   11   'BEGIN'                                                                    LSF1T010                                BLOCK5
   12         'SWITCH'SF:=F1,F2,F3,F4,F5,F6,F7,F8;                                 LSF1T011
   13         'GOTO'SF[M];                                                         LSF1T012
   14          F1: F:=A1[1]*F(H*X);                    'GOTO'EF;                  LSF1T013
   15          F2: F:=A*X+B;                           'GOTO'EF;                  LSF1T014
   16          F3: F:=A*X*(X+1)*B;                     'GOTO'EF;                  LSF1T015
   17          F4: F:=A*X*(X+3)*B;                     'GOTO'EF;                  LSF1T016
   18          F5: F:=A*EXP(B*SQRT(X))*X;              'GOTO'EF;                  LSF1T017
   19          F6: F:=A*EXP(B*X)*X;                    'GOTO'EF;                  LSF1T018
   20          F7: F:=A*EXP(B*SQRT(X));                'GOTO'EF;                  LSF1T019
   21          F8: F:=A/2*(EXP(H*X)+EXP(-H*X));                                   LSF1T020                                BLOCK E.D
   22   EF:'END'F;                                                                 LSF1T021
   23         'REAL''PROCEDURE'FA(X);                                              LSF1T022
   24               'REAL'X;                                                      LSF1T023                                BLOCK8
   25   'BEGIN''SWITCH'SFA:=FA1,FA2,FA3,FA4,FA5,FA6,FA7,FA8; 'GOTO'SFA[M];        LSF1T024
   26          FA1: FA:=EXP(B*X);                     'GOTO'EFA;                  LSF1T025
   27          FA2: FA:=X*B;                          'GOTO'EFA;                  LSF1T026
   28          FA3: FA:=X*(X+1)*B;                    'GOTO'EFA;                  LSF1T027
   29          FA4: FA:=X*(X+3)*B;                    'GOTO'EFA;                  LSF1T028
   30          FA5: FA:=EXP(B*SQRT(X))*X;             'GOTO'EFA;                  LSF1T029
   31          FA6: FA:=EXP(B*X)*X;                   'GOTO'EFA;                  LSF1T030
   32          FA7: FA:=EXP(B*SQRT(X));               'GOTO'EFA;                  LSF1T031
   33          FA8: FA:=1/2*(EXP(H*X)+EXP(-H*X));                                 LSF1T032                                BLOCK E.D
   34   EFA:'END' FA;                                                              LSF1T033
   35         'REAL''PROCEDURE'FB(X);                                              LSF1T034
   36               'REAL'X;                                                      LSF1T035                                BLOCK8
   37   'BEGIN''SWITCH'SFB:=FB1,FB2,FB3,FB4,FB5,FB6,FB7,FB8; 'GOTO'SFB[M];        LSF1T036
   38          FB1: FB:=A*EXP(B*X);                   'GOTO'EFB;                  LSF1T037
   39          FB2: FB:=A*X*(1-X);                    'GOTO'EFB;                  LSF1T038
   40          FB3: FB:=A*X*(X-1)*POL(X+1);           'GOTO'EFB;                  LSF1T039

   41          FB4: FB:=A*X*(X+3)*POL(X+3);           'GOTO'EFB;                  LSF1T040
   42          FB5: FB:=A*EXP(H*SQRT(X))*X*(3/2);     'GOTO'EFB;                  LSF1T041
   43          FB6: FB:=A*EXP(B*X)*X*2;               'GOTO'EFB;                  LSF1T042
   44          FB7: FB:=A*EXP(H*SQRT(X))*SQRT(X);     'GOTO'EFB;                  LSF1T043
   45          FB8: FB:=A/2*X*(EXP(-6*X)+EXP(-6*X));                              LSF1T044                                BLOCK E.D
   46   EFB:'END'FB;                                                               LSF1T045
   47       'INTEGER'K,L;                                                          LSF1T046
   48       'REAL' S11,S12,S22,Y1,Y2,D,S0,S01;                                     LSF1T047
   49       'ARRAY' YCA[1:M];                                                      LSF1T048
   50          L:=0;                                                               LSF1T049
   51       'FOR'K:=1'STEP'1'UNTIL'M'DO' YCA[K]:=F(X[K]);                         LSF1T050
   52   A1:    S0:=S11:=S12:=S22:=Y1:=Y2:=0;                                      LSF1T051
   53       'FOR'K:=1'STEP'1'UNTIL'M'DO'                                          LSF1T052
   54   'BEGIN' S11:=S11+FA1Y(K))*2;                                              LSF1T053
   55          S22:=S22+FA(X[K])*2;                                               LSF1T054
   56          S12:=S12+FA(X[K])*FA1X[K]);                                        LSF1T055
   57          Y1:=Y1+(Y[K]-YCA[K])*FA(X[K]);                                     LSF1T056
   58          Y2:=Y2+(Y[K]-YCA[K])*FA(X[K]);                                     LSF1T057
   59          S0:=S0+(Y[K]-YCA[K])*2;                                            LSF1T058
   60   'END'K;                                                                   LSF1T059
   61          D:=DET(S11,S12,S12,S22);                                           LSF1T060
   62       'IF'L=0'THEN'"PRINT"'''L'SQUARES'',SAMELINE,SCALED(4),L,'3'',         LSF1T061
   63                                 S0,''S3'A='',A,''S3'B='',B;                 LSF1T062
   64          A:=DET(Y1,S12,Y2,S22)/D;                                           LSF1T063
   65          B:=DET(S11,Y1,S12,Y2)/D;                                           LSF1T064
   66          S01:=0;                                                            LSF1T065
   67       'FOR'K:=1'STEP'1'UNTIL'M'DO'                                          LSF1T066
   68   'BEGIN' YCA[K]:=F(X[K]);                                                  LSF1T067
   69          S01:=S01+(Y[K]-YCA[K])*2;                                          LSF1T068
   70   'END'K;                                                                   LSF1T069
   71       'PRINT'"/,'SQUARES',SAMELINE,SCALED(4),L+1,'3',S01,                   LSF1T070
   72                  ''S3'A='',A,''S3'B='',B;                                   LSF1T071
   73       'IF'L<5''THEN'                                                        LSF1T072
   74                                  'BEGIN' L:=L+1;                           LSF1T073
   75                                          'GOTO'A                           LSF1T074
   76                                  'END';                                    LSF1T075
   77       'FOR'K:=1'STEP'1'UNTIL'M'DO'                                          LSF1T076
   78       'PRINT'"/,'L',SAMELINE,SCALED(4),X[K],''S3'',Y[K],''S3'',             LSF1T077
   79                 YCA[K],''S3'',(Y[K]-YCA[K])*2;                             LSF1T078                                PLOCK E :
   80   'END' OF PROCEDURE LSF1T;                                                 LSF1T079
   81                                                                             LSF1T080
   82       'ARRAY'P,Q[1:3,1:3];  'BOOLEAN'BOOL;  'INTEGER'J,K0;                  LSF1T081
   83        BOOL:='ON';  J:=0;  'FOR'J:=J+1'WHILE'BOOL'DO'                       LSF1T082
   84   'BEGIN''REAL'D,E[J],J[J];                                                 LSF1T083
   85         'IF'ABS(P[J,J])<3*10**-8'AND'ABS(Q[J,J])<3*10**-8'THEN' BOOL:=1<0   LSF1T084
   86   'END'J;                                                                   LSF1T085
   87       'FOR'L:=1'STEP'1'UNTIL'6'DO'                                          LSF1T086
   88   'BEGIN''REAL'A,B;                                                         LSF1T087
   89          LSF1T(L-2,P,Q,M);                                                  LSF1T088
   90   'END'M;                                                                   LSF1T089                                BLOCK E :
   91   'END' OF PROGRAMME LSF1T;
  48a     MC
 1204  CODE
 1694  TOTAL


&D[AG:                                                                   CPU TIME =  0000  11.673
R[AG
```